in co-tutela con UNIVERSITE' DE LAUSANNE

DOTTORATO DI RICERCA IN

MATEMATICA

Ciclo 37

Settore concorsuale: 01/A3 – ANALISI MATEMATICA, PROBABILITÀ E STATISTICA MATEMATICA

Settore Scientifico Disciplinare: MAT/05 – ANALISI MATEMATICA

SEVERAL ASPECTS OF MODERN SIGNAL ANALYSIS: OPTIMAL TUNING PARAMETERS IN MRI INVERSE PROBLEMS AND SYMPLECTIC TIME-FREQUENCY ANALYSIS OF MODULATION SPACES

Presentata da: Gianluca Giacchi

Coordinatore Dottorato

Giovanni Mongardi

Supervisori

Nicola Arcozzi

Micah Murray

Co-supervisori

Elena Cordero

Benedetta Franceschiello

Esame finale anno 2025

Quando si parte il gioco de la zara,
colui che perde si riman dolente,
repetendo le volte, e tristo impara;

con l'altro se ne va tutta la gente;
qual va dinanzi, e qual di dietro il prende,
e qual dallato li si reca a mente;

el non s'arresta, e questo e quello intende;
a cui porge la man, più non fa pressa;
e così da la calca si difende.

Tal era io in quella turba spessa,
volgendo a loro, e qua e là, la faccia,
e promettendo mi sciogliea da essa.

[D. Alighieri, Purgatorio - Canto VI, vv. 1—12]

Abstract

Signal analysis, in all its forms, has proven to be effective in addressing challenges across modern branches of applied sciences, engineering, data analysis, medicine, and imaging. A prototypical example is Magnetic Resonance Imaging (MRI), which exploits electromagnetism to produce anatomical and functional images safely and without radiation. The numerous Nobel Prizes awarded to MRI research since its introduction forty years ago underscore its ongoing significance. However, despite our complete understanding of its mechanisms, medical advances require refining of the current techniques, improvement of image quality and reduction of the patient's scanning time. The modern challenges in this field are primarily twofold, both stemming from the physical nature of MRI, discussed in Chapter 1:

- Undersampling below the Nyquist threshold: to reduce acquisition time, MRI signals are often sampled below the Nyquist rate, necessitating the use of denoising and artifact removal techniques. Since MRI signals are highly compressible, Compressed Sensing (CS) techniques enable the reconstruction of missing information by solving a minimization problem known as the generalized LASSO. This process involves three parameters, selected based on mathematical and empirical criteria: the measurement matrix, which incorporates the sampling trajectory; regularization, which encodes signal sparsity; and a tuning parameter that balances fidelity and regularization.

- Motion sensitivity: MRI requires the patient to remain motionless during scanning, complicating the imaging of organs with involuntary and unavoidable movements, such as the heart and lungs. These movements also affect the imaging of nearby organs. Modern techniques introduce separate hardware to track these movements, allowing for the acquisition of data that can be divided to produce a dynamic sequence following the various phases of motion.

In this thesis, we explore two prominent aspects of the mathematics involved in MRI signal analysis. In Chapters 3 and 4, we focus on CS-MRI, and we introduce an iterative algorithm inspired by convex analysis that efficiently determines the tuning parameter for Total Variation (TV) regularized LASSO (TV-LASSO). The selection of the tuning parameter is crucial for minimizing noise and artifacts in the reconstructed image, and this choice is often made manually, which is time-consuming. Many of the techniques introduced in recent years suffer from two flaws: some are overly specific and not easily adaptable, while others involve learning algorithms that require extensive datasets, which are often unavailable.

Although tested on TV-LASSO with Cartesian acquisition, our algorithm can be easily extended to other regularizations and sampling strategies, always converging within a reasonable number of iterations.

In Chapters 5, 6 and 7, we discuss new time-frequency representations, which allow for the analysis of time-evolving signals, such as the MRI signal. Despite this, the application of these techniques to the analysis of time-varying signals is currently limited to a few examples in the literature, and it remains unclear how they can be effectively applied to MRI post-processing. However, we believe that the MRI signal of moving organs can be effectively processed through time-frequency representations with the appropriate properties. Our work involves the generalization of the most well-known and widely used time-frequency representations, the short-time Fourier transform and the Wigner distribution, through the so-called metaplectic operators. This generalization enables us to explain the properties of what we called *metaplectic Wigner distributions* in terms of the symplectic group, to which they are closely related. Thanks to these techniques it is possible to construct metaplectic Wigner distributions with the right properties, according to the applications.

In conclusion, we introduce ALMA, a novel algorithm to compute well performing tuning parameters for TV-LASSO problem, and use it to reconstruct images in a MRI framework. The results show near-optimality of our reconstructions in terms of multiscale structural similarity, peak signal-to-noise ratio and coefficient of joint variation. We introduce metaplectic Wigner distributions as natural generalizations of the most popular time-frequency representations, through metaplectic operators, and we study their main properties, relating them to the structure of the related symplectic matrices.

Résumé

L'analyse du signal, sous toutes ses formes, s'est avérée efficace pour relever des défis dans les branches modernes des sciences appliquées, de l'ingénierie, de l'analyse de données, de la médecine et de l'imagerie. Un exemple prototypique est l'Imagerie par Résonance Magnétique (IRM), qui exploite l'électromagnétisme pour produire des images anatomiques et fonctionnelles de manière sûre et sans rayonnement. Les nombreux Prix Nobel attribués à la recherche sur l'IRM depuis son introduction il y a quarante ans soulignent son importance continue. Cependant, malgré notre compréhension complète de ses mécanismes, les avancées médicales nécessitent un raffinement des techniques actuelles, une amélioration de la qualité des images et une réduction du temps de scan pour le patient. Les défis modernes dans ce domaine sont principalement de deux ordres, découlant tous deux de la nature physique de l'IRM, discutée au Chapitre 1:

- Sous-échantillonnage en dessous du seuil de Nyquist : Pour réduire le temps d'acquisition, les signaux IRM sont souvent échantillonnés en dessous de la fréquence de Nyquist, ce qui nécessite l'utilisation de techniques de débruitage et de suppression des artefacts. Étant donné que les signaux IRM sont hautement compressibles, les techniques de Compressed Sensing (CS) permettent de reconstruire les informations manquantes en résolvant un problème de minimisation connu sous le nom de LASSO généralisé. Ce processus implique trois paramètres, sélectionnés en fonction de critères mathématiques et empiriques : la matrice de mesure, qui incorpore la trajectoire d'échantillonnage ; la régularisation, qui encode la parcimonie du signal ; et un paramètre de réglage qui équilibre la fidélité et la régularisation.

- Sensibilité au mouvement : L'IRM nécessite que le patient reste immobile pendant le scan, ce qui complique l'imagerie des organes soumis à des mouvements involontaires et inévitables, comme le cœur et les poumons. Ces mouvements affectent également l'imagerie des organes adjacents. Les techniques modernes introduisent du matériel séparé pour suivre ces mouvements, permettant l'acquisition de données qui peuvent être divisées pour produire une séquence dynamique suivant les différentes phases du mouvement.

Dans cette thèse, nous explorons deux aspects importants des mathématiques impliquées dans l'analyse des signaux IRM. Aux Chapitres 3 et 4, nous nous concentrons sur le CS-IRM et introduisons un algorithme itératif inspiré par l'analyse convexe qui détermine efficacement le paramètre de réglage pour le LASSO régularisé par Variation Totale (TV-LASSO). La sélection du paramètre de réglage

est cruciale pour minimiser le bruit et les artefacts dans l'image reconstruite, et ce choix est souvent fait manuellement, ce qui est chronophage. Beaucoup des techniques introduites ces dernières années souffrent de deux défauts : certaines sont trop spécifiques et difficilement adaptables, tandis que d'autres impliquent des algorithmes d'apprentissage nécessitant de vastes ensembles de données, qui sont souvent indisponibles. Bien que testé sur le TV-LASSO avec acquisition cartésienne, notre algorithme peut être facilement étendu à d'autres régularisations et stratégies d'échantillonnage, tout en convergeant toujours en un nombre raisonnable d'itérations.

Aux Chapitres 5, 6 et 7, nous discutons de nouvelles représentations temps-fréquence, qui permettent l'analyse des signaux évoluant dans le temps, tels que le signal IRM. Malgré cela, l'application de ces techniques à l'analyse des signaux variant dans le temps est actuellement limitée à quelques exemples dans la littérature, et il reste incertain comment elles peuvent être appliquées efficacement au post-traitement des signaux IRM. Cependant, nous croyons que le signal IRM d'organes en mouvement peut être traité efficacement à l'aide de représentations temps-fréquence ayant les propriétés appropriées. Notre travail consiste en la généralisation des représentations temps-fréquence les plus connues et les plus largement utilisées, la transformation de Fourier à court terme et la distribution de Wigner, à travers les opérateurs métraplectiques. Cette généralisation nous permet d'expliquer les propriétés de ce que nous avons appelé les *distributions de Wigner métraplectiques* en termes du groupe symplectique, auquel elles sont étroitement liées. Grâce à ces techniques, il est possible de construire des distributions de Wigner métraplectiques avec les bonnes propriétés, selon les applications.

En conclusion, nous introduisons ALMA, un nouvel algorithme pour calculer des paramètres de réglage performants pour le problème TV-LASSO, et l'utilisons pour reconstruire des images dans un cadre IRM. Les résultats montrent la quasi-optimalité de nos reconstructions en termes de similarité structurelle multiscale, de rapport signal-sur-bruit de crête et de coefficient de variation conjointe. Nous introduisons les distributions de Wigner métaplectiques comme des généralisations naturelles des représentations temps-fréquence les plus populaires, via les opérateurs métaplectiques, et nous étudions leurs principales propriétés, en les reliant à la structure des matrices symplectiques associées.

Contents

Introduction

1.1 History of MRI

Magnetic Resonance Imaging (MRI) has emerged as a seminal technology in the realm of neuroscience, fundamentally transforming our capacity to non-invasively probe the intricacies of the human brain's structure, function, and connectivity. By leveraging the principles of nuclear magnetic resonance (NMR), MRI offers a non-ionizing radiation method to generate high-resolution images of soft tissues, particularly the brain.

The inception of MRI can be traced back to the pioneering work in the late 1930s and 1940s. In 1939, Rabi, Millman, Kusch, and Zacharias laid the groundwork for NMR with their investigations into molecular beams [106]. Their innovative work provided the theoretical framework that underpins MRI's ability to detect and differentiate between various tissue types based on their magnetic properties. Recognizing the significance of their contributions, they were awarded the Nobel Prize in Physics in 1944.

Building on this foundation, 1946 marked another pivotal year with the parallel research efforts of Bloch, Hansen, Packard, Purcell, Torrey, and Pound. Their studies elucidated the behavior of spins in liquids and solids when subjected to magnetic fields, paving the way for the development of MRI as a viable imaging technique [7, 97, 105]. Bloch and Purcell's seminal contributions were recognized with the Nobel Prize in Physics in 1952.

The true breakthrough in MRI came in the early 1970s with the work of Lauterbur. In 1973, Lauterbur demonstrated the feasibility of MRI by producing the first two-dimensional MR image of water-filled tubes [81]. This groundbreaking achievement laid the groundwork for the development of modern MRI techniques. In his subsequent work in 1974, Lauterbur introduced the term *zeugmatograms* to describe images obtained through NMR, which later evolved into the commonly used term MRI. Moreover, he expanded the scope of MRI by capturing the first MR images of living organisms, including a small Venus mercenaria and the thoracic cavity of a live mouse. For his pioneering contributions

to the field of MRI, Lauterbur was awarded the Nobel Prize in Physiology or Medicine in 2003, underscoring the transformative impact of his work on both scientific research and clinical practice. Today, MRI has evolved into a multifaceted imaging modality, encompassing a range of techniques such as functional MRI (fMRI), diffusion MRI (dMRI), magnetic resonance spectroscopy (MRS), and magnetic resonance elastography (MRE), each offering unique insights into the structure and function of the human brain and body.

Despite being such a powerful technique, MRI poses formidable challenges to modern research, related to both acquisition and processing of the MRI signal. As explained in the following, the MRI signal is acquired below its Nyquist frequency to reduce the dimensionality of the MRI data, which consists indeed of a high-dimensional complex vector. To retrieve the missing information due to undersampling, compressed sensing techniques, such LASSO inverse problems, are widely used. Another challenge that modern research faces involves the dynamic nature of MRI acquisition, particularly when imaging moving organs. The motion of a patient in the scanner causes artifacts, yielding to blurred regions in the reconstruction. MRI signal is actually a concrete example of time-evolving signal, therefore necessitating of robust methodologies to capture and interpret temporal variations accurately. Time-frequency analysis addresses time-varying signals by localizing and decomposing them into their frequency content over time allowing, in principle, to extract local features of time-evolving signals. Precisely, time-frequency analysis is a branch of Fourier analysis that studies the phase-space concentration of signals, with applications to operator theory, signal analysis, engineering, medical sciences, where it is deployed in the processing of echocardiographic signals, electroencephalograms, evoked potentials and MR spectroscopy, [6], in fMRI to study the correlation between coupled time-series functions by their frequencies and phases, [62]. Time-frequency analysis was also applied to MRI of moving organs, where the frequency information varies in time as a consequence of motion by M. Sushma et al. in [115]. To build upon the strengths of time-frequency analysis, a closely related method—wavelet analysis on graphs—has recently been employed to analyze brain fMRI signals, as demonstrated by I. M. Bulai and S. Saliani in [13]. Keeping the increasing interest of researchers in the applications of time-frequency analysis to concrete problems in MRI, part of this thesis work consists of generalizing classical time-frequency representations, such as the short-time Fourier transform (STFT) and the Wigner distribution, to enable a broader perspective on their properties and limitations, shedding new light on the nature of these representation and their construction, according to the necessity.

With this historical context in mind and motivated by the impact that we believe time-frequency analysis technique may have in MRI, we will now delve into the fundamental physics that govern MRI and introduce compressed sensing (CS) as a fundamental tool to processing of MRI signals, both at the acquisition level, where it deals with designing measurement matrices, and to the reconstruction

level, where it provides techniques to retrieve partially sampled, noisy and sparse data.

1.2   The MRI signal

In order to introduce the acquisition process of the MRI signal, understanding the theoretical principles and physics behind MRI is crucial. This acquisition is indeed modelled as a sampling operator applied to the MRI signal, which is as a function in $\mathcal{C}^\infty(\mathbb{R}^3)$, as detailed below.

MR scanners utilize coils made primarily of superconducting materials, such as niobium-titanium or niobium-tin alloys, which are cooled to extremely low temperatures (close to absolute zero) to achieve superconductivity. This superconducting state allows the coils to conduct electricity without resistance, generating a powerful and uniform magnetic field, denoted by $\boldsymbol{B_0}$, essential for high-quality MRI images [1]. Before illustrating the physical nature of the MRI signal, let us synthesize how the MRI signal is generated.

1. The patient is placed within the strong static magnetic field of the MRI machine. This causes the magnetic moments of atomic nuclei (typically protons) in the body to align with the magnetic field.

2. Additional magnetic field gradients are applied, which encode spatial information into the detected signal, allowing the MRI system to determine the location of the signal origin within the body.

3. A radiofrequency (RF) pulse is applied perpendicular to the static magnetic field. This pulse perturbs the aligned magnetic moments, causing them to precess (or spin) around the direction of the magnetic field.

4. The protons absorb energy from the RF pulse, causing them to transition from a low-energy state to a higher-energy state. This energy is typically in the radiofrequency range.

5. After the RF pulse is turned off, the protons gradually return to their original alignment with the magnetic field.

6. During the relaxation processes, the protons release the absorbed RF energy as they return to their equilibrium states. This emitted energy consists of RF waves, which induce a weak alternating current in *receiver* coils of the MRI scanner.

---

[1]The notation employed in MRI physics utilizes bold lettering to signify vectors. The bold notation will be discontinued shortly to avoid confusion and maintain consistency.

Loosely speaking, the MRI signal is related to the electromotor force (emf) induced by the variation of a magnetic field $\boldsymbol{B}$ passing though receiving coils. Consider a sample located in a region $V \subseteq \mathbb{R}^3$, with magnetization $\boldsymbol{M}$. The magnetic field due to to $\boldsymbol{M}$ is given by:

$$\boldsymbol{B}(\boldsymbol{r}) = \mathrm{rot}(\boldsymbol{V_M}(\boldsymbol{r})),$$

where the curl is computed with respect to the spatial variables $\boldsymbol{r} = (x, y, z)$,

$$\boldsymbol{V_M}(\boldsymbol{r}) = \frac{\mu_0}{4\pi}\int_V \frac{\boldsymbol{J_M}(\boldsymbol{r}')}{|\boldsymbol{r}-\boldsymbol{r}'|}d\boldsymbol{r}' = \frac{\mu_0}{4\pi}\oint \frac{I d\boldsymbol{l}}{|\boldsymbol{r}-\boldsymbol{r}'|}$$

is the potential of the associated to the effective current density $\boldsymbol{J_M} = \mathrm{rot}(\boldsymbol{M})$, and I is the intensity of the current generated in the coils. Here, μ_0 denotes the vacuum permeability constant. The flux generated by the variation of $\boldsymbol{B}$ is given by:

$$\Phi_{\boldsymbol{M}}(t) = \int_{\mathbb{R}^3} \boldsymbol{B}(\boldsymbol{r}') \cdot \boldsymbol{M}(\boldsymbol{r}', t)d\boldsymbol{r}',$$

where $\boldsymbol{B}$ is the magnetic field per unit of current produced by the coil:

$$\boldsymbol{\mathcal{B}}(\boldsymbol{r}') = \mathrm{rot}\Big(\frac{\boldsymbol{V_M}(\boldsymbol{r}')}{I}\Big) = \frac{\boldsymbol{B}(\boldsymbol{r}')}{I}.$$

The MRI signal is proportional to the emf induced by $\Phi_{\boldsymbol{M}}$:

$$\tilde{s}(t) \propto -\frac{d}{dt}\int_{\mathbb{R}^3}\Big(\mathcal{B}_x(\boldsymbol{r}')M_x(\boldsymbol{r}', t) + \mathcal{B}_y(\boldsymbol{r}')M_y(\boldsymbol{r}', t) + \mathcal{B}_z(\boldsymbol{r}')M_z(\boldsymbol{r}', t)\Big)d\boldsymbol{r}', \quad (1.1)$$

(the non-bold symbols denote the corresponding components of $\boldsymbol{\mathcal{B}}$ and $\boldsymbol{M}$). Each tissue of interest has signature *relaxation times* T_1 and T_2. In physics terms, T_1 is the time it takes for the protons to re-align with the magnetic field $\boldsymbol{B}_0$ after the RF pulse is turned off, while T_2 is the time it takes for the protons to lose the energy gained from the RF pulse. T_1 is usually longer than T_2. The Bloch equations relate relaxation times to the magnetization:

$$\begin{cases} \frac{dM_x}{dt} = \omega_0 M_y - \frac{M_x}{T_2}, \\ \frac{dM_y}{dt} = -\omega_0 M_x - \frac{M_y}{T_2}, \\ \frac{dM_z}{dt} = \frac{M_0 - M_z}{T_1}, \end{cases} \quad (1.2)$$

where ω_0 is the Larmor frequency, and M_0 is the equilibrium value of the magnetization before the application of the RF pulse. The solution $\boldsymbol{M}$ of (1.2) is explicitly given by:

$$\begin{cases} M_x(t) = e^{-t/T_2}(M_x(0)\cos(\omega_0 t) + M_y(0)\sin(\omega_0 t)), \\ M_y(t) = e^{-t/T_2}(M_y(0)\cos(\omega_0 t) + M_x(0)\sin(\omega_0 t)), \\ M_z(t) = M_z(0)e^{-t/T_1} + M_0(1 - e^{-t/T_1}). \end{cases}$$

To see how Fourier analysis comes into play in the MRI framework, the expression (1.1) of $\tilde{s}$ undergoes further manipulations and approximations. For simplicity of exposition, consider the case in which the scanner magnetic field $\boldsymbol{B}_0$ is directed along the z-axis. In this case, it is useful to decompose the magnetization $\boldsymbol{M}$ along its longitudinal and orthogonal components, $\boldsymbol{M}_z = M_z \boldsymbol{e}_z$ and $\boldsymbol{M}_\perp = M_x \boldsymbol{e}_x + M_y \boldsymbol{e}_y$, where $\boldsymbol{e}_x$, $\boldsymbol{e}_y$ and $\boldsymbol{e}_z$ are the unit vectors of the coordinate axes. Under this notation, the orthogonal component of the solution $\boldsymbol{M}(\boldsymbol{r}, t)$ of (1.2) can be represented as a complex vector $\boldsymbol{M}_+(\boldsymbol{r}, t)$:

$$\boldsymbol{M}_+(\boldsymbol{r}, t) = e^{-t/T_2} e^{-i\omega_0 t + i\phi_0(\boldsymbol{r})} \boldsymbol{M}_\perp(\boldsymbol{r}, 0),$$

where ϕ_0 and $\boldsymbol{M}_\perp(\boldsymbol{r}, 0)$ are determined by the initial conditions on the RF pulse. The next step is differentiating (1.1) and neglecting the exponentials e^{-t/T_1} and e^{-t/T_2}. This can be done because in the applications $\omega_0 T_1, \omega_0 T_2 \approx 10^4$. The obtained approximated signal is:

$$\tilde{s}(t) \propto \omega_0 \int_{\mathbb{R}^3} e^{-t/T_2} \boldsymbol{M}_\perp(\boldsymbol{r}, 0)[\mathcal{B}_x(\boldsymbol{r})\sin(\omega_0 t - \phi_0(\boldsymbol{r})) + \mathcal{B}_y(\boldsymbol{r})\cos(\omega_0 t - \phi_0(\boldsymbol{r}))]d\boldsymbol{r}.$$

Writing $\mathcal{B}_x = \mathcal{B}_\perp \cos(\vartheta_B)$ and $\mathcal{B}_y = \mathcal{B}_\perp \sin(\vartheta_B)$,

$$\tilde{s}(t) \propto \omega_0 \int_{\mathbb{R}^3} e^{-t/T_2} M_\perp(\boldsymbol{r}, 0)\mathcal{B}_\perp(\boldsymbol{r})\sin(\omega_0 + \vartheta_B(\boldsymbol{r}) - \phi_0(\boldsymbol{r}))d\boldsymbol{r}. \qquad (1.3)$$

In 3D MRI, the application of a *gradient* changes the direction of the scanner magnetic field $\boldsymbol{B}_0$. In this cae, (1.3) must be modified accordingly, by replacing ω_0 with $\omega(\boldsymbol{r}) = \omega_0 + \Delta\omega(\boldsymbol{r})$, and the rapid oscillations due to ω_0 are removed using rotating frames (*demodulation*). For suitable constant Λ and introducing a *demodulation frequency* $\Omega = \omega_0 + \delta\omega$, the resulting *demodulated signal* is:

$$\tilde{s}(t) = \Lambda \omega_0 \int_{\mathbb{R}^3} e^{-t/T_2} M_\perp(\boldsymbol{r}, 0)\mathcal{B}_\perp(\boldsymbol{r})e^{i((\Omega - \omega_0)t + \phi_0(\boldsymbol{r}) - \vartheta_B(\boldsymbol{r}))}d\boldsymbol{r}. \qquad (1.4)$$

Assuming that ϑ_B and ϕ_0 to be independent on $\boldsymbol{r}$, (1.4) becomes:

$$\tilde{s}(t) = \omega_0 \Lambda \int_{\mathbb{R}^3} \mathcal{B}_\perp(\boldsymbol{r})M_\perp(\boldsymbol{r}, 0)e^{i(\Omega t + \phi(\boldsymbol{r}, t))}d\boldsymbol{r}, \qquad (1.5)$$

where:

$$\phi(\boldsymbol{r}, t) = -\int_0^t \omega(\boldsymbol{r}, t')dt' \qquad (1.6)$$

is the accumulated phase. Applying a $\pi/2$ RF pulse, the function $\mathcal{B}_\perp(\boldsymbol{r})M_\perp(\boldsymbol{r}, 0)$ becomes proportional to the density of proton spins $\rho(\boldsymbol{r})$. Ignoring this proportionality constant, (1.5) becomes the relation between the density of proton spins and the MRI signal:

$$s(t) = \int_{\mathbb{R}^3} \rho(\boldsymbol{r})e^{i(\Omega + \phi(\boldsymbol{r}, t))}d\boldsymbol{r}. \qquad (1.7)$$

The key observation is that the application of a gradient to modify the direction and the intensity of $\boldsymbol{B}$, allows to control accumulated phase as follows. Consider a vector $\boldsymbol{G} \in \mathbb{R}^3$, which we call *gradient* and perturb the static magnetic field: $\boldsymbol{B}(\boldsymbol{r},t) = \boldsymbol{B}_0 + \boldsymbol{G}$. By choosing $\omega(\boldsymbol{r},t) = \omega_0 + \boldsymbol{r} \cdot \boldsymbol{G}$ in (1.6), and by demodulating with frequency $\Omega = \omega_0$ in (1.7), we get:

$$s(t) = C \int_{\mathbb{R}^3} \rho(\boldsymbol{r}) e^{-2\pi i t \boldsymbol{G} \cdot \boldsymbol{r}} d\boldsymbol{r}, \tag{1.8}$$

where the constant $C > 0$ is chosen properly for 2π to appear in the phase factor. Neglecting C, (1.8) tells that the signal at time t is equal to the Fourier transform of the density of proton spins:

$$s(t) = \hat{\rho}(t\boldsymbol{G}).$$

Observe that the proton density function ρ vanishes outside a cube of length $L > 0$. Therefore, s is a finite-energy signal, i.e., $s \in L^2(\mathbb{R}^3)$ and since $\rho \in L^1(\mathbb{R}^3)$, we also have that $s \in \mathcal{C}_0(\mathbb{R}^3)$, i.e., s is continuous and goes to 0 at infinity. The function of one real variable s is a function on $\mathbb{R}^3$ undercover. This can be stressed by defining $\boldsymbol{\xi}(t) := t\boldsymbol{G} \in \mathbb{R}^3$ and writing:

$$s(t) = s(\boldsymbol{\xi}(t)) = \hat{\rho}(\boldsymbol{\xi}(t)) \tag{1.9}$$

(the caret denoting the Fourier transform). Assuming that $s \in L^1(\mathbb{R}^3)$, the Fourier transform in (1.9) can be inverted:

$$\rho(\boldsymbol{r}) = \int_{\mathbb{R}^3} s(\boldsymbol{\xi}) e^{2\pi i r \cdot \boldsymbol{\xi}} d\boldsymbol{\xi}. \tag{1.10}$$

Equation (1.10) is the fundamental relation between the MRI signal s and the proton density ρ, which outlines the anatomical image. This justifies the abuse of language:

the MR image of an organ of interest is
the inverse Fourier transform of the MR signal.

1.3 Compressed Sensing MRI

In order to digitally process and reconstruct these anatomical images, the continuous MRI signal must be discretized through a process known as *sampling*. This transition from continuous to discrete data through sampling is fundamental, as computers are unable to process analog signals directly, and it is guided by a classic principle of signal analysis, which dictates the necessary conditions for retrieving the analog signal in its digital form.
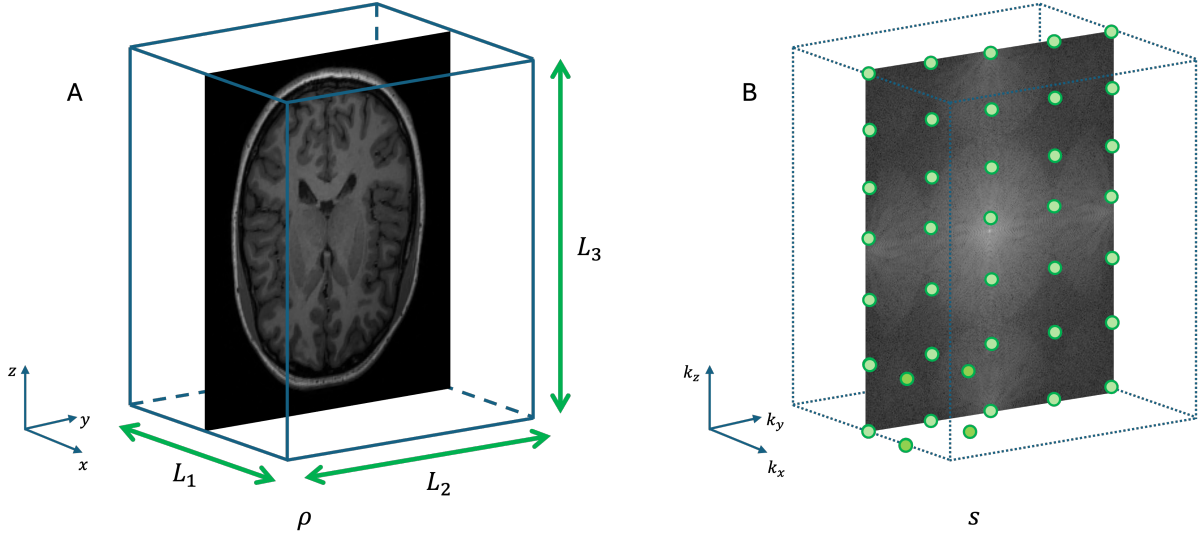
Figure 1.1: Full salmpling of 3D MRI signal. (A) The proton density ρ is supported in a cube of sides L_1, L_2 and L_3 of the image domain, i.e., the Fourier transform of s is supported in $[-L_1/2, L_1/2] \times [-L_2/2, L_2/2] \times [-L_3/2, L_3/2]$. (B) Every coordinate direction of the k-space is sampled at its Nyquist frequency.

Theorem 1.1 (Shannon, Nyquist, Whittaker, Kotelnikov). *Let $f \in L^2(\mathbb{R})$ be such that $supp(\hat{f}) \subseteq [-A, A]$ (i.e., $\hat{f}(\xi) = 0$ if $|\xi| > A$) for some $A > 0$. Then,*

$$f(t) = \sum_{k=-\infty}^{\infty} f(kT) \operatorname{sinc}(\frac{t - kT}{T}), \qquad t \in \mathbb{R},$$

where $\operatorname{sinc}(x) = \frac{\sin(\pi x)}{\pi x}$ *and* $T \leq T_A = 1/2A$ *(T_A is called Nyquist frequency).*

The 3D MRI signal s enjoys the property that its inverse Fourier transform ρ is supported in a cube, as illustrated in Fig. 1.1 (A). Full sampling for the MRI signal corresponds to sampling s across every direction of the k-space (the domain of the Fourier transform) at the corresponding Nyquist frequency, see Fig. 1.1 (B). Concretely, the sampling trajectory $\boldsymbol{\xi}(t)$ is controlled by means of time and gradients, choosing $\boldsymbol{\xi}(t) = t\boldsymbol{G}$ in (1.9), as in formula (1.8). The theoretical framework described so far is implemented by approximating the MRI signals by sampling within a limited cubic neighborhood of the k-space center. However, even when restricting the sampling to a neighborhood around the origin, the sampling of MRI signals is in general extremely time-consuming, due to the large amount of points needed to reach good resolution reaching orders of magnitude that make MRI post-processing computationally prohibitive. This extensive data gathering process not only renders MRI signal acquisition economically burdensome but also contributes to patient discomfort, necessitating

prolonged periods of immobility during the procedure. Furthermore, for some patients with specific conditions, remaining still for even a brief period could even be impossible. Given the burden posed by the large number of samples required for conventional MRI post-processing, alternative approaches such as compressed sensing (CS) have gained prominence. CS is a modern discipline that combines mathematics, signal processing and computer science to extract essential information from data that is sampled below the Nyquist frequency, thereby paving the way for faster, more efficient, and more economical data acquisition. It finds applications in image and video processing [9, 50, 41, 104, 100, 126], electrical engineering [70, 15, 56, 71, 42], geophysics [91, 80, 95], remote sensing [57, 99], machine learning [10, 84, 113, 98, 77] and medical imaging techniques, such as computer tomography [67, 125] and, of course, MRI. Notably, the application of compressed sensing to MRI is known as *CS-MRI* and it was firstly address in the celebrated work by M. Lustig, et al., [87]. In CS-MRI, the sparsity or compressibility of MRI signals with respect to several *sparsity-promoting transforms* is exploited to enable significant undersampling (sampling below the Nyquist frequency), thereby reducing the number of acquired samples while still allowing for accurate signal reconstruction. By strategically acquiring a subset of samples in k-space, CS techniques offer a promising avenue for accelerating MRI acquisition and overcoming the limitations associated with conventional sampling trajectories.

Definition 1.2. A vector $x \in \mathbb{R}^d$ is *m-sparse* if $\|x\|_0 := \#\{j : x_j \neq 0\} \leq m$, where $\#S$ denotes the cardinality of a set S. When m is clear from the context or irrelevant, we say that x is *sparse*.

Sparsity is related on constrained optimization by the following result, whose proof is a slight modification of the proof of [49, Theorem 3.1].

Theorem 1.3. *Let $A \in \mathbb{R}^{m \times n}$ be a measurement matrix and $\eta \geq 0$. If the minimizer $x^\#$ of the constrained LASSO:*

$$minimize \qquad \|x\|_1 \ subject \ to \ x \in \mathbb{R}^n, \ \|Ax - b\|_2 \leq \eta \qquad (1.11)$$

is unique, then $x^\#$ is $\mathrm{rank}(A)$-sparse, where $\mathrm{rank}(A)$ denotes the rank of A.

LASSO has many equivalent formulations, where the equivalence notion is specified in [49, Proposition 3.2]. We limit ourselves to delineate the relationship between the constrained LASSO (1.11) and its unconstrained counterpart:

$$minimize \qquad \frac{1}{2}\|x\|_1 + \frac{\lambda}{2}\|Ax - b\|_2^2. \qquad (1.12)$$

Theorem 1.4. *Let $A \in \mathbb{R}^{m \times n}$, $b \in \mathbb{R}^m$ and $\eta > 0$. Let $x^\#$ be a minimizer of the constrained LASSO (1.11). Then, there exists $\lambda' \geq 0$ such that $x^\#$ is also a minimizer of (1.12) with $\lambda = \lambda'$. Conversely, if $x^\#$ is a minimizer of (1.12), there exists $\eta' \geq 0$ such that $x^\#$ is also a minimizer of (1.11) with $\eta = \eta'$.*

Consequently, solving (4.2) with the corresponding Lagrange multiplier provides a rank(A)-sparse solution. MRI images and MRI data, however, may not be sparse themselves, but with respect to so-called *sparsity-promoting transforms*, such as discrete Fourier transform, discrete cosine transform, wavelets [87]. That is, Φx is sparse, where Φ denotes a sparsity-promoting transform. LASSO problem can be modified to encompass this a-priori information. Specifically, the generalized LASSO (g-LASSO):

$$minimize \qquad \frac{1}{2}\|Ax - b\|_2^2 + \frac{\lambda}{2}\|\Phi x\|_1, \qquad (1.13)$$

allows for the retrieval of vectors that are compressible with respect to Φ. The rescaling by the factor $1/2$ in (1.13) is needed for computational purposes, but it is irrelevant to the analysis of (4.3). Also, for the purposes of our work, observe that (1.13) with $\lambda \neq 0$ is equivalent to:

$$minimize \qquad \frac{1}{2}\|\Phi x\|_1 + \frac{\lambda^*}{2}\|Ax - b\|_2^2, \qquad (1.14)$$

where the equivalence follows by choosing $\lambda^* = \lambda^{-1}$.

For the purpose of this introduction, let us focus on the unconstrained form of g-LASSO expressed in (1.13), a more exhaustive treatment of CS is contained in Chapter 3. In the MRI framework, the matrix A models the acquisition procedure of the MRI signal, and it is called *measurement matrix*. Specifically,

$$A = UFC \qquad (1.15)$$

is the composition of three operators. U encodes the undersampling trajectory that can be 2D, 3D, 4D, when time evolution is considered, and even 5D, when respiratory phases are considered. F is the discrete Fourier transform, and C is the so-called *coil sensitivity*. The coil sensitivity map corrects the intensity inhomogeneity of the images across nCh channels, crucial to reconstruct high-quality images from undersampled k-space data.

The second operator appearing in (1.15) is the discrete Fourier transform (DFT), which we denoted by F. Sampling the MRI signal over a finite sampling set results in an approximation, which is effectively described by the DFT. Let $L > 0$ play the role of a scale length and fix an integer $n > 0$, related to number of samples. The DFT of a vector of $x = (x_{-n}, \ldots, x_{n-1})^T \in \mathbb{C}^{2n}$ is the vector $Fx \in \mathbb{C}^{2n}$ with coordinates[2]:

$$Fx_k = \sum_{j=-n}^{n-1} x_j e^{-2\pi i \frac{jk}{2n}}, \qquad k = -n, \ldots, n-1.$$

---

[2]For the sake of simplicity, we will omit the transposition superscript and denote with the same symbols vectors and covectors. This shall not cause confusion.

In our context, x is related to samples of the MRI signal, which is a function over $\mathbb{R}^2$, as in our experiments, or in general on a real vector space. Let us express this relation in dimension 1. Under the notation above, let $s \in L^2(\mathbb{R})$ with $x_k = s(k\Delta k)$, and define $\Delta k := 1/L$. Equation Fx reads as:

$$Fs(k\Delta k) = \sum_{j=-n} s(j\Delta x)e^{-2\pi ijk\Delta x\Delta k}, \qquad k = -n, \ldots, n-1,$$

and the corresponding inversion formula is:

$$s(j\Delta x) = \frac{1}{2n} \sum_{k=-n}^{n-1} Fs(k\Delta k)e^{2\pi i\frac{jk}{2n}}, \qquad j = -n, \ldots, n-1.$$

The last operation appearing in (1.15) is represented by the undersampling operator U. This sampling procedure is implemented by a discretization to fit the reconstructed image to the pixels/voxels. Sampling the MRI signal can be modelled in the framework of tempered distributions. For the sake of simplicity, we put ourselves in the 1D setting. The *sampling function* is the distribution given by:

$$u = \Delta k \sum_{j=-\infty}^{\infty} \delta_{j\Delta k} \in \mathcal{S}'(\mathbb{R}),$$

where δ_{x_0} is the point mass measure in x_0. By Poisson's summation formula, it's inverse Fourier transform is

$$F^{-1}u = \Delta k \sum_{k=-\infty}^{\infty} \delta_{j/\Delta k}. \tag{1.16}$$

Since $\hat{s} = \rho$ is compactly supported, $s \in \mathcal{C}^\infty(\mathbb{R})$ and it has moderate growth. Infinite sampling can be modelled by u as the tempered distribution:

$$s_\infty = s \cdot u \tag{1.17}$$

and the reconstructed image would be approximated by taking the inverse Fourier transform, using (1.17) and (1.16), as:

$$\tilde{\rho}_\infty(x) = \Delta k \sum_{j=-\infty}^{\infty} \rho(x - j/\Delta k), \qquad x \in \mathbb{R}. \tag{1.18}$$

Since ρ is compactly supported, (1.18) shows that the infinitely-sampled approximated image $\tilde{\rho}_\infty$ is the juxtaposition of infinitely many copies of ρ. Specifically, it is a $1/\Delta k$ periodic function and the number $1/\Delta k$ is called *Field Of View* (FOV). In the practice, sampling is limited to a cubic region around the origin of the k-space, which is in turns automatically defined once the origin in the

image domain is fixed. IN the 1D framework the truncation is modelled using the characteristic function:

$$\chi_{[-1/2,1/2]}(\xi) = \begin{cases} 1 & \text{if } |\xi| \leq 1/2, \\ 0 & \text{if } |\xi| > 1/2, \end{cases}$$

and the sampling distribution becomes:

$$U(\xi) = u(\xi)\chi_{[-1/2,1/2]}\Big(\frac{\xi + \Delta k/2}{2n\Delta k}\Big) = \Delta k \sum_{j=-n}^{n-1} \delta_{j\Delta k}(\xi),$$

where $2n$ indicates the number of sampled points. The undersampled signal is:

$$s_m(\xi) = s(\xi)U(\xi) = \Delta k \sum_{j=-n}^{n-1} s(j\Delta k)\delta_{j\Delta k}(\xi),$$

and the reconstructed spin density is:

$$\tilde{\rho}(x) = \mathcal{F}^{-1}s_m(x) = \Delta k \sum_{j=-n}^{n-1} s(j\Delta k)e^{2\pi i j\Delta k x}, \qquad x \in \mathbb{R}.$$

The reconstruction in the image domain undergoes further discretization due to the voxel resolution, which defines the smallest distinguishable unit of the 3D space within the MRI scan, ultimately impacting the image's clarity and detail. This is modelled by means of the tempered distribution

$$v = \Delta x \sum_{k=-\infty}^{\infty} \delta_{k\Delta x}.$$

Emulating the preceding argument,

$$\tilde{\rho}_m(x) = \tilde{\rho}(x)v(x)\chi_{[-1/2,1/2]}\Big(\frac{x + \Delta x/2}{2n\Delta x}\Big) = \sum_{k=-n}^{n-1} \tilde{\rho}(k\Delta x)\delta_{k\Delta x}(x), \qquad x \in \mathbb{R},$$

(1.19)

is a truncated approximation of the MR image. The resolution of the reconstructed image is related to n by $\Delta x = \frac{L}{2n}$, where L is the *pixel/voxel size*, and $2n$ is also the number of pixels/voxels along the considered direction.

The argument above extends naturally to the 3D framework, where sampling along grids is referred to as Cartesian sampling (fig. 1.2 (A)). However, alternative patterns such as radial, spiral, or other sampling methods require distinct approaches for assigning values to each pixel or voxel. In any case, it is a relevant point in MRI reconstructions that in the case of non-Cartesian trajectories, the samples are rearranged into a Cartesian grid before reconstruction. This by done

by assigning a value to each point of the grid, usually obtained as a Gaussian-weighted average of the sampled signal (the Gaussian centered on the considered point of the Cartesian grid), mathematically speaking a discrete convolution with a Gaussian weight. Moreover, according to CS theory, undersampling trajectories are designed to satisfy *incoherence* properties while sampling points in the k-space below the Nyquist frequency, though we will not delve into the specifics of this topic here, we refer to [49] as an exhaustive source in this direction.

In MRI, we can leverage the a-priori information that the Fourier transform of the MRI signal is concentrated around the center of the k-space to optimize the sampling strategy, thereby improving the reconstruction quality and efficiency. Consequently, the most commonly implemented MRI sampling trajectories involve sampling the center of the k-space, which captures the finer details of the MR image, at the Nyquist frequency, while sampling the periphery of the k-space, which captures the coarsest details, less densely. In Cartesian sampling, data is collected along parallel lines in k-space, with undersampling achieved by selectively omitting some of these lines, or segments. A specified portion of the sampling lines covers a neighborhood of the k-space center at the Nyquist frequency, while the remaining lines are randomly selected based on a normal distribution, as depicted in fig. 1.2 (A). In contrast, radial sampling consists of acquiring data along radial lines extending from the center of k-space outwards towards its periphery, ensuring wider coverage of the k-space center, while undersampling the peripheral regions, see fig. 1.2 (B). 3D sampling strategies encompass various methods, including 3D Cartesian sampling, which extends the principles of 2D Cartesian sampling into three dimensions for volumetric data acquisition. Additionally, spiral sampling, serving as a 3D counterpart to 2D radial sampling, involves data acquisition along segments radiating from the center of k-space, following a spiral phyllotaxis pattern. Notably, these spirals rotate by the golden angle, $\alpha = (3 - \sqrt{5})\pi$ radians, robustly reducing motion artifacts, cf. [82, 61, 52], preserving a uniform readout distribution, which facilitates simple density compensation, and reducing significantly the impact of eddy current, cf. [101]. In our research, we only consider 2D Cartesian sampling and, therefore, do not discuss the methodologies and complexities associated with these other sampling techniques, which are still relevant in many application such as cardiac imaging, eye imaging, and in general on MRI of moving organs, [47, 101, 12, 39, 88, 51].

1.4   Main contributions

In this work, we address both the two key challenges in modern MRI, reconstruction and motion correction, from specific perspectives. In Chapter 4, we present an iterative algorithm designed to compute tuning parameters for the TV-LASSO problem, that is problem (1.14), where Φ is represented by the discrete gradient. In Chapter 5, we introduce a new class of time-frequency representations with
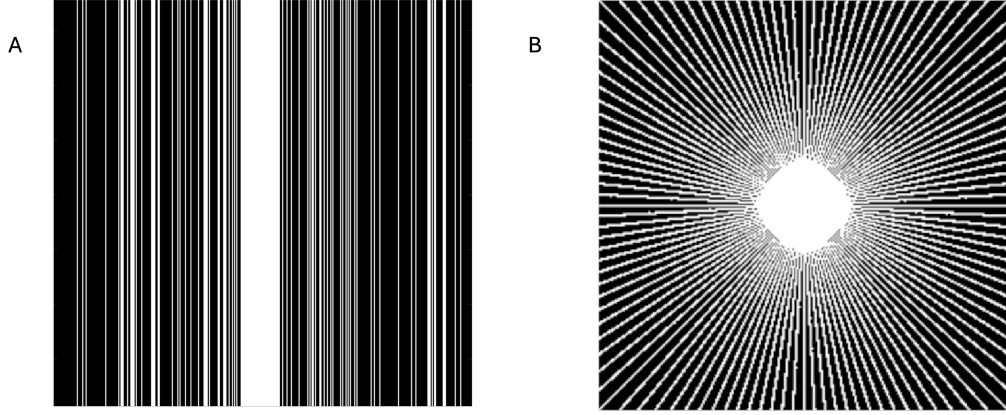
Figure 1.2: MRI 2D sampling trajectories. Cartesian sampling (A) and radial sampling (B).

potential applications in MRI of moving organs. This section delves into the specifics of these findings and explains their significance within the context of MRI.

1.4.1   Tuning parameters

The first major challenge in modern MRI involves performing the reconstruction of MRI data. When employing the generalized LASSO framework, this challenge can be approached from three primary angles:

- Designing sampling patterns.

- Defining appropriate regularization functions.

- Automatically selecting optimal tuning parameters.

In this work, we focus on the third aspect.

The equivalence between (1.11) and (1.12) requires the a-priori knowledge either of the upper-bound η or the Lagrange multiplier λ. To have insights on this relation, in Chapter 3, we studied it for a weighted LASSO problem, a case where computations can be performed directly. This information is difficult to obtain in the practice and these problems are usually interpreted as bi-criterion optimization problems. Moreover, the question was still open whether Lagrange multipliers yield to solutions of (1.13) presenting some degree of sparsity. Let us delve into the bi-criterion interpretation of (1.13). For a given image vector x, the generalized LASSO consists of minimizing the sum of two terms: the *fidelity* $\|Ax - b\|_2$ quantifies the distance between the noisy undersampled measurements b, acquired across channels, and the model Ax; and the *regularization* $\|\Phi x\|_1$

Figure 1.3: The choice of λ in (1.13) affects the quality of the reconstructions. When $\lambda \ll 1$, the reconstructions are noisy and exhibit artifact bias. Conversely, when $\lambda \gg 1$, the reconstructions are overly smooth.

measures the sparsity of Φx. Images satisfying $Ax = b$ (i.e., $\|Ax - b\|_2 = 0$) tend to be noisy and corrupted by a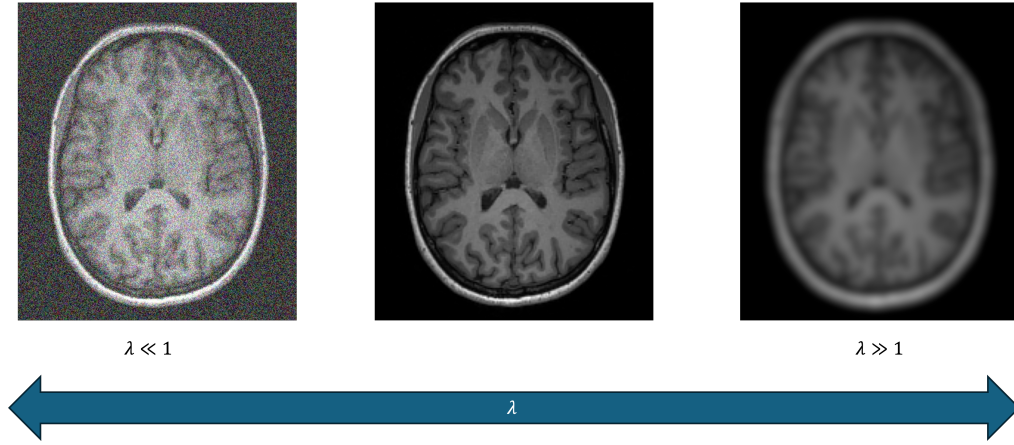rtifacts due to undersampling. Thus, the fidelity term should be minimized but not to the extent of strictly adhering to the measurements, to prevent biased reconstructions. Similarly, $\|\Phi x\|_1$ is minimized when $x \in \ker(\Phi)$. For instance, if $\Phi = D$ represents the discrete gradient, then $\|\Phi x\|_1 = 0$ for any constant vector x. Therefore, the regularization term should be small enough to promote sparsity, but not too small, to avoid overly smooth or inaccurate reconstructions. The first main subject of this work involves the choice of the parameter $\lambda > 0$, which acts as a trade-off between fidelity and regularization (see Fig. 1.3). Namely, when λ is small,

$$\|Ax - b\|_2^2 + \lambda \|\Phi x\|_1 \approx \|Ax - b\|_2^2,$$

resulting in a noisy solution to (1.13). Conversely, when λ is large, $\|\Phi x\|_1$ must be small to keep $\lambda \|\Phi x\|_1$ small, leading to a reconstruction with poor resolution.

Therefore, the selection of the tuning parameter λ significantly affects the denoising and artifact removal effectiveness of (1.14). However, λ is still chosen manually, despite the extensive literature in this direction, since no effective, automatic and general procedure has been proposed yet, lengthening the MRI post-processing. In this work, we formulate ALMA (Algorithm for Lagrange Multipliers Approximation), synthesised in Figure 1.4, an iterative algorithm to approximate the Lagrange multipliers of TV-regularized LASSO and we prove that the obtained approximate Lagrange multipliers can be used to retrieve MR images.

We evaluate the quality of the retrieved images using three quantitative metrics. The multiscale structural similarity index (mSSIM) is employed to assess
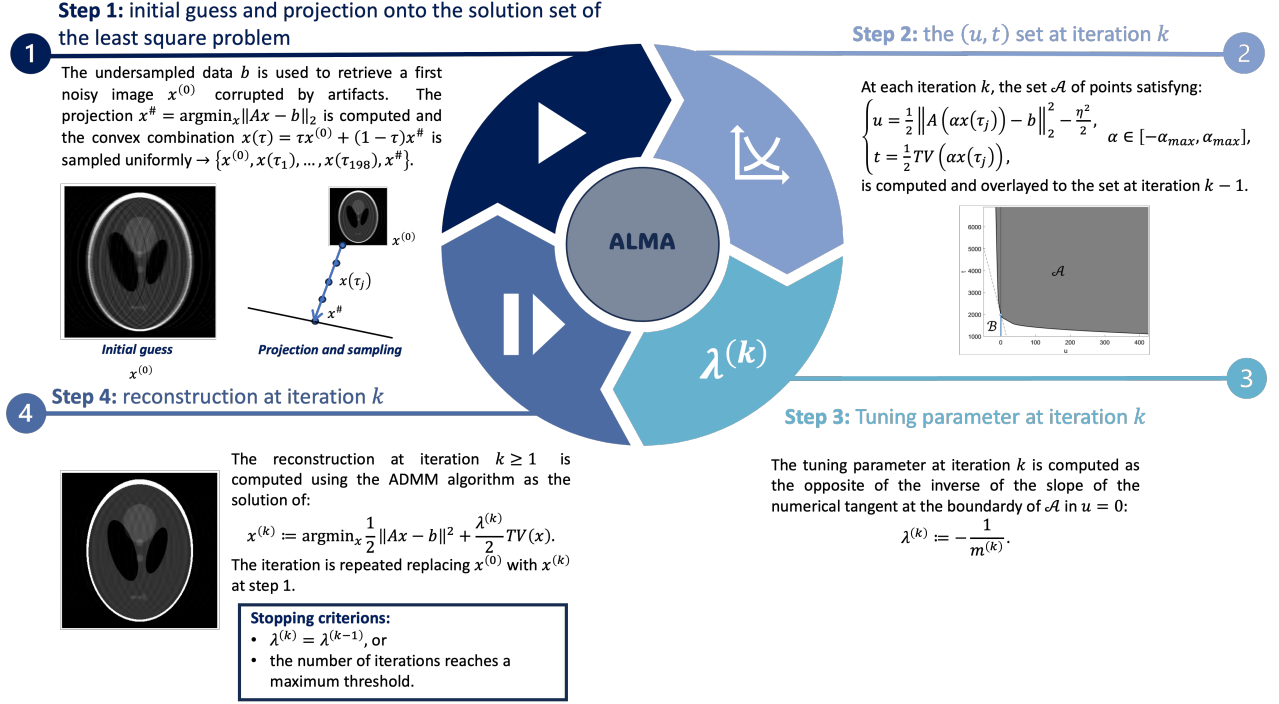
Figure 1.4: A schematic representation of ALMA.

reconstruction quality across various scales, approximating human visual perception [122, 38]. The peak Signal-to-Noise Ratio (pSNR) quantifies noise corruption in compressed images, independent of human visual quality [1]. Finally, the Coefficient of Joint Variation (CJV) measures the presence of intensity non-uniformity (INU) artifacts in MRI images [83, 55].

ALMA was tested using the Shepp-Logan brain phantom, (see figure 1.5 below), with its discrete Fourier transform corrupted by artificial noise and sampled below the Nyquist frequency. For comparison, Figure 1.6 displays an example of reconstruction using the tuning parameter approximated by ALMA, that we called Approximate Lagrange Multipliers (ALM), alongside the reconstruction using the parameter determined by the classical L-curve method. The performance of the ALM is comparable to that of the L-curve method. However, the L-curve method is not iterative and requires reconstructions for numerous tuning parameters, unlike ALMA.

1.4.2 Time-frequency analysis

As detailed above, motion during MRI acquisition causes artifacts. The main sources of motion in MRI are gathered into two groups. Bulk motion, consisting of rototranslations of the organ that is being imaged, and is mostly caused by

Figure 1.5: The Shepp-Logan brain phantom.

patient movement, and organ motion, such as cardiac, respiratory and eye motion, [118]. These movements cannot be always modeled as linear transformations and consequently corrected exploiting the well-known intertwining relation between the Fourier transform and rescalings.

Consequently, strategies are needed to address time-evolving signals for both time-wise analysis of MRI signals and correction of motion artifacts. Time-frequency analysis provides a robust framework for addressing these challenges by offering tools that can simultaneously represent the temporal and spectral characteristics of signals. As a branch of Fourier analysis, it stands at the intersection between harmonic analysis, engineering, (audio, video, radar) signal processing, and medical imaging [8, 96].

The *global nature* of the Fourier transform limits its ability to localize signals in time, making it poorly suited for such time-wise analysis of distributions. Specifically, the inversion formula of the Fourier transform:

$$f(x) = \int_{\mathbb{R}^d} \hat{f}(\xi) e^{2\pi i \xi \cdot x} d\xi, \qquad f \in \mathcal{S}(\mathbb{R}^d),$$

tells that (almost) every frequency of f is needed to retrieve the value of the signal f at time x. This loss of local information highlights the inadequacy of this operator to describe the evolution of time-varying signals. In fact, the concept of *local frequencies* remains ambiguous, and the Fourier transform alone is insufficient for defining what local frequencies should be. This fact is mathematically quantified by the so-called *uncertainty principles*, which emerge whenever a meaningful definition of *localization* is given. The idea of an instantaneous frequency, essentially the frequency of a signal at a specific point in time, poses therefore significant challenges. The uncertainty principles highlight a critical
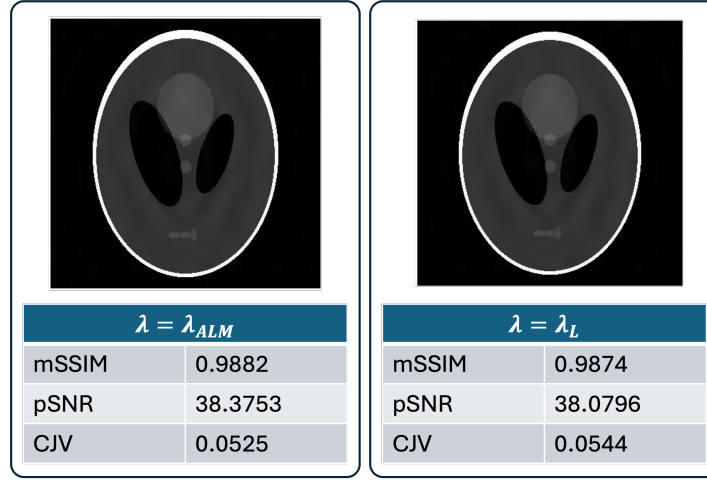
$\lambda = \lambda_{ALM}$	
mSSIM	0.9882
pSNR	38.3753
CJV	0.0525

$\lambda = \lambda_L$	
mSSIM	0.9874
pSNR	38.0796
CJV	0.0544

Figure 1.6: An example of reconstruction with the approximate Lagrange multiplier returned by ALMA, λ_{ALM} and with the L-curve parameter λ_L, the quality of each reconstruction is assessed by means of the mSSIM, the pSNR and the CJV, and the measurements are reported below the reconstructions.

point: attempting to define or measure instantaneous frequencies without considering the context of time localization is fundamentally flawed. This is because the uncertainty principles quantify the inherent trade-offs between the precision of time and frequency localizations and reveal how it is essential first to localize the signal in time to gain meaningful insights into the local frequency content of a signal. This localization allows us to analyze the frequency components over short intervals, rather than at an instantaneous point, thereby respecting the constraints imposed by the uncertainty principles. This is the idea behind the definition of the *short-time Fourier transform*, hereafter shortened as STFT. Consider a *window* function $g \in L^2(\mathbb{R}^d) \setminus \{0\}$, such as a cut-off function centered at the origin, and a signal $f \in L^2(\mathbb{R}^d)$. To localize f around a specific time $x \in \mathbb{R}^d$, we translate g around x and multiply f by $T_x\bar{g}$, the translation of the complex conjugate of g, see fig. 1.7. The use of the complex conjugate has an analytical justification. The resulting function $f \cdot T_x\bar{g}$ represents a *localization of f around x*. By taking the Fourier transform $\mathcal{F}(f \cdot T_x\bar{g})$, we obtain the frequency content of the localization of f. This allows us to interpret these frequencies as the local frequency components of f at the point x.

Specifically, the STFT of $f \in L^2(\mathbb{R}^d)$ with respect to $g \in L^2(\mathbb{R}^d)$ is the function:

$$V_g f(x, \xi) = \int_{\mathbb{R}^d} f(t)\overline{g(t-x)}e^{-2\pi i \xi \cdot t} dt, \qquad x, \xi \in \mathbb{R}^d. \qquad (1.20)$$

The operators $g \mapsto \pi(x, \xi)g(t) = e^{2\pi i \xi \cdot t}g(t-x)$ are called *time-frequency shift*. Denoting by $\langle \cdot, \cdot \rangle$ the unique extension of the sesquilinear inner product of $L^2(\mathbb{R}^d)$ to a duality pairing $\mathcal{S}' \times \mathcal{S}$ (antilinear in the second component), (1.20) extends
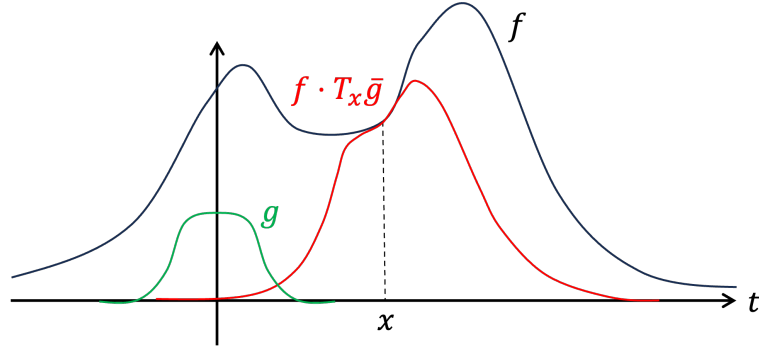
Figure 1.7: The localization of the signal f by means of the window g around the time x.

to $(f,g) \in \mathcal{S}'(\mathbb{R}^d) \times \mathcal{S}(\mathbb{R}^d)$ as:

$$V_g f(x,\xi) = \langle f, \pi(x,\xi)g \rangle, \qquad x,\xi \in \mathbb{R}^d. \tag{1.21}$$

The main properties of the STFT can be found in any time-frequency analysis standard reference book, see e.g., [65, 29].

The short-time Fourier transform can be used to measure the *local time-frequency content* of signals, i.e., the local L^p integrability of f, the local L^q integrability of $\hat{f}$ and their growth - or decay - in the phase space. For fixed $0 < p,q \leq \infty$, $g \in \mathcal{S}(\mathbb{R}^d) \setminus \{0\}$ and v-moderate weight $m \in \mathcal{M}_v(\mathbb{R}^{2d})$ [3], the weighted mixed Lebesgue (quasi-)norm of $V_g f$:

$$\|V_g f\|_{L_m^{p,q}} = \left\| y \mapsto \|m(\cdot,y)V_g f(\cdot,y)\|_p \right\|_q,$$

define (quasi-)norms on subspaces of $\mathcal{S}'(\mathbb{R}^d)$, called *modulation spaces*, see fig. 1.8. Namely,

$$M_m^{p,q}(\mathbb{R}^d) = \left\{ f \in \mathcal{S}'(\mathbb{R}^d) : \|f\|_{M_m^{p,q}} := \|V_g f\|_{L_m^{p,q}} < \infty \right\}.$$

If $p = q$, we write $M^p = M^{p,p}$, and if $m = 1$ we write $M^{p,q} = M_1^{p,q}$.

Different windows g define equivalent (quasi-)norms. Modulation spaces were first introduced by Feichtinger in [44] for $1 \leq p,q \leq \infty$ and later extended to the quasi-Banach setting by Galperin and Samarah in [54]. A large part of this work involves *metaplectic operators*. In time-frequency analysis, metaplectic operators play a crucial role as they are unitary operators on the Hilbert space $L^2(\mathbb{R}^d)$ that generalize the Fourier transform and preserve the structure of modulation spaces.

---

[3] A weight function $v : \mathbb{R}^{2d} \to [0,+\infty)$ is *submultiplicative* if $v(x+y) \leq v(x)v(y)$ for every $x,y \in \mathbb{R}^{2d}$. A weight function $m : \mathbb{R}^{2d} \to [0,+\infty)$ is v-moderate, and we write $m \in \mathcal{M}_v(\mathbb{R}^{2d})$ if $m(x+y) \lesssim v(x)m(y)$. We refer to [64] as an exhaustive source about weight functions and their deployment in time-frequency analysis.
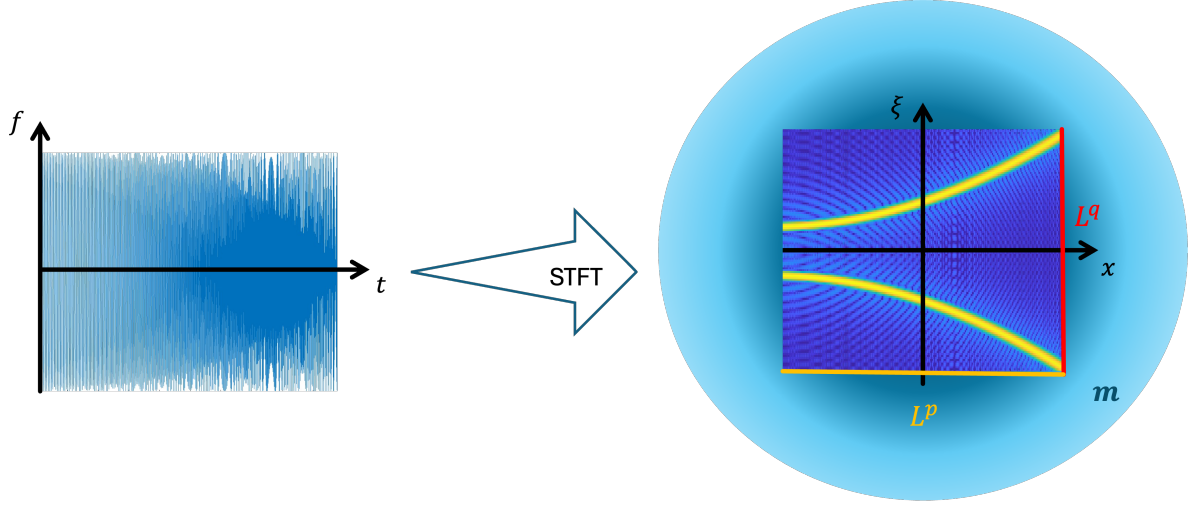
Figure 1.8: Using weighted mixed-norm Lebesgue spaces to measure local time-frequency content of signals. The local L^p integrability of f and the local L^q integrability of $\hat{f}$ is measured by the global $L^{p,q}$ integrability of $V_g f$, the weight m measures the growth, or decay, of $V_g f$.

These operators are closely related to the symplectic group $\mathrm{Sp}(2n, \mathbb{R})$, which consists of matrices $S \in \mathbb{R}^{2d \times 2d}$ with block decompositions

$$S = \begin{pmatrix} A & B \\ C & D \end{pmatrix}, \qquad A, B, C, D \in \mathbb{R}^{d \times d}$$

satisfying:

$$\begin{cases} A^T C = C^T A, \\ B^T D = D^T B, \\ A^T D - C^T B = I_{d \times d}. \end{cases}$$

We write $S \in \mathrm{Sp}(d, \mathbb{R})$. For a given symplectic matrix $S \in \mathrm{Sp}(d, \mathbb{R})$ there exists a unitary operator $\hat{S} : L^2(\mathbb{R}^d) \to L^2(\mathbb{R}^d)$ such that:

$$\hat{S}\pi(x, \xi)\hat{S}^{-1} = c_S \pi(S(x, \xi)), \qquad x, \xi \in \mathbb{R}^d,$$

for $c_S \in \mathbb{C}$, $|c_S| = 1$. The matrix S does not determine the metaplectic operator $\hat{S}$ uniquely, however $\{\hat{S} : S \in \mathrm{Sp}(d, \mathbb{R})\}$ has a subgroup, denoted by $\mathrm{Mp}(d, \mathbb{R})$, containing precisely two such operators for every $S \in \mathrm{Sp}(d, \mathbb{R})$. The projection $\pi^{Mp}(\hat{S}) := S$ is a group homomorphism with kernel $\ker(\pi^{Mp}) = \{\pm I_{L^2}\}$ and the symplectic projection of certain metaplectic operators is known, see table 1.9.

The restrictions of metaplectic operators to $\mathcal{S}(\mathbb{R}^d)$ are homeomorphisms of $\mathcal{S}(\mathbb{R}^d)$, and the extension of any $\hat{S} \in \mathrm{Mp}(d, \mathbb{R})$ to $\mathcal{S}'(\mathbb{R}^d)$, given by

$$\langle \hat{S}f, g \rangle = \langle f, \hat{S}^{-1}g \rangle, \qquad f, g \in \mathcal{S}'(\mathbb{R}^d),$$

Metaplectic operator	Associated symplectic projection
Fourier transform, $\mathcal{F} = i^{-d/2}(\cdot)^{\wedge}$	$J = \begin{pmatrix} 0_{d\times d} & I_{d\times d} \\ -I_{d\times d} & 0_{d\times d} \end{pmatrix}$
Chirp-products, $\mathfrak{p}_Q f(t) = e^{i\pi Qt\cdot t} f(t)$, $Q^T = Q$	$V_Q = \begin{pmatrix} I_{d\times d} & 0_{d\times d} \\ Q & I_{d\times d} \end{pmatrix}$
Rescalings, $\mathfrak{T}_L f(t) = i^m |\det(L)|^{1/2} f(Lt)$, $L \in \mathrm{GL}(d,\mathbb{R})$	$\mathcal{D}_L = \begin{pmatrix} L^{-1} & 0_{d\times d} \\ 0_{d\times d} & L^T \end{pmatrix}$
Multipliers, $\mathfrak{m}_P f = \mathcal{F}^{-1}(e^{i\pi Pu\cdot u}\hat{f})$, $P^T = P$	$U_P = V_P^T = \begin{pmatrix} I_{d\times d} & P \\ 0_{d\times d} & I_{d\times d} \end{pmatrix}$

Figure 1.9: The symplectic projections of certain metaplectic operators. Observe that the projection of the Fourier transform is the matrix of the canonical symplectic form of $\mathbb{C}^d$.

defines a homeomorphism of $\mathcal{S}'(\mathbb{R}^d)$.

Formulas (1.20) and (1.21) can be further generalized by means of metaplectic operators to allow $f, g \in \mathcal{S}'(\mathbb{R}^d)$. Let us consider the partial Fourier transform with respect to the frequency variables:

$$\mathcal{F}_2 F(x, \xi) = \int_{\mathbb{R}^d} F(x, y) e^{-2\pi i y \cdot \xi} dy, \qquad F \in \mathcal{S}(\mathbb{R}^{2d}),$$

and the rescaling $\mathfrak{T}_{L_{st}}$, where

$$L_{ST} = \begin{pmatrix} 0_{d\times d} & I_{d\times d} \\ -I_{d\times d} & I_{d\times d} \end{pmatrix},$$

then:

$$V_g f = \mathcal{F}_2 \mathfrak{T}_{L_{st}}(f \otimes \bar{g}), \qquad f, g \in \mathcal{S}'(\mathbb{R}^d)$$

is the unique extension of the STFT to $\mathcal{S}'(\mathbb{R}^d) \times \mathcal{S}'(\mathbb{R}^d)$. Since $\mathcal{F}_2$ is a metaplectic operator in $\mathrm{Sp}(2d, \mathbb{R})$ with projection:

$$A_{FT2} = \begin{pmatrix} I_{d\times d} & 0_{d\times d} & 0_{d\times d} & 0_{d\times d} \\ 0_{d\times d} & 0_{d\times d} & 0_{d\times d} & I_{d\times d} \\ 0_{d\times d} & 0_{d\times d} & I_{d\times d} & 0_{d\times d} \\ 0_{d\times d} & -I_{d\times d} & 0_{d\times d} & 0_{d\times d} \end{pmatrix},$$

$\mathcal{F}_2 \mathfrak{T}_{L_{ST}}$ is a metaplectic operator in $\mathrm{Mp}(2d, \mathbb{R})$ with symplectic projection having $d \times d$ block decomposition:

$$A_{ST} = \begin{pmatrix} I_{d\times d} & -I_{d\times d} & 0_{d\times d} & 0_{d\times d} \\ 0_{d\times d} & 0_{d\times d} & I_{d\times d} & I_{d\times d} \\ 0_{d\times d} & 0_{d\times d} & 0_{d\times d} & -I_{d\times d} \\ -I_{d\times d} & 0_{d\times d} & 0_{d\times d} & 0_{d\times d} \end{pmatrix}.$$

Along the STFT, other time-frequency representations can be found in the literature. The (cross-)τ-Wigner distributions, defined for $\tau \in \mathbb{R}$ as

$$W_\tau(f,g) = \mathcal{F}_2 \mathfrak{T}_{L_\tau}(f \otimes \bar{g}), \qquad f,g \in \mathcal{S}'(\mathbb{R}^d),$$

where

$$L_\tau = \begin{pmatrix} I_{d \times d} & \tau I_{d \times d} \\ I_{d \times d} & -(1-\tau)I_{d \times d} \end{pmatrix},$$

generalize both the classical *(cross-)Wigner distribution*, given for $f,g \in L^2(\mathbb{R}^d)$ by:

$$W(f,g)(x,\xi) = W_{1/2}(f,g)(x,\xi) = \int_{\mathbb{R}^d} f(x+t/2)\overline{g(x-t/2)}e^{-2\pi i \xi \cdot t}dt, \quad (1.22)$$

$x, \xi \in \mathbb{R}^d$, and the *(cross-)Rihacek distribution*, defined for $f,g \in \mathcal{S}(\mathbb{R}^d)$ by:

$$W_0(f,g)(x,\xi) = f(x)\overline{\hat{g}(\xi)}e^{-2\pi i \xi \cdot x}, \qquad x, \xi \in \mathbb{R}^d,$$

corresponding to the cases $\tau = 1/2$ and $\tau = 0$ respectively. The associated projections define a one-parameter family of symplectic matrices:

$$\mathcal{A}_\tau = \begin{pmatrix} (1-\tau)I_{d \times d} & \tau I_{d \times d} & 0_{d \times d} & 0_{d \times d} \\ 0_{d \times d} & 0_{d \times d} & \tau I_{d \times d} & -(1-\tau)I_{d \times d} \\ 0_{d \times d} & 0_{d \times d} & I_{d \times d} & I_{d \times d} \\ -I_{d \times d} & I_{d \times d} & 0_{d \times d} & 0_{d \times d} \end{pmatrix}.$$

The idea of employ metaplectic operators in the generalization of time-frequency representations such as the STFT and the Wigner distribution stemmed in 2012. In [3], the authors propose to replace the factor $e^{-2\pi i \xi \cdot t}$ in (1.22) with the kernel of metaplectic operators with free symplectic projections. A wider generalization was obtained in [128]. Parallel to these works, matrix Wigner distributions (that in this work are called *totally Wigner-decomposable metaplectic Wigner distributions*) were defined in [32]. Carried to extremes, a possible generalization of all of these distributions can be defined by means of metaplectic operators:

Definition 1.5. Let $\hat{\mathcal{A}} \in \mathrm{Mp}(2d,\mathbb{R})$. The *metaplectic Wigner distribution* associated to $\hat{\mathcal{A}}$ is the time-frequency representation:

$$W_{\mathcal{A}}(f,g) = \hat{\mathcal{A}}(f \otimes \bar{g}), \qquad f,g \in L^2(\mathbb{R}^d).$$

A fascinating question that arises naturally when defining a time-frequency representations $W_{\mathcal{A}}$ by letting the metapletic operator $\hat{\mathcal{A}}$ act on tensor products is how the properties of $W_{\mathcal{A}}$ are related to the symplectic projection

$$\mathcal{A} = \begin{pmatrix} A_{11} & A_{12} & A_{13} & A_{14} \\ A_{21} & A_{22} & A_{23} & A_{24} \\ A_{31} & A_{32} & A_{33} & A_{34} \\ A_{41} & A_{42} & A_{43} & A_{44} \end{pmatrix}, \qquad A_{i,j} \in \mathbb{R}^{d \times d}, \; i,j = 1,\dots,4. \quad (1.23)$$

In our works, we studied which metaplectic Wigner distributions can be used to measure local time-frequency content and which are generalized spectrograms. Modulation spaces are classically defined using the STFT, but every τ-Wigner distribution ($\tau \neq 0, 1$) satisfies:

$$\|W_\tau(f,g)\|_{L_m^{p,q}} \asymp \|f\|_{M_m^{p,q}}, \qquad f \in M_m^{p,q}(\mathbb{R}^d),$$

for $g \in \mathcal{S}(\mathbb{R}^d) \setminus \{0\}$ fixed. For $\tau = 0, 1$ this property fails, for instance:

$$\|W_0(f,g)\|_p = \|f\|_p \|\hat{g}\|_p \not\asymp \|f\|_{M^p}.$$

The question arises which metaplectic Wigner distributions can be used to measure local time-frequency concentration of signals or, stated differently, which metaplectic Wigner distributions satisfy:

$$\|W_{\mathcal{A}}(f,g)\|_{L_m^{p,q}} \asymp \|f\|_{M_m^{p,q}}, \qquad f \in M_m^{p,q}(\mathbb{R}^d). \tag{1.24}$$

The following inequalities, that can be found in [31, Theorem 2.22], tell that if $E_{\mathcal{A}} \in \mathrm{GL}(d, \mathbb{R})$, then:

$$\|f\|_{M^p} \lesssim \||W_{\mathcal{A}}(f,g_1) * W_{\mathcal{A}}(g_1,g_2)|(-E_{\mathcal{A}}\cdot)|\|_p \leq \|W_{\mathcal{A}}(f,g_1)\|_p \|W_{\mathcal{A}}(g_1,g_2)\|_1.$$

That is,

$$\|f\|_{M^p} \lesssim \|W_{\mathcal{A}}(f,g_1)\|_p,$$

one of the two inequalities of the equivalence $\|f\|_{M^p} \asymp \|W_{\mathcal{A}}(f,g_1)\|_p$.

Therefore, Cordero and Rodino conjecture that the condition $E_{\mathcal{A}} \in \mathrm{GL}(d, \mathbb{R})$ is fundamental in describing modulation spaces by means of metaplectic Wigner distributions, and they formulate the definition of *shift-invertibility*.

Definition 1.6. A metaplectic Wigner distribution $W_{\mathcal{A}}$ is *shift-invertible* if the submatrix:

$$E_{\mathcal{A}} = \begin{pmatrix} A_{11} & A_{13} \\ A_{21} & A_{23} \end{pmatrix} \tag{1.25}$$

is invertible.

With an abuse of notation, we say that $\mathcal{A}$ or $\hat{\mathcal{A}}$ are shift-invertible if $W_{\mathcal{A}}$ is shift-invertible.

Theorem 1.7. *Let $0 < p, q \leq \infty$, $W_{\mathcal{A}}$ be a metaplectic Wigner distribution. $W_{\mathcal{A}}$ is shift-invertible if and only if there exist $E \in \mathrm{GL}(2d, \mathbb{R})$, $C \in \mathrm{Sym}(2d, \mathbb{R})$ and $\hat{\delta} \in \mathrm{Mp}(d, \mathbb{R})$ so that:*

$$W_{\mathcal{A}}(f,g)(z) = |\det(E)|^{1/2} e^{i\pi E^T C E z \cdot z} V_{\hat{\delta}g} f(Ez), \qquad z \in \mathbb{R}^{2d}, \tag{1.26}$$

for every $f, g \in L^2(\mathbb{R}^d)$. Moreover, $E = E_{\mathcal{A}}^{-1}$.
Consequently,

(i) If $W_\mathcal{A}$ is shift-invertible, $A_{21} = 0_{d \times d}$ and $m \asymp m \circ E_\mathcal{A}$, then (1.24) holds for every $0 < p, q \leq \infty$. If $p = q$ the condition on A_{21} can be dropped.
(ii) If $W_\mathcal{A}$ is not shift-invertible, then:

$$M^p(\mathbb{R}^d) \neq \left\{ f \in \mathcal{S}'(\mathbb{R}^d) : \|W_\mathcal{A}(f, g)\|_p < \infty \right\}$$

for every $0 < p \leq \infty$, $p \neq 2$.

In this thesis, we trace the story of Theorem 1.7, that was proved between 2022 and 2023 in a series of works with Cordero and Rodino. Namely, Chapter 5 contains [23], where we started considering the particular case of what we called metaplectic Wigner distributions *of the classic type*. These distributions are in the form:

$$W_\mathcal{A}(f, g) = \mathcal{F}_2 \mathfrak{T}_L(f \otimes \bar{g}), \qquad f, g \in L^2(\mathbb{R}^d),$$

for some $L \in \mathrm{GL}(2d, \mathbb{R})$.

Thanks to the rsults in [53], where the boundedness of linear rescalings $f \mapsto f \circ L$ on $L_m^{p,q}$ is characterized by means of a block-diagonality condition on E, we were able to prove Theorem 1.7 without knowing (1.26), in the Banach case $1 \leq p, q \leq \infty$, as outlined in Chapter 6, which contains [19].

Incidentally, while studying metaplectic Gabor frames in [20], we ran into the characterization of shift-invertible metaplectic Wigner distributions by means of the STFT, which yield to a straighforward proof of Theorem 1.7 covering the entire quasi-Banach setting $0 < p, q \leq \infty$, see Chapter 7 for the details.

Theorem 1.7 can be interpreted as a relation between the property of being shift-invertible, related to the blocks (1.23) of the projection $\mathcal{A}$, and the property of measuring local time-frequency content. Similar statements can be formulated in a similar fashion for covariance, for the Cohen's class and for the class of generalized spectrograms, as pointed out in [30, 31, 22].

1.5   Thesis outline

The remainder of this thesis is organized as follows. We gathered in Chapter 2 the main notation and prerequisites. Chapter 3 is dedicated to the theoretical study of tuning parameters for LASSO problems. We use convex analysis techniques to gain insights into the relationship between these parameters and concrete estimates, such as noise energy estimates. Specifically, we examine the framework of the weighted LASSO, where explicit computations can be performed. However, when more general regularizations are considered, numerical methods are required to determine the tuning parameters explicitly. While asymptotic estimates of tuning parameters are available for cases involving significant noise corruption, this is not the situation in MRI, where the contaminating noise is only a small fraction of the total energy content.

In Chapter 4, we study our algorithm designed to approximate tuning parameters in a MRI framework. We test it on TV-LASSO, retrieving the 2D Shepp-Logan brain phantom, which is piecewise constant and, therefore, sparse with respect to total variation. We retrace the creation of the dataset, obtained by adding artificial white noise to the undersampled Fourier transform of the phantom. We assess the performance of ALMA quantitatively via mSSIM, pSNR and CJV and draw our conclusions. In particular, we observe that ALMA has the potential to be applied to different sampling patterns, such as radial, spiral, and higher noise levels.

The following chapters retrace the history of the research on shift-invertibility. In Chapter 5 we study decomposable metaplectic Wigner distribution, characterizing which of these representations is suited for measuring local time-frequency content of signals, this chapter is immersed in the framework of Wigner analysis of operators, a topic that we developed in subsequent works with Cordero, Pucci, Rodino and Valenzano. In Chapter 6, we use standard analysis to prove that shift-invertible distributions do characterize modulation spaces (and some Wiener amalgam space) in the Banach framework, and provide concrete non-trivial examples of metaplectic Wigner distributions having this property. Finally, in Chapter 7, we characterize definitively all the metaplectic Wigner distributions that define modulation spaces, from two different aspects: the form of the corresponding symplectic projection and the form of the distribution itself, which is revealed to be a rescaled short-time Fourier transform. Metaplectic Gabor frames are analyzed and the discrete representation of modulation spaces is retrieved.

Finally, we draw the conclusions and discuss further research directions in Chapter 8.

Prerequisites and notation

In this chapter, we introduce the main notation that will be used throughout this work. Minor notation will be introduced across each chapter. The content of this chapter can be found in [5, 44, 43, 65, 54, 79, 49, 11, 112, 45, 107].

2.1 Linear algebra

2.1.1 Vector notation

We denote by $\mathbb{R}^d$ the real vector space of dimension d, endowed with the canonical basis $e_1, \ldots, e_d$, unless stated otherwise. If $x, y \in \mathbb{R}^d$, $x \cdot y = \langle x, y \rangle = \sum_{j=1}^d x_j y_j$ denotes the inner product between x and y. If $L \subseteq \mathbb{R}^d$ is a linear subspace of $\mathbb{R}^d$, $L^\perp$ denotes its orthogonal complement. Moreover, we write $x \preceq y$ if $x_j \leq y_j$ for every $j = 1, \ldots, d$. The symbol $\succeq$ is used similarly. If $x \in \mathbb{R}^d$, we denote by x_j $(j = 1, \ldots, d)$ the j-th coordinate of x. Also, x^+ is the positive part of x, i.e., the vector with coordinates $(x^+)_j = \max\{0, x_j\}$. We denote with $\mathcal{M}_d$ the family of all the signature matrices, that are the diagonal matrices

$$S = \begin{pmatrix} \lambda_1 & \ldots & 0 \\ \vdots & \ddots & \vdots \\ 0 & \ldots & \lambda_d \end{pmatrix}$$

with $|\lambda_j| = 1$ for every $j = 1, \ldots, d$. Moreover, $\mathrm{sgn}(x) = \{S \in \mathcal{M}_d : Sx \succeq 0\}$. Observe that if $S \in \mathcal{M}_d$, then $S^2 = I_{d \times d}$, and consequently $S^{-1} = S$.

For $0 < p < \infty$,

$$\|x\|_p := \left(\sum_{j=1}^d |x_j|^p \right)^{1/p}, \qquad x \in \mathbb{R}^d,$$

is the p-norm of x. Moreover,

$$\|x\|_\infty = \max_{j=1,\ldots,d} |x_j|.$$

Similar notation will be used for the d-dimensional complex space $\mathbb{C}^d$, with standard inner product $zw = \sum_{j=1}^{d} z_j \overline{w_j}$, the bar denoting the complex conjugation.

2.1.2 Matrix notation

We denote by $\mathbb{R}^{r \times d}$ the space of $r \times d$ matrices with real entries. $I_{d \times d}$ and $0_{r \times d}$ denote the $d \times d$ identity matrix and the $r \times d$ matrix with all zero entries, respectively.

If $M \in \mathbb{R}^{r \times d}$, M^T denotes its conjugate, $\ker(M)$ denotes its kernel, $\Im(M)$ denotes its range, and $\mathrm{rank}(M)$ denotes its rank. If $M \in \mathbb{R}^{d \times d}$, $\det(M)$ denotes the determinant of M.

We denote by $\mathrm{GL}(d, \mathbb{R})$ the space of $d \times d$ invertible matrices. We denote by $\mathrm{Sym}(d, \mathbb{R})$ the space of $d \times d$ symmetric matrices, i.e., $M \in \mathrm{Sym}(d, \mathbb{R})$ if $M^T = M$.

If $M \in \mathbb{R}^{2d \times 2d}$ has block decomposition:

$$M = \begin{pmatrix} A & B \\ C & D \end{pmatrix},$$

$A, B, C, D \in \mathbb{R}^{d \times d}$, we say that M is upper block triangular if $C = 0_{d \times d}$, lower block triangular if $B = 0_{d \times d}$, and block diagonal if $B = C = 0_{d \times d}$.

2.1.3 Topological notation

We always consider the Euclidean topology on $\mathbb{R}^d$. If $\Omega \subseteq \mathbb{R}^d$, $\mathring{\Omega}$ denotes the set of the interior points of Ω, whereas $\partial \Omega$ denotes its boundary.

2.1.4 Multi-indices

For $\alpha \in \mathbb{N}^d$ and $x \in \mathbb{R}^d$, $x^\alpha = \prod_{j=1}^{d} x_j^{\alpha_j}$. We denote by $|\alpha| = \sum_{j=1}^{d} \alpha_j$. If $f : \mathbb{R}^d \to \mathbb{C}$,

$$D^\alpha f(x) = \frac{\partial^{|\alpha|}}{\partial x_1^{\alpha_1} \ldots \partial x_d^{\alpha_d}} f(x).$$

2.2 Function and distribution spaces

We always consider measurable (with respect to the Lebesgue measure) complex-valued functions on $\mathbb{R}^d$. If g is a function and Ω is a subset of its domain, $g|_\Omega$ denotes the restriction of g to Ω. Finally, if $\Omega \subseteq \mathbb{R}^n$, χ_Ω denotes the characteristic function of Ω. We denote by $\mathcal{C}_0^\infty(\mathbb{R}^d)$ the space of complex-valued smooth functions on $\mathbb{R}^d$. If f, g are functions on $\mathbb{R}^d$, the notation $f \lesssim g$ means that there

exists $C > 0$ such that $f(x) \leq Cg(x)$ for every $x \in \mathbb{R}^d$, whereas $f \asymp g$ means that $C_1 f \leq g \leq C_2 f$ for some $C_1, C_2 > 0$.

2.2.1 Lebesgue spaces

We always consider the Lebesgue measure on $\mathbb{R}^d$, and if $f : \mathbb{R}^d \to \mathbb{C}$ is measurable, and $0 < p < \infty$,

$$\|f\|_p := \left(\int_{\mathbb{R}^d} |f(x)|^p dx \right)^{1/p},$$

were dx denotes the Lebesgue measure on $\mathbb{R}^d$, and

$$\|f\|_\infty = \operatorname*{ess\,sup}_{x \in \mathbb{R}^d} |f(x)|.$$

We denote by $L^p(\mathbb{R}^d)$ the space of p-integrable functions. We denote by

$$\langle f, g \rangle = \int_{\mathbb{R}^d} f(x) \overline{g(x)} dx, \qquad f, g \in L^2(\mathbb{R}^d),$$

the sesquilinear inner product of $L^2(\mathbb{R}^d)$.

2.2.2 Test functions and distributions

We denote by $\mathcal{S}(\mathbb{R}^d)$ the Schwartz space of rapidly decreasing functions, and its topological dual $\mathcal{S}'(\mathbb{R}^d)$ is the space of tempered distributions. We endow $\mathcal{S}(\mathbb{R}^d)$ with the initial topology associated to the seminorms

$$\rho_{\alpha,\beta}(f) = \sup_{x \in \mathbb{R}^d} |x^\alpha D^\beta f(x)|,$$

whereas $\mathcal{S}'(\mathbb{R}^d)$ is endowed with the weak-$*$ topology.

The inner product $\langle \cdot, \cdot \rangle$ of $L^2(\mathbb{R}^d)$ defined above extends uniquely to a duality pairing $\mathcal{S}' \times \mathcal{S}$, antilinear in its second component: if $f \in \mathcal{S}'(\mathbb{R}^d)$,

$$\langle f, \varphi \rangle = f(\bar{\varphi}), \qquad \varphi \in \mathcal{S}(\mathbb{R}^d).$$

We have:

$$\mathcal{S}(\mathbb{R}^d) \hookrightarrow L^p(\mathbb{R}^d) \hookrightarrow \mathcal{S}'(\mathbb{R}^d)$$

for every $0 < p \leq \infty$, and the inclusions are dense if $p \neq \infty$.

For $t \in \mathbb{R}^d$, we denote by δ_t the Dirac delta distribution centered in t, i.e.,

$$\langle \delta_t, \varphi \rangle = \overline{\varphi(t)}, \qquad \varphi \in \mathcal{S}(\mathbb{R}^d).$$

2.2.3 Tensor products

If f, g are complex-valued Lebesgue-measurable functions on $\mathbb{R}^d$, we denote with $f \otimes g$ the function

$$(f \otimes g)(x, y) = f(x)g(y), \quad x, y \in \mathbb{R}^d.$$

We have that $\mathrm{span}\{f \otimes g \ : \ f, g \in \mathcal{S}(\mathbb{R}^d)\}$ is dense in $\mathcal{S}(\mathbb{R}^{2d})$, and $\mathrm{span}\{f \otimes g : f, g \in L^p(\mathbb{R}^d)\}$ is dense in $L^p(\mathbb{R}^d)$, $1 \le p < \infty$.

If $f, g \in \mathcal{S}'(\mathbb{R}^d)$, $f \otimes g$ is defined as the tempered distribution on $\mathbb{R}^{2d}$ such that

$$\langle f \otimes g, \Phi \rangle = \langle f, \langle g, \Phi^x \rangle \rangle = \langle g, \langle f, \Phi^y \rangle \rangle, \quad \Phi \in \mathcal{S}(\mathbb{R}^{2d}),$$

where $\Phi^x = \Phi(x, \cdot)$, $x \in \mathbb{R}^d$, and $\Phi^y = \Phi(\cdot, y)$, $y \in \mathbb{R}^d$, are the sections of Φ. Again, $\mathrm{span}\{f \otimes g \ : \ f, g \in \mathcal{S}'(\mathbb{R}^d)\}$ is dense in $\mathcal{S}'(\mathbb{R}^{2d})$.

2.2.4 Weights

In this work, v is a continuous, positive, submultiplicative weight function on $\mathbb{R}^d$, i.e., $v(z_1 + z_2) \le v(z_1)v(z_2)$, for all $z_1, z_2 \in \mathbb{R}^d$. A weight function m is in $\mathcal{M}_v(\mathbb{R}^d)$ if m is a positive, continuous weight function on $\mathbb{R}^d$ and it is v-*moderate*: $m(z_1 + z_2) \lesssim v(z_1)m(z_2)$. This notation means that there exists a universal constant $C > 0$ such that the inequality $m(z_1 + z_2) \le Cv(z_1)m(z_2)$ holds for all $z_1, z_2 \in \mathbb{R}^d$.

In the following, we will work with weights on $\mathbb{R}^{2d}$ of the type

$$v_s(z) = \langle z \rangle^s = (1 + |z|^2)^{s/2}, \quad z \in \mathbb{R}^d.$$

For $s < 0$, v_s is $v_{|s|}$-moderate.

In particular, we shall use the weight functions on $\mathbb{R}^{4d}$:

$$(v_s \otimes 1)(z, \zeta) = (1 + |z|^2)^{s/2}, \quad (1 \otimes v_s)(z, \zeta) = (1 + |\zeta|^2)^{s/2}, \quad z, \zeta \in \mathbb{R}^{2d}.$$

Two weights m_1, m_2 are equivalent if $m_1 \asymp m_2$. For example, $v_s(z) \asymp (1 + |z|^2)^{s/2}$. We refer to [64] for a comprehensive source about weight functions in time-frequency analysis.

2.2.5 Weighted mixed norm spaces

If $m \in \mathcal{M}_v(\mathbb{R}^{2d})$, $0 < p, q \le \infty$ and $f : \mathbb{R}^{2d} \to \mathbb{C}$ measurable, we set

$$\|f\|_{L_m^{p,q}} := \left(\int_{\mathbb{R}^d} \left(\int_{\mathbb{R}^d} |f(x,y)|^p m(x,y)^p \right)^{q/p} dy \right)^{1/q} = \left\| y \mapsto \|f(\cdot, y)m(\cdot, y)\|_p \right\|_q,$$

with the obvious adjustments when $\min\{p, q\} = \infty$. The space of measurable functions f having $\|f\|_{L_m^{p,q}} < \infty$ is denoted by $L_m^{p,q}(\mathbb{R}^{2d})$. If $m \in \mathcal{M}_v(\mathbb{R}^{2d})$ and $1 \le p, q \le \infty$, then $L_m^{p,q}(\mathbb{R}^{2d}) * L_v^1(\mathbb{R}^{2d}) \hookrightarrow L_m^{p,q}(\mathbb{R}^{2d})$.

2.3   Fourier transforms

The Fourier transform of a function $f \in \mathcal{S}(\mathbb{R}^d)$ is

$$\hat{f}(\xi) = \int_{\mathbb{R}^d} f(x)e^{-2\pi i \xi \cdot x} dx, \qquad \xi \in \mathbb{R}^d.$$

The operator (also called Fourier transform) $\mathcal{F} : f \in \mathcal{S}(\mathbb{R}^d) \to \hat{f} \in \mathcal{S}(\mathbb{R}^d)$ is a homeomorphism, and it extends to a unitary operator on $L^2(\mathbb{R}^d)$, meaning that it is surjective and

$$\langle \hat{f}, \hat{g} \rangle = \langle f, g \rangle, \qquad f, g \in L^2(\mathbb{R}^d).$$

The Fourier transform of $f \in \mathcal{S}'(\mathbb{R}^d)$ is the tempered distribution $\hat{f}$ defined by its action on $\mathcal{S}(\mathbb{R}^d)$ by

$$\langle \hat{f}, \varphi \rangle = \langle f, \mathcal{F}^{-1}\varphi \rangle, \qquad \varphi \in \mathcal{S}(\mathbb{R}^d).$$

The operator $\mathcal{F} : f \in \mathcal{S}'(\mathbb{R}^d) \to \mathcal{S}'(\mathbb{R}^d)$ is a homeomorphism.

If $1 \leq j \leq d$, the *partial Fourier transform* with respect to the jth coordinate is defined as

$$\mathcal{F}_j f(t_1, \ldots, t_{j-1}, \xi_j, t_{j+1} \ldots, t_d) = \int_{-\infty}^{\infty} f(t_1, \ldots, t_d)e^{-2\pi i t_j \xi_j} dt_j, \quad f \in L^1(\mathbb{R}^d).$$

$$(2.1)$$

Analogously, the definition is transported on $\mathcal{S}'(\mathbb{R}^d)$ in terms of antilinear duality pairing: for all $f \in \mathcal{S}'(\mathbb{R}^d)$,

$$\langle \mathcal{F}_j f, \varphi \rangle := \langle f, \mathcal{F}_j^{-1}\varphi \rangle, \qquad \varphi \in \mathcal{S}(\mathbb{R}^d).$$

Observe that $\mathcal{F}_j \mathcal{F}_k = \mathcal{F}_k \mathcal{F}_j$ for all $1 \leq j, k \leq d$. In particular,

$$\mathcal{F} = \mathcal{F}_{\sigma(1)} \circ \ldots \circ \mathcal{F}_{\sigma(d)}$$

holds that for all permutation $\sigma : \{1, \ldots, d\} \to \{1, \ldots, d\}$. Finally, for all $1 \leq j \leq d$,

$$\mathcal{F}_j^2 f(x_1, \ldots, x_d) = f(x_1, \ldots, x_{j-1}, -x_j, x_{j+1}, \ldots, x_d).$$

Moreover, for $F \in \mathcal{S}(\mathbb{R}^{2d})$, the partial Fourier transform with respect to the frequency variables is

$$\mathcal{F}_2 F(x, \xi) = \int_{\mathbb{R}^d} F(x, t)e^{-2\pi i \xi \cdot t} dt, \qquad \xi \in \mathbb{R}^d.$$

The choice of denoting with the symbol $\mathcal{F}_2$ both the partial Fourier transform with respect to the second variable and the partial Fourier transform with respect to the frequency variables shall not cause confusion in this work.

2.4 Tools from time-frequency analysis

For $x, \xi \in \mathbb{R}^d$, we denote with T_x and M_ξ the translation and the modulation operators respectively, i.e., the unitary operators on $L^2(\mathbb{R}^d)$ defined as

$$T_x g(t) = g(t - x), \quad M_\xi g(t) = e^{2\pi i \xi \cdot t} g(t), \quad g \in L^2(\mathbb{R}^d).$$

These operators extend to $\mathcal{S}'(\mathbb{R}^d)$ by setting for $f \in \mathcal{S}'(\mathbb{R}^d)$,

$$\langle T_x f, g \rangle = \langle f, T_{-x} g \rangle, \quad \text{and} \quad \langle M_\xi f, g \rangle = \langle f, M_{-\xi} g \rangle, \qquad g \in \mathcal{S}(\mathbb{R}^d).$$

If $z = (x, \xi) \in \mathbb{R}^{2d}$, the operator

$$\pi(x, \xi) f(t) = M_\xi T_x f(t) = e^{2\pi i \xi \cdot t} f(t - x), \qquad f \in L^2(\mathbb{R}^d) \tag{2.2}$$

is called *time-frequency shift*. Observe that:

$$\pi(z) \pi(w) = e^{-2\pi i x \cdot \eta} \pi(z + w),$$

and

$$\pi(z)^{-1} = \pi(z)^* = e^{-2\pi i x \cdot \xi} \pi(-z). \tag{2.3}$$

for every $z = (x, \xi), w = (y, \eta) \in \mathbb{R}^{2d}$.

2.4.1 The short-time Fourier transform

For a fixed $g \in \mathcal{S}(\mathbb{R}^d) \setminus \{0\}$, the *short-time Fourier transform* (STFT) of $f \in L^2(\mathbb{R}^d)$ is defined as

$$V_g f(x, \xi) = \int_{\mathbb{R}^d} f(t) \overline{g(t - x)} e^{-2\pi i \xi \cdot t} dt, \quad x, \xi \in \mathbb{R}^d.$$

The definition of STFT can be extended to all tempered distributions: fixed $g \in \mathcal{S}(\mathbb{R}^d) \setminus \{0\}$, $f \in \mathcal{S}'(\mathbb{R}^d)$

$$V_g f(x, \xi) = \langle f, \pi(x, \xi) g \rangle.$$

Defined as above, the STFT is a uniformly continuous function on $\mathbb{R}^{2d}$ that grows at most polynomially. In particular $V_g f \in \mathcal{S}'(\mathbb{R}^{2d})$. Finally, it is easy to see that if

$$\mathfrak{T}_{L_{ST}} F(x, t) = F(t, t - x), \qquad F \in \mathcal{S}(\mathbb{R}^{2d}), \quad x, t \in \mathbb{R}^d,$$

then,

$$V_g f = \mathcal{F}_2 \mathfrak{T}_{L_{ST}} (f \otimes \bar{g}),$$

defines a tempered distribution, which extends the STFT to $(f, g) \in \mathcal{S}'(\mathbb{R}^d) \times \mathcal{S}'(\mathbb{R}^d)$. Here, $\mathfrak{T}_{L_{ST}}$ of a tempered distribution f is defined as

$$\langle \mathfrak{T}_{L_{ST}} f, g \rangle = \langle f, \mathfrak{T}_{L_{ST}}^{-1} g \rangle, \qquad g \in \mathcal{S}(\mathbb{R}^d).$$

Similar notation will be used in the up-coming sections.

We will use the fundamental identity of time-frequency analysis: for $f \in \mathcal{S}'(\mathbb{R}^d)$ and $g \in \mathcal{S}(\mathbb{R}^d)$,

$$V_g f(x,\xi) = e^{-2\pi i \xi \cdot x} V_{\hat{g}} \hat{f}(\xi,-x), \qquad x, \xi \in \mathbb{R}^d. \tag{2.4}$$

Moreover, if $f \in L^2(\mathbb{R}^d)$, and $g, \gamma \in L^2(\mathbb{R}^d)$ are such that $\langle \gamma, g \rangle \neq 0$, the following inversion formula holds:

$$f = \frac{1}{\langle \gamma, g \rangle} \int_{\mathbb{R}^{2d}} V_g f(x,\xi) \pi(x,\xi) \gamma \, dx d\xi,$$

where the integral must be interpreted in the weak sense of distributions.

2.4.2 Other time-frequency representations

We will also consider the (cross-)Wigner distribution, which is defined as

$$W(f,g)(x,\xi) = \int_{\mathbb{R}^d} f\left(x + \frac{t}{2}\right) \overline{g\left(x - \frac{t}{2}\right)} dt, \qquad f,g \in L^2(\mathbb{R}^d).$$

If $f = g$, we write $Wf = W(f,f)$, the Wigner distribution of f. Similarly, for $\tau \in \mathbb{R}$, we will consider the (cross-)τ-Wigner distribution

$$W_\tau(f,g)(x,\xi) = \int_{\mathbb{R}^d} f(x + \tau t) \overline{g(x - (1-\tau)t)} dt, \qquad f,g \in L^2(\mathbb{R}^d). \tag{2.5}$$

In particular, we retrieve for $\tau = 0$ the (cross-)RIhacek distribution

$$W_0(f,g)(x,\xi) = f(x) \overline{\hat{g}(\xi)} e^{-2\pi i \xi \cdot x}, \qquad f,g \in \mathcal{S}(\mathbb{R}^d), \quad x, \xi \in \mathbb{R}^d, \tag{2.6}$$

and for $\tau = 1$ the (cross-)conjugate RIhacek distribution

$$W_1(f,g)(x,\xi) = \hat{f}(\xi) \overline{g(x)} e^{2\pi i \xi \cdot x}, \qquad f,g \in \mathcal{S}(\mathbb{R}^d), \quad x, \xi \in \mathbb{R}^d. \tag{2.7}$$

If $f = g$, we write $W_\tau f = W_\tau(f,f)$, the τ-Wigner distribution of f. Observe that the case $\tau = 1/2$ corresponds to the Wigner distribution.

Similarly to the STFT, the τ-Wigner distributions extend to $(f,g) \in \mathcal{S}'(\mathbb{R}^d) \times \mathcal{S}'(\mathbb{R}^d)$ by setting:

$$W_\tau(f,g) = \mathcal{F}_2 \mathfrak{T}_{L_\tau}(f \otimes \bar{g}),$$

where

$$\mathfrak{T}_{L_\tau} F(x,t) = F(x + \tau t, x - (1-\tau)t), \qquad F \in \mathcal{S}(\mathbb{R}^{2d}), \quad x, t \in \mathbb{R}^d.$$

2.4.3   Modulation spaces

Fix $0 < p, q \leq \infty$, $m \in \mathcal{M}_v(\mathbb{R}^{2d})$, and $g \in \mathcal{S}(\mathbb{R}^d) \setminus \{0\}$. The *modulation space* $M_m^{p,q}(\mathbb{R}^d)$ is classically defined as the space of tempered distributions $f \in \mathcal{S}'(\mathbb{R}^d)$ such that

$$\|f\|_{M_m^{p,q}} := \|V_g f\|_{L_m^{p,q}} < \infty.$$

If $p = q$, we write $M_m^{p,p} = M_m^p$, and if $m = 1$, we write $M_m^{p,q} = M^{p,q}$. The space M^1 is known as Feichtinger's algebra, and the spaces $M_{1 \otimes v_s}^{\infty,1}$ are known as Sjöstrand classes. If $\min\{p, q\} \geq 1$, the quantity $\|\cdot\|_{M_m^{p,q}}$ defines a norm, otherwise a quasi-norm. Different windows give rise to equivalent (quasi-)norms. Modulation spaces are (quasi-)Banach spaces and the following continuous inclusions hold: if $0 < p_1 \leq p_2 \leq \infty$, $0 < q_1 \leq q_2 \leq \infty$ and $m_1, m_2 \in \mathcal{M}_v(\mathbb{R}^{2d})$ satisfy $m_2 \lesssim m_1$:

$$\mathcal{S}(\mathbb{R}^d) \hookrightarrow M_{m_1}^{p_1,q_1}(\mathbb{R}^d) \hookrightarrow M_{m_2}^{p_2,q_2}(\mathbb{R}^d) \hookrightarrow \mathcal{S}'(\mathbb{R}^d).$$

In particular, $M_v^1(\mathbb{R}^d) \hookrightarrow M_m^{p,q}(\mathbb{R}^d)$ whenever $m \in \mathcal{M}_v(\mathbb{R}^{2d})$ and $\min\{p, q\} \geq 1$. We will also use the inclusion $M_{m \otimes 1}^1(\mathbb{R}^{2d}) \hookrightarrow L_m^1(\mathbb{R}^{2d})$. We denote with $\mathcal{M}_m^{p,q}(\mathbb{R}^d)$ the closure of $\mathcal{S}(\mathbb{R}^d)$ in $M_m^{p,q}(\mathbb{R}^d)$, which coincides with the latter whenever $p, q < \infty$. Moreover, if $1 \leq p, q < \infty$, $(M_m^{p,q}(\mathbb{R}^d))' = M_{1/m}^{p',q'}(\mathbb{R}^d)$, where p' and q' denote the Lebesgue conjugate exponents of p and q respectively. Finally, if $m_1 \asymp m_2$, then $M_{m_1}^{p,q}(\mathbb{R}^d) = M_{m_2}^{p,q}(\mathbb{R}^d)$ for all p, q.

2.4.4   Wiener amalgam spaces

For $0 < p, q \leq \infty$, and $m_1, m_2 \in \mathcal{M}_v(\mathbb{R}^{2d})$, $W(\mathcal{F}L_{m_1}^p, L_{m_2}^q)(\mathbb{R}^d)$ is the space of tempered distributions $f \in \mathcal{S}'(\mathbb{R}^d)$ such that for some (hence, all) window $g \in \mathcal{S}(\mathbb{R}^d) \setminus \{0\}$,

$$\|f\|_{W(\mathcal{F}L_{m_1}^p, L_{m_2}^q)} := \left\| x \mapsto m_2(x) \|V_g f(x, \cdot) m_1\|_p \right\|_q < \infty.$$

Using (2.4), we have that $\|f\|_{W(\mathcal{F}L_{m_1}^p, L_{m_2}^q)} = \left\| \hat{f} \right\|_{M_{m_1 \otimes m_2}^{p,q}}$, so that

$$\mathcal{F}M_{m_1 \otimes m_2}^{p,q}(\mathbb{R}^d) = W(\mathcal{F}L_{m_2}^p, L_{m_1}^q)(\mathbb{R}^d).$$

Also, for $p = q$,

$$W(\mathcal{F}L_{m_1}^p, L_{m_2}^p)(\mathbb{R}^d) = M_{m_1 \otimes m_2}^p(\mathbb{R}^d). \tag{2.8}$$

2.4.5   Gabor frames

For a fixed $\Lambda \subseteq \mathbb{R}^{2d}$ and $g \in L^2(\mathbb{R}^d)$, the system $\mathcal{G}(g, \Lambda) = \{\pi(\lambda)g\}_{\lambda \in \Lambda}$ is a Gabor frame if there exist $A, B > 0$ such that

$$A \|f\|_2^2 \leq \sum_{\lambda \in \Lambda} |\langle f, \pi(\lambda)g \rangle|^2 \leq B \|f\|_2^2, \qquad f \in L^2(\mathbb{R}^d).$$

Theorem 2.1. *If $\mathcal{G}(g, \Lambda)$, with $g \in \mathcal{S}(\mathbb{R}^d)$, is a Gabor frame, there exists $\gamma \in \mathcal{S}(\mathbb{R}^d)$ such that for every $f \in M_m^{p,q}(\mathbb{R}^d)$,*

$$f = \sum_{\lambda \in \Lambda} \langle f, \pi(\lambda)g \rangle \pi(\lambda)\gamma,$$

where the series is unconditionally convergent in the $M_m^{p,q}$ quasi-norm if $p, q \neq \infty$, and weak-$*$ convergent otherwise. If $p, q \geq 1$, the window can be taken in $M_v^1(\mathbb{R}^d)$.

Proof. See [46]. □

2.5 Symplectic group and metaplectic operators

2.5.1 The Lie group of symplectic matrices

We denote by

$$J = \begin{pmatrix} 0_{d \times d} & I_{d \times d} \\ -I_{d \times d} & 0_{d \times d} \end{pmatrix} \tag{2.9}$$

the matrix that defines the standard symplectic form of $\mathbb{C}^d$. Consider a matrix $S \in \mathbb{R}^{2d \times 2d}$ with block decomposition:

$$S = \begin{pmatrix} A & B \\ C & D \end{pmatrix}, \qquad A, B, C, D \in \mathbb{R}^{d \times d}.$$

We say that S is symplectic, and we write $S \in \mathrm{Sp}(d, \mathbb{R})$ if one of these equivalent conditions holds:
(1) S satisfies

$$S^T J S = J,$$

(2) The blocks of S satisfy

$$\begin{cases} A^T C = C^T A, \\ B^T D = D^T B, \\ A^T D - C^T B = I_{d \times d}, \end{cases} \tag{2.10}$$

(3) The inverse of S has block decomposition

$$S^{-1} = \begin{pmatrix} D^T & -B^T \\ -C^T & A^T \end{pmatrix}.$$

(4) The blocks of S satisfy

$$\begin{cases} DC^T = CD^T, \\ AB^T = BA^T, \\ DA^T - CB^T = I_{d \times d}. \end{cases}$$

The Lie algebra of $\mathrm{Sp}(d, \mathbb{R})$ is denoted by $\mathfrak{sp}(d, \mathbb{R})$.

Example 2.2. (i) The matrix J is trivially symplectic. Observe that $J^{-1} = -J$.
(ii) The matrices

$$V_C = \begin{pmatrix} I_{d\times d} & 0_{d\times d} \\ C & I_{d\times d} \end{pmatrix} \quad and \quad \mathcal{D}_L = \begin{pmatrix} L^{-1} & 0_{d\times d} \\ 0_{d\times d} & L^T \end{pmatrix}, \tag{2.11}$$

for $C \in \mathrm{Sym}(d,\mathbb{R})$ and $L \in \mathrm{GL}(d,\mathbb{R})$ are symplectic. Observe that $V_C^{-1} = V_{-C}$ and $\mathcal{D}_L^{-1} = \mathcal{D}_{L^{-1}}$
(iii) If $S \in \mathrm{Sp}(d,\mathbb{R})$, also $S^T \in \mathrm{Sp}(d,\mathbb{R})$, and in particular every

$$U_C = V_C^T = \begin{pmatrix} I_{d\times d} & C \\ 0_{d\times d} & I_{d\times d} \end{pmatrix}, \qquad C \in \mathrm{Sym}(d,\mathbb{R}),$$

is symplectic. Also, S^{-1} is symplectic.
(iv) For a subset of indices $\mathcal{J} \subseteq \{1,\ldots,d\}$, consider $I_\mathcal{J}$ the diagonal matrix with diagonal entries

$$(I_\mathcal{J})_{jj} = \begin{cases} 1 & \text{if } j \in \mathcal{J}, \\ 0 & \text{otherwise.} \end{cases}$$

If $\mathcal{J} = \{j\}$, we write $\Pi_\mathcal{J} = \Pi_j$. Observe that $\prod_j \Pi_j = J$. The matrix

$$\Pi_\mathcal{J} = \begin{pmatrix} I_{d\times d} - I_\mathcal{J} & I_\mathcal{J} \\ -I_\mathcal{J} & I_{d\times d} - I_\mathcal{J} \end{pmatrix}$$

is symplectic. In particular,

$$\mathcal{A}_{FT2} = \begin{pmatrix} I_{d\times d} & 0_{d\times d} & 0_{d\times d} & 0_{d\times d} \\ 0_{d\times d} & 0_{d\times d} & 0_{d\times d} & I_{d\times d} \\ 0_{d\times d} & 0_{d\times d} & I_{d\times d} & 0_{d\times d} \\ 0_{d\times d} & -I_{d\times d} & 0_{d\times d} & 0_{d\times d} \end{pmatrix} \tag{2.12}$$

is symplectic.

Definition 2.3. A symplectic matrix S with block decomposition (7.3) is *free* if $B \in \mathrm{GL}(d,\mathbb{R})$.

Lemma 2.4. *Let $S \in \mathrm{Sp}(d,\mathbb{R})$. There exist S_1, S_2 free such that $S = S_1 S_2$.*

Proof. See [35, Theorem 60]. □

For the next result we refer the reader to [48, Proposition 4.10].

Proposition 2.5. The symplectic group is generated by J, and by matrices of the form V_C and $\mathcal{D}_L$, for $C \in \mathrm{Sym}(d,\mathbb{R})$ and $L \in \mathrm{GL}(d,\mathbb{R})$.

2.5.2 Metaplectic operators

Let ρ be the Schrödinger representation of the Heisenberg group, that is

$$\rho(x, \xi; \tau) = e^{2\pi i \tau} e^{-\pi i \xi \cdot x} \pi(x, \xi),$$

for all $x, \xi \in \mathbb{R}^d$, $\tau \in \mathbb{R}$. We will use the following tensor product property: for all $f, g \in L^2(\mathbb{R}^d)$, $z = (z_1, z_2), w = (w_1, w_2) \in \mathbb{R}^{2d}$,

$$\rho(z; \tau) f \otimes \rho(w; \tau) g = e^{2\pi i \tau} \rho(z_1, w_1, z_2, w_2; \tau)(f \otimes g).$$

For all $S \in \mathrm{Sp}(d, \mathbb{R})$, $\rho_S(x, \xi; \tau) := \rho(S(x, \xi); \tau)$ defines another representation of the Heisenberg group that is equivalent to ρ, i.e., there exists a unitary operator $\hat{S} : L^2(\mathbb{R}^d) \to L^2(\mathbb{R}^d)$ such that

$$\hat{S}\rho(x, \xi; \tau)\hat{S}^{-1} = \rho(S(x, \xi); \tau), \qquad x, \xi \in \mathbb{R}^d, \ \tau \in \mathbb{R}. \qquad (2.13)$$

This operator is not unique, but if $\hat{S}'$ is another unitary operator satisfying (2.13), then $\hat{S}' = c\hat{S}$, for some constant $c \in \mathbb{C}$, $|c| = 1$. The set $\{\hat{S} : S \in \mathrm{Sp}(d, \mathbb{R})\}$ is a group under composition and it admits a subgroup that contains exactly two operators for each $S \in \mathrm{Sp}(d, \mathbb{R})$. This subgroup is called **metaplectic group**, denoted by $\mathrm{Mp}(d, \mathbb{R})$. It is a realization of the two-fold cover of $\mathrm{Sp}(d, \mathbb{R})$ and the projection

$$\pi^{Mp} : \mathrm{Mp}(d, \mathbb{R}) \to \mathrm{Sp}(d, \mathbb{R})$$

is a group homomorphism with kernel $\ker(\pi^{Mp}) = \{-id_{L^2}, id_{L^2}\}$.

Throughout this work, if $\hat{S} \in \mathrm{Mp}(d, \mathbb{R})$, the matrix S (without the caret) will always be the unique symplectic matrix such that $\pi^{Mp}(\hat{S}) = S$. The next result is proved in [48, Proposition 4.27].

Proposition 2.6. Every operator $\hat{S} \in \mathrm{Mp}(d, \mathbb{R})$ maps $\mathcal{S}(\mathbb{R}^d)$ homeomorphically to $\mathcal{S}(\mathbb{R}^d)$. Moreover, for every $f \in \mathcal{S}'(\mathbb{R}^d)$, the tempered distribution $\hat{S}f \in \mathcal{S}'(\mathbb{R}^d)$ defined by

$$\langle \hat{S}f, g \rangle = \langle f, \hat{S}^{-1}g \rangle, \qquad g \in \mathcal{S}(\mathbb{R}^d)$$

is the unique extension of $\hat{S}$ to an operator on $\mathcal{S}'(\mathbb{R}^d)$, which is a homeomorphism of $\mathcal{S}'(\mathbb{R}^d)$.

Example 2.7. (i) The Fourier transform is a metaplectic operator, and

$$\pi^{Mp}(\mathcal{F}) = J.$$

(ii) For every $L \in \mathrm{GL}(d, \mathbb{R})$, the rescaling operator

$$\mathfrak{T}_L f(t) = |\det(L)|^{1/2} f(Lt), \qquad f \in L^2(\mathbb{R}^d),$$

is a metaplectic operator, and

$$\pi^{Mp}(\mathfrak{T}_L) = \mathcal{D}_L.$$

(iii) For every $C \in \mathrm{Sym}(d, \mathbb{R})$, the corresponding chirp function is

$$\Phi_C(t) = e^{i\pi Ct \cdot t}, \qquad t \in \mathbb{R}^d. \tag{2.14}$$

The product operator

$$\mathfrak{p}_C f(t) = \Phi_C(t) f(t), \qquad f \in L^2(\mathbb{R}^d) \tag{2.15}$$

is a metaplectic operator with projection

$$\pi^{Mp}(\mathfrak{p}_C) = V_C.$$

(iv) For every $C \in \mathrm{Sym}(d, \mathbb{R})$, the operator

$$\mathfrak{m}_C f = \mathcal{F}^{-1}(\Phi_C \hat{f}) = \mathcal{F}^{-1}\Phi_C * f, \qquad f \in L^2(\mathbb{R}^d) \tag{2.16}$$

is metaplectic, with

$$\pi^{Mp}(\mathfrak{m}_C) = U_C = V_C^T.$$

Observe that, if $C \in \mathrm{GL}(d, \mathbb{R})$,

$$\mathcal{F}^{-1}\Phi_C = |\det(C)|\Phi_{-C^{-1}},$$

and consequently,

$$\mathfrak{m}_C f = |\det(C)|\Phi_{-C^{-1}} * f, \qquad f \in L^2(\mathbb{R}^d).$$

(v) Let $\mathcal{F}_j$, $1 \leq j \leq d$, be the partial Fourier transform with respect to the jth coordinate defined in (2.1). Then

$$\mathcal{F}_j \rho(x, \xi, \tau) \mathcal{F}_j^{-1} = \rho(\Pi_j(x, \xi), \tau), \quad x, \xi \in \mathbb{R}^d, \, \tau \in \mathbb{R}.$$

In fact, take any $f \in L^1(\mathbb{R}^d)$ and compute $\mathcal{F}_j \rho(x, \xi, \tau) \mathcal{F}_j^{-1} f$ as follows:

$$\mathcal{F}_j \rho(x, \xi, \tau) \mathcal{F}_j^{-1} f(t_1, \ldots, t_d) e^{-2\pi i \tau} e^{i\pi x \cdot \xi}$$

$$= e^{2\pi i \sum_{k \neq j} t_k \cdot \xi_k} \int_{\mathbb{R}} e^{-2\pi t_j \zeta_j} e^{2\pi i \zeta_j \xi_j} \mathcal{F}_j^{-1} f(t_1 - x_1, \ldots, \zeta_j - x_j, \ldots, t_d - x_d) \, d\zeta_j$$

$$= e^{2\pi i \sum_{k \neq j} t_k \cdot \xi_k} \int_{\mathbb{R}} e^{-2\pi i (u_j + x_j)(t_j - \xi_j)} \mathcal{F}_j^{-1} f(t_1 - x_1, \ldots, u_j, \ldots, t_d - x_d) \, du_j$$

$$= e^{2\pi i \sum_{k \neq j} t_k \cdot \xi_k} e^{2\pi i t_j (-x_j)} e^{2\pi i x_j \xi_j} \int_{\mathbb{R}} e^{-2\pi u_j (\xi_j - \zeta_j)}$$

$$\times \quad \mathcal{F}_j^{-1} f(t_1 - x_1, \ldots, u_j, \ldots, t_d - x_d) \, du_j$$

$$= e^{-2\pi i \tau} e^{i\pi x \cdot \xi} \rho(\Pi_j(x, \xi), \tau) f(t_1, \ldots, t_d).$$

Consequently, $\mathcal{F}_j$ is a metaplectic operator, and $\pi^{Mp}(\mathcal{F}_j) = \Pi_j$. More generally, if $\mathcal{J} = \{j_1, \ldots, j_r\} \subseteq \{1, \ldots, d\}$, the partial Fourier transform with respect to the variables indexed by $\mathcal{J}$ is

$$\mathcal{F}_{\mathcal{J}} = \mathcal{F}_{j_1} \circ \ldots \circ \mathcal{F}_{j_r}.$$

We have
$$\pi^{Mp}(\mathcal{F}_{\mathcal{J}}) = \Pi_{\mathcal{J}}.$$

In particular, the partial Fourier transform with respect to the frequency variables $\mathcal{F}_2$ is a metaplectic operator and
$$\pi^{Mp}(\mathcal{F}_2) = \mathcal{A}_{FT2}.$$

Remark 2.8. With an abuse of notation, if $\hat{S}$ is a metaplectic operator on $L^2(\mathbb{R}^d)$, we write $\hat{S} \in \mathrm{Mp}(d, \mathbb{R})$. Stated otherwise, we write $\hat{S} \in \mathrm{Mp}(d, \mathbb{R})$ if there exists $c \in \mathbb{C}$ with $|c| = 1$ so that $c\hat{S} \in \mathrm{Mp}(d, \mathbb{R})$. The reason is that all the properties treated in this work are independent on c.

Proposition 2.9. The operators $\mathcal{F}$, $\mathfrak{p}_C$ and $\mathfrak{T}_L$ generate the group of metaplectic operators.

Proof. It is a straightforward restatement of Proposition 2.5, together with the fact that π^{Mp} is a homomorphism. $\qquad\square$

For the next result is contained in [48, Theorems 4.51 and 4.53].

Lemma 2.10. *If* $\hat{S} \in \mathrm{Mp}(d, \mathbb{R})$ *and* $S = \pi^{Mp}(\hat{S})$ *is free, then for every* $f \in \mathcal{S}(\mathbb{R}^d)$,
$$\hat{S}f(x) = |\det(B)|^{-1/2} \Phi_{-DB^{-1}}(x) \int_{\mathbb{R}^d} f(t) e^{2\pi i B^{-1}x \cdot t} e^{-i\pi B^{-1}At \cdot t} dt,$$

and, if $\hat{S} \in \mathrm{Mp}(d, \mathbb{R})$ *and* $S = \pi^{Mp}(\hat{S})$ *has* $A \in \mathrm{GL}(d, \mathbb{R})$, *then*
$$\hat{S}f(x) = |\det(A)|^{-1/2} \Phi_{CA^{-1}}(x) \int_{\mathbb{R}^d} \Phi_{-A^{-1}B}(\xi) \hat{f}(\xi) e^{2\pi i A^{-1}x \cdot \xi} d\xi$$

for every $f \in \mathcal{S}(\mathbb{R}^d)$.

2.6   Metaplectic Wigner distributions

Let $\hat{\mathcal{A}} \in \mathrm{Mp}(2d, \mathbb{R})$.

Definition 2.11. The **metaplectic Wigner distribution** associated to $\hat{\mathcal{A}}$ is defined for all $f, g \in L^2(\mathbb{R}^d)$ as
$$W_{\mathcal{A}}(f, g) = \hat{\mathcal{A}}(f \otimes \bar{g}).$$

The most popular time-frequency representations are metaplectic Wigner distributions. Namely, $V_g f = \hat{\mathcal{A}}_{ST}(f \otimes \bar{g})$ and $W_\tau(f, g) = \hat{\mathcal{A}}_\tau(f \otimes \bar{g})$, where:

$$A_{ST} = \begin{pmatrix} I_{d\times d} & -I_{d\times d} & 0_{d\times d} & 0_{d\times d} \\ 0_{d\times d} & 0_{d\times d} & I_{d\times d} & I_{d\times d} \\ 0_{d\times d} & 0_{d\times d} & 0_{d\times d} & -I_{d\times d} \\ -I_{d\times d} & 0_{d\times d} & 0_{d\times d} & 0_{d\times d} \end{pmatrix} \qquad (2.17)$$

and

$$A_{\tau,2d} = \begin{pmatrix} (1-\tau)I_{d\times d} & \tau I_{d\times d} & 0_{d\times d} & 0_{d\times d} \\ 0_{d\times d} & 0_{d\times d} & \tau I_{d\times d} & -(1-\tau)I_{d\times d} \\ 0_{d\times d} & 0_{d\times d} & I_{d\times d} & I_{d\times d} \\ -I_{d\times d} & I_{d\times d} & 0_{d\times d} & 0_{d\times d} \end{pmatrix}, \qquad (2.18)$$

when d is clear from the context, we limit to write $\mathcal{A}_\tau$.

We recall the following continuity properties.

Proposition 2.12. Let $W_{\mathcal{A}}$ be a metaplectic Wigner distribution. Then,
(i) $W_{\mathcal{A}} : L^2(\mathbb{R}^d) \times L^2(\mathbb{R}^d) \to L^2(\mathbb{R}^{2d})$ is continuous;
(ii) $W_{\mathcal{A}} : \mathcal{S}(\mathbb{R}^d) \times \mathcal{S}(\mathbb{R}^d) \to \mathcal{S}(\mathbb{R}^{2d})$ is continuous;
(iii) $W_{\mathcal{A}} : \mathcal{S}'(\mathbb{R}^d) \times \mathcal{S}'(\mathbb{R}^d) \to \mathcal{S}'(\mathbb{R}^{2d})$ is continuous.

Proof. See [31, Proposition 2.3]. □

Lemma 2.13. *For every* $f_1, f_2, g_1, g_2 \in L^2(\mathbb{R}^d)$,

$$\langle W_{\mathcal{A}}(f_1, f_2), W_{\mathcal{A}}(g_1, g_2)\rangle = \langle f_1, g_1\rangle\overline{\langle f_2, g_2\rangle}. \qquad (2.19)$$

Proof. See [31, Proposition 2.9]. □

The projection of a metaplectic operator $\hat{\mathcal{A}} \in \mathrm{Mp}(2d, \mathbb{R})$ is a symplectic matrix $\mathcal{A} \in \mathrm{Sp}(2d, \mathbb{R})$ with block decomposition

$$\mathcal{A} = \begin{pmatrix} A_{11} & A_{12} & A_{13} & A_{14} \\ A_{21} & A_{22} & A_{23} & A_{24} \\ A_{31} & A_{32} & A_{33} & A_{34} \\ A_{41} & A_{42} & A_{43} & A_{44} \end{pmatrix}. \qquad (2.20)$$

For a $4d \times 4d$ symplectic matrix with block decomposition (2.20), relations (2.10) read as:

$$\begin{cases} (R1a) & A_{11}^T A_{31} + A_{21}^T A_{41} = A_{31}^T A_{11} + A_{41}^T A_{21}, \\ (R1b) & A_{11}^T A_{32} + A_{21}^T A_{42} = A_{31}^T A_{12} + A_{41}^T A_{22}, \\ (R1c) & A_{12}^T A_{32} + A_{22}^T A_{42} = A_{32}^T A_{12} + A_{42}^T A_{22}, \end{cases}$$

$$\begin{cases} (R2a) & A_{13}^T A_{33} + A_{23}^T A_{43} = A_{33}^T A_{13} + A_{43}^T A_{23}, \\ (R2b) & A_{13}^T A_{34} + A_{23}^T A_{44} = A_{33}^T A_{14} + A_{43}^T A_{24}, \\ (R2c) & A_{14}^T A_{34} + A_{24}^T A_{44} = A_{34}^T A_{14} + A_{44}^T A_{24}, \end{cases}$$

$$\begin{cases} (R3a) & A_{11}^T A_{33} + A_{21}^T A_{43} - (A_{31}^T A_{13} + A_{41}^T A_{23}) = I_{d\times d}, \\ (R3b) & A_{11}^T A_{34} + A_{21}^T A_{44} = A_{31}^T A_{14} + A_{41}^T A_{24}, \\ (R3c) & A_{12}^T A_{33} + A_{22}^T A_{43} = A_{32}^T A_{13} + A_{42}^T A_{23}, \\ (R3d) & A_{12}^T A_{34} + A_{22}^T A_{44} - (A_{32}^T A_{14} + A_{42}^T A_{24}) = I_{d\times d}. \end{cases}$$

We identify four $2d \times 2d$ submatrices of $4d \times 4d$ symplectic matrices. Namely, if $\mathcal{A} \in \mathrm{Sp}(2d, \mathbb{R})$ has block decomposition (2.20), we set:

$$E_{\mathcal{A}} = \begin{pmatrix} A_{11} & A_{13} \\ A_{21} & A_{23} \end{pmatrix}, \quad F_{\mathcal{A}} = \begin{pmatrix} A_{31} & A_{33} \\ A_{41} & A_{43} \end{pmatrix}, \tag{2.21}$$

and

$$\mathcal{E}_{\mathcal{A}} = \begin{pmatrix} A_{12} & A_{14} \\ A_{22} & A_{24} \end{pmatrix}, \quad \mathcal{F}_{\mathcal{A}} = \begin{pmatrix} A_{32} & A_{34} \\ A_{42} & A_{44} \end{pmatrix}. \tag{2.22}$$

A simple comparison shows that relationships $(R1a) - (R3d)$ read, in terms of these four submatrices, as

$$\begin{cases} E_{\mathcal{A}}^T F_{\mathcal{A}} - F_{\mathcal{A}}^T E_{\mathcal{A}} = J, \\ \mathcal{E}_{\mathcal{A}}^T \mathcal{F}_{\mathcal{A}} - \mathcal{F}_{\mathcal{A}}^T \mathcal{E}_{\mathcal{A}} = J, \\ E_{\mathcal{A}}^T \mathcal{F}_{\mathcal{A}} - F_{\mathcal{A}}^T \mathcal{E}_{\mathcal{A}} = 0_{d \times d}. \end{cases} \tag{2.23}$$

We will also consider

$$B_{\mathcal{A}} = \begin{pmatrix} A_{13} & \frac{1}{2} I_{d \times d} - A_{11} \\ \frac{1}{2} I_{d \times d} - A_{11}^T & -A_{21} \end{pmatrix}. \tag{2.24}$$

Finally, the following matrices will appear ubiquitously throughout this work:

$$L = \begin{pmatrix} 0_{d \times d} & I_{d \times d} \\ I_{d \times d} & 0_{d \times d} \end{pmatrix} \quad and \quad P = \begin{pmatrix} 0_{d \times d} & I_{d \times d} \\ 0_{d \times d} & 0_{d \times d} \end{pmatrix}. \tag{2.25}$$

In this work, we often denote by L also a general invertible matrix. However, this shall not cause confusion.

Lemma 2.14. *Let $\mathcal{A} \in \mathrm{Sp}(2d, \mathbb{R})$ have block decomposition (2.20) and $E_{\mathcal{A}}$, $F_{\mathcal{A}}$, $\mathcal{E}_{\mathcal{A}}$, and $\mathcal{F}_{\mathcal{A}}$ be defined as in (2.21) and (2.22). Let L be defined as in (2.25). If $E_{\mathcal{A}} \in \mathrm{GL}(2d, \mathbb{R})$, then,*
(i) $\mathcal{F}_{\mathcal{A}} = E_{\mathcal{A}}^{-T} F_{\mathcal{A}}^T \mathcal{E}_{\mathcal{A}}$;
(ii) the matrix $G_{\mathcal{A}} := L E_{\mathcal{A}}^{-1} \mathcal{E}_{\mathcal{A}}$ is symplectic;
(iii) $\mathcal{E}_{\mathcal{A}} \in \mathrm{GL}(2d, \mathbb{R})$ and $\det(\mathcal{E}_{\mathcal{A}}) = (-1)^d \det(E_{\mathcal{A}})$.
If $\mathcal{E}_{\mathcal{A}} \in \mathrm{GL}(2d, \mathbb{R})$, then,
(iv) $F_{\mathcal{A}} = \mathcal{E}_{\mathcal{A}}^{-T} \mathcal{F}_{\mathcal{A}}^T E_{\mathcal{A}}$;
(v) the matrix $\mathfrak{G}_{\mathcal{A}} = L \mathcal{E}_{\mathcal{A}}^{-1} E_{\mathcal{A}}$ is symplectic;
(vi) $E_{\mathcal{A}} \in \mathrm{GL}(2d, \mathbb{R})$ and $\det(E_{\mathcal{A}}) = (-1)^d \det(\mathcal{E}_{\mathcal{A}})$.
In particular, $E_{\mathcal{A}}$ is invertible if and only if $\mathcal{E}_{\mathcal{A}}$ is invertible.

Proof. Relation (i) follows directly from the third equation in (2.23), using the invertibility of $E_{\mathcal{A}}$.

Item (ii) is a consequence of (2.23) and (i). For, observe that $LJL = -J$, so that:

$$
\begin{aligned}
G_{\mathcal{A}}^T J G_{\mathcal{A}} &= (L E_{\mathcal{A}}^{-1} \mathcal{E}_{\mathcal{A}})^T J (L E_{\mathcal{A}}^{-1} \mathcal{E}_{\mathcal{A}}) = \mathcal{E}_{\mathcal{A}}^T E_{\mathcal{A}}^{-T} (LJL) E_{\mathcal{A}}^{-1} \mathcal{E}_{\mathcal{A}} \\
&= -\mathcal{E}_{\mathcal{A}}^T E_{\mathcal{A}}^{-T} J E_{\mathcal{A}}^{-1} \mathcal{E}_{\mathcal{A}} = \mathcal{E}_{\mathcal{A}}^T E_{\mathcal{A}}^{-T} (F_{\mathcal{A}}^T E_{\mathcal{A}} - E_{\mathcal{A}}^T F_{\mathcal{A}}) E_{\mathcal{A}}^{-1} \mathcal{E}_{\mathcal{A}} \\
&= \mathcal{E}_{\mathcal{A}}^T (E_{\mathcal{A}}^{-T} F_{\mathcal{A}}^T - F_{\mathcal{A}} E_{\mathcal{A}}^{-1}) \mathcal{E}_{\mathcal{A}} = \mathcal{E}_{\mathcal{A}}^T (E_{\mathcal{A}}^{-T} F_{\mathcal{A}}^T \mathcal{E}_{\mathcal{A}}) - (\mathcal{E}_{\mathcal{A}}^T F_{\mathcal{A}} E_{\mathcal{A}}^{-1}) \mathcal{E}_{\mathcal{A}} \\
&= \mathcal{E}_{\mathcal{A}}^T \mathcal{F}_{\mathcal{A}} - \mathcal{F}_{\mathcal{A}}^T \mathcal{E}_{\mathcal{A}} = J.
\end{aligned}
$$

Finally, (iii) follows directly from (ii). Items (iv)-(vi) are proved analogously. $\quad\square$

Definition 2.15. We say that $W_{\mathcal{A}}$ or, by extension, $\mathcal{A}$ and $\hat{\mathcal{A}}$, is shift-invertible if $E_{\mathcal{A}} \in \mathrm{GL}(d, \mathbb{R})$.

Tuning parameters for LASSO problems

In Section 3.1, we establish the notation we use in this work. In Section 3.2 we compute the deterministic relationships between the parameters λ_j's and the τ_j's in order for problems

$$minimize \quad \|Ax - b\|_2^2, \qquad x \in \mathbb{R}^n, \quad |x_j| \leq \tau_j, \quad j = 1, \dots, n. \qquad (3.1)$$

and

$$minimize \quad \|Ax - b\|_2^2 + \sum_{j=1}^{n} \lambda_j |x_j|, \qquad (3.2)$$

to be equivalent, under the following specific assumptions: e.g., A is a subsampling matrix (i.e., the k-th row of A, $a_{k,*}$ is either the k-th vector of the canonical basis of $\mathbb{R}^n$, or the null vector), A is the matrix of the discrete Fourier transform, or simply the identity matrix. In those cases A is such that $A^T A$ is diagonal, and the Lagrange multipliers are explicitly given by:

$$\lambda_j^{\#} = 2 \|a_{*,j}\|_2^2 \left(\frac{|\langle b, a_{*,j} \rangle|}{\|a_{*,j}\|_2^2} - \tau_j \right) \chi_{\left[0, \frac{|\langle b, a_{*,j} \rangle|}{\|a_{*,j}\|_2^2} \right]} (\tau_j), \qquad (3.3)$$

where $a_{*,j}$ denotes the j-th column of A and $\chi_{\left[0, \frac{|\langle b, a_{*,j} \rangle|}{\|a_{*,j}\|_2^2} \right]}$ is the characteristic function on $\left[0, \frac{|\langle b, a_{*,j} \rangle|}{\|a_{*,j}\|_2^2} \right]$, $j = 1, ..., n$. We also provide deterministic results under assumptions on the sign of the gradient of $\|Ax - b\|_2^2$. Specifically, we provide the explicit expression of the Lagrange multipliers when $\frac{\partial}{\partial x_j}(\|Ax - b\|_2^2) \leq 0$, for every $j = 1, \dots, n$ in $\{|x_j| \leq \tau_j : j = 1, \dots, n\}$.

We point out that our result is interesting for two main reasons: to the best of our knowledge, the analytic dependence that we investigate was never fully understood, neither computed. Formula (3.3) can be applied directly for denoising in some transform domain, i.e., if A is orthogonal or the identity itself.

Furthermore, if A is the matrix of an undersampling pattern, $A^T A$ is diagonal and (3.3) can be exploited to control the Lagrange multipliers of the weighted LASSO problem (3.2) in terms of voxel-wise estimates. We presume that such estimates are relatively easy to obtain. For example, one may first reconstruct a highly undersampled image, apply filters using convolution techniques and estimate the tuning parameters λ from the filtered image, therefore obtaining a denoised image.

This chapter is part of an article published in *Applied Mathematics and Optimization* in 2024, cf. [60].

3.1 Convex analysis of LASSO problems

3.1.1 Lagrange duality

Consider a constrained optimization problem in the form

$$\text{minimize } F_0(x), \qquad \Psi x = y, \ F_l(x) \le b_l, \ l = 1, \ldots, M, \qquad (3.4)$$

where $\Psi \in \mathbb{R}^{m \times n}$, $y \in \mathbb{R}^m$ and $F_0, F_1, \ldots, F_M : \mathbb{R}^n \to (-\infty, +\infty]$ are convex. We always assume that a minimizer of (3.4) exists.

A point $x \in \mathbb{R}^n$ is called *feasible* if it belongs to the constraints, that is if:

$$x \in K := \left\{ \zeta \in \mathbb{R}^n \ : \ \Psi\zeta = y \text{ and } F_l(\zeta) \le b_l, \ l = 1, \ldots, M \right\}$$

and K is called the *set of feasible points*. To avoid triviality, we always assume $K \ne \emptyset$, in which case problem (3.4) is called *feasible*. In view of the definition of K, problem (3.4) can be implicitly written as:

$$minimize \quad F_0(x), \qquad x \in K.$$

Convex problems such as (1.11) and (3.1) can be approached by considering their Lagrange formulation, see Subsection 3.1.3 below. The *Lagrange function* related to (3.4) is the function $L : \mathbb{R}^n \times \mathbb{R}^m \times [0, +\infty)^M \to (-\infty, +\infty]$ defined as:

$$L(x, \xi, \lambda) := F_0(x) + \langle \xi, \Psi x - y \rangle + \sum_{l=1}^{M} \lambda_l (F_l(x) - b_l).$$

Observe that for all ξ, λ and $x \in K$:

$$L(x, \xi, \lambda) = F_0(x) + \underbrace{\langle \xi, \Psi x - y \rangle}_{= \, 0} + \sum_{l=1}^{M} \underbrace{\lambda_l}_{\ge \, 0} \underbrace{(F_l(x) - b_l)}_{\le \, 0} \le F_0(x),$$

so that:

$$\inf_{x \in \mathbb{R}^n} L(x, \xi, \lambda) \le \inf_{x \in K} L(x, \xi, \lambda) \le \inf_{x \in K} F_0(x). \qquad (3.5)$$

Definition 3.1. The function $H : \mathbb{R}^m \times [0, +\infty)^M \to [-\infty, +\infty]$ defined as:

$$H(\xi, \lambda) := \inf_{x \in \mathbb{R}^n} L(x, \xi, \lambda)$$

is called *Lagrange dual function*.

Inequalities (3.5) read as:

$$H(\xi, \lambda) \leq \inf_{x \in K} F_0(x) \tag{3.6}$$

for all $\xi \in \mathbb{R}^m$ and all $\lambda \in [0, +\infty)^M$. Stating (3.6) differently, we have the *weak duality inequality*:

$$\sup_{\substack{\xi \in \mathbb{R}^m \\ \lambda \succeq 0}} H(\xi, \lambda) \leq \inf_{x \in K} F_0(x). \tag{3.7}$$

We point out that (3.7) is equivalent to:

$$\sup_{\xi, \lambda} \inf_x L(x, \xi, \lambda) \leq \inf_x \sup_{\xi, \lambda} L(x, \xi, \lambda) \tag{3.8}$$

(see [11, Subsection 5.4.1]).

We are interested in computing the parameters (ξ, λ) such that (3.7) is an equality, in which case (3.7) becomes:

$$\sup_{\substack{\xi \in \mathbb{R}^m \\ \lambda \succeq 0}} H(\xi, \lambda) = \inf_{x \in K} F_0(x), \tag{3.9}$$

so that *strong duality* (3.9) holds for problem (3.4).

3.1.2 Subdifferential

Definition 3.2 (Subdifferential)**.** Let $\Omega \subseteq \mathbb{R}^n$ be open and $g : \Omega \to \mathbb{R}$. Let $x_0 \in \Omega$. The *subdifferential* of g at x_0 is the set:

$$\partial g(x_0) := \{v \in \mathbb{R}^n \ : \ g(x) \geq g(x_0) + v^T(x - x_0) \ \forall x \in \Omega\}.$$

We refer to any $v \in \partial g(x_0)$ as a *subgradient* of g at x_0.

We will use the following standard result of convex analysis.

Proposition 3.3. Let $\Omega \subseteq \mathbb{R}^n$ be open and convex, and $g : \Omega \to \mathbb{R}$ be convex and continuous on Ω. Let $x_0 \in \Omega$. Then, $\partial g(x_0) \neq \emptyset$.

Proof. See e.g. [110, Theorem 23.4]. $\qquad\qquad\square$

3.1.3   Lagrange formulation of constrained problems

Under the notation above, let $F(x) := (F_1(x), ..., F_M(x))$. In the convex framework, if the constraint $F(x) \preceq b$ does not reduce to $F(x) = b$, namely if for all $l = 1, \ldots, M$ the inequality $F_l(x) < b_l$ holds for some $x \in \mathbb{R}^n$, then strong duality holds.

Theorem 3.4 (Cf. [11], Section 5.3.2). *Assume that $F_0, F_1, \ldots, F_M$ are convex functions defined on $\mathbb{R}^n$. Let $x^\#$ be such that $F_0(x^\#) = \inf_{x \in \mathbb{R}^n} F_0(x)$. If:*

(i) there exists $\tilde{x} \in \mathbb{R}^n$ such that $\Psi\tilde{x} = y$ and $F(\tilde{x}) \prec b$ or,

(ii) in absence of inequality constraints, if $K \neq \emptyset$ (i.e., if there exists $\tilde{x} \in \mathbb{R}^n$ such that $\Psi\tilde{x} = y$),

then, there exists $(\xi^\#, \lambda^\#) \in \mathbb{R}^m \times [0, +\infty)^M$ such that

$$H(\xi^\#, \lambda^\#) = \sup_{\xi, \lambda} H(\xi, \lambda)$$

and $H(\xi^\#, \lambda^\#) = F_0(x^\#)$.

The proof of Theorem 3.4 contains the fundamental construction we will use in the next sections and we report it for this reason. We refer to [11, Subsection 5.3.2] for the complete proof. First, we need a result from functional analysis, which is well-known as (geometrical) *Hahn-Banach theorem.*

Definition 3.5 (Separating hyperplane). Consider two subsets $\mathcal{A}, \mathcal{B} \subseteq \mathbb{R}^n$. A hyperplane $\Gamma := \{x \in \mathbb{R}^n \; : \; \langle \xi, x \rangle = \alpha\}$ satisfying:

$$\langle \xi, x \rangle \leq \alpha < \langle \xi, y \rangle, \qquad x \in \mathcal{A}, \quad y \in \mathcal{B}, \tag{3.10}$$

is a *separating hyperplane* between $\mathcal{A}$ and $\mathcal{B}$.

Theorem 3.6 (Cf. [112] Theorem 3.4). *Let $\mathcal{A}, \mathcal{B} \subset \mathbb{R}^n$ be two convex and disjoint subsets. If $\mathcal{B}$ is open, there exists $\xi \in \mathbb{R}^n$ and $\alpha \in \mathbb{R}$ such that (3.10) holds for all $x \in \mathcal{A}$ and all $y \in \mathcal{B}$.*

Idea of the proof of Theorem 3.4. First, one assumes that A has full row-rank. Moreover, one reduces to consider the situation in which $p^* := \inf_{x \in K} F_0(x) > -\infty$, otherwise the assertion is trivial.

Consider the set:

$$\mathcal{G} := \left\{ (F(x) - b, \Psi x - y, F_0(x)) \in \mathbb{R}^M \times \mathbb{R}^m \times \mathbb{R} \; : \; x \in \mathbb{R}^n \right\},$$

where, with an abuse of notation, $\Psi x - y$ denotes the row vector with the same (ordered) entries of $\Psi x - y$, and $\mathcal{A}$ be defined as the epigraph:

$$
\begin{aligned}
\mathcal{A} &:= \mathcal{G} + ((\mathbb{R}_{\geq 0})^M \times \mathbb{R}^m \times \mathbb{R}_{\geq 0}) \\
&= \Big\{ (u, v, t) \in \mathbb{R}^M \times \mathbb{R}^m \times \mathbb{R} \ : \ u \succeq F(x) - b, \\
& \qquad v = \Psi x - y, \ t \geq F_0(x) \ for \ some \ x \in \mathbb{R}^n \Big\}.
\end{aligned}
$$

It is easy to verify that if $F_0, F_1, \dots, F_M$ are convex, than $\mathcal{A}$ is convex. Then, consider the set:

$$
\mathcal{B} := \Big\{ (0, 0, s) \in \mathbb{R}^M \times \mathbb{R}^m \times \mathbb{R} \ : \ s < p^* \Big\}.
$$

$\mathcal{A}$ and $\mathcal{B}$ are clearly disjoint, $\mathcal{B}$ (which is an open half-line) being trivially convex and open. Therefore, the assumptions of Theorem 3.6 are satisfied and we conclude that there exists a triple of parameters $(\tilde{\lambda}, \tilde{\xi}, \mu) \neq 0$ and $\alpha \in \mathbb{R}$ such that:

$$
\begin{aligned}
(u, v, t) \in \mathcal{A} &\implies \tilde{\lambda}^T u + \langle \tilde{\xi}, v \rangle + \mu t \geq \alpha, && (3.11) \\
(u, v, t) \in \mathcal{B} &\implies \tilde{\lambda}^T u + \langle \tilde{\xi}, v \rangle + \mu t \leq \alpha. && (3.12)
\end{aligned}
$$

It is easy to see that the definition of $\mathcal{A}$, together with (3.11), imply that $\tilde{\lambda}_l \geq 0$ for all $l = 1, \dots, M$ and $\mu \geq 0$. Also, applying the definition of $\mathcal{B}$ to (3.12), one finds that $\mu t \leq \alpha$ for all $t < p^*$, which implies that $\mu p^* \leq \alpha$. Therefore, for all $x \in \mathbb{R}^n$,

$$
\sum_{l=1}^{M} \tilde{\lambda}_l (F_l(x) - b_l) + \langle \tilde{\xi}, \Psi x - y \rangle + \mu F_0(x) \geq \alpha \geq \mu p^*. \qquad (3.13)
$$

If $\mu > 0$, then (3.13) gives that $L(x, \tilde{\xi}/\mu, \tilde{\lambda}/\mu) \geq p^*$ for all $x \in \mathbb{R}^n$, which implies that $H(\tilde{\xi}/\mu, \tilde{\lambda}/\mu) \geq p^*$. Since the other inequality holds trivially by the weak duality inequality, we conclude that $H(\tilde{\xi}/\mu, \tilde{\lambda}/\mu) = p^*$. Finally, using the assumptions on the rank of Ψ and on the existence of a point satisfying the strict inequality constraint, one proves by contradiction that it must be $\mu > 0$. $\qquad \square$

Definition 3.7 (Lagrange Multipliers)**.** We refer to a couple $(\xi^\#, \lambda^\#) \in \mathbb{R}^m \times [0, +\infty)^M$ as to *Lagrange multipliers* for the problem (3.4) if $(\xi^\#, \lambda^\#)$ attend the supremum in (3.9).

As a consequence of Theorem 3.4, we have the following result, which relates the minimizers of (3.4) and those of the dual problem $\max_{\xi, \lambda} H(\xi, \lambda)$, providing also the Lagrange multipliers, that may not be unique.

Corollary 3.8 (Cf. [49] Theorem B.28)**.** *Let* $F_0 : \mathbb{R}^n \to [0, +\infty)$ *and* $\phi : [0, +\infty) \to \mathbb{R}$ *be such that* ϕ *is monotonically increasing and* $\phi \circ F_0$ *is convex. Let*

$\tau_j > 0 \ (j = 1, \ldots, M)$ and $\psi_j : \mathbb{R}^n \to \mathbb{R} \ (j = 1, \ldots, M)$ be convex functions such that $\psi_j^{-1}([0, \tau_j)) \neq \emptyset$ for all $j = 1, \ldots, M$. Let $x^\#$ be a minimizer of the problem:

$$minimize \quad F_0(x), \qquad x \in \mathbb{R}^n \ \psi(x) \preceq \tau, \tag{3.14}$$

where $\tau = (\tau_1, \ldots, \tau_M)$. Then, there exist $\lambda_j \geq 0 \ (j = 1, \ldots, M)$ such that $x^\#$ is a minimizer of:

$$minimize \quad \phi(F_0(x)) + \sum_{j=1}^{M} \lambda_j \psi_j(x).$$

Proof. Since ϕ is monotonically increasing, (3.14) is obviously equivalent to:

$$minimize \quad \phi(F_0(x)), \qquad x \in \mathbb{R}^n \ \psi_j(x) \leq \tau_j,$$

$(j = 1, \ldots, M)$ whose Lagrangian is given by:

$$L(x, \lambda) = \phi(F_0(x)) + \sum_{j=1}^{M} \lambda_j(\psi_j(x) - \tau_j). \tag{3.15}$$

By the assumption, $\phi \circ F_0$ and each ψ_j are convex and the inequalities $\psi_j(\tilde{x}) < \tau_j$ are satisfied by some $\tilde{x} \in \mathbb{R}^n$ (observe that here we need $\tau_j > 0$), so we can apply Theorem 3.4 to get $H(\lambda^\#) = \phi(F_0(x^\#))$ for some $\lambda^\# \in [0, +\infty)^M$. By (3.8), for all $x \in \mathbb{R}^n$:

$$L(x^\#, \lambda^\#) \leq L(x, \lambda^\#),$$

so that $x^\#$ is also a minimizer of the function $x \in \mathbb{R}^n \mapsto L(x, \lambda^\#)$. Since the constant terms $-\lambda_j \tau_j$ in (3.15) do not affect the set of minimizers, we have that $x^\#$ is a minimizer of:

$$minimize \quad \phi(F_0(x)) + \sum_{j=1}^{M} \lambda_j^\#(\psi_j(x) - \tau), \qquad x \in \mathbb{R}^n.$$

$\square$

Remark 3.9. Theorem 3.6 has a complex version that holds with $\Re\langle z, w \rangle = \Re\left(\sum_{j=1}^{n} \overline{z_j} w_j\right)$ ($\Re$ denotes the real part of a complex number) instead of $\langle \cdot, \cdot \rangle$. In particular, the entire theory presented in this work is applicable in the complex framework as well. This extension involves replacing the canonical real inner product of $\mathbb{R}^n$ with the real inner product on $\mathbb{C}^n$ defined above. Therefore, we do not need to study the complex case separately, as only the structure of $\mathbb{C}^n$ as a real vector space is involved.

Remark 3.10. To sum up, Theorem 3.4 and Corollary 3.8 together tell that, up to the sign, the coefficients of any hyperplane separating the two sets:

$$\mathcal{A} = \left\{(u, t) \in \mathbb{R}^{M+1} \ : \ u \succeq F(x) - b, \ t \geq F_0(x) \ for \ x \in \mathbb{R}^n\right\}$$

and

$$\mathcal{B} = \left\{ (0, t) \in \mathbb{R}^{M+1} \ : \ t < \inf_{x \in K} F_0(x) \right\}$$

define Lagrange multipliers for problem (3.4), in absence of equality constraints, i.e., if $y = 0$ and $\Psi = 0$ in (3.4). This is the geometric idea that we will apply in the following sections to the weighted LASSO.

3.1.4 Existence of solutions for LASSO problems

Since we did not find a direct proof in the existing literature, we provide a formal proof of the existence of the minimizer of the generalized LASSO problem:

$$\arg \min_{x \in \mathbb{R}^n} \|Ax - b\|_2^2 + \lambda \|\Phi x\|_1, \tag{3.16}$$

where $b \in \mathbb{R}^m$, $A \in \mathbb{R}^{m \times n}$ and $\Phi \in \mathbb{R}^{N \times n}$.

We state the result in the general framework of finite-dimensional vector spaces: we denote by X, Y, Z three finite-dimension real vector spaces. We denote by $\langle \cdot, \cdot \rangle_X$ an inner product on X and with $\|\cdot\|_X$ the induced norm. Analogous notation will be used for Y, whereas we set:

$$\|z\|_p = \left(\sum_{j=1}^{\dim(Z)} |z_j|^p \right)^{1/p}, \qquad z \in Z$$

for $0 < p \le \infty$. Recall that $\|\cdot\|_p$ is a Banach quasi-norm (meaning that there exists $C_p \ge 1$ such that $\|x + y\|_p \le C_p(\|x\|_p + \|y\|_p)$ for all $x, y \in Z$) replaces the triangular inequality for $0 < p < 1$, and it is a norm for $1 \le p \le \infty$.

Then, for given $\lambda \ge 0$, $b \in Y$, $A : X \to Y$ and $\Phi : X \to Z$ linear, we define for all $x \in X$,

$$f(x) = \|Ax - b\|_Y^2 + \lambda \|\Phi x\|_p.$$

Theorem 3.11. *For all $0 < p \le \infty$, $\lambda \ge 0$ there exists $x^\# \in X$ such that*

$$\inf_{x \in X} f(x) = f(x^\#).$$

In particular, the generalized LASSO problem (3.16) has at least one solution.

Proof. Clearly, the function $f(x) = \|b\|_Y^2 + \lambda \|\Phi x\|_p$ attains its minimum in $x^\# = 0$. Hence, we may assume that

$$\Im(A) \neq \{0\}.$$

Since $\Im(A)$ is a vector subspace of Y, for all $b \in Y$ there exists a unique $y^{\#} \in \Im(A)$ such that $\inf_{y \in Y} \|y - b\|_Y^2 = \|y^{\#} - b\|_Y^2$. By definition, $y^{\#} = Ax^{\#}$ for some $x^{\#} \in X$. Hence,

$$\inf_{x \in X} \|Ax - b\|_Y^2 = \inf_{y \in \Im(A)} \|y - b\|_Y^2 = \min_{y \in Y} \|y - b\|_2^2 = \left\|Ax^{\#} - b\right\|_Y^2$$

and the assertion follows also for the case in which $\lambda = 0$ or $\Im(B) = \{0\}$. We will thereby assume that $\Im(A) \neq \{0\}$, $\Im(B) \neq \{0\}$ and $\lambda > 0$. Let $L := \ker(A) \cap \ker(B) = \{x \in X : Ax = 0, \Phi x = 0\}$ and denote the closed ball of X of center 0 and radius $r > 0$ by $B_X(0, r) = \{x \in X : \|x\|_X \leq r\}$. The rest of the proof is devided into three graded steps.

Step 1. *We prove that if $L = \{0\}$, then $\lim_{\|x\|_X \to +\infty} f(x) = +\infty$.*

By convexity of $\|\cdot\|_Y$,

$$\|y_1\|_Y^2 \leq 2(\|y_1 - y_2\|_Y^2 + \|y_2\|_Y^2)$$

for all $y_1, y_2 \in Y$. Therefore,

$$\|Ax - b\|_2^2 \geq \frac{1}{2}\|Ax\|_Y^2 - \|b\|_Y^2,$$

so that:

$$\|Ax - b\|_Y^2 + \lambda\|\Phi x\|_p \geq \frac{1}{2}\|Ax\|_Y^2 + \lambda\|\Phi x\|_p - \|b\|_Y^2.$$

Let

$$\mathbb{S}_X := \{x \in X : \|x\|_X = 1\}$$

denote the unit sphere of X and set $\eta := \min_{x \in \mathbb{S}_X} \frac{1}{2}\|Ax\|_Y^2 + \lambda\|\Phi x\|_p$. If $\eta = 0$, then,

$$\min_{x \in \mathbb{S}_X} \frac{1}{2}\|Ax\|_Y^2 + \lambda\|\Phi x\|_p = 0,$$

together with the assumptions on $\Im(A)$, $\Im(B)$ and λ, yields to the existence of $x^{\#} \in \mathbb{S}_X$ such that $\frac{1}{2}\left\|Ax^{\#}\right\|_Y^2 + \lambda\left\|\Phi x^{\#}\right\|_p = 0$. But $\|\cdot\|_Y$ and $\|\cdot\|_p$ are (quasi-)norms, so $x^{\#} = 0 \notin \mathbb{S}_X$. This is a contradiction. Hence, $\eta > 0$.

Next, for $\|x\|_X > 1$, we have:

$$\frac{1}{2}\|Ax\|_Y^2 + \lambda\|\phi x\|_p - \|b\|_Y^2 = \frac{1}{2}\|x\|_X^2 \left\|A\frac{x}{\|x\|_X}\right\|_Y^2 + \lambda\|x\|_X \left\|\Phi\frac{x}{\|x\|_X}\right\|_p - \|b\|_Y^2$$

$$> \|x\|_X \left(\frac{1}{2}\left\|A\frac{x}{\|x\|_X}\right\|_Y^2 + \lambda\left\|B\frac{x}{\|x\|_X}\right\|_p\right) - \|b\|_Y^2$$

$$\geq \eta\|x\|_X - \|b\|_Y^2.$$

Therefore, for all $x \in X$ such that $\|x\|_X > 1$,

$$f(x) = \|Ax - b\|_Y^2 + \lambda \|\Phi x\|_p > \eta \|x\|_X + \|b\|_Y^2$$

and the assertion follows, since $\eta > 0$ implies that the right hand-side goes to $+\infty$ as $\|x\|_X \to +\infty$.

Step 2. *We prove the assertion for $L = \{0\}$.*

Let $m := \inf_{x \in X} f(x)$. By Step 1, there exist $R > 0$ such that $f(x) > m + 1$ for $\|x\|_X > R$. $B_X(0, R)$ is compact and convex, and $\inf_{x \in X} f(x) = \inf_{x \in B_X(0,R)} f(x)$ by definition of R. Let $(x_j)_j \subseteq B_X(0, R)$ be a minimizing sequence. By compactness, it admits a converging subsequence and, without loss of generality, we may assume that $\lim_{j \to +\infty} x_j = x^\# \in B_X(0, R)$. By continuity, $f(x^\#) = \lim_{j \to +\infty} f(x_j) = m$.

Step 3. *We prove the assertion for $L \neq \{0\}$.*

Recall that $X = L \oplus L^\perp$, where the orthogonality is defined with respect to the inner product $\langle \cdot, \cdot \rangle_X$. By definition of direct sum, for all $x \in X$ there exist unique $x_1 \in L$ and $x_2 \in L^\perp$ such that $x = x_1 + x_2$. Observe that since $x_1 \in L$,

$$f(x) = \|Ax_2 - b\|_Y^2 + \lambda \|\Phi x_2\|_p = f(x_2).$$

In particular,

$$\inf_{x \in X} f(x) = \inf_{x \in L^\perp} f(x).$$

The restrictions of A and Φ to $L^\perp$ are linear mappings between vector spaces. We denote them with $A|_{L^\perp} L^\perp \to Y$ and $\Phi|_{L^\perp} : L^\perp \to Z$ respectively and set $f|_{L^\perp} : L^\perp \to Y$ as the restriction of f to $L^\perp$. Obviously,

$$f|_{L^\perp}(x) = \|A|_{L^\perp}x - b\|_Y^2 + \lambda \|\Phi|_{L^\perp}x\|_p = f(x)$$

for all $x \in L^\perp$, so that:

$$\inf_{x \in X} f(x) = \inf_{x \in L^\perp} f(x) = \inf_{x \in L^\perp} f|_{L^\perp}(x).$$

Obviously,

$$L^\perp := \ker(A|_{L^\perp}) \cap \ker(\Phi|_{L^\perp}) = \ker(A) \cap \ker(B) \cap L^\perp = L \cap L^\perp = \{0\}.$$

Therefore, by Step 2, it follows that there exists $x^\# \in L^\perp$ such that:

$$\inf_{x \in L^\perp} f|_{L^\perp}(x) = f|_{L^\perp}(x^\#).$$

This implies that:

$$\inf_{x \in X} f(x) = f|_{L^\perp}(x^\#) = f(x^\#),$$

since $x^\# \in L^\perp$. $\qquad\qquad\qquad\qquad\qquad\qquad\qquad\qquad\qquad\qquad\qquad\qquad\qquad$ $\square$

3.2   The weighted LASSO

Let $A \in \mathbb{R}^{m \times n}$, $b \in \mathbb{R}^m$ and $\tau_1, \ldots, \tau_n \geq 0$. We denote with $a_{*,j}$ the j-th column of A and set $b = (b_1, \ldots, b_m)$. We consider the constrained minimization problem:

$$minimize \quad \|Ax - b\|_2^2, \qquad x \in \mathbb{R}^n, \ |x_j| \leq \tau_j, \ j = 1, \ldots, n. \qquad (3.17)$$

We also assume that $\tau_j \neq 0$ for all $j = 1, \ldots, n$. In fact, if $\tau_j = 0$ for some $j = 1, \ldots, n$, then the solution $x = (x_1, \ldots, x_n)$ has $x_j = 0$. In this case, problem (3.17) reduces to

$$minimize \quad \left\| \tilde{A}y - b \right\|_2^2, \qquad y \in \mathbb{R}^{n-r}, \ |y_{i_j}| \leq \tau_{i_j}, \ j = 1, \ldots, n - r,$$

where $r = \text{card}\{j : \tau_j = 0\} \leq m$, $J = \{1 \leq i_1 < \ldots < i_{n-r} \leq n\} := \{j : \tau_j \neq 0\}$ and $\tilde{A} = (a_{*,j})_{j \in J} \in \mathbb{R}^{m \times (n-r)}$.

Let K denote the set of the feasible points of problem (3.17), that is:

$$K = \{x \in \mathbb{R}^n \ : \ |x_j| \leq \tau_j \ \forall j = 1, \ldots, n\}$$

and consider the Lagrange function associated to (3.17), i.e.

$$L(x, \lambda_1, \ldots, \lambda_n) = \|Ax - b\|_2^2 + \sum_{j=1}^n \lambda_j (|x_j| - \tau_j).$$

We are interested in a vector of Lagrange multipliers $\lambda^\# \succeq 0$ for (3.17). Based on the proofs of Theorem 3.4 and Corollary 3.8, $\lambda^\#$ can be chosen as the direction of any hyperplane separating the sets:

$$\mathcal{A} = \Big\{ (u, t) \in \mathbb{R}^n \times \mathbb{R} \ : \ u_l \geq |x_l| - \tau_l \ (l = 1, \ldots, n),$$
$$t \geq \|Ax - b\|_2^2 \text{ for some } x \in \mathbb{R}^n \Big\} \qquad (3.18)$$

and

$$\mathcal{B} = \Big\{ (0, t) \in \mathbb{R}^n \times \mathbb{R} \ : \ t < p^* \Big\} \qquad (3.19)$$

where $p^* := \inf_{x \in K} \|Ax - b\|_2^2$.

3.2.1   The scalar case

To clarify the general procedure, we focus on the simple case $m = n = 1$ first, in which (3.17) becomes:

$$minimize \quad (Ax - b)^2, \qquad x \in \mathbb{R}, \ |x| \leq \tau, \qquad (3.20)$$

where $A \in \mathbb{R} \setminus \{0\}$ and $b \in \mathbb{R}$. To find the Lagrange multipliers, we consider the set $\mathcal{G}$ of points $(u,t) \in \mathbb{R}^2$ that satisfy:

$$\begin{cases} u = |x| - \tau, \\ t = (Ax - b)^2, \end{cases}$$

which give a curve of the half-plane $U = \{(u,t) \in \mathbb{R}^2 \ : \ u \geq -\tau, \ t \geq 0\}$ parametrized by $x \in \mathbb{R}$. More precisely:

- if $x \geq 0$,
$$\begin{cases} x = u + \tau, \\ t = \big(A(u + \tau) - b\big)^2 = (Au + (A\tau - b))^2, \end{cases}$$
  which is a branch of parabola in U with vertex in $(\frac{b}{A} - \tau, 0)$.

- If $x < 0$
$$\begin{cases} x = -u - \tau, \\ t = \big(-A(u + \tau) - b\big)^2 = (Au + (A\tau + b))^2, \end{cases}$$
  which is, again, a branch of parabola in U, having its vertex in $(-\frac{b}{A} - \tau, 0)$.

Proposition 3.12. Let $\tau > 0$, $A \in \mathbb{R} \setminus \{0\}$, $b \in \mathbb{R}$. A Lagrange multiplier for (3.20) is given by:

$$\lambda^{\#} = \begin{cases} 2A^2(|b/A| - \tau) & \text{if } 0 < \tau < |b/A|, \\ 0 & \text{if } \tau \geq |b/A| \end{cases} = 2A^2(|b/A| - \tau)^+.$$

Namely, if $x^{\#}$ is a minimizer of (3.20), then it is also a minimizer for the problem:

$$minimize \quad (Ax - b)^2 + \lambda^{\#}|x|, \qquad x \in \mathbb{R}.$$

3.2.2   Properties of $\mathcal{A}$

Consider $A \in \mathbb{R}^{m \times n}$ and $b = (b_1, ..., b_m) \in \mathbb{R}^m$, with:

$$A = \begin{pmatrix} a_{11} & \cdots & a_{1n} \\ \vdots & \ddots & \vdots \\ a_{m1} & \cdots & a_{mn} \end{pmatrix}.$$

We consider the problem (3.17) and the associated Lagrange function:

$$L(x, \lambda) := \|Ax - b\|_2^2 + \sum_{j=1}^{n} \lambda_j(|x_j| - \tau_j).$$

Recall that p^* was defined as $p^* := \min_{x \in K} \|Ax - b\|_2^2$, being K the set of the points $x \in \mathbb{R}^n$ such that $|x_j| \leq \tau_j$ for all $j = 1, \ldots, n$. It is not difficult to verify that:

$$p^* = \inf \left\{ t \in \mathbb{R} \ : \ (u, t) \in \mathcal{G}, \ u_j \leq 0 \ \ \forall j = 1, \ldots, n \right\}. \qquad (3.21)$$

Let $\mathcal{M}_n$ be the set of the n-dimensional signature matrices, that are the diagonal matrices $S = (s_{ij})_{i,j=1}^n \in \mathbb{R}^{n \times n}$ such that $|s_{jj}| = 1$ for all $j = 1, \ldots, n$. Observe that if $S \in \mathcal{M}_n$, then $S^2 = I_{n \times n}$, where $I_{n \times n}$ denotes the identity matrix in $\mathbb{R}^{n \times n}$, in particular S is invertible with $S^{-1} = S$. If $x \in \mathbb{R}^n$ and $S \in \mathcal{M}_n$ is such that $Sx \in \prod_{j=1}^n [0, +\infty)$, we write $S \in \mathrm{sgn}(x)$.

Lemma 3.13. *Let $A \in \mathbb{R}^{m \times n}$, $b \in \mathbb{R}^m$ and $\tau_j > 0$ for $j = 1, \ldots, n$. Let $S \in \mathcal{M}_n$. There exists $u \in \prod_{j=1}^n [-\tau_j, 0]$ such that $ASu + AS\tau - b = 0$ if and only if $S \in \mathrm{sgn}(x)$ for some $x \in \mathbb{R}^n$ such that $Ax = b$ and $|x_j| \leq \tau_j$.*

Proof. Assume that there exists $u \in \prod_{j=1}^n [-\tau_j, 0]$ such that $ASu + AS\tau - b = 0$ and let $x := S(u + \tau)$. Then, $Sx = u + \tau \in \prod_{j=1}^n [0, \tau_j]$, so that $S \in \mathrm{sgn}(x)$, $|x_j| \leq \tau_j$ for all $j = 1, \ldots, n$ and

$$0 = AS(u + \tau) - b = Ax - b.$$

Vice versa, assume that $Ax = b$ for some $x \in \prod_{j=1}^n [0, \tau_j]$. Let $S \in \mathrm{sgn}(x)$ and $u := Sx - \tau$. Then, $u \in \prod_{j=1}^n [-\tau_j, 0]$ and

$$0 = Ax - b = A(Su + \tau) - b = ASu + AS\tau - b.$$

$\square$

Recall the definitions of the two sets $\mathcal{A}$ and $\mathcal{B}$ given in (3.18) and (3.19) respectively. First, if $\mathcal{G}$ is the set of the points $(u, t) \in \mathbb{R}^{n+1}$ such that:

$$\begin{cases} u_j = |x_j| - \tau_j & j = 1, \ldots, n, \\ t = \|Ax - b\|_2^2, \end{cases} \qquad (3.22)$$

for some $x \in \mathbb{R}^n$, then

$$\mathcal{A} = \mathcal{G} + [0, +\infty)^{n+1},$$

that is, $(u, t) \in \mathcal{A}$ if and only if

$$\begin{cases} u_j \geq |x_j| - \tau_j & j = 1, \ldots, n, \\ t \geq \|Ax - b\|_2^2, \end{cases} \qquad (3.23)$$

for some $x \in \mathbb{R}^n$. Finally, $(u, t) \in \mathcal{B}$ if and only if $t < p^* = \min_{x_j \leq \tau_j} \|Ax - b\|_2^2$.

We will prove that the equations (3.22) defining $\mathcal{G}$ can be written in terms of $\mathcal{M}_n$.

Lemma 3.14. *Let $\tau_1, \ldots, \tau_n > 0$ and let $\mathcal{G}$ be the set of points satisfying (3.22). Then,*

  (i) $\mathcal{G}$ is closed.

  (ii) $(u, p^*) \in \mathcal{G}$ for some $u \in \mathbb{R}^n$ such that $-\tau_j \leq u_j \leq 0$ for all $j = 1, \ldots, n$. Moreover, $p^* = \min \left\{ t \in \mathbb{R} \ : \ (u, t) \in \mathcal{G}, \ u_j \leq 0 \ \ \forall j = 1, \ldots, n \right\}$.

  (iii) For every $(u, t) \in \mathcal{G}$ there exists $S \in \mathcal{M}_n$ such that

$$t = \|ASu + (AS\tau - b)\|_2^2.$$

  Vice versa, if $t = \|ASu + (AS\tau - b)\|_2^2$ for some $u \in \mathbb{R}^n$ such that $u_j \geq -\tau_j$ and some $S \in \mathcal{M}_n$, then $(u, t) \in \mathcal{G}$.

Proof. We prove that $\mathcal{G}$ is closed. For, let $(u^k, t^k) \in \mathcal{G}$ converge to $(u, t) \in \mathbb{R}^{n+1}$. We prove that $(u, t) \in \mathcal{G}$. Let $x^k \in \mathbb{R}^n$ be such that (3.22) is satisfied for (u^k, t^k). Then, $|x_j^k| = u_j^k - \tau_j \leq u_j + 1 - \tau_j$ for j sufficiently large. In particular, the sequence $\{x^k\}_k$ is bounded and, thus, it converges up to subsequences. Without loss of generality, we may assume that $(x^k)_k$ converges to $x := \lim_{k \to +\infty} x^k$ in $\mathbb{R}^n$. Then, for all $j = 1, \ldots, n$,

$$|x_j| = \lim_{k \to +\infty} |x_j^k| = \lim_{k \to +\infty} u_j^k + \tau_j = u_j + \tau_j$$

and, by continuity,

$$\|Ax - b\|_2^2 = \lim_{k \to +\infty} \left\|Ax^k - b\right\|_2^2 = \lim_{k \to +\infty} t^k = t.$$

This proves that $(u, t) \in \mathcal{G}$ and, thus, that $\mathcal{G}$ is closed. (ii) follows by (i) and (3.21).

It remains to check (iii). If $(u, t) \in \mathcal{G}$, there exists $x \in \mathbb{R}^n$ satisfying (3.22). Let $S \in \mathcal{M}_n$ be such that $|x| = Sx$, where $|x| := (|x_1|, \ldots, |x_n|)$. Then, using the fact that $S^{-1} = S$,

$$|x| = u + \tau \quad \implies \quad Sx = (u + \tau) \quad \implies \quad x = S(u + \tau).$$

By the last equation of (3.22), we have:

$$t = \|Ax - b\|_2^2 = \|ASu + (AS\tau - b)\|_2^2.$$

Viceversa, assume that $t = \|ASu + (AS\tau - b)\|_2^2$ for some $S \in \mathcal{M}_n$ and $u \in \mathbb{R}^n$ is such that $u \succeq -\tau$. Let $x := S(u + \tau)$, then $|x_j| = |u_j + \tau_j| = u_j + \tau_j$ for all $j = 1, \ldots, n$ and $t = \|Ax - b\|_2^2$. This proves that $(u, t) \in \mathcal{G}$ and the proof of (iii) is concluded. $\square$

Lemma 3.15. *Let* $u \in \prod_{j=1}^{n}[-\tau_j, +\infty)$,

$$h_G(u) := \min_{S \in \mathcal{M}_n} \|ASu + AS\tau - b\|_2^2 \tag{3.24}$$

and

$$g_G(u) := \min_{(u,s) \in \mathcal{G}} s.$$

Then, $h_G(u) = g_G(u)$.

Proof. By Lemma 3.14 (iii), if $(u, s) \in \mathcal{G}$, then $s = \|AS_0u + AS_0\tau - b\|_2^2$ for some $S_0 \in \mathcal{M}_n$. Hence,

$$h_G(u) = \min_{S \in \mathcal{M}_n} \|ASu + AS\tau - b\|_2^2 \leq \|AS_0u + AS_0\tau - b\|_2^2 = s$$

for all s such that $(u, s) \in \mathcal{G}$. Taking the minimum, we get $h_G(u) \leq g_G(u)$. On the other hand, $(u, h_G(u)) \in \mathcal{G}$ by Lemma 3.14 (iii). Therefore, $g_G(u) \leq h_G(u)$ by definition of g_G. $\square$

Lemma 3.16. *Let* $\mathcal{G}$ *be the set of points satisfying (3.22) and* $\mathcal{A}$ *be the set of points satisfying (3.23). Then,*

(i) $\mathcal{G} \subseteq \mathcal{A}$;

(ii) $\mathcal{A}$ *is closed.*

Proof. (i) is obvious. We prove (ii).

Let $(u^k, t^k) \in \mathcal{A}$ be a sequence such that $(u^k, t^k) \xrightarrow[k \to +\infty]{} (u, t)$ in $\mathbb{R}^{n+1}$. We need to prove that $(u, t) \in \mathcal{A}$. For all k, let $x^k \in \mathbb{R}^n$ be such that:

$$\begin{cases} u_1^k \geq |x_1^k| - \tau_1, \\ \vdots \\ u_n^k \geq |x_n^k| - \tau_n, \\ t^k \geq \|Ax^k - b\|_2^2. \end{cases}$$

The sequence $\{x^k\}_k$ is bounded, in fact for all $j = 1, \ldots, n$, $|x_j^k| \leq u_j^k + \tau_j \leq u_j + 1 + \tau_j$ for k sufficiently large. Therefore, up to subsequences, we can assume $x^k \xrightarrow[k \to +\infty]{} x$ in $\mathbb{R}^n$. For all $j = 1, \ldots, n$,

$$|x_j| = \lim_{k \to +\infty} |x_j^k| \leq \lim_{k \to +\infty} u_j^k + \tau_j = u_j + \tau_j.$$

Moreover, by continuity,

$$\|Ax - b\|_2^2 = \lim_{k \to +\infty} \left\|Ax^k - b\right\|_2^2 \leq \lim_{k \to +\infty} t^k = t.$$

$\square$

Lemma 3.17. *Let $\mathcal{A}$ be the set of points satisfying (3.23).*

   (i) $\mathcal{A}$ is the epigraph of a convex non-negative function function

$$g : \prod_{j=1}^{n} [-\tau_j, +\infty) \to \mathbb{R}$$

   which is continuous in $\prod_{j=1}^{n}(-\tau_j, +\infty)$;

  (ii) $\partial g(0) \neq \emptyset$;

 (iii) $g(u) = 0$ if and only if $(u, t) \in \mathcal{A}$ for all $t \geq 0$.

Proof. First, observe that $\mathcal{A} \subseteq \{(u, t) \ : \ t \geq 0\}$ since $t \geq \|Ax - b\|_2^2 \geq 0$ for some $x \in \mathbb{R}^n$ whenever $(u, t) \in \mathcal{A}$.

For the sake of completeness, we check that $\mathcal{A}$ is the epigraph of the function:

$$g(u) = \min_{(u,s) \in \mathcal{A}} s, \qquad u \in \prod_j [-\tau_j, +\infty), \tag{3.25}$$

which is well defined by Lemma 3.16.

By the observation at the beginning of the proof, $g(u) \geq 0$. Let

$$epi(g) := \{(u, t) \ : \ t \geq g(u)\}$$

be the epigraph of g. If $(u, t) \in \mathcal{A}$, then $t \geq \min_{(u,s) \in \mathcal{A}} s = g(u)$, this means that $(u, t) \in epi(g)$. On the other hand, if $(u, t) \in epi(g)$, then $t \geq s$ for some $(u, s) \in \mathcal{A}$. But, if $t \geq s$ (and $(u, s) \in \mathcal{A}$), then $(u, t) \in \mathcal{A}$ as well, since $\mathcal{A}$ contains the vertical upper half-lines having their origins in (u, s), namely $(u, s) + (\{0\} \times [0, +\infty))$.

This proves that $\mathcal{A}$ is an epigraph. Moreover, g is convex because $\mathcal{A}$ is convex (see [111] Proposition 2.4). The continuity of g on $\prod_j(-\tau_j, +\infty)$ follows from [110], Theorem 10.1. This proves (i).

Moreover, since $\tau_j > 0$ for all $j = 1, \ldots, n$, $0 \in \mathbb{R}^n$ is an interior point of $\prod_j[-\tau_j, +\infty)$. Since g is continuous and convex in $\prod_j(-\tau_j, +\infty)$, the subdifferential of g in 0 is non-empty and (ii) follows.

To prove (iii), assume that $g(u) = 0$. Then, $\min_{(u,s) \in \mathcal{A}} s = 0$ implies $(u, 0) \in \mathcal{A}$. Since for all $t \geq 0$, $(u, 0) + (\{0\} \times [0, +\infty)) \in \mathcal{A}$, we have that $(u, t) \in \mathcal{A}$ for all $t \geq 0$. For the converse, assume that $(u, t) \in \mathcal{A}$ for all $t \geq 0$. Then, $(u, 0) \in \mathcal{A}$, so that (by the non-negativity of g) $0 \leq g(u) \leq 0$. This proves the equivalence in (iii). $\qquad\square$

Remark 3.18. As we observed in the general theory situation, $(0, s) \in \mathcal{A}$ if and only if $s \geq p^*$. This tells that $g(0) = p^*$ and $(0, p^*) \in \mathcal{A}$.

We want to prove formally that $g(u)$ defines the boundary $\partial \mathcal{A}$ of $\mathcal{A}$ in a neighborhood of $u = 0$ and, then, find an explicit formula for $g(u)$. Observe that, $\mathcal{A} = \partial \mathcal{A} \cup \mathring{\mathcal{A}}$, where $\mathring{\mathcal{A}}$ denotes the topologic interior of $\mathcal{A}$. Since $\mathcal{A}$ is closed and convex in $\mathbb{R}^n$, $\mathring{\mathcal{A}}$ coincides with the algebraic interior of $\mathcal{A}$, which is defined as follows:

Definition 3.19. Let X be a vector space and $\mathcal{A} \subseteq X$ be a subset. The *algebraic interior* of $\mathcal{A}$ is defined as:

$$\text{a-int}(\mathcal{A}) := \{a \in \mathcal{A} \ : \ \forall x \in X \ \exists \varepsilon_x > 0 \ s.t. \ a + tx \in \mathcal{A} \ \forall t \in (-\varepsilon_x, \varepsilon_x)\}.$$

Lemma 3.20. *Let $\mathcal{A}$ be as in Lemma 3.16. Then,*

$$\begin{aligned} \partial \mathcal{A} = &\{(u, t) \in \mathcal{A} \ : \ t = g(u), \ u_j > -\tau_j \ \forall j = 1, \ldots, n\} \cup \\ &\cup \{(u, t) \in \mathcal{A} \ : \ u_j = -\tau_j \ \text{for some } j = 1, \ldots, n\} \end{aligned} \qquad (3.26)$$

and the union is disjoint. Moreover,

$$\{(u, t) \in \mathcal{A} \ : \exists j = 1, \ldots, n, \ u_j = -\tau_j\} = \{(u, t) \in \partial \mathcal{A} : (u, t + \alpha) \in \partial \mathcal{A} \ \forall \alpha \geq 0\}.$$

Proof. Observe that the union in (3.26) is clearly disjoint. We first prove (3.26).

($\supseteq$) None of the sets on the RHS of (3.26) is contained in $\mathring{\mathcal{A}}$. In fact,

- the definition of $g(u)$ implies that for all $\varepsilon > 0$, $-\varepsilon < t < \varepsilon$, $(u, t) \in \mathcal{A}$ if and only if $t \geq 0$, so that $(u, g(u)) \notin \text{a-int}(\mathcal{A}) = \mathring{\mathcal{A}}$. This proves that the graph of g in $\prod_j (-\tau_j, +\infty)$ is a subset of $\partial \mathcal{A}$.

- Analogously, assume that $u_j = -\tau_j$ for some $j = 1, \ldots, n$, and for all $\varepsilon > 0$ consider the point (u_ε, t), where $(u_\varepsilon)_l = u_l$ for all $l \neq j$ and $(u_\varepsilon)_j = -\tau_j - \varepsilon$. But g is defined on $\prod_j [-\tau_j, +\infty)$ and $\mathcal{A}$ is its epigraph, hence all the points of $\mathcal{A}$ must be in the form $(u, g(u) + \alpha)$ for some $u \in \prod_j [-\tau_j, +\infty)$, $t = g(u) + \alpha$ ($\alpha \geq 0$), hence $(u_\varepsilon, t) \notin \mathcal{A}$ and this proves that $(u, t) \notin \text{a-int}(\mathcal{A})$.

The fact that $\partial \mathcal{A} = \mathcal{A} \setminus \mathring{\mathcal{A}}$ proves the first inclusion.

($\subseteq$) We prove that the complementary of the RHS of (3.26) in $\mathbb{R}^{n+1}$ is contained in $\mathring{\mathcal{A}}$. Let (u, t) be such that $u > -\tau_j$ for all j and $t > g(u)$ (as it is easy to check, these are the conditions for (u, t) to belong to the complementary of the union of the two set at the LHS of (3.26)).

Let $d := t - g(u) > 0$. Since g is continuous on $\prod_j (-\tau_j, +\infty)$, there exists $\delta > 0$ such that $|g(u) - g(v)| < d/4$ for all $v \in B_\delta(u) := \{w \in \mathbb{R}^n \ : \ |w - u| < \delta\}$. In particular, for all $v \in B_\delta(u)$, $g(v) < t - \frac{3}{4}d < t$. Then, $B_\delta(u) \times (t - \frac{3}{4}d, +\infty)$ is all contained in $\mathcal{A}$ (because $\mathcal{A}$ is the epigraph of g) and it is an open neighborhood of (u, t). Hence, $(u, t) \in \mathring{\mathcal{A}} = \mathcal{A} \setminus \partial \mathcal{A}$.

Next, we check the second part of the lemma:

($\subseteq$) assume $(u,t) \in \mathcal{A}$ is such that $u_j = -\tau_j$ for some j. Then, by the first part of this Lemma, $(u, t+\alpha) \in \partial\mathcal{A}$ for all $\alpha \geq 0$, since (3.26) is a partition of $\partial\mathcal{A}$.

($\supseteq$) Assume that $(u, t+\alpha) \in \partial\mathcal{A}$ for all $\alpha \geq 0$. Then, $(u,t) \in \partial\mathcal{A}$. Assume by contradiction that $u_j > -\tau_j$ for all j. Then, since (3.26) is a partition of $\partial\mathcal{A}$, $g(u) = t + \alpha$ for all $\alpha \geq 0$, which cannot be the case.

$\square$

The function g, defined in Lemma 3.17, is expressed in terms of the function h_G, as shown in the following result.

Theorem 3.21. *Let $\mathcal{A}$ be the set of points satisfying (3.23), h_G and g be the functions defined in (3.24) and (3.25), respectively. For $u \in \prod_{j=1}^{n}[-\tau_j, +\infty)$, $u = (u_1, \ldots, u_n)$, let $Q(u) := \prod_{j=1}^{n}[-\tau_j, u_j]$ and*

$$h(u) := \min_{S \in \mathcal{M}_n,\ v \in Q(u)} \|AS(v+\tau) - b\|_2^2 = \min_{v \in Q(u)} h_G(v). \qquad (3.27)$$

Then, $h(u) = g(u)$ for all $u \in \prod_j [-\tau_j, +\infty)$.

Proof. We first prove that $g(u) \leq h(u)$. For, it is enough to prove that $(u, h(u)) \in \mathcal{A}$, so that $g(u) \leq h(u)$ would follow by the definition of g. By definition of h, there exist $S_0 \in \mathcal{M}_n$ and $v \in Q(u)$ so that:

$$h(u) = \|AS_0 v + AS_0\tau - b\|_2^2.$$

By Lemma 3.14 (iii), $(v, h(u)) \in \mathcal{G}$. Since $u_j \geq v_j$ for all $j = 1, \ldots, n$, it follows that $(u, h(u)) \in \mathcal{A}$ by definition of $\mathcal{A}$.

For the converse, since $(u, g(u)) \in \mathcal{A}$, there exists $(v', t) \in \mathcal{G}$ such that $v'_j \leq u_j$ for all $j = 1, \ldots, n$ and $g(u) \geq t$. In particular, $v' \in Q(u)$. By Lemma 3.14 (iii), $t = \|AS_1 v' + AS\tau - b\|_2^2$ for some $S_1 \in \mathcal{M}_n$. Therefore,

$$g(u) \geq \|AS_1 v' + AS_1\tau - b\|_2^2 \geq \min_{S \in \mathcal{M}_n,\ v \in Q(u)} \|ASv + AS\tau - b\|_2^2 = h(u).$$

This concludes the proof.

$\square$

Even if $g = h$, in what follows we still distinguish h and g when we want to stress the explicit definitions of both. Namely, we write $g(u)$ when we refer to $\min_{(u,s) \in \mathcal{A}} s$ and $h(u)$ when we refer to (3.27).

Corollary 3.22. *Under the same notation as above,*

$$g(u) = \min_{-u-\tau \preceq v \preceq u+\tau} \|Av - b\|_2^2.$$

Proof. Using the second expression in (3.27),

$$g(u) = \min_{S \in \mathcal{M}_n} \min_{v \in Q(u)} \|AS(v+\tau) - b\|_2^2.$$

But,

$$f_S(v) = \|AS(v+\tau) - b\|_2^2 = f(S(v+\tau)),$$

for $f(v) = \|Av - b\|_2^2$, that gives:

$$\min_{-\tau \preceq v \preceq u} f_S(v) = \min_{v \in Q(u)} f(S(v+\tau)) = \min_{v \in S(Q(u)+\tau)} \|Av - b\|_2^2,$$

so that:

$$\min_{S \in \mathcal{M}_n} \min_{-\tau \preceq v \preceq u} f_S(v) = \min_{\bigcup_{S \in \mathcal{M}_n} S(Q(u)+\tau)} \|Av - b\|_2^2$$

and the assertion follows by observing that

$$\bigcup_{S \in \mathcal{M}_n} S(Q(u) + \tau) = \{v \in \mathbb{R}^n : -u - \tau \preceq v \preceq u + \tau\}.$$

$\square$

3.2.3   A result under conditions on the gradient of the fidelity

In general, the geometry of $\mathcal{A}$ is so complicated that expressing g explicitly may turn into a tough task. Nevertheless, it is obvious that if u is itself one of the minimizers of (3.27), then $g(u) = h_G(u) = \min_{S \in \mathcal{M}_n} \|ASu + AS\tau - b\|_2^2$. So, under further assumptions on $\nabla(\|ASu - b\|_2^2)$ granting the equality $g(u) = h_G(u)$ holds in a neighborhood of 0, we can compute explicitly the Lagrange multipliers.

Theorem 3.23. *Let $f(v) = \|Av - b\|_2^2$ and assume that for all $k = 1, \ldots, n$ the condition:*

$$\sum_{j=1}^n u_j \langle a_{*,j}, a_{*,k} \rangle \le \langle b, a_{*,k} \rangle \qquad (-\tau \preceq u \preceq \tau) \tag{3.28}$$

holds. Then, $g(u) = f(u+\tau)$ for all $u \in Q(0)$ and $\lambda^\# = A^T(b - A\tau)$ is a set of Lagrange multipliers for problem (3.17).

Proof. The set of conditions (3.28) is equivalent to $(Au - b)^T A \preceq 0$ for all $-\tau \preceq u \preceq \tau$, that is $\nabla f(u) \preceq 0$ for $-\tau \preceq u \preceq \tau$. We prove that, under this further

condition, $g(u) = f(u + \tau)$ for all $u \in Q(0)$. Let $u \in Q(0)$ and $\mathfrak{n} \succ 0$ be a unit vector. For all $t \in \mathbb{R}$, define:

$$f_{\mathfrak{n}}(t) := f(u + \tau + t\mathfrak{n}) = \|A(u + \tau + t\mathfrak{n}) - b\|_2^2$$
$$= \|A\mathfrak{n}\|_2^2 \, t^2 + 2\langle A(u + \tau) - b, A\mathfrak{n}\rangle t + \|A(u + \tau) - b\|_2^2,$$

which is the restriction of f to the line $\{u + t\mathfrak{n} : t \in \mathbb{R}\}$. If $\mathfrak{n} \in \ker(A)$, then $f_{\mathfrak{n}} \equiv 0$ and it has a global minimum in $t = 0$. Assume $\mathfrak{n} \notin \ker(A)$. The intersection of this line with $\{-\tau \preceq v \preceq \tau\}$ is contained in $(-\infty, 0]$. If we prove that, for all $\mathfrak{n} \succ 0$, $f_{\mathfrak{n}}$ has a constrained minimum in $t = 0$, we get the first assertion. For, it's enough to observe that

$$f'_{\mathfrak{n}}(0) = \nabla f(u + \tau) \cdot \mathfrak{n} \leq 0,$$

because if $u \in Q(0)$, then $\{-u - \tau \preceq v \preceq u + \tau\} \subseteq \{-\tau \preceq v \preceq \tau\}$. This proves that $g(u) = f(u + \tau)$ for all $u \in Q(0)$. In particular,

$$-\nabla g(0) = -\nabla f(\tau) = (b - A\tau)^T A \succeq 0$$

is a set of Lagrange multipliers for (3.17).   □

Remark 3.24. It is not difficult to generalize Theorem 3.23 a bit further. If the hyperparallelogram $\{-\tau \preceq u \preceq \tau\}$ is all contained in the region $\{u \in \mathbb{R}^n : S\nabla f(u) \preceq 0\}$ for some $S \in \mathcal{M}_n$, then $g(u) = f(S(u + \tau))$ for all $u \in Q(0)$ and

$$\lambda^{\#} = -\nabla g(0) = -S\nabla f(S(u + \tau))^T$$

defines a vector of Lagrange multipliers for (3.17). The proof goes exactly as in Theorem 3.23.

3.2.4   Decoupling the variables

In this subsection, we focus on the situation in which $A^T A$ is a diagonal matrix. Since:

$$A^T A = \begin{pmatrix} \|a_{*,1}\|_2^2 & \langle a_{*,1}, a_{*,2}\rangle & \dots & \langle a_{*,1}, a_{*,n}\rangle \\ \langle a_{*,2}, a_{*,1}\rangle & \|a_{*,2}\|_2^2 & \dots & \langle a_{*,2}, a_{*,n}\rangle \\ \vdots & \vdots & \ddots & \vdots \\ \langle a_{*,n}, a_{*,1}\rangle & \langle a_{*,n}, a_{*,2}\rangle & \dots & \|a_{*,n}\|_2^2 \end{pmatrix}$$

and the rank of $A^T A$ is equal to that of A, it follows that in this case:

$$A^T A = \mathrm{diag}(\|a_{*,1}\|_2^2, ..., \|a_{*,n}\|_2^2). \tag{3.29}$$

Remark 3.25. If $m \leq n$ and $A^T A$ is diagonal, $n - m$ of the norms in (3.29) above vanish. In this case, we assume that $a_{*,m+1} = ... = a_{*,n} = 0$, so that A can be written in terms of its columns as:

$$A = \left(A' | 0_{m \times (n-m)}\right),$$

where $A' = (a_{*,1}|...|a_{*,m}) \in \mathrm{GL}(m,\mathbb{R})$. Observe that:

$$\|Ax - b\|_2^2 = \|A'x' - b\|_2^2,$$

where $x' = (x_1, ..., x_m)^T$, so that $x^\#$ is a mimizer of (3.17) if and only if $(x^\#)' = (x_1^\#, \ldots, x_m^\#)$ is a minimizer of the problem:

$$minimize \quad \|A'y - b\|_2^2, y \in \mathbb{R}^m, \ |y_j| \leq \tau_j, \ j = 1, \ldots, m, \qquad (3.30)$$

under the further condition that the remaining coordinates of x vanish.

For this reason, for the rest of this subsection, we focus on (3.30), both for the cases $n \leq m$ and $m \leq n$, and provide the Lagrange multipliers.

Remark 3.26. We point out that in this situation the Lagrange multipliers can be computed directly from Proposition 3.12. Indeed, under the *orthogonality* assumption on A, the target function in problem (3.30) becomes:

$$\sum_{j=1}^m (\|a_{*,j}\|_2^2 \, y_j^2 - 2y \langle a_{*,j}, n \rangle y_j) + \|b\|_2^2.$$

Since the variables of all the addenda are decoupled, and the addenda are non-negative,

$$\min_y \sum_{j=1}^m (\|a_{*,j}\|_2^2 y_j^2 - 2y \langle a_{*,j}, n \rangle y_j) + \|b\|_2^2$$

$$= \sum_{j=1}^m \min_{y_j} \left(\|a_{*,j}\|_2^2 \, y_j^2 - 2y \langle a_{*,j}, n \rangle y_j + \frac{\|b\|_2^2}{m} \right)$$

and a minimizer of (3.30) is also a minimizer of the problem:

$$minimize \quad \|a_{*,j}\|_2^2 \, y_j^2 - 2y \langle a_{*,j}, n \rangle y_j + \frac{\|b\|_2^2}{m}, \qquad |y_j| \leq \tau_j$$

for all $j = 1, ..., m$. In other words, it is enough to treat (3.30) as m 1-dimensional constrained minimization problems. However, our interest is testing the tools presented in the previous section, computing the function g and the separating hyperplane.

To exhibit a vector of Lagrange multipliers, we start by the set

$$\mathcal{G} := \{(u,t) \in \mathbb{R}^{m+1} : \exists y \in \mathbb{R}^m, \ u_j = |y_j| - \tau_j \ (j = 1, \ldots, m), \ t = \|A'y - b\|_2^2\}.$$

By Lemma 3.14 (iii), $(u,t) \in \mathcal{G}$ if and only if $u \succeq -\tau$ and $t = \|A'S(u+\tau) - b\|_2^2$ for some $S \in \mathcal{M}_m$. Let $f_S(u) = \|A'S(u+\tau) - b\|_2^2$ and observe that:

$$f_S(u) = \sum_{j=1}^m \|a_{*,j}\|_2^2 \, (u_j + \tau_j)^2 - 2 \sum_{j=1}^m s_{jj} \langle b, a_{*,j} \rangle (u_j + \tau_j) + \|b\|_2^2.$$

The functions f_S are the equivalent of the parabolas in the 1-dimensional case and they describe elliptic paraboloids. As it clear by Subsection 3.2.1, we need to understand what is $h_G(u) := \min_{S \in \mathcal{M}_m} f_S(u)$. Observe that for all $S \in \mathcal{M}_n$,

$$f_S(u) \geq \sum_{j=1}^m \|a_{*,j}\|_2^2 (u_j + \tau_j)^2 - 2 \sum_{j=1}^m |\langle b, a_{*,j} \rangle| (u_j + \tau_j) + \|b\|_2^2 = f_{S_\beta}(u),$$

where $S_\beta = (s_j^\beta)_{j=1}^m \in \mathcal{M}_m$ is a diagonal matrix such that $s_j^\beta \langle b, a_{*,j} \rangle \geq 0$.

Lemma 3.27. *Under the notation and the assumptions of this subsection,*

$$h_G(u) = f_{S_\beta}(u) = \sum_{j=1}^m \|a_{*,j}\|_2^2 (u_j + \tau_j)^2 - 2 \sum_{j=1}^m |\langle b, a_{*,j} \rangle| (u_j + \tau_j) + \|b\|_2^2.$$

h_G defines an elliptic paraboloid whose vertex $V = (c,0) \in \mathbb{R}^{m+1}$ is characterized both by $c = -\tau + S_\beta (A')^{-1} b$ and

$$c_j = -\tau_j + \frac{|\langle b, a_{*,j} \rangle|}{\|a_{*,j}\|_2^2}$$

($j = 1, \ldots, m$). Moreover,

$$h_G(u) = \sum_{j=1}^m \|a_{*,j}\|_2^2 (u_j - c_j)^2.$$

Proof. We already proved the first part of the Lemma. We only need to compute the vertex of f_{S_β}. For, observe that the minimum of f_{S_β} is $(c, 0)$, where c satisfies $f_S(c) = 0$. This equation is satisfied if and only if $c = -\tau + S_\beta (A')^{-1} b$. Moreover, the minimum of f_{S_β} is also characterized by $\nabla f_{S_\beta}(c) = 0$, that is:

$$c_j + \tau_j - \frac{|\langle b, a_{*,j} \rangle|}{\|a_{*,j}\|_2^2} = 0$$

($j = 1, \ldots, m$). Finally, using the first characterization of c,

$$h_G(u) = \|AS_\beta(u + \tau) - b\|_2^2 = \|AS_\beta(u - c) + AS_\beta(c + \tau) - b\|_2^2$$

$$= \|AS_\beta(u - c)\|_2^2 = \sum_{j=1}^m \|a_{*,j}\|_2^2 (u_j - c_j)^2.$$

This concludes the proof. $\square$

In order to compute the Lagrange multipliers for the decoupled problem, we observe that $\mathcal{A} + [0, +\infty)^{m+1}$ is the epigraph of the function $g(u)$ whose first properties are proved in Lemma 3.17. Hence, this function describes the lower boundary of $\mathcal{A}$, that is the part of $\mathcal{A}$ we need to compute a separating hyperplane. By (3.27), $g(u) = \min_{v \in Q(u)} h_G(v)$, where $Q(u) = \prod_{j=1}^m [-\tau_j, u_j]$.

Theorem 3.28. *Under the notation and the assumptions of this subsection,*

$$g(u) = h_G(Pu),$$

where $P : \prod_{j=1}^{m}[-\tau_j, +\infty) \to Q(c)$ *is the projection defined by*

$$(Pu)_j = \begin{cases} u_j & \text{if } -\tau_j \leq u_j \leq c_j, \\ c_j & \text{if } u_j > c_j \end{cases} = \min\{c_j, u_j\}, \qquad j = 1, \dots, m,$$

$u \in \prod_{j=1}^{m}[-\tau_j, +\infty)$. *Explicitly, under the assumptions of this subsection,*

$$g(u) = \sum_{j=1}^{m} \|a_{*,j}\|_2^2 (u_j - c_j)^2 \chi_{[-\tau_j, c_j]}(u_j). \tag{3.31}$$

In particular, $g \in \mathcal{C}^1(\prod_{j=1}^{n}(-\tau_j, +\infty))$ *with:*

$$\frac{\partial g}{\partial u_j}(u) = 2 \|a_{*,j}\|_2^2 (u_j - c_j) \chi_{[-\tau_j, c_j]}(u_j) \tag{3.32}$$

for all $u \in \prod_{j=1}^{n}(-\tau_j, +\infty)$.

Proof. Obviously, P is a projection of $\prod_{j=1}^{n}[-\tau_j, +\infty)$ onto $Q(c)$. For all $j = 1, \dots, m$,

$$\operatorname{argmin}_{-\tau_j \leq v_j \leq u_j} \|a_{*,j}\|_2^2 (v_j - c_j)^2 = \begin{cases} u_j & \text{if } -\tau_j \leq u_j \leq c_j, \\ c_j & \text{otherwise} \end{cases} = (Pu)_j.$$

Hence,

$$g(u) = \min_{v \in Q(u)} h_G(v) = \sum_{j=1}^{m} \min_{-\tau_j \leq v_j \leq u_j} \|a_{*,j}\|_2^2 (v_j - c_j)^2 =$$

$$= \sum_{j=1}^{m} \|a_{*,j}\|_2^2 ((Pu)_j - c_j)^2 = h_G(Pu).$$

The explicit definition of Pu gives (3.31) and (3.32). The differentiability and formula (3.32) are obvious by the expression (3.31) of g. $\qquad\square$

Remark 3.29. As a consequence of Theorem 3.28,

$$p^* = g(0) = \sum_{j=1}^{m} \|a_{*,j}\|_2^2 \left(-\tau_j + \frac{|\langle b, a_{*,j} \rangle|}{\|a_{*,j}\|_2^2} \right)^2 \chi_{[-\tau_j, c_j]}(0).$$

Then, observe that:

$$-\tau_j \leq 0 \leq -\tau_j + \frac{|\langle b, a_{*,j} \rangle|}{\|a_{*,j}\|_2^2} \quad \Longleftrightarrow \quad 0 \leq \tau_j \leq \frac{|\langle b, a_{*,j} \rangle|}{\|a_{*,j}\|_2^2}, \tag{3.33}$$

so that:

$$p^* = \sum_{j=1}^{m} \|a_{*,j}\|_2^2 \left(-\tau_j + \frac{|\langle b, a_{*,j}\rangle|}{\|a_{*,j}\|_2^2} \right)^2 \chi_{\left[0, \frac{|\langle b, a_{*,j}\rangle|}{\|a_{*,j}\|_2^2}\right]}(\tau_j).$$

Theorem 3.30. *Under the notation of this subsection, the vector $\lambda^{\#} \in [0, +\infty)^m$ given by*

$$\lambda_j^{\#} = 2 \|a_{*,j}\|_2^2 \left(\frac{|\langle b, a_{*,j}\rangle|}{\|a_{*,j}\|_2^2} - \tau_j \right)^+$$

defines a vector of Lagrange multipliers for (3.30).

Proof. We apply (3.32) to $u = 0$ and use (3.33). Namely,

$$t = p^* + \langle \nabla g(0), u \rangle$$

is the tangent hyperplane of g in $u = 0$, which is also the hyperplane that separates $\mathcal{A}$ and $\mathcal{B}$. The direction of this hyperplane is $(\nabla g(0), -1)$, so that:

$$\lambda^{\#} = -\nabla g(0),$$

i.e., the assertion. $\square$

Remark 3.31. As far as the original problem (3.17) with $m \leq n$ is concerned, we get the Lagrange multipliers for free by Theorem 3.30 simply observing that if $A = (a_{*1}|\ldots|a_{*m}|0|\ldots|0) \in \mathbb{R}^{m\times n}$, $A' = (a_{*1}|\ldots|a_{*m})$ and $x = (x', x'') \in \mathbb{R}^m \times \mathbb{R}^{n-m}$, then

$$\min_{x \in \mathbb{R}^n} \|Ax - b\|_2^2 + \sum_{j=1}^{n} \lambda_j(|x_j| - \tau_j) = \min_{x' \in \mathbb{R}^m} \|A'x' - b\|_2^2 + \sum_{j=1}^{m} \lambda_j(|x_j'| - \tau_j) +$$

$$+ \underbrace{\min_{x'' \in \mathbb{R}^{n-m}} \sum_{j=m+1}^{n} \lambda_j(|x_j| - \tau_j)}_{= -\sum_{j=m+1}^{n} \lambda_j \tau_j},$$

so that, if $\lambda^{\#} \in \mathbb{R}^m$ defines a vector of Lagrange multipliers for (3.30), then $(\lambda^{\#}|0) \in \mathbb{R}^m \times \mathbb{R}^{n-m}$ defines a vector of Lagrange multipliers for (3.17).

3.2.5   Explicit solution

The conditions $|x_j| \leq \tau_j$ are equivalent to $x_j^2 \leq \tau_j^2$. Under this point of view, (3.17) can be restated as:

$$minimize \quad \|Ax - b\|_2^2, \qquad x_j^2 \leq \tau_j^2, \tag{3.34}$$

that can be interpreted as a weighted Tikhonov problem. Assume that $\lambda^{\#}$ is a vector of Lagrange multipliers for (3.17) or, equivalently, for (3.34). We are interested in computing

$$x^{\#} = \arg\min_{x} L(x, \lambda),$$

where L is the Lagrange function associated to (3.34), i.e.

$$L(x, \lambda^{\#}) = \|Ax - b\|_2^2 + \sum_{j=1}^{n} \lambda_j^{\#}(x_j^2 - \tau_j^2).$$

Since $L \in \mathcal{C}^{\infty}(\mathbb{R}^n)$ and it is convex, they satisfy $\nabla L(x, \lambda^{\#}) = 0$, that is:

$$(A^T A + \Delta_\lambda)x = A^T b,$$

where $\Delta_\lambda = \text{diag}(\lambda_1^{\#}, ..., \lambda_n^{\#})$. Hence, $x^{\#}$ satisfies:

$$(A^T A + \Delta_\lambda)x^{\#} = A^T b, \tag{3.35}$$

that is, $x^{\#} \in (A^T A + \Delta_\lambda)^{-1} A^T b$.

Remark 3.32. Another way to compute the Lagrange multipliers associated to (3.17), or equivalently to (3.34), can be by means of strong duality condition, namely using:

$$\lambda^{\#} = \arg\max_{\lambda \succeq 0} \min_{x} L(x, \lambda).$$

However, we stress that the explicit value of $\min_x L(x, \lambda)$ is still hard to compute since the implicit relation (3.35) satisfied by $x^{\#}$ cannot be made explicit by means of Dini's theorem.

3.3 Applications

Despite the apparently heavy assumptions on A, Theorem 3.30 has itself interesting applications. For instance, it can be applied to denoising problems, where $A = I_{n \times n}$, i.e., problems in the form:

$$minimize \quad \|x - b\|_2^2, \qquad x \in \mathbb{R}^n, \ |x_j| \leq \tau_j, \ j = 1, \ldots, n. \tag{3.36}$$

By Theorem 3.30, $\lambda^{\#} = (\lambda_j^{\#})_{j=1}^n$ is a vector of Lagrange multipliers for (3.36), where:

$$\lambda_j^{\#} = 2(|b_j| - \tau_j)^+. \tag{3.37}$$

We can also apply Theorem 3.30 to the discrete Fourier transform, i.e., given a noisy fully-sampled signal $b \in \mathbb{C}^n$, we want to find a vector $z \in \mathbb{C}^n$ such that $\|\Phi z - b\|_2^2$ is minimized under the constrains $|z_j| \leq \tau_j$, where $\Phi \in \mathbb{C}^{n \times n}$ denotes

the (complex) DFT matrix. Since $\Phi^*\Phi = I_{n\times n}$, we can apply Theorem 3.30 to deduce that a set of Lagrange multipliers for this problem is:

$$\lambda_j^{\#} = 2\Big(|\langle b, \phi_{*,j}\rangle| - \tau_j\Big)^{+},$$

$(j = 1, \dots, n)$, being $\phi_{*,j}$ the j-th column of Φ.

The question that naturally arises in the applications is whether the dependence of $\lambda_1, \dots, \lambda_n$ on $\tau_1, \dots, \tau_n$ can be a critical issue in the applicability of the theory. Indeed, $\tau_1, \dots, \tau_n$ are upper bounds for $|x_1|, \dots, |x_n|$ respectively, which are not available in the practice. However, whenever it is possible to estimate these local upper bounds, our result may lead to high-quality imaging perfomances. For instance, for denoising, (3.37) may be approximated by replacing $\tau_1, \dots, \tau_n$ with the voxel values obtained by applying a Gaussian filter (or other types of filtering) to the noisy image. This opens the question of which filtering technique could lead to optimal approximations of the $\tau_1, \dots, \tau_n$ depending on the field of research in which (3.17) can be implemented. We intend to investigate this topic in the immediate future.

An iterative algorithm to compute tuning parameters

In Section 4.1, we discuss the theoretical model underlying the approximation of Lagrange multipliers, outline the main challenges, and describe the MRI model used in our experiments. In Section 4.2, we present our experiment and ALMA, detailing the metrics employed for data analysis. Section 4.3 presents the results, while Section 4.4 provides a comprehensive discussion.

This chapter has been published on arXiv in 2024, cf. [59].

4.1 Theoretical model

4.1.1 Mathematical rationale

Within the domain of MRI, Lustig and colleagues [87, 86, 34, 120, 119] pioneered the applications of both LASSO and g-LASSO. The purpose of this section is to motivate our conjecture that Lagrange multipliers could be used as effective tuning parameters for imaging reconstruction with g-LASSO.

As we discussed in Chapter 3, the constrained LASSO problem

$$minimize \qquad \|x\|_1 \text{ subject to } x \in \mathbb{R}^n, \ \|Ax - b\|_2 \leq \eta \qquad (4.1)$$

has many equivalent formulations, where the equivalence notion is specified in [49, Proposition 3.2]. We limit ourselves to delineate the relationship between the constrained LASSO (4.1) and its unconstrained counterpart:

$$minimize \qquad \frac{1}{2}\|x\|_1 + \frac{\lambda}{2}\|Ax - b\|_2^2. \qquad (4.2)$$

Theorem 4.1. *Let* $A \in \mathbb{R}^{m \times n}$, $b \in \mathbb{R}^m$ *and* $\eta > 0$. *Let* $x^{\#}$ *be a minimizer of the constrained LASSO* (4.1). *Then, there exists* $\lambda' \geq 0$ *such that* $x^{\#}$ *is also a minimizer of* (4.2) *with* $\lambda = \lambda'$. *Conversely, if* $x^{\#}$ *is a minimizer of* (4.2), *there exists* $\eta' \geq 0$ *such that* $x^{\#}$ *is also a minimizer of* (4.1) *with* $\eta = \eta'$.

Consequently, solving (4.2) with the corresponding Lagrange multiplier provides a rank(A)-sparse solution. Theorem 4.1 holds also for g-LASSO:

$$minimize \qquad \frac{1}{2}\|Ax - b\|_2^2 + \frac{\lambda}{2}\|\Phi x\|_1, \qquad (4.3)$$

the rescaling by the factor $1/2$ is needed for computational purposes, but it is irrelevant to the analysis of (4.3). Also, observe that (4.3) with $\lambda \neq 0$ is equivalent to:

$$minimize \qquad \frac{1}{2}\|\Phi x\|_1 + \frac{\lambda}{2}\|Ax - b\|_2^2, \qquad (4.4)$$

where the equivalence follows by choosing $\lambda^* = \lambda^{-1}$.

4.1.2   Construction of Lagrange multipliers

The construction of a Lagrange multiplier is detailed in the proof of [11, Theorem 4.8], which uses Hahn-Banach theorem to find a hyperplane that separates two convex sets, which for (4.4) read as: the epigraph $\mathcal{A} = \Big\{(u,t) \in \mathbb{R}^2 : u \geq \frac{1}{2}\|Ax - b\|_2^2 - \frac{\eta^2}{2},\ t \geq \frac{1}{2}\|\Phi x\|_1\ for\ some\ x \in \mathbb{R}^n\Big\}$ and the lower half-line $\mathcal{B} = \Big\{(0,t) \in \mathbb{R}^2 : t < p^*\Big\}$, where $p^* = \min\{\|\Phi x\|_1 : \|Ax - b\|_2 \leq \eta\}$ (see fig. 4.1).
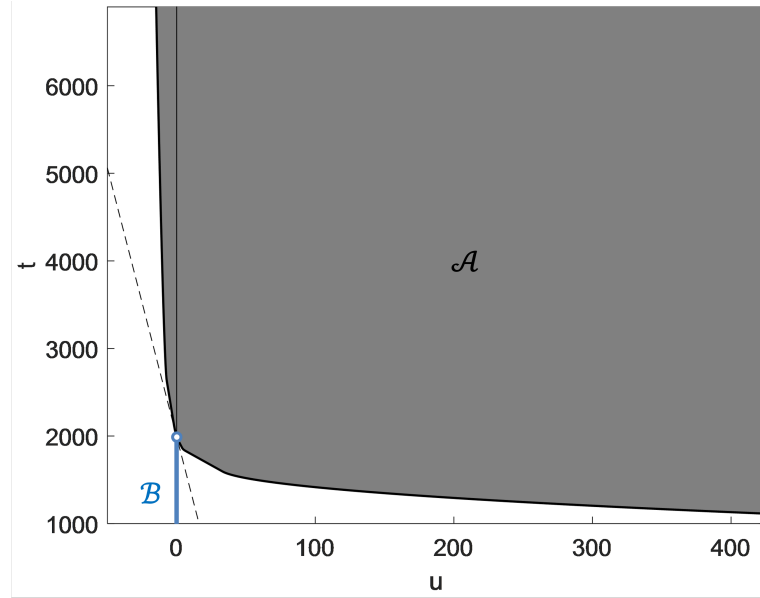

Figure 4.1: A graphic representation of the sets $\mathcal{A}$ and $\mathcal{B}$, and the separating hyperplane (dashed line). Observe that $\mathcal{A}$ is an epigraph and $\mathcal{B}$ is an open lower half-line. The closure of $\mathcal{B}$ intersects the boundary of $\mathcal{A}$.

In the particular case of g-LASSO, separating hyperplanes are lines, and if $t = mu + q$ is any separating line, then a Lagrange multiplier can be chosen as $\lambda^* = -m$ or, equivalently, $\lambda = -1/m$. Let us observe that set $\mathcal{B}$ serves no essential purpose in determining a separating line, as it merely constitutes a lower half-line intersecting $\mathcal{A}$ at its boundary. Additionally, when the lower boundary of $\mathcal{A}$ is $\mathcal{C}^1$ regular in a neighborhood of $u = 0$, a numerical approach enables the identification of a separating line by delineating $\mathcal{A}$ and computing the tangent at 0 along the graph of its boundary.

4.1.3 Main challenges

A direct application of the theory described so far for deriving tuning parameters poses three main challenges.

- **Necessity of numerical methods:** in the vast majority of convex optimization problems, the expression of the dependence $\lambda = \lambda(x^{\#})$ or even $\lambda = \lambda(\eta)$, is a challenging task. We refer to [60] for examples of weighted LASSO problems where this relation is instead explicit. Hence, finding a Lagrange multiplier with the construction in [11] requires a separating line to be found numerically.

- **Unknown constraints:** theoretically, the numerical machinery described above necessitates prior knowledge of $\eta = \|Ax^{\#} - b\|_2$, where $x^{\#}$ is the solution of g-LASSO. Consequently, the cylinder $\Gamma_\eta = \{x : \|Ax - b\|_2 \leq \eta\}$ is not only unknown, but it depends heavily on the outcome of g-LASSO.

- **Dimensionality:** outlining $\mathcal{A}$ or its boundary necessitates plotting ∞^n points in $\mathbb{R}^2$, rendering it an impractical endeavor.

While acknowledging the necessity of numerical analysis, we may resort to an escamotage to overcome the two remaining challenges. However, this entails abandoning the pursuit of exact Lagrange multipliers in favor of approximations. The constraint bound η depends intrinsically on the solution $x^{\#}$ of g-LASSO, which in general differs from the ground truth f which, in the case of our experimental setting, consists of the Shepp-Logan phantom (see fig. 4.3 (A)).

Defining a constrained bound η induces a solution $x^{\#}$ and reversely, a given solution $x^{\#}$ sets the constraint bound η. In practice the solution $x^{\#}$ is of course unknown and it is a subtle task to choose η appropriately so that the solution $x^{\#}$ is, hopefully, as close as possible to the ground truth. Choosing η is equivalent to choosing the allowed amount of error on the raw data. It follows that η must be at least as large as the noise amplitude. Other sources of error can also add to the noise so that in general η may be larger than the noise amplitude. This being said, in the present study, we chose to set η to be equal to the norm of the added noise

$$\eta = \|Af - b\|_2 = \|\varepsilon\|_2.$$

This situation is still far from concrete, since $\|\varepsilon\|_2$ is not known in the practice. However, we note that the purpose of the present study is to present an ideal situation to test if it is possible to use approximations of Lagrange multipliers as well-performing tuning parameters for generalized LASSO problems, shifting the focus from selecting the tuning parameter to estimating the noise energy.

Consequently, the tuning parameter returned by ALMA serves as an *approximate Lagrange multiplier*, rather than the exact one. Achieving this approximation involves outlining the corresponding epigraph $\mathcal{A}$. The essence of ALMA lies in a technicality allowing for the approximation of $\mathcal{A}$ by sketching infinitely many of its points simultaneously, as outlined below.

4.1.4   The MRI model

For the sake of concreteness, we simulate the reconstruction of a MR signal. Let us spend a few words about how g-LASSO is used, and why the correct choice of λ is fundamental, in the context of MRI. Roughly speaking, the (inverse) spatial Fourier transform of the MR signal is the anatomical image of a tissue, which is supported in a cube $[-L_x/2, L_x/2] \times [-L_y/2, L_y/2] \times [-L_z/2, L_z/2]$. By Shannon's theorem full Cartesian (uniform) sampling consists of sampling n_x points in the k_x direction, n_y points along the k_y direction and n_z points along the k_z direction of the k-space, where:

$$\Delta x = \frac{L_x}{n_x}, \ \ \Delta y = \frac{L_y}{n_y}, \ \ \Delta z = \frac{L_y}{n_z},$$

and

$$\Delta k_x = \frac{1}{L_x}, \ \ \Delta k_y = \frac{1}{L_y}, \ \ \Delta k_z = \frac{1}{L_z},$$

we mention [90] as reference therein.

For various reasons, sampling the MRI signal at its Nyquist frequency poses several challenges, necessitating techniques that can accurately reconstruct the MRI signal from samples taken below the Nyquist frequency. First, in our 2D experiments the dimensionality of the problem is of the order of $n = n_x n_y = 384^2 \sim 10^5$. For a 3D image, it increases to $n = n_x n_y n_z \sim 10^8$, making the processing of the MRI signal extremely time-consuming and computationally expensive. Secondly, MRI requires patients to remain still throughout the entire acquisition process, making it challenging to image moving organs and to perform scans on patients with conditions such as movement disorders. Furthermore, MRI

is extremely expensive, and reducing the amount of information to be acquired can lead to significant cost savings.

In light of these reasons, CS offers a valuable solution for reducing both acquisition time and computational costs. However, there are situations where CS transcends being merely advantageous: it becomes imperative. Take, for example, 3D-CINE MRI, where sampling a full-Cartesian grid would be excessively time-consuming to the extent that achieving full sampling becomes practically infeasible. The application of CS to MRI is called CS-MRI. Since the MR signal is known to be sparse with respect to the DFT, DWT, and other sparsity promoting transforms, cf. [87], g-LASSO is used for the purpose. In this work, we use the Shepp-Logan phantom and corrupt the data with artificial noise. The Shepp-Logan phantom is piecewise constant and, therefore, its gradient is sparse. For this reason, we use the discrete gradient as sparsity promoting transform:

$$
D = \begin{pmatrix}
-1 & 1 & 0 & \ldots & 0 & 0 \\
0 & -1 & 1 & \ldots & 0 & 0 \\
\vdots & \vdots & \vdots & \ddots & \vdots & \vdots \\
0 & 0 & 0 & \ldots & -1 & 1
\end{pmatrix},
$$

and we set $TV(x) = \|Dx\|_1$ (discrete anisotropic spatial total variation).

4.2   Experimental design

The experiments were conducted using MATLAB_R2023b. The Monalisa toolbox was used for MRI reconstructions.

4.2.1   The simulated MR signal

To simulate the acquisition of an MR signal, we considered the Shepp-Logan brain phantom $f \in \mathbb{R}^{384 \times 384}$, simulate coil sensitivity, undersampling, and Gaussian noise. MR data is sampled by a certain number nCh of coils simultaneously (parallel imaging). Let us delve into a detailed exposition of the data simulation, briefly summarized in the previous lines.

1. **Channel extension and acquisition across coils:** by juxtaposition, f is replicated $nCh = 8$ times and each replica $f_j \in \mathbb{R}^{384 \times 384}$, $j = 1, \ldots, nCh$, is pointwise multiplied by a simulated coil sensitivity matrix $C_j \in \mathbb{C}^{384 \times 384}$:

$$
f_k(i, j) = C_k(i, j) f(i, j),
$$

$k = 1, \ldots, nCh$, $i, j = 1, \ldots, 384$ (fig. 4.2).

2. **Fourier transform:** the spatial discrete Fourier transform of each f_j is computed (see fig. 9B).
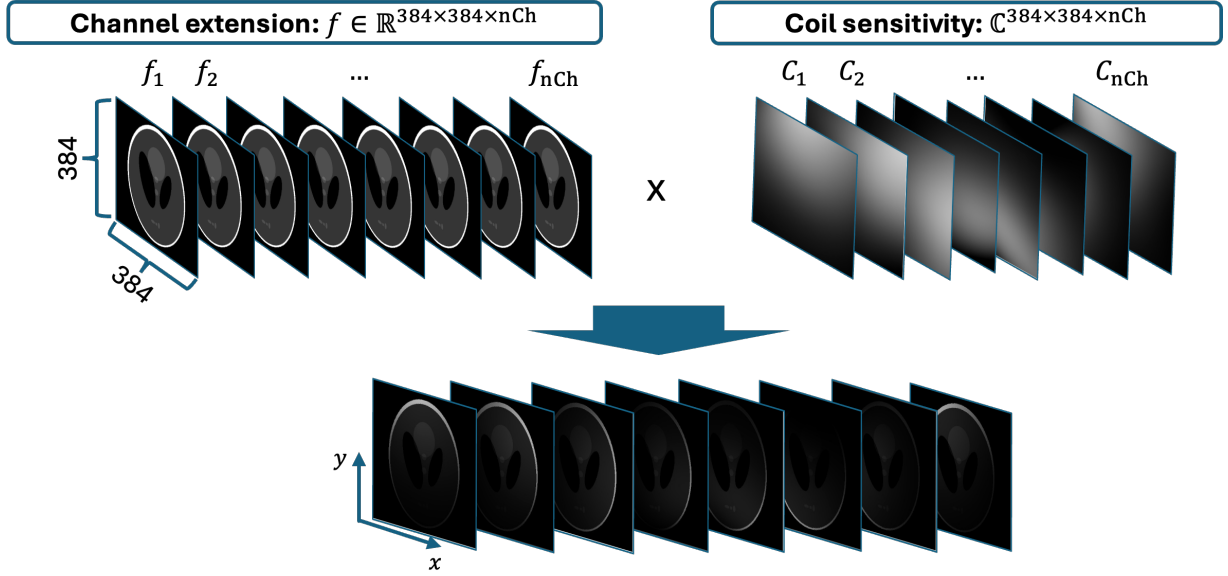
Figure 4.2: Simulated channel extension and acquisition across coils.

3. **Undersampling:** full Cartesian sampling consists of sampling $nLines = 384$ lines evenly spaced, whereas undersampling entails sampling only a certain fraction of these 384 lines, which we denote by $UR_\%$. In our study, we tested undersampling rates of 10%, 15% and 20%, that is $UR_\% \in \{10/100, 15/100, 20/100\}$. For a fixed $UR_\%$, the sampling trajectory comprises $n(UR_\%) = \lceil nLines \cdot UP_\% \rceil$ lines. The 30% of the $n(UR_\%)$ lines are used to sample the center of the k-space at the Nyquist frequency. Specifically, $\lceil n(UR_\%) \cdot 30/100 \rceil$ lines sample the center of the k-space, while the remaining lines sample the periphery of the k-space following a normal distribution $\mathcal{N}(\mu, \sigma^2)$ with $\mu = nLines/2 + 1$ and $\sigma^2 = nLines \cdot UR_\%$ (see fig. 9C). The Fourier transform of each coil-image is sampled according to the Cartesian undersampled trajectory established before. Consequently, the resulting simulated MR data consists of a tensor $y \in Y = \mathbb{C}^{(nLines \cdot n(UR_\%)) \times nCh}$ (see fig. 9D).

4. **Noise corruption:** we tested ALMA under three distinct noise levels. Specifically, the simulated MR data is given by: $b = y + \varepsilon$, where $\varepsilon \in Y$ and $\Re(\varepsilon_{i,j}), \Im(\varepsilon_{i,j}) \sim \mathcal{N}(0, \sigma^2)$ $(i = 1, \ldots, nLines \cdot n(UR_\%)$ and $j = 1, \ldots, nCh)$. We refer to σ^2 as to noise level, which is computed as $\sigma^2 = \|y\| \cdot NL_\%$, where in our experiments $NL_\% \in \{3/100, 5/100, 7/100\}$. For instance, the terminology 3% noise means that we are considering $NL_\% = 3/100$.

4.2.2   ALMA

ALMA is synthesised in fig. 1.4 and schematized in Algorithm 1, here we limit to comment how ALMA computes an ALM. Note that the scalar product $a^T b$, $a, b \in \mathbb{R}^n$, must be replaced with $\Re(a^T b)$ when $a, b \in \mathbb{C}^n$. Moreover, for non-Cartesian MRI trajectories, the scalar product that shall be considered is $\langle a, b \rangle = \Re(a^T H b)$, with H Hermitian positive-definite matrix encoding the non-Cartesian gridding of the k-space.

In the previous paragraphs we observed that finding an ALM is a matter of tracing the tangent line in 0 to the epigraph $\mathcal{A} = \{(u, t) \in \mathbb{R}^2 : u \geq \|Ax - b\|_2^2/2 - \eta^2/2, \ t \geq TV(x)/2 \ for \ some \ x \in \mathbb{R}^n\}$, where $\eta = \|Af - b\|_2$, being $f \in \mathbb{R}^{384 \times 384}$ the 384×384 Shepp-Logan phantom. We pointed out that outlining $\mathcal{A}$ is technically difficult due to the unfeasible dimensionality: in principle, for every $x \in \mathbb{R}^n$ ($n = 384^2$), once the point $(u, t) = (u(x), t(x)) = 1/2 \cdot (\|Ax - b\|_2^2 - \eta^2, TV(x))$ is computed, one has that all the points of the first quadrant centered in $(u(x), t(x))$ belong to $\mathcal{A}$. Clearly, it would be enough to compute $(u(x), t(x))$ only for $x \in \mathbb{R}^n$ such that $(u(x), t(x))$ belongs to the boundary $\partial \mathcal{A}$ of $\mathcal{A}$, but we do not have access to those points. On top of that, computing $(u(x), t(x))$ for a fixed x is computationally expensive, because of the measurement operator A. However, a meaningful family of points $(u(x), t(x))$ that would be enough to approximate the tangent line in 0 to its boundary can be found as follows:

1. Choose $x \in \mathbb{R}^n$ so that the corresponding $(u(x), t(x))$ is as far to the left of $\mathcal{A}$ as possible. Clearly, this task is accomplished by any minimizer of $\phi(x) = \|Ax - b\|_2^2$, which consists of iterative reconstructions. Let us call this point $x^\#$.

2. Choose another point, for instance, the reconstructed image obtained by the gridded reconstruction of the noisy undersampled data, b. Let us call this point $x^{(0)}$.

3. Consider the segment that joins $x^\#$ to $x^{(0)}$ in the image domain and sample it at a rate decided a priori, e.g. 201 uniformly spaced samples.

4. Let x be one of this samples. Compute $\|Ax\|_2^2$, $b^T Ax$ and $TV(x)$.

5. The curve γ_x parametrized by $\alpha \in \mathbb{R}$ as:

$$\gamma_x(\alpha) = (u(\alpha x), t(\alpha x)) = \frac{1}{2} \Big(\alpha \|Ax\|_2^2 - 2\alpha b^T Ax + \|b\|_2^2 - \eta^2, |\alpha| TV(x) \Big)$$

consists of a couple of branches of parabolas. The parameters α_1 and α_2 such that $\gamma_x(\alpha_1)$ and $\gamma_x(\alpha_2)$ are the vertices of these parabolas can be computed explicitly by the expression of $\gamma_x(\alpha)$.

6. Let $\alpha_{max} = \max\{|\alpha_1|, |\alpha_2|\}$. Compute and plot $\gamma_x(\alpha)$ for $\alpha_{max} \leq \alpha \leq \alpha_{max}$. Since $\|Ax\|_2^2$, $b^T Ax$ and $TV(x)$ have been computed in 4., the computational cost of this operation is low.

Algorithm 1 ALMA

Require: : maximal number of iterations: n_{max}.
Require: : $A \in \mathbb{C}^{m \times n}$ and $b \in \mathbb{C}^m$.
Require: : $x^{\#}$ ground-truth and set $\eta = \|Ax^{\#} - b\|_2$.
Require: : $x^{(0)} = \arg\min_{x \in \mathbb{C}^n} \|Ax - b\|_2$.
  while $n \leq n_{max}$ **do**
  1. Project $x^{(n-1)}$ onto the solution set of the least-square problem, call $x_{proj}^{(n-1)}$ the projection.
  2. Consider the convex combination $x_\tau^{(n)} = \tau x^{(n-1)} + (1 - \tau)x_{proj}^{(n-1)}$ $(0 \leq \tau \leq 1)$.
  3. Consider a partition $\tau_1 = 0, \ldots, \tau_{200} = 1$ of $[0, 1]$ and the related $x_{\tau_j}^{(n)}$.

  while $1 \leq j \leq 200$ **do** Plot the set $\mathcal{A}$ of points $(u, t) \in \mathbb{C}^2$ in the form

$$\begin{cases} u = \frac{1}{2}\|A(\alpha_k x_{\tau_j}^{(n)}) - b\|_2^2 - \frac{\eta^2}{2}, \\ t = \frac{1}{2}TV(\alpha_k x_{\tau_j}^{(n)}), \end{cases}$$

  where $\alpha_k \in [-\alpha_{max}, \alpha_{max}]$ is an equally spaced sequence $(k = 1, \ldots, k_{max})$,

$$\alpha_{max} = \frac{|b^T A x_{\tau_j}^{(n)}|}{\|A x_{\tau_j}^{(n)}\|_2^2}.$$

  end while
  4. Compute the slope $m^{(n)}$ of the tangent to the lower boundary of $\mathcal{A}$, in $u = 0$. Set $\lambda^{(n)} = -1/m^{(n)}$.
  5. Solve

$$\arg\min_{x \in \mathbb{C}^n} \frac{1}{2}\|Ax - b\|_2^2 + \frac{\lambda^{(n)}}{2}TV(x)$$

  with the ADMM algorithm. Call $x^{(n)}$ the solution.

    if $n > 1$ and $\lambda^{(n)} = \lambda^{(n-1)}$ **then** Break
    end if
  end while
  Result: $x_{out} = x^{(r)}$, where r is the number of iterations at the end of **while**.

---

7. Repeat the procedure for every x belonging to the segment that joins $x^{\#}$ to $x^{(0)}$.

8. Since $\mathcal{A}$ is known to be convex, compute the convex hull of the outlined points.

The convex hull at the end of 8. is the approximation of $\mathcal{A}$ at iteration 1.

9. Choose $\lambda^{(1)} = -1/m^{(1)}$, where $m^{(1)}$ is the slope of the tangent and reconstruct an image using $\lambda^{(1)}$ as tuning parameter for TV-LASSO. Call this image $x^{(1)}$.

Indicatively, $x^{(1)}$ has the advantage of being more regular than $x^{(0)}$, that is $TV(x^{(1)}) \leq TV(x^{(0)})$.

10. Repeat steps 1-9. replacing $x^{(0)}$ with $x^{(1)}$, to outline points of $\mathcal{A}$ that are narrower with respect to the points outlined in steps 1)-7). Overlaying these new points to the ones already outlined in 7), improves the approximation of $\mathcal{A}$.

11. Compute the slope $m^{(2)}$ of the new tangent in 0 to the convex boundary of $\mathcal{A}$ and define $\lambda^{(2)} = -1/m^{(2)}$.

4.2.3 Image quality metrics

We measured quantitatively the quality of the output of ALMA by means of three metrics: the mSSIM, the pSNR and the CJV.

- The mSSIM is an extension of the structural similarity index, designed to assess the quality of reconstructions across various scales in a manner that approximates human perception, cf. [122, 38]. It compares the brightness, contrast, and structural details of reconstructions with ground truth images, assigning values on a scale from 0 to 1, where a score of 1 indicates optimal similarity. Good quality reconstructions typically correspond to mSSIM values of ≥ 0.9. In the present work, the mSSIM is computed via the command `multissim(I,Iref)`, where `Iref` is the reference image (the Shepp-Logan brain phantom) and `I` is the image to be assessed.

- The pSNR quantifies noise corruption of compressed images, independently on the quality as perceived by human vision and good visual quality requires pSNR to be at least 30dB, cf. [1].

- CJV measures the presence of intensity non-uniformity (INU) artifacts in MRI, cf. [83, 55]. In the current paper, we use it as a measure of artifact bias in reconstructions. Lower values of CJV indicate better quality of
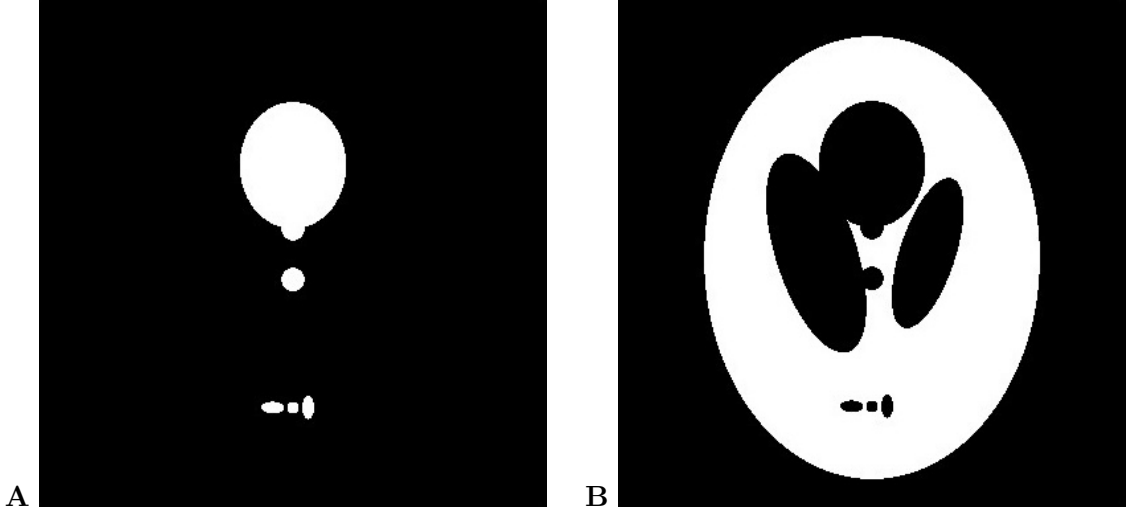
Figure 4.3: Grey matter (A) and white matter (B) masks for CJV computation.

MR images in terms of artifacts. CJV is defined based on the intensity difference between grey and white matter. Fig. 4.3 illustrates the masks corresponding to grey matter (A) and white matter (B) in the Shepp-Logan phantom, used for the computation of the CJV, as inspired by [75].

The notation $mSSIM(\lambda)$ stands for the mSSIM of the reconstruction obtained by solving:
$$\arg\min_{x\in\mathbb{C}^n} \frac{1}{2}\|Ax - b\|_2^2 + \frac{\lambda}{2}TV(x).$$
Analogous notations for $pSNR(\lambda)$ and $CJV(\lambda)$. The mSSIM takes values in $[0,1]$ and optimality corresponds to $mSSIM(\lambda) = 1$ (maximum). The pSNR and the CJV take values in $[0, +\infty)$ and are optimized in correspondence of their maxima and their minima respectively. Good quality with respect to mSSIM corresponds to $mSSIM \geq 0.9$, good quality with respect to pSNR corresponds to $pSNR \geq 30$dB. Assessing good quality for CJV is harder, since, differently from the mSSIM and the pSNR, the CJV is optimized in correspondence of its minima $\arg\min(CJV(\lambda))$, whereas $\max(CJV(\lambda))$ potentially grows to infinity. For these reasons, we considered good quality with respect to CJV as:

$$CJV(\lambda) \leq \min(CJV) + \frac{\max(CJV) - \min(CJV)}{10}$$
$$= 0.0493 \approx 0.05,$$

where
$$\max(CJV) = \max\{CJV(\lambda) : \lambda \geq 0\}$$

and
$$\min(CJV) = \min\{CJV(\lambda) : \lambda \geq 0\},$$

analogous notations are used for the minima and the maxima of mSSIM and pSNR.

4.2.4 Data analysis

The mSSIM, pSNR, and CJV, along with their respective relative versions, serve as quantitative measures for assessing the quality of reconstructions. Additionally, the (unique, in our experiments) tuning parameters $\lambda_{mSSIM}, \lambda_{pSNR}$ and λ_{CJV} which optimize each metric can be considered. Specifically, $\lambda_{mSSIM} = \arg\max\{mSSIM(\lambda) : \lambda \geq 0\}$, $\lambda_{pSNR} = \arg\max\{pSNR(\lambda) : \lambda \geq 0\}$ and $\lambda_{CJV} = \arg\min\{CJV(\lambda) : \lambda \geq 0\}$. The ratios $\lambda_{mSSIM}/\lambda_{ALM}$, $\lambda_{pSNR}/\lambda_{ALM}$ and $\lambda_{CJV}/\lambda_{ALM}$ express the distance between optimal tuning parameters (with respect to the metrics) and ALM in terms of the orders of magnitude of the corresponding ratios. We term the ratio λ_{mSSIM}/λ the magnitude ratio corresponding to λ (with respect to mSSIM), and similar notations are reserved for the other metrics. For every pair $(UR_\%, NL_\%)$ and every reconstruction, we calculate the mSSIM, pSNR and CJV, alongside their corresponding magnitude rations. Within each fixed pair $(UR_\%, NL_\%)$, we employ violin plots to illustrate the distributions of mSSIM, pSNR and CJV across the 50 runs, for analysis. Additionally, shaded error bars for the functions $mSSIM(\lambda/\lambda_{ALM})$, $pSNR(\lambda/\lambda_{ALM})$ and $CJV(\lambda/\lambda_{ALM})$ are incorporated to evaluate the optimality of ALM as tuning parameters. A value of $\lambda_{mSSIM}/\lambda_{ALM} = 1$ signifies that λ_{ALM} is the optimal tuning parameter with respect to mSSIM. Similar interpretations apply for the other magnitude ratios. For a comparison, we compute the L-curve tuning parameter λ_L, and execute reconstructions using TV-LASSO with this parameter. Subsequently, we compute $mSSIM(\lambda_L)$, $pSNR(\lambda_L)$ and $CJV(\lambda_L)$, along with the corresponding magnitude ratios pertaining to λ_L with respect to these three metrics.

4.2.5 The dataset

The dataset is obtained reconstructing an image for a fixed pair $(UR_\%, NL_\%)$ 50 times (number of runs), to ensure statistical robustness with respect to the sampling randomisation. The dataset consists of $3 \times 3 \times 50$ reconstructions.

4.3 Results

4.3.1 Analysis of convergence

For fixed noise level and undersampling rate, ALMA approximates an ALM by conducting reconstructions, updating the ALM approximation at each iteration. We have selected two stopping criteria:
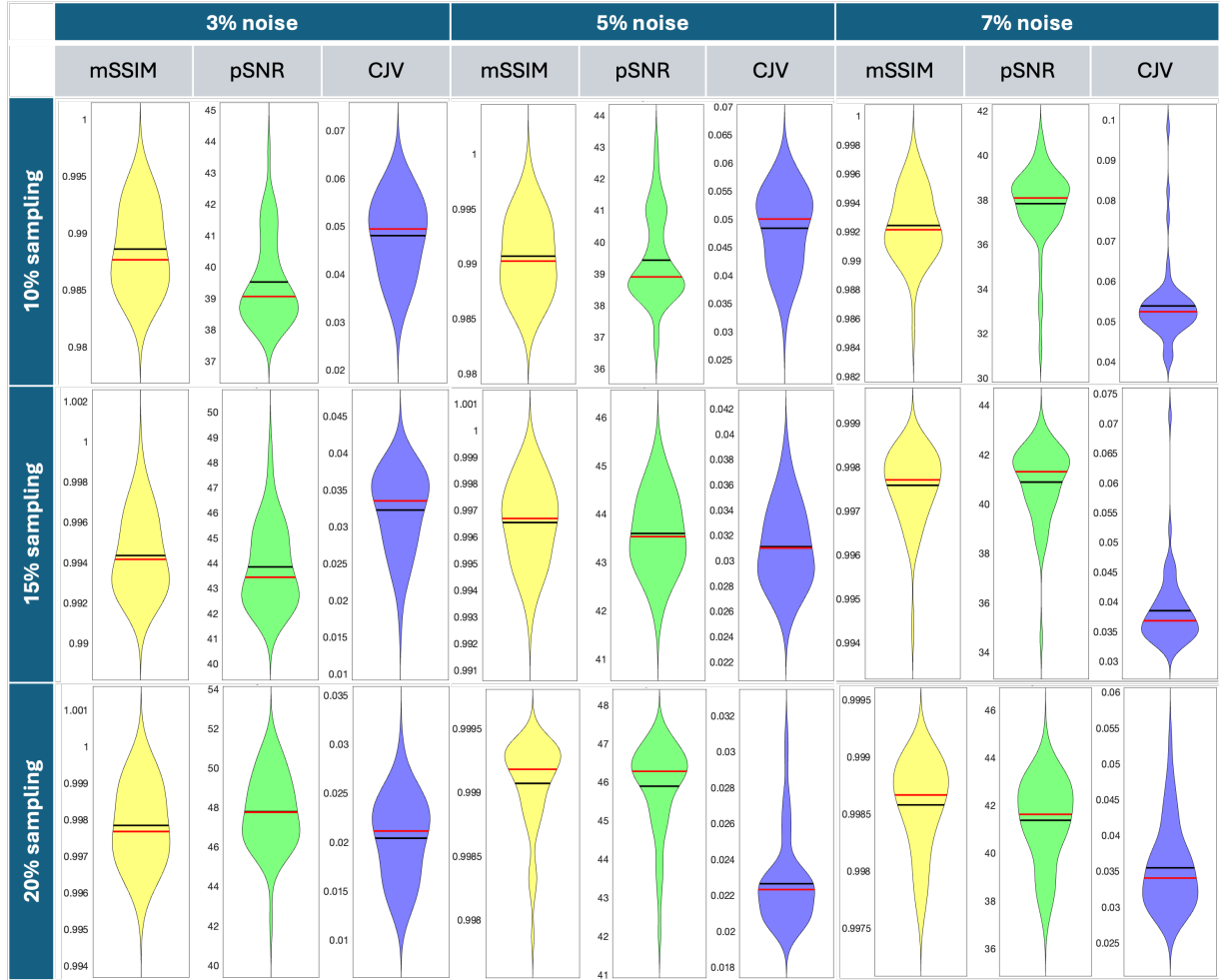
Figure 4.4: Violin plots of the three metrics across noise levels and undersampling rates. Yellow violins correspond to mSSIM, green violins correspond to pSNR and purple violins correspond to CJV. The black lines correspond to the means and the red lines correspond to the medians.
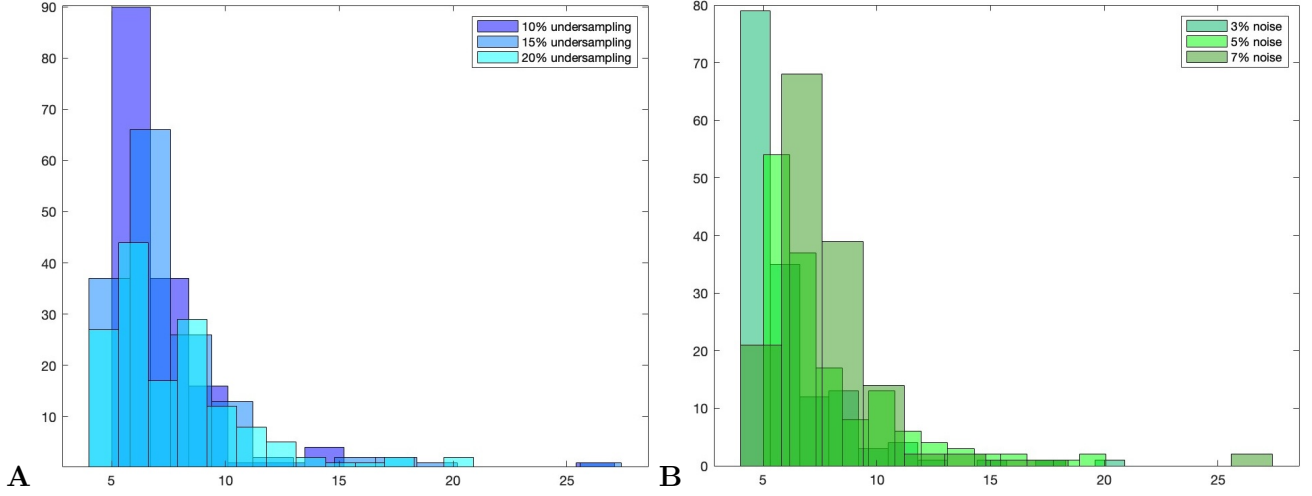
Figure 4.5: Convergence analysis. Histograms of the number of iterations needed for ALMA's convergence across undersampling rates (A) and noise levels (B). The number of bins for each histogram is the ceiling of the square root of the number of points, i.e., $\lceil \sqrt{150} \rceil = 13$. Observe that the number of iterations for ALMA to stop is mostly concentrated in the interval $[0, 10]$ independently of the noise level and the undersampling rate, while the standard deviations increase with the undersampling rate and the noise percentage. This demonstrates that the number of iterations required for ALMA to converge is relatively low even when processing larger amounts of information (20% undersampling) and higher noise percentages (7% noise).

- The number of iterations k reaches a predefined maximum (set to $k_{max} = 100$).

- At iteration $k_0 + 1$, $\lambda^{(k_0+1)} = \lambda^{(k_0)}$, in which case $\lambda^{(k)} = \lambda^{(k_0)}$ for every $k \geq k_0$.

Note that the second criterion serves as a convergence criterion for ALMA. This means that if it is satisfied, ALMA not only stops but actually *converges* (i.e., the sequence $(\lambda^{(k)})_k$ of ALM at step k converges). Observe that in all of our experiments, the sequence of the ALM is eventually constant. Therefore, in what follows, the term *convergence* will refer to ALMA stopping due to the fulfillment of the second stopping criterion.

Through empirical analysis, we investigated the convergence of ALMA across various noise levels and undersampling rates. As aforementioned, ALMA converges in a finite time for every undersampling rate and noise level.

The histograms in fig. 4.5 (A) illustrates the number of iterations required for the convergence of ALMA across different noise levels and undersampling rates. Both histograms follow Gaussian distributions that become less concentrated

around 0 as the undersampling rate increases (fig. 4.5 (A)) or as the noise level rises (fig. 4.5 (B)). In both scenarios, the increase in the number of iterations can be attributed to the amount of information processed by ALMA, which grows with the number of sampling points and the noise level. Let us delve deeper into these cases. On average, ALMA stops after 7.2089 ± 2.9773 iterations (see fig. 4.9). For the 10% sampling rate, both the average number of iterations and the standard deviation increase with the noise level. A similar trend is observed for the 15% undersampling rate, as detailed in fig. 4.9. However, the 20% sampling rate exhibits a distinct pattern: the average number of iterations increases from 3% to 5% noise levels and reaches its minimum at a noise level of 7%.

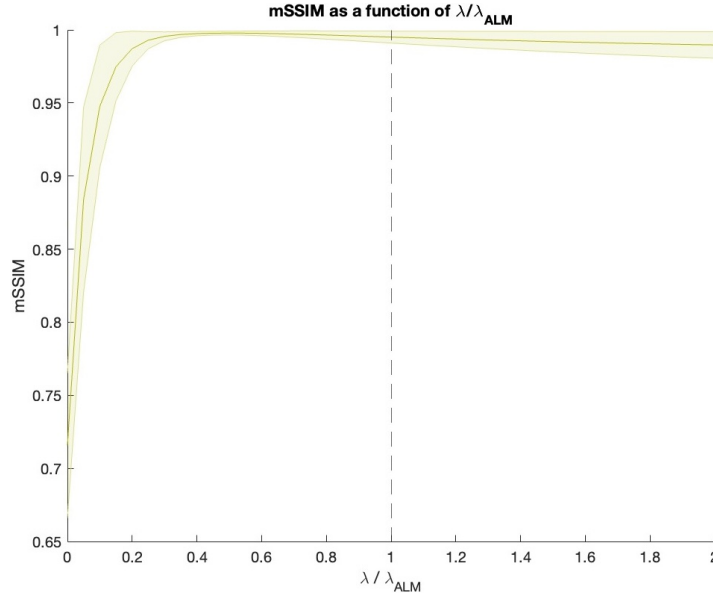### 4.3.2   Performance of ALMA with respect to mSSIM

Figure 4.6: Shaded error bars of the mSSIM, the shades representing the corresponding standard deviations. The values 1 on the horizontal axes correspond to $\lambda = \lambda_{\mathrm{ALM}}$. Observe that the corresponding mSSIM values lie on the plateau of the mSSIM graph, just to the right of the maximum. This indicates that the ALM performs nearly optimally with respect to the mSSIM metric.

Images reconstructed utilizing the ALM computed by ALMA consistently exhibit an average $mSSIM \geq 0.99$, irrespective of the noise level or the undersampling rate (see fig. 4.9). The violin plots for the mSSIM are displayed in figure 4.4 (color yellow).

Across noise levels and undersampling rates, the tuning parameter that optimizes the mSSIM (λ_{mSSIM}) is around half of the ALM (λ_{ALM}), i.e., $\lambda_{mSSIM} \approx 0.52 \cdot \lambda_{ALM}$ (see fig. 4.9). However, even if λ_{ALM} does not maximize the mSSIM,

the points $(1, mSSIM(1))$, which correspond to the mSSIM of the reconstructions obtained with ALM, always lie on the plateau of the graph of the function $mSSIM(\lambda/\lambda_{ALM})$, indicating that λ_{ALM} is in the range of tuning parameters corresponding to almost-optimal mSSIM values (see fig. 4.6).

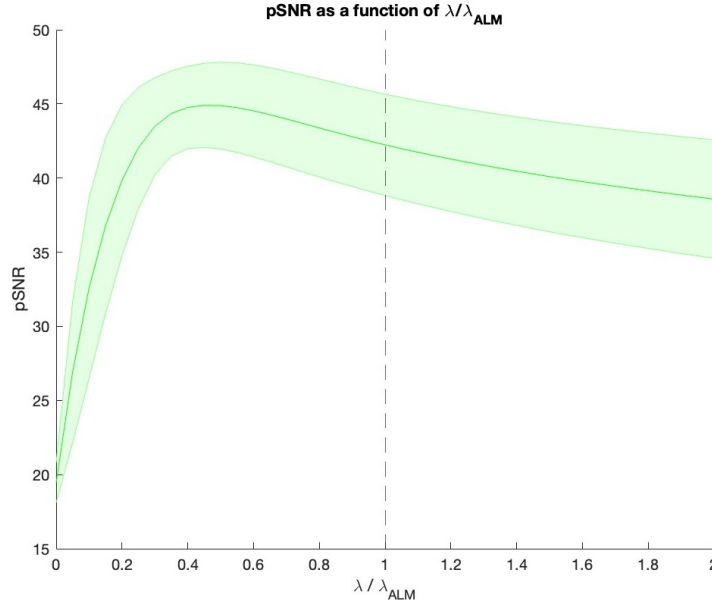### 4.3.3 Performance of ALMA with respect to pSNR

Figure 4.7: Shaded error bars of the pSNR, the shades representing the corresponding standard deviations. The values 1 on the horizontal axes correspond to $\lambda = \lambda_{\mathrm{ALM}}$. Observe that the corresponding mSSIM values lie on the plateau of the mSSIM graph, just to the right of the maximum. This indicates that the ALM performs nearly optimally with respect to the mSSIM metric.

Reconstructions obtained using ALMA exhibit high pSNR for every noise level and undersampling rate. As expected the pSNR decreases across noise levels. On average, the pSNR is ≥ 40dB for reconstructions of images corresponding to 15% and 20% undersampling rates, whereas the average pSNR of reconstructions with 10% undersampling rate is at least 35dB (see fig. 4.9). Other than demonstrating the quality of reconstructions obtained via ALMA in terms of pSNR, this reflects the fact that solving TV-LASSO with ALM as tuning parameters tend to produce highly regularized images. Again, across noise levels and undersampling rates, the tuning parameter that optimizes the pSNR (λ_{pSNR}) tends to be approximately 0.47 times the corresponding ALM, i.e., $\lambda_{pSNR} \approx 0.47 \cdot \lambda_{ALM}$ (see fig. 4.9). Compared to the graphs $mSSIM(\lambda/\lambda_{ALM})$, the plateau of the functions $pSNR(\lambda/\lambda_{pSNR})$ near their maxima is less pronounced, and the points $(1, pSNR(1))$, corresponding to the pSNR of reconstructions obtained with ALM,

are shifted to the right of their peaks (see fig. 4.7). In conclusion, ALM perform almost-optimally with respect to pSNR.

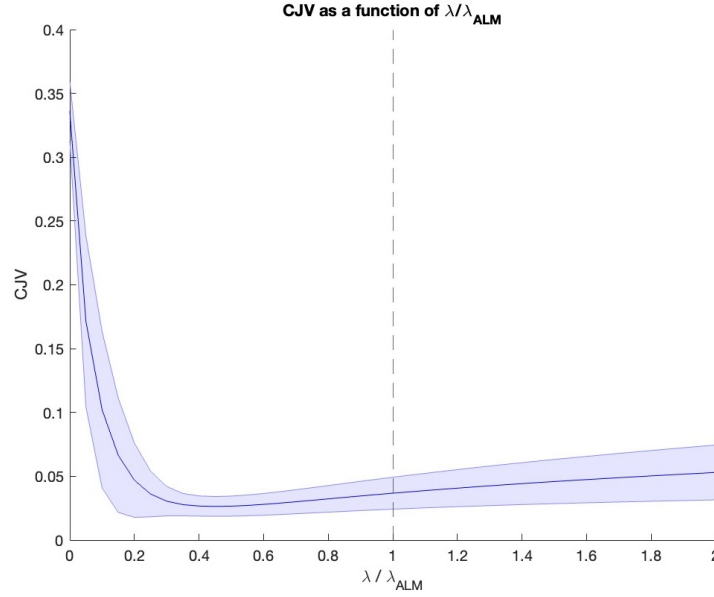### 4.3.4 Performance of ALMA with respect to CJV

Figure 4.8: Shaded error bars of the CJV, the shades representing the corresponding standard deviations. The values 1 on the horizontal axes correspond to $\lambda = \lambda_{\text{ALM}}$. Observe that the corresponding mSSIM values lie on the plateau of the mSSIM graph, just to the right of the maximum. This indicates that the ALM performs nearly optimally with respect to the mSSIM metric.

Except for the worst-case scenario $UR_\% = 10\%$, $NL_\% = 7\%$, the reconstructions obtained by ALMA display CJV values no larger than 0.05, showing that ALMA performs well with respect to CJV as well (see fig. 4.9). The tuning parameter that minimizes the CJV (λ_{CJV}) is on average 0.45 times the corresponding ALM, i.e., $\lambda_{CJV} \approx 0.45 \cdot \lambda_{ALM}$ (see fig. 4.9). However, ALM still perform almost optimally with respect to CJV, and the points $(1, CJV(1))$, corresponding to the CJV of reconstructions obtained with ALM, are shifted to the right of their minima, in accordance with the behavior of the graphs $pSNR(\lambda/\lambda_{CJV})$ (see fig. 4.8).

4.3.5 Comparison with the L-curve parameter

For a comparison, we report on the quantitative measurement regarding the reconstructions obtained utilizing the parameter λ_L, computed by $L-$curve. These

		iterations	mSSIM	pSNR (dB)	CJV	$\lambda_{mSSIM}/\lambda_{ALM}$	$\lambda_{pSNR}/\lambda_{ALM}$	$\lambda_{CJV}/\lambda_{ALM}$
10% sampling	3% noise	5.3600 ± 0.6627	0.9886 ± 0.0036	39.5220 ± 1.3622	0.0481 ± 0.0078	0.2680 ± 0.0705	0.3680 ± 0.0705	0.3890 ± 0.0865
	5% noise	6.8000 ± 2.2497	0.9907 ± 0.0034	39.4282 ± 1.3789	0.0484 ± 0.0069	0.4610 ± 0.0680	0.4610 ± 0.0680	0.4930 ± 0.0572
	7% noise	8.1000 ± 3.3089	0.9924 ± 0.0024	37.8291 ± 1.7134	0.0538 ± 0.0095	0.4460 ± 0.0748	0.4460 ± 0.0748	0.4430 ± 0.0553
15% sampling	3% noise	5.4800 ± 1.4741	0.9943 ± 0.0019	43.8485 ± 1.5849	0.0323 ± 0.0053	0.4210 ± 0.0881	0.4210 ± 0.0881	0.3770 ± 0.0771
	5% noise	7.5600 ± 2.9496	0.9965 ± 0.0015	43.5978 ± 0.8036	0.0311 ± 0.0032	0.6190 ± 0.0832	0.6190 ± 0.0832	0.5510 ± 0.0576
	7% noise	8.7000 ± 3.4181	0.9976 ± 0.0008	40.8857 ± 1.4965	0.0385 ± 0.0063	0.4700 ± 0.0953	0.4700 ± 0.0953	0.4700 ± 0.0964
20% sampling	3% noise	7.6000 ± 3.2514	0.9978 ± 0.0011	47.7808 ± 1.8292	0.0204 ± 0.0041	0.5460 ± 0.0903	0.5460 ± 0.0903	0.5030 ± 0.0785
	5% noise	9.5600 ± 3.0650	0.9991 ± 0.0003	45.8925 ± 1.1229	0.0226 ± 0.0024	0.5290 ± 0.1306	0.5290 ± 0.1306	0.5080 ± 0.1144
	7% noise	5.7200 ± 1.6293	0.9986 ± 0.0004	41.3764 ± 1.7199	0.0355 ± 0.0058	0.3590 ± 0.0973	0.3590 ± 0.0973	0.3530 ± 0.0928
Averages and stds		7.2089 ± 2.9473	0.9951 ± 0.0041	42.2401 ± 3.4208	0.0367 ± 0.0125	0.4688 ± 0.1200	0.4688 ± 0.1200	0.4541 ± 0.1034

Figure 4.9: Means and standard deviations of the number of iterations, the three metrics, and the magnitude ratios across undersampling rate and noise level, for the reconstructions obtained using the ALM. Observe that the average number of iterations is 7, and the three metrics exhibit average values of approximately 0.9951, 42.2401 dB, and 0.0367, respectively, indicating optimal performance of ALMA.

raconstructions exhibit an average $mSSIM \geq 0.99$, across noise levels and undersampling rates (see fig. 4.11), they also exhibit an average pSNR of 42.6351 and an average CJV of 0.035. Therefore, they perform well regarding the metrics criterion. Moreover, the tuning parameter that minimizes the mSSIM (λ_{mSSIM}) is on average 0.6 times the corresponding λ_L, i.e., $\lambda_{mSSIM} \approx 0.6 \cdot \lambda_L$, while the tuning parameters optimizing the pSNR and the CJV (λ_{pSNR} and λ_{CJV}, resp.) are on average 0.5 times λ_L (see fig. 4.11). All these data together show that the performance of the L-curve parameter is slightly better compared to the performance of the ALM. However, the difference is marginal and amounts to only a matter of decimals. Moreover, ALMA is an iterative procedure to compute tuning parameters and, consequently, solving TV-LASSO, whereas the L-curve method is heuristic and does not involve an iterative process. Despite yielding similar results, ALMA's iterative nature ensures a more robust and accurate determination of tuning parameters for solving TV-LASSO, offering a superior alternative to the heuristic approach of the L-curve method. Therefore, both methods perform similarly overall, indicating that the ALM is a reliable parameter, performing on par with the well-established L-curve method.

4.4   Discussion

We introduced ALMA for TV-LASSO, which demonstrated promising results in reconstructing undersampled and noisy MRI phantom data, achieving high-quality reconstructions without extensive manual tuning. We assessed the quality of the reconstructions quantitatively by means of mSSIM, pSNR and CJV.

As illustrated in fig. 4.10, the reconstruction quality using ALMA, even in the worst case scenario ($UR_\% = 10\%$ and $NL_\% = 7\%$), is notably superior when compared to parameter choices as powers of ten (see fig. 4.10). The reconstructed image via ALMA exhibits finer structural details and improved contrast, which are crucial for accurate diagnosis and analysis in clinical radiology.

To further validate ALMA's robustness, we compared its reconstructions to those obtained using parameters optimized for the three metrics (mSSIM, pSNR, and CJV). Figure 4.9 encapsulates this comparison, while fig. 4.10 provides a visual example of the reconstructions. The results indicate that ALMA's performance is nearly optimal, matching closely with the parameters that optimize each metric.

We also compared the performance of ALMA against the well-established L-curve method. As presented in fig. 4.9 and 4.11, and exemplified in fig. 4.10, both methods show comparable performance across the metrics. However, ALMA stands out as the first iterative algorithm to compute the parameter dynamically during reconstruction. This active, iterative approach grants ALMA significant advantages in computational efficiency and ease of implementation, which are particularly beneficial in clinical settings where a rapid and optimized reconstruction is essential.

Qualitatively, ALMA-reconstructed images maintain the anatomical integrity and structural fidelity necessary for clinical interpretation. This is evident in fig. 4.10, where even under severe noise and undersampling, the critical features are preserved. Quantitatively, ALMA achieves high mSSIM, pSNR, and low CJV values, closely approximating the optimal values for these metrics obtained through extensive parameter optimization.
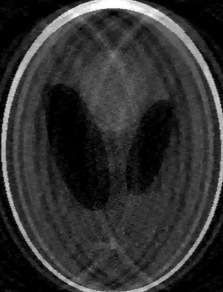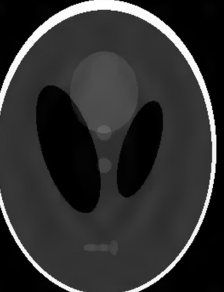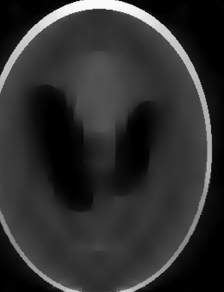
$\lambda = \lambda_{ALM}$	$\lambda = \lambda_L$	$\lambda = \lambda_{mSSIM} = \lambda_{pSNR}$	$\lambda = \lambda_{CJV}$

mSSIM = 0.9882	mSSIM = 0.9874	mSSIM = 0.9964	mSSIM = 0.9952
pSNR = 38.3753	pSNR = 38.0796	pSNR = 41.5552	pSNR = 41.2745
CJV = 0.0525	CJV = 0.0544	CJV = 0.0386	CJV = 0.0375

$\lambda = 0.0001$	$\lambda = 0.001$	$\lambda = 0.01$	$\lambda = 0.1$

mSSIM = 0.7091	mSSIM = 0.9422	mSSIM = 0.9865	mSSIM = 0.9038
pSNR = 20.0032	pSNR = 29.4250	pSNR = 37.7847	pSNR = 23.1956
CJV = 0.3037	CJV = 0.1261	CJV = 0.0554	CJV = 0.2113

Figure 4.10: Example of reconstruction of simulated MRI data ($NL_\% = 7/100$, $UR_\% = 10/100$) with different tuning parameters: the ALM and the tuning parameter computed with the L-curve method, the tuning parameters that optimize each metric and tuning parameters that are powers of 10. The corresponding quantitative quality assessments are reported below each reconstruction. Observe that the quality of the reconstructions obtained using the ALM and the L-curve parameter are nearly indistinguishable, and close to the quality of the images reconstructed with the tuning parameters that optimize the metrics.

		mSSIM	pSNR (dB)	CJV	$\lambda_{mSSIM}/\lambda_L$	λ_{pSNR}/λ_L	λ_{CJV}/λ_L
10% sampling	3% noise	0.9881 ± 0.0032	39.5421 ± 1.0556	0.0484 ± 0.0073	0.7348 ± 0.2026	0.7494 ± 0.2053	0.7947 ± 0.2359
	5% noise	0.9911 ± 0.0027	39.6677 ± 1.1756	0.0440 ± 0.0046	0.8564 ± 0.0790	0.7768 ± 0.0952	0.8351 ± 0.1159
	7% noise	0.9923 ± 0.0034	37.6640 ± 2.3154	0.0555 ± 0.0147	0.5962 ± 0.2733	0.5241 ± 0.2601	0.5112 ± 0.2293
15% sampling	3% noise	0.9963 ± 0.0016	44.2511 ± 1.4122	0.0275 ± 0.0042	0.3228 ± 0.1609	0.3137 ± 0.1512	0.2846 ± 0.1555
	5% noise	0.9975 ± 0.0010	43.7773 ± 0.9432	0.0286 ± 0.0026	0.5337 ± 0.2205	0.5077 ± 0.1786	0.4600 ± 0.1785
	7% noise	0.9978 ± 0.0006	40.9865 ± 1.5365	0.0379 ± 0.0053	0.5896 ± 0.1991	0.4742 ± 0.1392	0.4724 ± 0.1309
20% sampling	3% noise	0.9988 ± 0.0006	48.7886 ± 1.1751	0.0170 ± 0.0024	0.4246 ± 0.0996	0.4022 ± 0.0751	0.3723 ± 0.0762
	5% noise	0.9992 ± 0.0002	45.6172 ± 1.3660	0.0228 ± 0.0027	0.5787 ± 0.2013	0.4753 ± 0.1449	0.4580 ± 0.1376
	7% noise	0.9989 ± 0.0003	43.4215 ± 1.4928	0.0301 ± 0.0040	0.7700 ± 0.2300	0.5675 ± 0.1725	0.5579 ± 0.1168
Averages and stds		0.9956 ± 0.0043	42.6351 ± 3.5832	0.0346 ± 0.0135	0.6008 ± 0.2493	0.5323 ± 0.2174	0.5273 ± 0.2372

Figure 4.11: Means and standard deviations of the number of iterations, the three metrics, and the magnitude ratios across undersampling rate and noise level, for the reconstructions obtained using λ_L, the tuning parameter of the L-curve.

Wigner analysis and metaplectic Wigner distributions

We open this chapter with Section 5.1, where we provide the main definitions and discuss Wigner analysis of Schrödinger equations, the reason that yield Cordero and Rodino in defining metaplectic Wigner distributions. In Section 5.2 we present the main properties of metaplectic Wigner distributions and introduce their related pseudodifferential operators. Different symplectic matrices give rise to different quantizations: we show the link between different quantizations and generalize the equality in (5.1) to any metaplectic Wigner distribution and metaplectic pseudodifferential operator. This is a valuable result of its own, we believe it could be useful in the framework of operator theory and quantum mechanics. Section 5.3 is devoted to study subclasses of metaplectic Wigner distributions and pseudodifferential operators: covariant, totally Wigner-decomposable and Wigner-decomposable. The last ones provide a new characterization of modulation spaces. Next, we show that covariant matrices belong to the Cohen class and compute the related kernel. As for the Wigner case, we are able to give an explicit expression of the metaplectic Wigner when $\mathcal{A}$ is covariant. Section 5.4 contains a deep study of metaplectic pseudodifferential operators on modulation spaces, which will be used in the applications to Schrödinger equations (Section 5.6). Section 5.5 introduces new algebras of generalized metaplectic operators and their main properties. Finally, Sections 5.6 and 5.7 exhibit some application of the theory developed so far to Schrödinger equations and wavefront sets, respectively.

This chapter is part of an article published in *Communications in Mathematical Physics* in 2024, cf. [23].

5.1 Schrödinger equations and Wigner analysis

Cauchy problems for Schrödinger equations have been studied by a variety of authors in many different frameworks. Limiting attention to the microlocal analysis

context, let us mention as a partial list of contributions [2, 33, 69, 73, 74, 93, 94, 109, 124].

As more recent issues, under the influence of the new time-frequency methods, we may refer to [5, 14, 25, 27, 28, 30, 29, 31, 40, 35, 37, 78, 103, 102, 121].

In this chapter, we propose a new approach, in terms of phase-space concentration of suitable time-frequency distributions. The basic idea in terms of Wigner distribution is not new, though. It goes back to Wigner 1932 [123] (later developed by Cohen and many other authors, see e.g. [16, 17]). For a given linear operator P acting on $L^2(\mathbb{R}^d)$ (or a more general functional space), Wigner considered an operator K on $L^2(\mathbb{R}^{2d})$ such that

$$W(Pf) = KWf \tag{5.1}$$

and its kernel k

$$W(Pf)(x,\xi) = \int_{\mathbb{R}^{2d}} k(x,\xi,y,\eta) Wf(y,\eta)\, dy d\eta. \tag{5.2}$$

We continue the development of a theory started in the Part I [30], addressed to P pseudodifferential operators with W replaced by the more general τ-Wigner distributions. Here the main concern is the study of Cauchy propagators for linear Schrödinger equations

$$\begin{cases} i\dfrac{\partial u}{\partial t} + Hu = 0 \\ u(0,x) = u_0(x), \end{cases} \tag{5.3}$$

with $t \in \mathbb{R}$ and the initial condition $u_0 \in \mathcal{S}(\mathbb{R}^d)$ (Schwartz class) or in some modulation space as explained below. The Hamiltonian has the form

$$H = Op_w(a) + Op_w(\sigma), \tag{5.4}$$

where $Op_w(a)$ is the Weyl quantization of a real homogeneous quadratic polynomial on $\mathbb{R}^{2d}$ and $Op_w(\sigma)$ is a pseudodifferential operator with a symbol σ in suitable modulation spaces, namely $\sigma \in M^{\infty,q}_{1 \otimes v_s}(\mathbb{R}^{2d})$, $s \geq 0$, $0 < q \leq 1$ (see Section 2.2 below for the definitions) which guarantee that $Op_w(\sigma)$ is bounded on $L^2(\mathbb{R}^d)$ (and in more general spaces). This implies that the operator H in (5.4) is a bounded perturbation of the generator $H_0 = Op_w(a)$ of a unitary group (cf. [108] for details).

As special instances of the Hamiltonian above we find the Schrödinger equation $H = \Delta - V(x)$ and the perturbation of the harmonic oscillator $H = \Delta - |x|^2 - V(x)$ with a potential $V \in M^{\infty,q}(\mathbb{R}^d)$. Observe that V is bounded, but not necessarily smooth.

The unperturbed case $\sigma = 0$, was already considered in [31]

$$\begin{cases} i\dfrac{\partial u}{\partial t} + Op_w(a)u = 0 \\ u(0,x) = u_0(x). \end{cases} \tag{5.5}$$

The solution is given by the metaplectic operators $u = \widehat{\chi}_t u_0$, for a suitable symplectic matrix χ_t, see for example the textbooks [48, 35]. Precisely, if $a(x,\xi) = \frac{1}{2}xAx + \xi Bx + \frac{1}{2}\xi C\xi$, with A, C symmetric and B invertible, we can consider the classical evolution, given by the linear Hamiltonian system

$$\begin{cases} 2\pi \dot{x} = \nabla_\xi a = Bx + C\xi \\ 2\pi \dot{\xi} = -\nabla_x a = -Ax - B^T\xi \end{cases}$$

(the factor 2π is due to our normalization of the Fourier transform) with Hamiltonian matrix $\mathbb{D} := \begin{pmatrix} B & C \\ -A & -B^T \end{pmatrix} \in \mathfrak{sp}(d, \mathbb{R})$. Then we have $\chi_t = e^{t\mathbb{D}} \in \mathrm{Sp}(d, \mathbb{R})$.

The solution to (5.5) is the Schrödinger propagator

$$u(t,x) = e^{itOp_w(a)}u_0(x) = \widehat{\chi}_t u_0, \tag{5.6}$$

and the Wigner transform with respect to the space variable x is given by

$$Wu(t,z) = Wu_0(\chi_t^{-1}z), \quad z = (x,\xi),$$

as already observed in the works of Wigner [123] and Moyal-Bartlett [92]. Hence (5.2) reads in this case

$$W(e^{itOp_w(a)}u_0)(z) = \int_{\mathbb{R}^{2d}} k(t,z,w)Wu_0(w)\,dw, \tag{5.7}$$

with $k(t,z,w)$ given by the delta density $\delta_{z=\chi_t w}$.

The aim of [31] was to reconsider (5.6) and (5.7) in the functional frame of the modulation spaces, in terms of the general metaplectic Wigner transform introduced in [30]. The propagator of the perturbed problem (5.3) is a generalized metaplectic operator, as already exhibited in Theorem 4.1 [25] for symbols in the Sjöstrand class.

Here, to deal with further non-smooth potentials $Op_w(\sigma)$ in (5.4), where we consider $\sigma \in M^{\infty,q}_{1\otimes v_s}(\mathbb{R}^{2d})$, and we expand the class of generalized metaplectic operators, including quasi-algebras of operators, which allow faster decay at infinity than the original Sjöstrand class. To quantify the decay we use the Wiener amalgam spaces $W(C, L^p_{v_s})(\mathbb{R}^{2d})$, which consist of the continuous functions F on $\mathbb{R}^{2d}$ such that

$$\|F\|_{W(C,L^p)} := \left(\sum_{k\in\mathbb{Z}^{2d}} (\sup_{z\in[0,1]^{2d}} |F(z+k)|)^p v_s(k)^p \right)^{\frac{1}{p}} < \infty \tag{5.8}$$

(obvious changes for $p = \infty$), where $v_s(k) = (1 + |k|^2)^{1/2}$.

Definition 5.1. Given $\chi \in \mathrm{Sp}(d, \mathbb{R})$, $g \in \mathcal{S}(\mathbb{R}^d)$, $0 < q \leq 1$, we say that a linear operator $T : \mathcal{S}(\mathbb{R}^d) \to \mathcal{S}'(\mathbb{R}^d)$ is a *generalized metaplectic operator* in the class $FIO(\chi, q, v_s)$ if there exists a function $H \in W(C, L^q_{v_s})(\mathbb{R}^{2d})$, such that the kernel of T with respect to time-frequency shifts satisfies the decay condition

$$|\langle T\pi(z)g, \pi(w)g \rangle| \leq H(w - \chi z), \qquad \forall w, z \in \mathbb{R}^{2d} \tag{5.9}$$

(where the time-frequency shifts $\pi(z)$, $\pi(w)$ are defined in Subsection 2.2).

We infer boundedness, quasi-algebras and spectral properties of the previous operators, see Section 6 below. Moreover, we shall show that they can be represented as

$$T = Op_w(\sigma_1)\hat{\chi} \quad \text{or} \quad T = \hat{\chi}Op_w(\sigma_1),$$

that is, they can be viewed as composition of metaplectic operators with Weyl operators with symbols in the modulation spaces $M^{\infty,q}_{1 \otimes v_s}(\mathbb{R}^{2d})$.

The solution $e^{itH}u_0$ to (5.3) is a generalized metaplectic operator of this type for every $t \in \mathbb{R}$, so that it enjoys the phase-space concentration of this class.

The main work of this paper relies in preparing all the instruments we need to study the Wigner kernel of e^{itH}, namely $k(t, z, w)$, $w, z \in \mathbb{R}^{2d}$, such that

$$W(e^{itH}u_0)(z) = \int k(t, z, w)Wu_0(w)\,dw$$

and possible generalizations to metaplectic Wigner distributions, defined as follows.

We shall focus on $\mathcal{A}$ shift-invertible, covariant symplectic matrices, see Definitions 4.5 and Subsection 4.1 and 4.2 below for definitions and properties. Furthermore we limit to $\mathcal{A}$ shift-invertible, covariant symplectic matrices such that the related metaplectic Wigner distribution $W_{\mathcal{A}}$ is in the Cohen class Q_Σ, namely it can be written as

$$W_{\mathcal{A}}(f, g) = W(f, g) * \Sigma_{\mathcal{A}}$$

where the kernel $\Sigma_{\mathcal{A}}$ is related to $\mathcal{A}$ by (5.43), (5.41) below.

Let us define $\Sigma_{\mathcal{A},t}(z) = \Sigma_{\mathcal{A}}(\chi_t(z))$ and denote by $\mathcal{A}_t$ the covariant matrix such that

$$W_{\mathcal{A}_t} = Wf * \Sigma_{\mathcal{A}_t, t}.$$

Then from the results of [31] we have from the unperturbed equation (5.5), as counterpart of (5.7)

$$W_{\mathcal{A}}(e^{itOp_w(a)}u_0)(z) = \int_{\mathbb{R}^{2d}} \delta_{z = \chi_t w}(W_{\mathcal{A}_t}u_0)(w)\,dw.$$

So we keep the action of the classical Hamiltonian flow according to the original idea of Wigner [123], provided the matrix $\mathcal{A}_t$ is defined as before.

We prove that the result does not change so much for the perturbed equation. Namely, under the stronger assumption $\sigma \in S_{0,0}^0(\mathbb{R}^{2d})$, we prove (see Proposition 5.50 below)

$$W_{\mathcal{A}}(e^{itH}u_0)(z) = \int_{\mathbb{R}^{2d}} k_{\mathcal{A}}(t, z, w)(W_{\mathcal{A}_t}u_0)(w)\, dw$$

where, for every $N \geq 0$,

$$k_{\mathcal{A}}(t, z, w)\langle z - \chi_t(w)\rangle^{2N}$$

is the kernel of an operator bounded on $L^2(\mathbb{R}^d)$.

Starting from this, we may obtain the propagation result for the Wigner wave front set

$$\mathcal{WF}_{\mathcal{A}}(e^{itH}u_0) = \chi_t(\mathcal{WF}_{\mathcal{A}}u_0),$$

see Definition 5.52 in the sequel. In particular, for $W_{\mathcal{A}} = W = W_t$, defining as in [30, 31] $z_0 \notin \mathcal{WF}f$, $z_0 \neq 0$, if there exists a conic neighbourhood $\Gamma_{z_0} \subset \mathbb{R}^{2d}$ of z_0 such that for all $N \geq 0$,

$$\int_{\Gamma_{z_0}} \langle z\rangle^N |Wf(z)|^2\, dz < \infty,$$

we obtain

$$\mathcal{WF}(e^{itH}u_0) = \chi_t(\mathcal{WF}u_0).$$

5.2 Metaplectic analysis of pseudodifferential operators

In this section we study several properties of metaplectic pseudodifferential operators in the context of time-frequency analysis. Integrals that must be intended in the weak sense are clear by the context.

First, we recall their definition, cf. [30, Section 4].

If $\mathcal{A} \in \mathrm{Sp}(2d, \mathbb{R})$ is a general symplectic matrix, we can write explicitly $W_{\mathcal{A}}(f, g)$ as a FIO of type II, using Lemma 2.10.

Proposition 5.2. Let $\mathcal{A} \in \mathrm{Sp}(2d, \mathbb{R})$ have factorization $\mathcal{A} = \mathcal{A}_1\mathcal{A}_2$ with $\mathcal{A}_j$, $j = 1, 2$, free with block decomposition

$$\mathcal{A}_j = \begin{pmatrix} A_j & B_j \\ C_j & D_j \end{pmatrix}.$$

Then, up to a unitary factor, for every $F \in \mathcal{S}(\mathbb{R}^{2d})$,

$$
\begin{aligned}
\hat{\mathcal{A}}F(x, \xi) = {}& \left|\frac{\det(B_1)}{\det(B_2)}\right|^{1/2} \Phi_{-D_1 B_1^{-1}}(x, \xi) \\
& \times \int_{\mathbb{R}^{4d}} F(z, \zeta)e^{-2\pi i[\Phi_{\mathcal{A}}(z,\zeta,y,\eta) - (x,\xi)\cdot(y,\eta)]}\tau_{\mathcal{A}}(z, \zeta, y, \eta)dz d\zeta dy d\eta,
\end{aligned}
\tag{5.10}
$$

where the phase is given by

$$\Phi_{\mathcal{A}}(z,\zeta,y,\eta) = \frac{1}{2}[B_2^{-1}A_2(z,\zeta)\cdot(z,\zeta) + B_1(B_1^{-1}A_1 + D_2B_2^{-1})B_1^T(y,\eta)\cdot(y,\eta)]$$

and the symbol is given by the tempered distribution

$$\tau_{\mathcal{A}}(z,\zeta,y,\eta) = e^{2\pi i B_2^{-1}B_1^T(y,\eta)\cdot(z,\zeta)}.$$

In particular, for every $f, g \in \mathcal{S}(\mathbb{R}^d)$,

$$W_{\mathcal{A}}(f,g)(x,\xi) = \left|\frac{\det(B_1)}{\det(B_2)}\right|^{1/2} \Phi_{-D_1B_1^{-1}}(x,\xi)$$

$$\times \int_{\mathbb{R}^{4d}} f(z)\overline{g(\zeta)} e^{-2\pi i[\Phi_{\mathcal{A}}(z,\zeta,y,\eta)-(x,\xi)\cdot(y,\eta)]}\tau_{\mathcal{A}}(z,\zeta,y,\eta)\,dz\,d\zeta\,dy\,d\eta.$$

$$(5.11)$$

Proof. Let $\widehat{\mathcal{A}_1}, \widehat{\mathcal{A}_2} \in \mathrm{Mp}(2d,\mathbb{R})$ having free projections be such that $\hat{\mathcal{A}} = \widehat{\mathcal{A}_1}\widehat{\mathcal{A}_2}$. We can write, for every $F \in \mathcal{S}(\mathbb{R}^{2d})$, and up to a unitary factor,

$$\hat{\mathcal{A}}F(x,\xi) = \widehat{\mathcal{A}_1}\widehat{\mathcal{A}_2}F(x,\xi).$$

For the rest of the proof, we write

$$X = (x,\xi), \quad Y = (y,\eta), \quad Z = (z,\zeta),$$

while $dY = dy\,d\eta$ and $dZ = dz\,d\zeta$.
Applying Lemma 2.10 and changing variables, up to a unitary constant,

$$\hat{\mathcal{A}}F(X) = |\det(B_1)|^{-1/2}e^{-i\pi D_1B_1^{-1}X\cdot X}\int_{\mathbb{R}^{2d}}(\widehat{\mathcal{A}_2}F)(Z)e^{2\pi i[B_1^{-1}X\cdot Y - \frac{1}{2}B_1^{-1}A_1Y\cdot Y]}dY$$

$$= |\det(B_1B_2)|^{-1/2}e^{-i\pi D_1B_1^{-1}X\cdot X}\int_{\mathbb{R}^{2d}}e^{-i\pi D_2B_2^{-1}Y\cdot Y}$$

$$\times \int_{\mathbb{R}^{2d}}F(Z)e^{2\pi i[B_2^{-1}Y\cdot Z - \frac{1}{2}B_2^{-1}A_2Z\cdot Z]}dZ\,e^{2\pi i[B_1^{-1}X\cdot Y - \frac{1}{2}B_1^{-1}A_1Y\cdot Y]}dY$$

$$= \left|\frac{\det(B_1)}{\det(B_2)}\right|^{1/2}\Phi_{-D_1B_1^{-1}}(X)$$

$$\int_{\mathbb{R}^{4d}}F(Z)e^{2\pi i[-\frac{1}{2}(B_1(B_1^{-1}A_1+D_2B_2^{-1})B_1^TY\cdot Y + B_2^{-1}A_2Z\cdot Z)+X\cdot Y]}e^{2\pi i B_2^{-1}B_1^TY\cdot Z}dY\,dZ.$$

This proves (5.10) and (5.11) follows plugging $F = f \otimes \bar{g}$ in (5.10). □

Moreover, we also have explicit integral formulas for metaplectic Wigner distributions in terms of their factorization via free symplectic matrices.

Corollary 5.3. *Under the same notation of Lemma 5.2, up to a unitary factor and for every $f, g \in \mathcal{S}(\mathbb{R}^d)$,*

$$W_{\mathcal{A}}(f, g)(x, \xi) = |\det(B_1 B_2)|^{-1/2} \Phi_{-D_1 B_1^{-1}}(x, \xi) \int_{\mathbb{R}^{2d}} f(y)\overline{g(\eta)} \Phi_{-B_2^{-1} A_2}(y, \eta)$$

$$\times \mathcal{F}^{-1}(\Phi_{-(B_1^{-1} A_1 + D_2 B_2^{-1})})(B_1^{-1}(x, \xi) + B_2^{-T}(y, \eta)) dy d\eta$$

$$= |\det(B_1 B_2)|^{-1/2} \Phi_{-D_1 B_1^{-1}}(x, \xi)$$

$$\times [((f \otimes \bar{g})\Phi_{-B_2^{-1} A_2}) * (\mathcal{F}^{-1}\Phi_{-(B_1^{-1} A_1 + D_2 B_2^{-1})} \circ (-B_2^{-T}))] \circ (-B_2^T B_1^{-1})(x, \xi),$$

where the chirp Φ is defined in (2.14). In particular, if $B_1^{-1} A_1 + D_2 B_2^{-1}$ is invertible, then, up to a phase factor,

$$W_{\mathcal{A}}(f, g)(x, \xi) = |\det(B_1 B_2)|^{-1/2} |\det(B_1^{-1} A_1 + D_2 B_2^{-1})|^{-1} \Phi_{-D_1 B_1^{-1}}(x, \xi)$$

$$\times \int_{\mathbb{R}^{2d}} f(y)\overline{g(\eta)} \Phi_{-B_2^{-1} A_2}(y, \eta) \Phi_{(B_1^{-1} A_1 + D_2 B_2^{-1})^{-1}}(B_1^{-1}(x, \xi) + B_2^{-T}(y, \eta)) dy d\eta.$$

Proof. Using (5.10), we can write, for every $F \in \mathcal{S}(\mathbb{R}^{2d})$, and up to a unitary factor,

$$\hat{\mathcal{A}} F(x, \xi) = \widehat{\mathcal{A}_1} \widehat{\mathcal{A}_2} F(x, \xi).$$

Applying Lemma 2.10, up to a unitary constant,

$$\hat{\mathcal{A}} F(x, \xi) = |\det(B_1 B_2)|^{-1/2} e^{-i\pi D_1 B_1^{-1}(x, \xi) \cdot (x, \xi)} \int_{\mathbb{R}^{2d}} F(y, \eta) e^{-\pi i B_2^{-1} A_2(y, \eta) \cdot (y, \eta)}$$

$$\times \int_{\mathbb{R}^{2d}} e^{2\pi i [B_1^{-1}(x, \xi) \cdot (z, \zeta) - \frac{1}{2} B_1^{-1} A_1(z, \zeta) \cdot (z, \zeta) - \frac{1}{2} D_2 B_2^{-1}(z, \zeta) \cdot (z, \zeta) + B_2^{-1}(z, \zeta) \cdot (y, \eta)]} dz d\zeta dy d\eta$$

$$= |\det(B_1 B_2)|^{-1/2} \Phi_{-D_1 B_1^{-1}}(x, \xi) \int_{\mathbb{R}^{2d}} F(y, \eta) \Phi_{-B_2^{-1} A_2}(y, \eta)$$

$$\times \int_{\mathbb{R}^{2d}} e^{2\pi i [(B_1^{-1}(x, \xi) + B_2^{-T}(y, \eta)) \cdot (z, \zeta) - \frac{1}{2}(B_1^{-1} A_1 + D_2 B_2^{-1})(z, \zeta) \cdot (z, \zeta)]} dz d\zeta.$$

$$(5.12)$$

The inner integral is worked out as

$$\int_{\mathbb{R}^{2d}} e^{2\pi i [(B_1^{-1}(x, \xi) + B_2^{-T}(y, \eta)) \cdot (z, \zeta) - \frac{1}{2}(B_1^{-1} A_1 - D_2 B_2^{-1})(z, \zeta) \cdot (z, \zeta)]} dz d\zeta$$

$$= \int_{\mathbb{R}^{2d}} \Phi_{-(B_1^{-1} A_1 - D_2 B_2^{-1})}(z, \zeta) e^{2\pi i [B_1^{-1}(x, \xi) + B_2^{-T}(y, \eta)] \cdot (z, \zeta)} dz d\zeta \qquad (5.13)$$

$$= \mathcal{F}^{-1}(\Phi_{-(B_1^{-1} A_1 + D_2 B_2^{-1})})(B_1^{-1}(x, \xi) + B_2^{-T}(y, \eta)).$$

Observe that if $B_1^{-1} A_1 + D_2 B_2^{-1}$ is invertible, then

$$\mathcal{F}^{-1}(\Phi_{-(B_1^{-1} A_1 + D_2 B_2^{-1})}) = \frac{1}{|\det(B_1^{-1} A_1 + D_2 B_2^{-1})|} \Phi_{(B_1^{-1} A_1 + D_2 B_2^{-1})^{-1}}.$$

Plugging (5.13) into (5.11) with $F = f \otimes \bar{g}$ the assertion follows. $\qquad \square$

The integral expression of $W_\mathcal{A}$ provided by Corollary 5.3 is useful to establish continuity properties for $W_\mathcal{A}(f,g)$. In practice an explicit factorization of $\mathcal{A}$ via free matrices may be unknown.

Definition 5.4. Let $a \in \mathcal{S}'(\mathbb{R}^{2d})$. The *metaplectic pseudodifferential operator* with *symbol a* and symplectic matrix $\mathcal{A}$ is the operator $Op_\mathcal{A}(a) : \mathcal{S}(\mathbb{R}^d) \to \mathcal{S}'(\mathbb{R}^d)$ such that
$$\langle Op_\mathcal{A}(a)f, g \rangle = \langle a, W_\mathcal{A}(g,f) \rangle, \quad g \in \mathcal{S}(\mathbb{R}^d).$$

Observe that this operator is well defined by Proposition 2.12, item (iii). Moreover, when the context requires to stress the matrix $\mathcal{A}$ that defines $Op_\mathcal{A}$, we refer to $Op_\mathcal{A}$ to as the *metaplectic pseudodifferential operator* with symbol a.

Remark 5.5. In principle, the full generality of metaplectic framework provides a wide variety of unexplored time-frequency representations that fit many different contexts. Namely, in Definition 5.4, the symplectic matrix $\mathcal{A}$ plays the role of a quantization and the quantization of a pseudodifferential operator is typically chosen depending on the the properties that must be satisfied in a given setting.

Example 5.6. Definition 5.4 in the case of $\mathcal{A}_{1/2,2d} \in \mathrm{Sp}(2d, \mathbb{R})$ in (2.18), provides the well-known Weyl quantization for pseudodifferential operators, that we denote with $Op_{w,2d}(a)$, i.e., for $a \in \mathcal{S}(\mathbb{R}^{2d})$,
$$Op_{w,2d}(a)f(x) = \int_{\mathbb{R}^{2d}} a\left(\frac{x+y}{2}, \xi\right) f(y)e^{2\pi i (x-y)\cdot\xi} dy d\xi, \quad f \in \mathcal{S}(\mathbb{R}^d).$$

When d is clear from the context or irrelevant, we write Op_w instead of $Op_{w,2d}$.

In the following result, we see how the symbols of metaplectic pseudodifferential operators change when we modify the symplectic matrix.

Lemma 5.7. *Consider $\mathcal{A}, \mathcal{B} \in \mathrm{Sp}(2d, \mathbb{R})$ and $a, b \in \mathcal{S}'(\mathbb{R}^{2d})$. Then,*
$$Op_\mathcal{A}(a) = Op_\mathcal{B}(b) \quad \Longleftrightarrow \quad b = \widehat{\mathcal{B}\mathcal{A}^{-1}}(a). \tag{5.14}$$

Proof. Let $f, g \in \mathcal{S}(\mathbb{R}^d)$. Then,
$$\langle Op_\mathcal{A}(a)f, g \rangle = \langle a, \widehat{\mathcal{A}}(f \otimes \bar{g}) \rangle = \langle \widehat{\mathcal{A}^{-1}}a, f \otimes \bar{g} \rangle,$$
$$\langle Op_\mathcal{B}(b)f, g \rangle = \langle b, \widehat{\mathcal{B}}(f \otimes \bar{g}) \rangle = \langle \widehat{\mathcal{B}^{-1}}b, f \otimes \bar{g} \rangle.$$

Since the span of $\mathcal{S}(\mathbb{R}^d) \otimes \mathcal{S}(\mathbb{R}^d)$ is dense in $\mathcal{S}(\mathbb{R}^{2d})$, we deduce that the equality between the two lines holds if and only if
$$\widehat{\mathcal{A}^{-1}}a = \widehat{\mathcal{B}^{-1}}b,$$

which is the same as (5.14). $\square$

As a direct consequence of Lemma 5.7 we get two corollaries. The first one provides the distributional kernel of $Op_\mathcal{A}$.

Corollary 5.8. *Consider* $\mathcal{A} \in \mathrm{Sp}(2d, \mathbb{R})$, $a \in \mathcal{S}'(\mathbb{R}^{2d})$. *Then, for all* $f, g \in \mathcal{S}(\mathbb{R}^d)$,

$$\langle Op_\mathcal{A}(a)f, g \rangle = \langle k_\mathcal{A}(a), g \otimes \bar{f} \rangle, \tag{5.15}$$

where the kernel is given by $k_\mathcal{A}(a) = \widehat{\mathcal{A}^{-1}a}$.

Proof. Plug $\mathcal{B} = I_{4d \times 4d}$ into (5.14) to get (5.15). $\qquad\square$

Corollary 5.9 is a generalization of (5.1) for metaplectic Wigner distributions and pseudodifferential operators. For its statement, we introduce the following notation: if $a \in \mathcal{S}'(\mathbb{R}^{2d})$, $a \otimes 1$ denotes the tempered distribution of $\mathcal{S}'(\mathbb{R}^{4d})$ defined via tensor product as

$$(a \otimes 1)(r, y, \rho, \eta) := a(r, \rho), \quad r, y, \rho, \eta \in \mathbb{R}^d. \tag{5.16}$$

Corollary 5.9. *Consider* $\mathcal{A} \in \mathrm{Sp}(4d, \mathbb{R})$, $\mathcal{B} \in \mathrm{Sp}(2d, \mathbb{R})$ *and* $a \in \mathcal{S}'(\mathbb{R}^{2d})$. *Then, for all* $\mathcal{B}_0 \in \mathrm{Sp}(4d, \mathbb{R})$, $f, g \in \mathcal{S}(\mathbb{R}^d)$,

$$W_\mathcal{A}(Op_\mathcal{B}(a)f, g) = Op_{\mathcal{B}_0}(\widehat{\mathcal{B}_0\mathcal{A}_{1/2,4d}^{-1}}((\widehat{\mathcal{A}_{1/2,2d}\mathcal{B}^{-1}a}) \otimes 1) \circ \mathcal{A}^{-1}) \times \\ \times \quad W_\mathcal{A}(f, g). \tag{5.17}$$

In particular,
(i) if $\mathcal{B}_0 = \mathcal{A}_{1/2,4d}$, *then*

$$W_\mathcal{A}(Op_\mathcal{B}(a)f, g) = Op_{w,4d}(((\widehat{\mathcal{A}_{1/2,2d}\mathcal{B}^{-1}a}) \otimes 1) \circ \mathcal{A}^{-1})W_\mathcal{A}(f, g); \tag{5.18}$$

(ii) if $\mathcal{B}_0 = \mathcal{A}_{1/2,4d}$ *and* $\mathcal{B} = \mathcal{A}_{1/2,2d}$, *then*

$$W_\mathcal{A}(Op_{w,2d}(a)f, g) = Op_{w,4d}((a \otimes 1) \circ \mathcal{A}^{-1})W_\mathcal{A}(f, g). \tag{5.19}$$

Proof. By [30, Lemma 4.1], for all $f, g \in \mathcal{S}(\mathbb{R}^d)$ and $a \in \mathcal{S}'(\mathbb{R}^{2d})$,

$$(Op_{w,2d}(a)f) \otimes \bar{g} = Op_{w,4d}(\sigma)(f \otimes \bar{g}). \tag{5.20}$$

Moreover, for all $\mathcal{A} \in \mathrm{Sp}(4d, \mathbb{R})$,

$$\hat{A}Op_{w,4d}(\sigma)\hat{A}^{-1} = Op_{w,4d}(\sigma \circ \mathcal{A}^{-1}). \tag{5.21}$$

Therefore, using Lemma 5.7, (5.20) and (5.21) respectively,

$$W_\mathcal{A}(Op_\mathcal{B}(a)f, g) = \hat{A}(Op_\mathcal{B}(a)f \otimes \bar{g}) = \hat{A}(Op_{w,2d}(\widehat{\mathcal{A}_{1/2,2d}\mathcal{B}^{-1}a})f \otimes \bar{g})$$
$$= \hat{A}(Op_{w,4d}((\widehat{\mathcal{A}_{1/2,2d}\mathcal{B}^{-1}a}) \otimes 1)(f \otimes \bar{g}))$$
$$= Op_{w,4d}(((\widehat{\mathcal{A}_{1/2,2d}\mathcal{B}^{-1}a}) \otimes 1) \circ \mathcal{A}^{-1})\hat{A}(f \otimes \bar{g})$$
$$= Op_{w,4d}(((\widehat{\mathcal{A}_{1/2,2d}\mathcal{B}^{-1}a}) \otimes 1) \circ \mathcal{A}^{-1})W_\mathcal{A}(f, g).$$

Then, by Lemma 5.7,

$$W_{\mathcal{A}}(Op_{\mathcal{B}}(a)f, g) = Op_{\mathcal{B}_0}(\mathcal{B}_0\widehat{\mathcal{A}_{1/2,4d}^{-1}}((\widehat{\mathcal{A}_{1/2,2d}}\mathcal{B}^{-1}a) \otimes 1) \circ \mathcal{A}^{-1})W_{\mathcal{A}}(f, g)$$

and we are done.   □

Remark 5.10. Formula (5.17) will be used in the form of (5.19) to deduce boundedness properties on modulation spaces for metaplectic pseudodifferential operators. However, the strength of Corollary 5.9 relies on its generality: the matrix $\mathcal{B}_0$ in (5.17) can be chosen in $\mathrm{Sp}(4d, \mathbb{R})$ arbitrarily, depending on the context.

5.3   Decomposability and covariance

In this section, we focus on metaplectic Wigner distributions that are defined in terms of symplectic matrices that satisfy decomposability and covariance properties. Explicit expressions for $W_{\mathcal{A}}$ and $Op_{\mathcal{A}}$ are derived from $\mathcal{A}$ in terms of its blocks.

5.3.1   Decomposability and shift-invertibility

We define decomposable metaplectic Wigner distributions directly in terms of their factorization, as follows. Let $\mathcal{A}$ be a symplectic matrix that factorizes as

$$\mathcal{A} = \mathcal{A}_{FT2}\mathcal{D}_L, \tag{5.22}$$

where $\mathcal{D}_L$ is defined in (2.11) and

$$\mathcal{A}_{FT2} = \begin{pmatrix} I_{d\times d} & 0_{d\times d} & 0_{d\times d} & 0_{d\times d} \\ 0_{d\times d} & 0_{d\times d} & 0_{d\times d} & I_{d\times d} \\ 0_{d\times d} & 0_{d\times d} & I_{d\times d} & 0_{d\times d} \\ 0_{d\times d} & -I_{d\times d} & 0_{d\times d} & 0_{d\times d} \end{pmatrix}. \tag{5.23}$$

Up to a phase factor,

$$\widehat{\mathcal{A}_{FT2}} = \mathcal{F}_2.$$

Definition 5.11. We say that $\mathcal{A} \in \mathrm{Sp}(2d, \mathbb{R})$ is a *totally Wigner-decomposable* (symplectic) matrix if (5.22) holds for some $L \in \mathrm{GL}(2d, \mathbb{R})$. If $\mathcal{A}$ is totally Wigner-decomposable, we say that $W_{\mathcal{A}}$ is of the *classic type*.

Example 5.12. The matrices (2.18) and (2.17) are totally Wigner-decomposable with

$$L_\tau = \begin{pmatrix} I_{d\times d} & \tau I_{d\times d} \\ I_{d\times d} & -(1-\tau)I_{d\times d} \end{pmatrix}$$

and

$$L_{ST} = \begin{pmatrix} 0_{d\times d} & I_{d\times d} \\ -I_{d\times d} & I_{d\times d} \end{pmatrix}$$

respectively.

Wigner distributions of classic type are immediate generalizations of the classical time-frequency representations, such as the (cross)-Wigner distribution W and the STFT.

The following result characterizes totally Wigner-decomposable symplectic matrices in terms of their block decomposition.

Proposition 5.13. Let $\mathcal{A} \in \mathrm{Sp}(2d, \mathbb{R})$ be a totally Wigner-decomposable matrix having block decomposition

$$\mathcal{A} = \begin{pmatrix} A_{11} & A_{12} & A_{13} & A_{14} \\ A_{21} & A_{22} & A_{23} & A_{24} \\ A_{31} & A_{32} & A_{33} & A_{34} \\ A_{41} & A_{42} & A_{43} & A_{44} \end{pmatrix}, \tag{5.24}$$

with $A_{ij} \in \mathbb{R}^{d \times d}$ $(i, j = 1, \ldots, 4)$. Then,
(i) $\mathcal{A}$ has the block decomposition

$$\mathcal{A} = \begin{pmatrix} A_{11} & A_{12} & 0_{d \times d} & 0_{d \times d} \\ 0_{d \times d} & 0_{d \times d} & A_{23} & A_{24} \\ 0_{d \times d} & 0_{d \times d} & A_{33} & A_{34} \\ A_{41} & A_{42} & 0_{d \times d} & 0_{d \times d} \end{pmatrix}; \tag{5.25}$$

(ii) L and its inverse are related to $\mathcal{A}$ by:

$$L = \begin{pmatrix} A_{33}^T & A_{23}^T \\ A_{34}^T & A_{24}^T \end{pmatrix}, \quad L^{-1} = \begin{pmatrix} A_{11} & A_{12} \\ -A_{41} & -A_{42} \end{pmatrix}. \tag{5.26}$$

Proof. Let

$$L = \begin{pmatrix} L_{11} & L_{12} \\ L_{21} & L_{22} \end{pmatrix} \quad \text{and} \quad L^{-1} = \begin{pmatrix} L'_{11} & L'_{12} \\ L'_{21} & L'_{22} \end{pmatrix} \tag{5.27}$$

be the block decompositions of L and L^{-1} respectively, where $L_{ij}, L'_{ij} \in \mathbb{R}^{d \times d}$ $(i, j = 1, 2)$. Then, the identity (5.22) reads as

$$\begin{pmatrix} A_{11} & A_{12} & A_{13} & A_{14} \\ A_{21} & A_{22} & A_{23} & A_{24} \\ A_{31} & A_{32} & A_{33} & A_{34} \\ A_{41} & A_{42} & A_{43} & A_{44} \end{pmatrix} = \begin{pmatrix} L'_{11} & L'_{12} & 0_{d \times d} & 0_{d \times d} \\ 0_{d \times d} & 0_{d \times d} & L_{12}^T & L_{22}^T \\ 0_{d \times d} & 0_{d \times d} & L_{11}^T & L_{21}^T \\ -L'_{21} & -L'_{22} & 0_{d \times d} & 0_{d \times d} \end{pmatrix}.$$

Thus the expressions for the matrices in (i) and (ii) easily follow. $\qquad\square$

Remark 5.14. Under the hypothesis of Proposition 5.13, it is easy to check that the identities $LL^{-1} = L^{-1}L = I_{2d \times 2d}$ read in terms of the blocks of L and L^{-1} as

$$\begin{cases} A_{33}^T A_{11} - A_{23}^T A_{41} = I_{d \times d}, \\ A_{33}^T A_{12} = A_{23}^T A_{42}, \\ A_{34}^T A_{11} = A_{24}^T A_{41}, \\ A_{34}^T A_{12} - A_{24}^T A_{42} = I_{d \times d} \end{cases} \quad \text{and} \quad \begin{cases} A_{11} A_{33}^T + A_{12} A_{34}^T = I_{d \times d}, \\ A_{11} A_{23}^T = -A_{12} A_{24}^T, \\ A_{41} A_{33}^T = -A_{42} A_{34}^T, \\ A_{41} A_{23}^T + A_{42} A_{24}^T = -I_{d \times d}. \end{cases} \tag{5.28}$$

These are exactly the block relations that $\mathcal{A}$ and

$$\mathcal{A}^{-1} = \mathcal{D}_L^{-1} \mathcal{A}_{FT2}^{-1} = \begin{pmatrix} A_{33}^T & 0_{d\times d} & 0_{d\times d} & -A_{23}^T \\ A_{34}^T & 0_{d\times d} & 0_{d\times d} & -A_{24}^T \\ 0_{d\times d} & -A_{41}^T & A_{11}^T & 0_{d\times d} \\ 0_{d\times d} & -A_{42}^T & A_{12}^T & 0_{d\times d} \end{pmatrix} \tag{5.29}$$

satisfy as symplectic matrices.

As pointed out in [31], shift-invertibility of symplectic matrices appears to be the fundamental property that a metaplectic Wigner distribution shall satisfy in order for $W_{\mathcal{A}}(\cdot, g)$ to replace the STFT in the definition of modulation spaces.

Lemma 5.15. *Let $\mathcal{A} \in \mathrm{Sp}(2d, \mathbb{R})$ be a totally Wigner-decomposable as in (5.22) and (5.24). The following statements are equivalent:*
(i) L is right-regular;
(ii) the matrix

$$E_{\mathcal{A}} := \begin{pmatrix} A_{11} & 0_{d\times d} \\ 0_{d\times d} & A_{23} \end{pmatrix} \tag{5.30}$$

is invertible;
(iii) $W_{\mathcal{A}}$ is shift-invertible with $E_{\mathcal{A}}$ given as in (5.30).

Proof. The equivalence between (ii) and (iii) is proved in [31]. We prove that (i) and (ii) are equivalent.

$(i) \Rightarrow (ii)$. Assume that L is right-regular. We have to prove that both A_{23} and A_{11} are invertible. The right-regularity of L is equivalent to the invertibility of A_{23} and A_{24}, hence it remains to check that A_{11} is invertible.

It is easy to verify that L is right-regular if and only if L^{-T} is left-regular. By Proposition 5.13 (ii),

$$L^{-T} = \begin{pmatrix} A_{11}^T & -A_{41}^T \\ A_{12}^T & -A_{42}^T \end{pmatrix},$$

so that L^{-T} is left-regular if and only if A_{11} and A_{12} are invertible, which gives the invertibility of A_{11}.

$(i) \Leftarrow (ii)$. If $E_{\mathcal{A}}$ is invertible, then A_{11} and A_{23} are invertible. By the identity $A_{11} A_{23}^T = -A_{12} A_{24}^T$ in (5.28), we also have the invertibility of A_{12} and A_{24}. Hence, A_{23} and A_{24} are invertible. $\qquad\square$

Corollary 5.16. *Let $\mathcal{A}$ satisfy (5.22) with block decomposition as in (5.25). The following statements are equivalent:*
(i) L is right-regular;
(ii) A_{11}, A_{12}, A_{23} and A_{24} are invertible.
Moreover, if L is right-regular,
(iii) A_{33} is invertible if and only if A_{42} is invertible;
(iv) A_{34} is invertible if and only if A_{41} is invertible.

Proof. The equivalence between (i) and (ii) is just a restatement of Lemma 5.15. (iii) and (iv) follow directly from (ii) and the equalities in (5.28). $\qquad\square$

Remark 5.17. Assume that L is right-regular with block decomposition as in (5.27). Since L is also invertible by its definition, all the assumptions of Theorem 2.1 (ii) and Theorem 2.2 (i) of [85] are verified. Thus, we can write a Wigner-decomposable matrix $\mathcal{A}$, with L right-regular, explicitly in terms of the blocks of L both as

$$\mathcal{A} = \begin{pmatrix} A_{11} & A_{12} & 0_{d\times d} & 0_{d\times d} \\ 0_{d\times d} & 0_{d\times d} & L_{12}^T & L_{22}^T \\ 0_{d\times d} & 0_{d\times d} & L_{11}^T & L_{21}^T \\ A_{41} & A_{42} & 0_{d\times d} & 0_{d\times d} \end{pmatrix}$$

with

$$A_{11} = (L_{11} - L_{12}L_{22}^{-1}L_{21})^{-1},$$
$$A_{12} = -(L_{11} - L_{12}L_{22}^{-1}L_{21})^{-1}L_{12}L_{22}^{-1},$$
$$A_{41} = L_{22}^{-1}L_{21}(L_{11} - L_{12}L_{22}^{-1}L_{21})^{-1},$$
$$A_{42} = -L_{22}^{-1} - L_{22}^{-1}L_{21}(L_{11} - L_{12}L_{22}^{-1}L_{21})^{-1}L_{12}L_{22}^{-1};$$

or, equivalently, as

$$\mathcal{A} = \begin{pmatrix} A_{11} & A_{12} & 0_{d\times d} & 0_{d\times d} \\ 0_{d\times d} & 0_{d\times d} & L_{12}^T & L_{22}^T \\ 0_{d\times d} & 0_{d\times d} & L_{11}^T & L_{21}^T \\ A_{41} & A_{42} & 0_{d\times d} & 0_{d\times d} \end{pmatrix},$$

where

$$A_{11} = -(L_{21} - L_{22}L_{12}^{-1}L_{11})^{-1}L_{22}L_{12}^{-1},$$
$$A_{12} = (L_{21} - L_{22}L_{12}^{-1}L_{11})^{-1},$$
$$A_{41} = -L_{12}^{-1} - L_{12}^{-1}L_{11}(L_{21} - L_{22}L_{12}^{-1}L_{11})^{-1}L_{22}L_{12}^{-1}$$
$$A_{42} = -L_{12}^{-1}L_{11}(L_{21} - L_{22}L_{12}^{-1}L_{11})^{-1}L_{22}L_{12}^{-1}.$$

Theorem 5.18. *Let L be right-regular and $\mathcal{A}$ be as in (5.25). Then, for all $f, g \in L^2(\mathbb{R}^d)$ and for all $x, \xi \in \mathbb{R}^d$,*

$$W_\mathcal{A}(f,g)(x,\xi) = \sqrt{|\det(L)|}|\det(A_{23})|^{-1}e^{2\pi i A_{23}^{-1}\xi \cdot A_{33}^T x}V_{\widetilde{g}}f(c(x),d(\xi)), \quad (5.31)$$

where

$$\widetilde{g}(t) := g(A_{24}^T A_{23}^{-T}t), \ c(x) = (A_{33}^T - A_{23}^T A_{24}^{-T} A_{34}^T)x \ and \ d(\xi) = A_{23}^{-1}\xi. \quad (5.32)$$

Observe that all the inverses that appear in (5.31) exist if L is right-regular by Corollary 5.16 (ii) and Theorem 2.1 (ii) of [85].

Proof. The proof is a straightforward consequence of [32, Theorem 3.8]. $\qquad\square$

Theorem 5.19. *Let $0 < p, q \leq \infty$, L be right-regular and $\mathcal{A}$ be as in (5.25). Let $m \in \mathcal{M}_v$ be such that*

$$m((A_{33}^T - A_{23}^T A_{24}^{-T} A_{34}^T)\cdot, A_{23}^{-1}\cdot) \asymp m(\cdot, \cdot). \tag{5.33}$$

Then, for all $g \in \mathcal{S}(\mathbb{R}^d)$,

$$f \in M_m^{p,q}(\mathbb{R}^d) \quad \Longleftrightarrow \quad W_{\mathcal{A}}(f, g) \in L_m^{p,q}(\mathbb{R}^{2d}). \tag{5.34}$$

Moreover, if $1 \leq p, q \leq \infty$ and there exist $0 < C_1(L) \leq C_2(L)$ such that

$$C_1(L)v(x, \xi) \leq v((A_{23}^T(A_{24}^T)^{-1})x, A_{23}^{-1}A_{24}\xi) \leq C_2(L)v(x, \xi), \quad (x, \xi) \in \mathbb{R}^{2d}, \tag{5.35}$$

then g can be chosen in the larger class $M_v^1(\mathbb{R}^d)$.

Proof. The proof is a straightforward consequence of Theorem 5.18. In fact, for $g \in \mathcal{S}(\mathbb{R}^d)$ and L right-regular, the function $\widetilde{g}$ defined as in (5.32) is in $\mathcal{S}(\mathbb{R}^d)$ and by (5.31),

$$\|f\|_{M_m^{p,q}} \asymp \|V_{\widetilde{g}}f\|_{L_m^{p,q}} \asymp \|W_{\mathcal{A}}(f, g)((A_{33}^T - A_{23}^T(A_{24}^T)^{-1}A_{34}^T)^{-1}\cdot, A_{23}\cdot)\|_{L_m^{p,q}}$$
$$\asymp \|W_{\mathcal{A}}(f, g)\|_{L_m^{p,q}},$$

by assumption (5.33).

Assume that $\varphi \in \mathcal{S}(\mathbb{R}^d)$. Then,

$$V_{\varphi}\widetilde{g}(x, \xi) = \int_{\mathbb{R}^d} g(Ct)e^{-2\pi i\xi\cdot t}\overline{\varphi(t - x)}dt$$
$$\asymp \int_{\mathbb{R}^d} g(s)e^{-2\pi i((C^{-1})^T\xi)\cdot s}\overline{\varphi(C^{-1}(s - Cx))}ds$$
$$= V_{\widetilde{\varphi}}g(B(x, \xi)),$$

where

$$C = A_{24}^T A_{23}^{-T}, \qquad B = \begin{pmatrix} C & 0_{d\times d} \\ 0_{d\times d} & C^{-T} \end{pmatrix} = \mathcal{D}_{A_{24}^{-T}}\mathcal{D}_{A_{23}^T}$$

and $\widetilde{\varphi}(t) = \varphi(C^{-1}t)$. Condition (5.35) implies that $g \in M_v^1$ if and only if $\widetilde{g} \in M_v^1$:

$$\|\widetilde{g}\|_{M_v^1} \asymp \|V_{\varphi}\widetilde{g}\|_{L_v^1} \asymp \|V_{\widetilde{\varphi}}g(B\cdot)v(\cdot)\|_{L^1}$$
$$\asymp \|V_{\widetilde{\varphi}}g(\cdot)v(B^{-1}\cdot)\|_{L^1} \asymp \|V_{\widetilde{\varphi}}g(\cdot)v(\cdot)\|_{L^1} \asymp \|g\|_{M_v^1}.$$

Hence, for $1 \leq p, q \leq \infty$, we can choose g in $M_v^1(\mathbb{R}^d)$. $\qquad\square$

Next, we generalize the metaplectic Wigner distributions associated to Wigner-decomposable matrices in order to include multiplications by chirps. These Wigner distributions, along with the right-regularity condition on L, characterize modulation spaces.

Definition 5.20. We say that a matrix $\mathcal{A} \in \mathrm{Sp}(d, \mathbb{R})$ is *Wigner-decomposable* if $\mathcal{A} = V_C \mathcal{A}_{FT2} \mathcal{D}_L$ for some $C \in \mathbb{R}^d$ symmetric and $L \in \mathrm{GL}(d, \mathbb{R})$.

Theorem 5.21. *Let $\mathcal{A} \in \mathrm{Sp}(2d, \mathbb{R})$ be a Wigner-decomposable matrix with decomposition $\mathcal{A} = V_C \mathcal{A}_{FT2} \mathcal{D}_L$ (where $V_C, \mathcal{A}_{FT2}, \mathcal{D}_L$ are defined in (2.11), (5.23), and (2.11), respectively)*

$$C = \begin{pmatrix} C_{11} & C_{12} \\ C_{12}^T & C_{22,} \end{pmatrix}$$

$C_{11}^T = C_{11}$ *and* $C_{22}^T = C_{22}$*. Then, for all $f, g \in L^2(\mathbb{R}^d)$, up to a phase factor,*

$$W_{\mathcal{A}}(f, g)(x, \xi) = \widetilde{\Phi}_C(x, \xi) \int_{\mathbb{R}^d} f(x + (I_{d \times d} - A_{11})y) \overline{g(x - A_{11}y)} e^{-2\pi i \xi \cdot y} dy,$$

(5.36)

with

$$\widetilde{\Phi}_C(x, \xi) = e^{2\pi i C_{12}^T x \cdot \xi} \Phi_{C_{11}}(x) \Phi_{C_{22}}(\xi)$$

and the chirp functions $\Phi_{C_{11}}$, $\Phi_{C_{22}}$ are defined in (2.14). If the matrix L is right-regular,

$$W_{\mathcal{A}}(f, g)(x, \xi) = |\det(I_{d \times d} - A_{11})|^{-1} \widetilde{\Phi}'_C(x, \xi) V_{\tilde{g}} f(A_{11}^{-1} x, (I - A_{11}^T)^{-1} \xi), \quad (5.37)$$

where

$$\widetilde{\Phi}'_C(x, \xi) = \Phi_{C_{11}}(x) \Phi_{C_{22}}(\xi) e^{2\pi i (C_{12}^T + (I - A_{11})^{-1}) x \cdot \xi},$$

and $\tilde{g}(t) = g(-A_{11}(I_{d \times d} - A_{11})^{-1} t)$.

Proof. Formula (5.36) is proved using the explicit definitions of the operators associated to V_C, $\mathcal{A}_{FT2}$ and $\mathcal{D}_L$. In fact, up to a phase factor,

$$\widehat{\mathcal{A}_{FT2} \mathcal{D}_L}(f \otimes \bar{g})(x, \xi) = \mathcal{F}_2 \mathfrak{T}_L(f \otimes \bar{g})(x, \xi) = \int_{\mathbb{R}^d} (f \otimes \bar{g})(L(x, y)) e^{-2\pi i \xi \cdot y} dy$$

$$= \int_{\mathbb{R}^d} f(x + (I_{d \times d} - A_{11})y) \overline{g(x - A_{11}y)} e^{-2\pi i \xi \cdot y} dy.$$

For $z = (x, \xi)$ and V_C as in the statement, we have by (2.15)

$$\widehat{V_C} F(z) = e^{\pi i C z \cdot z} F(z) = e^{i\pi[(C_{11}x + C_{12}\xi) \cdot x + (C_{12}^T x + C_{22}\xi) \cdot \xi]} F(z), \quad F \in L^2(\mathbb{R}^{2d}).$$

Furthermore, formula (5.31) applied to the symplectic matrix $\mathcal{A}_{FT2} \mathcal{D}_L$ (L as in the statement, see [31, Theorem 2.27], where the formula was obtained in this particular case) tells that, up to a unitary constant,

$$W_{\mathcal{A}}(f, g)(z) = e^{\pi i (Cz) \cdot z} |\det(I_{d \times d} - A_{11})|^{-1} e^{2\pi i ((I_{d \times d} - A_{11}^T)^{-1} \xi) \cdot x}$$
$$\times V_{\tilde{g}} f(A_{11}^{-1} x, (I_{d \times d} - A_{11}^T)^{-1} \xi),$$

for $f, g \in L^2(\mathbb{R}^d)$ and $\tilde{g}$ being as in the statement.   □

As a consequence, we extend [31, Theorem 2.28] to all Wigner-decomposable matrices.

Corollary 5.22. *Under the notation of Theorem 5.25, the following statements are equivalent:*
(i) $\mathcal{A} = V_C \mathcal{A}_{FT2} \mathcal{D}_L$ is shift-invertible,
(ii) $\mathcal{A} = \mathcal{A}_{FT2} \mathcal{D}_L$ is shift-invertible,
(iii) L is right-regular.

Proof. The equivalence $(i) \Leftrightarrow (ii)$ is proved in Corollary 5.16. The equivalence $(ii) \Leftrightarrow (iii)$ follows from Theorem 5.21, which gives:

$$W_{\mathcal{A}}(f,g)(x,\xi) = e^{i\pi[(C_{11}x + C_{12}\xi)\cdot x + (C_{12}^T x + C_{22}\xi)\cdot \xi]} W_{\mathcal{A}_{FT2}\mathcal{D}_L}(f,g)(x,\xi),$$

so that:

$$|W_{\mathcal{A}}(f,g)(x,\xi)| = |W_{\mathcal{A}_{FT2}\mathcal{D}_L}(f,g)(x,\xi)|. \tag{5.38}$$

This gives

$$|W_{\mathcal{A}}(\pi(w)f,g)| = |W_{\mathcal{A}_{FT2}\mathcal{D}_L}(\pi(w)f,g)|, \quad \forall w \in \mathbb{R}^{2d},$$

which proves the claim. $\square$

Corollary 5.23. *Let $\mathcal{A} \in \mathrm{Sp}(2d,\mathbb{R})$ be Wigner-decomposable, with matrix L right-regular. Then, for any $g \in \mathcal{S}(\mathbb{R}^d)$, $0 < p,q \leq \infty$,*

$$f \in M_{v_s}^{p,q}(\mathbb{R}^d) \quad \Longleftrightarrow \quad W_{\mathcal{A}}(f,g) \in L_{v_s}^{p,q}(\mathbb{R}^{2d}).$$

For $1 \leq p,q \leq \infty$, the window g can be chosen in $M_{v_s}^1(\mathbb{R}^d)$.

Proof. With the same notations as Theorem 5.21, write $\mathcal{A} = V_C \mathcal{A}_{FT2} \mathcal{D}_L$, with L is right-invertible. By (5.38),

$$W_{\mathcal{A}}(f,g) \in L_{v_s}^{p,q}(\mathbb{R}^{2d}) \quad \Longleftrightarrow \quad W_{\mathcal{A}_{FT2}\mathcal{D}_L}(f,g) \in L_{v_s}^{p,q}(\mathbb{R}^{2d}).$$

By Corollary 5.22, $\mathcal{A}_{FT2}\mathcal{D}_L$ is a covariant (see Subsection 5.3.2 below), shift-invertible matrix. Then the claim follows from [31, Theorem 2.28]. $\square$

5.3.2   Covariance

According to [31, Proposition 2.10], for a given symplectic matrix $\mathcal{A}$, the metaplectic Wigner distribution $W_{\mathcal{A}}$ satisfies

$$W_{\mathcal{A}}(\pi(z)f, \pi(z)g) = T_z W_{\mathcal{A}}(f,g), \quad (f,g \in \mathcal{S}(\mathbb{R}^d)), \quad z \in \mathbb{R}^d, \tag{5.39}$$

if and only if $\mathcal{A}$ has block decomposition

$$
\mathcal{A} = \begin{pmatrix} A_{11} & I_{d\times d} - A_{11} & A_{13} & A_{13} \\ A_{21} & -A_{21} & I_{d\times d} - A_{11}^T & -A_{11}^T \\ 0_{d\times d} & 0_{d\times d} & I_{d\times d} & I_{d\times d} \\ -I_{d\times d} & I_{d\times d} & 0_{d\times d} & 0_{d\times d} \end{pmatrix}, \tag{5.40}
$$

with $A_{13} = A_{13}^T$ and $A_{21} = A_{21}^T$. We refer to such matrices as to *covariant matrices* and to property (5.39) as to the *covariance* property of $W_{\mathcal{A}}$. It was proved in [31] that a covariant matrix with block decomposition (5.40) is totally Wigner-decomposable if and only if $A_{21} = A_{13} = 0_{d\times d}$. Moreover, if

$$
B_{\mathcal{A}} := \begin{pmatrix} A_{13} & \frac{1}{2}I_{d\times d} - A_{11} \\ \frac{1}{2}I_{d\times d} & -A_{21} \end{pmatrix}, \tag{5.41}
$$

and W is the classical Wigner distribution, the following result holds:

Theorem 5.24. *Let $\mathcal{A} \in \mathrm{Sp}(2d, \mathbb{R})$ be a covariant matrix in the form (5.40). Then,*

$$
W_{\mathcal{A}}(f, g) = W(f, g) * \Sigma_{\mathcal{A}}, \quad f, g \in \mathcal{S}(\mathbb{R}^d), \tag{5.42}
$$

where

$$
\Sigma_{\mathcal{A}} = \mathcal{F}^{-1}(e^{-\pi i \zeta \cdot B_{\mathcal{A}} \zeta}) \in \mathcal{S}'(\mathbb{R}^{2d}), \tag{5.43}
$$

and $B_{\mathcal{A}}$ defined as in (5.41).

Recalling our chirp function in (2.14), the equality in (5.43) can be rewritten as

$$
\Sigma_{\mathcal{A}} = \mathcal{F}^{-1}\Phi_{-B_{\mathcal{A}}}. \tag{5.44}
$$

If a time-frequency representation $Q(f, g)$ satisfies

$$
Q(f, g) = W(f, g) * \Sigma, \quad f, g \in \mathcal{S}(\mathbb{R}^d),
$$

for some $\Sigma \in \mathcal{S}'(\mathbb{R}^{2d})$, we say that Q belongs to the *Cohen class*.

Theorem 5.24 sheds light on the importance of covariant matrices in the context of time-frequency analysis, stating that $\mathcal{A} \in \mathrm{Sp}(2d, \mathbb{R})$ is covariant if and only if $W_{\mathcal{A}}$ belongs to the Cohen class. The following result shows that covariant matrices are exactly those that decompose as the product of symplectic matrices V_C^T, $\mathcal{A}_{FT2}$ and $\mathcal{D}_L$ for some $d \times d$ symmetric matrix C and $L \in \mathrm{GL}(2d, \mathbb{R}^d)$.

Theorem 5.25. *Let $\mathcal{A} \in \mathrm{Sp}(2d, \mathbb{R})$ be covariant with block decomposition (5.40). Then,*

$$
\mathcal{A} = V_C^T \mathcal{A}_{FT2} \mathcal{D}_L, \tag{5.45}
$$

where

$$
C = \begin{pmatrix} A_{13} & 0_{d\times d} \\ 0_{d\times d} & -A_{21} \end{pmatrix} \quad and \quad L = \begin{pmatrix} I_{d\times d} & I_{d\times d} - A_{11} \\ I_{d\times d} & -A_{11} \end{pmatrix}. \tag{5.46}
$$

As a consequence, up to a phase factor, for all $f, g \in \mathcal{S}(\mathbb{R}^d)$,

$$W_{\mathcal{A}}(f,g)(x,\xi) = \int_{\mathbb{R}^d} [\mathcal{F}(\Phi_{-A_{13}}) * (f \otimes \bar{g})(L(\cdot, \eta))](x)\Phi_{A_{21}}(\eta)e^{-2\pi i\xi \cdot \eta}d\eta. \quad (5.47)$$

In particular, if $A_{13} = 0_{d \times d}$, *then*

$$W_{\mathcal{A}}(f,g)(x,\xi) = \int_{\mathbb{R}^d} f(x + (I_{d \times d} - A_{11})\eta)\overline{g(x - A_{11}\eta)}\Phi_{A_{21}}(\eta)e^{-2\pi i\xi \cdot \eta}d\eta. \quad (5.48)$$

Proof. Equality (5.45) is a straightforward computation. Then,

$$W_{\mathcal{A}}(f,g)(x,\xi) = \hat{\mathcal{A}}(f \otimes \bar{g})(x,\xi) = \widehat{V_C^T}\widehat{\mathcal{A}_{FT2}}\widehat{\mathcal{D}_L}(f \otimes \bar{g})(x,\xi)$$

$$= \mathcal{F}(\Phi_{-C}) * \left(\int_{\mathbb{R}^d} (f \otimes \bar{g})(L(\cdot, \eta))e^{-2\pi i\eta \cdot (\bullet)}d\eta \right)(x,\xi)$$

$$= \int_{\mathbb{R}^{2d}} \mathcal{F}(\Phi_{-C})(x - y, \xi - \omega)\left(\int_{\mathbb{R}^d} (f \otimes \bar{g})(L(y, \eta))e^{-2\pi i\eta \cdot \omega}d\eta \right)dyd\omega$$

$$= \int_{\mathbb{R}^{2d}} \left(\int_{\mathbb{R}^{2d}} e^{-i\pi[A_{13}u \cdot u - A_{21}v \cdot v]}e^{-2\pi i[(x-y) \cdot u + (\xi - \omega) \cdot v]}dudv \right)$$

$$\times \left(\int_{\mathbb{R}^d} (f \otimes \bar{g})(L(y, \eta))e^{-2\pi i\eta \cdot \omega}d\eta \right)dyd\omega.$$

Observe that

$$\int_{\mathbb{R}^{2d}} e^{i\pi A_{21}v \cdot v}e^{-2\pi i\xi \cdot v}e^{2\pi i\omega \cdot (v-\eta)}dvd\omega = e^{\pi iA_{21}\eta \cdot \eta}e^{-2\pi i\xi \cdot \eta},$$

so that

$$W_{\mathcal{A}}(f,g)(x,\xi)$$

$$= \int_{\mathbb{R}^d} \left(\int_{\mathbb{R}^{2d}} e^{-i\pi A_{13}u \cdot u}e^{2\pi iu \cdot (x-y)}(f \otimes \bar{g})(L(y, \eta))dudy \right)e^{\pi iA_{21}\eta \cdot \eta}e^{-2\pi i\xi \cdot \eta}d\eta.$$

Next, we apply

$$\int_{\mathbb{R}^{2d}} \varphi_1(u)\varphi_2(y)e^{2\pi iu \cdot x}e^{-2\pi iu \cdot y}dudy = \int_{\mathbb{R}^d} \left(\int_{\mathbb{R}^d} \varphi_2(y)e^{-2\pi iu \cdot y}dy \right)\varphi_1(u)e^{2\pi iu \cdot x}du$$

$$= \int_{\mathbb{R}^d} \hat{\varphi}_2(u)\varphi_1(u)e^{2\pi ix \cdot u}du = \mathcal{F}^{-1}(\varphi_1\hat{\varphi}_2)(x)$$

$$= (\mathcal{F}^{-1}(\varphi_1) * \varphi_2)(x)$$

to the inner integral, to get (5.47). $\qquad\square$

Remark 5.26. Theorem 5.25 states that the class of covariant symplectic matrices is invariant with respect to left-multiplication by matrices V_C^T. Equivalently, the class of metaplectic Wigner distributions associated to covariant matrices is invariant with respect to convolutions by kernels in the form Φ_C, C $d \times d$ real symmetric matrix.

Remark 5.27. Theorem 5.25 clarifies the roles that the blocks A_{13} and A_{21} have in Wigner metaplectic operators associated to covariant matrices. The block A_{13} appears in the convolution factor $\mathcal{F}(\Phi_{-A_{13}})(\cdot)$ and acts on $(f \otimes \bar{g}) \circ L(\cdot, \eta)$, whereas A_{21} produces the phase factor $\Phi_{A_{21}}$.

As we pointed out, covariant matrices play a key part in the theory of pseudodifferential operators, as they belong to the Cohen class. In the following result we prove an explicit integral formula for metaplectic pseudodifferential operators associated to covariant matrices.

Proposition 5.28. Let $\mathcal{A} \in \mathrm{Sp}(2d, \mathbb{R})$ be a covariant matrix with decomposition in (5.45). Then, for every $f \in \mathcal{S}(\mathbb{R}^d)$ and $a \in \mathcal{S}(\mathbb{R}^{2d})$, up to a phase factor,

$$Op_{\mathcal{A}}(a)f(x) = \int_{\mathbb{R}^{2d}} (\mathcal{F}(\Phi_C) * a)(A_{11}x + (I_{d\times d} - A_{11})y, \xi)f(y)e^{2\pi i\xi \cdot (x-y)}dyd\xi,$$

(5.49)

where the chirp function Φ_C is defined in (2.14).

Proof. We use the expression of $W_{\mathcal{A}}$ and Theorem 5.25. Namely, for every $f, g \in \mathcal{S}(\mathbb{R}^d)$, $a \in \mathcal{S}'(\mathbb{R}^{2d})$, up to a unitary factor,

$$\langle Op_{\mathcal{A}}(a)f, g \rangle = \langle a, W_{\mathcal{A}}(g, f) \rangle = \langle a, (V_C^T \mathcal{A}_{FT2} \mathcal{D}_L)^{\wedge}(g \otimes \bar{f}) \rangle$$
$$= \langle \mathfrak{T}_{L^{-1}} \mathcal{F}_2^{-1} \widehat{V_C^{-T}} a, g \otimes \bar{f} \rangle,$$

where we used $\widehat{V_C^T}^* = \widehat{V_C^{-T}}$. Since $|\det(L)| = 1$, we can write

$$\langle Op_{\mathcal{A}}(a)f, g \rangle = \int_{\mathbb{R}^{2d}} \mathcal{F}_2^{-1} \widehat{V_C^{-T}} a(L^{-1}(x, y))\overline{g(x)}f(y)dxdy$$
$$= \int_{\mathbb{R}^d} \left(\int_{\mathbb{R}^d} \mathcal{F}_2^{-1} \widehat{V_C^{-T}} a(L^{-1}(x, y))f(y)dy \right) \overline{g(x)}dx$$
$$= \left\langle \int_{\mathbb{R}^d} \mathcal{F}_2^{-1} \widehat{V_C^{-T}} a(L^{-1}(x, y))f(y)dy, g \right\rangle,$$

where the integrals must be interpreted in the weak sense. Hence,

$$Op_{\mathcal{A}}f(x) = \int_{\mathbb{R}^d} ((\mathcal{F}_2^{-1} \widehat{V_C^{-T}})a)(L^{-1}(x, y))f(y)dy.$$

(5.50)

Using

$$L^{-1} = \begin{pmatrix} A_{11} & I_{d\times d} - A_{11} \\ I_{d\times d} & -I_{d\times d} \end{pmatrix},$$

(5.51)

we compute

$$Op_{\mathcal{A}}f(x) = \int_{\mathbb{R}^d} \left(\int_{\mathbb{R}^d} (\widehat{V_C^{-T}}a)(A_{11}x + (I_{d\times d} - A_{11})y, \xi)e^{2\pi i\xi\cdot(x-y)}d\xi \right) f(y)dy$$

$$= \int_{\mathbb{R}^{2d}} (\widehat{V_C^{-T}}a)(A_{11}x + (I_{d\times d} - A_{11})y, \xi)e^{2\pi i\xi\cdot(x-y)} f(y)dyd\xi$$

$$= \int_{\mathbb{R}^{2d}} (\mathcal{F}(\Phi_C) * a)(A_{11}x + (I_{d\times d} - A_{11})y, \xi)e^{2\pi i\xi\cdot(x-y)} f(y)dyd\xi$$

where in the last step we used the expression of $\widehat{V_C^{-T}}$ computed in (2.16). $\qquad\square$

Remark 5.29. As in Remark 5.27, we stress that (5.49) sheds light on the role of the matrix V_C^T, in the decomposition of a covariant matrix $\mathcal{A}$, on the pseudodifferential operator with quantization given by $\mathcal{A}$. Basically, it produces the chirp $\mathcal{F}\Phi_C$ which acts on the symbol a via convolution.

To study the solution $u = u(x,t)$ to the Schrödinger equation in (5.5) we need to know information about his projection χ_t in (5.6).

Lemma 5.30. *Consider a covariant matrix $\mathcal{A} \in \mathrm{Sp}(2d, \mathbb{R})$ having block decomposition (5.40) and related matrix $B_{\mathcal{A}}$ in (5.41). For χ_t, $t \in \mathbb{R}$, in (5.6), assume that its inverse $\chi_t^{-1} \in \mathrm{Sp}(d, \mathbb{R})$, has the $d \times d$ block decomposition*

$$\chi_t^{-1} = \begin{pmatrix} X_t & Y_t \\ W_t & Z_t \end{pmatrix}.$$

Set $B_{\mathcal{A}_t} = \chi_t^{-T} B_{\mathcal{A}} \chi_t^{-1}$ and let $\mathcal{A}_t \in \mathrm{Sp}(2d, \mathbb{R})$ be the symplectic matrix associated to $B_{\mathcal{A}_t}$. Then, $\mathcal{A}_t$ is the covariant matrix having block decomposition

$$\mathcal{A}_t = \begin{pmatrix} A_{t,11} & I_{d\times d} - A_{t,11} & A_{t,13} & A_{t,13} \\ A_{t,21} & -A_{t,21} & I_{d\times d} - A_{t,11}^T & -A_{t,11}^T \\ 0_{d\times d} & 0_{d\times d} & I_{d\times d} & I_{d\times d} \\ -I_{d\times d} & I_{d\times d} & 0_{d\times d} & 0_{d\times d} \end{pmatrix}, \qquad (5.52)$$

with

$$A_{t,11} = -W_t^T Y_t - X_t^T[A_{13}Y_t - A_{11}Z_t] + W_t^T[A_{11}^T Y_t + A_{21}Z_t],$$

$$A_{t,13} = X_t^T W_t + X_t^T[A_{13}X_t - A_{11}W_t] - W_t^T[A_{11}^T X_t + A_{21}W_t],$$

$$A_{t,21} = -Z_t^T Y_t - Y_t^T[A_{13}Y_t - A_{11}Z_t] + Z_t^T[A_{11}^T Y_t + A_{21}Z_t].$$

Proof. Plugging $B_{\mathcal{A}_t} = \chi_t^{-T} B_{\mathcal{A}} \chi_t^{-1}$ into the block decomposition (5.41) for $B_{\mathcal{A}}$ and using the symplectic properties

$$W_t^T X_t = X_t^T W_t,$$

$$Z_t^T Y_t = Y_t^T Z_t,$$

$$Z_t^T X_t - Y_t^T W_t = I_{d\times d}$$

of χ_t^{-1} we get

$$B_{\mathcal{A}_t} = \begin{pmatrix} A_{t,13} & \frac{1}{2}I_{d\times d} - A_{t,11} \\ \frac{1}{2}I_{d\times d} - A_{t,11}^T & -A_{t,21} \end{pmatrix}, \tag{5.53}$$

where $A_{t,11}$, $A_{t,13}$ and $A_{t,21}$ are defined as in the assertion. Since the covariance of $\mathcal{A}$ is inherited by $\mathcal{A}_t$, we have that these blocks are exactly the ones defining the block decomposition of $\mathcal{A}_t$ as a covariant matrix. $\square$

We can now express the phase-space concentration of the solution $u(x,t)$ to the free particle equation in terms of metaplectic Wigner distribution.

Example 5.31 (The free particle)**.** We shall prove the formula originally announced in Part I, see Example 4.9 in [30], formula (126) therein (see also formula (108) in [31]).

In Example 4.9 in [30] we computed the τ-Wigner of the solution $u(t,x)$ to the Cauchy problem of the free particle equation:

$$\begin{cases} i\partial_t u + \Delta u = 0, \\ u(0,x) = u_0(x), \end{cases} \tag{5.54}$$

with $(t,x) \in \mathbb{R} \times \mathbb{R}^d$, $d \geq 1$. Namely, we obtained that

$$W_\tau u(t,x,\xi) = W_{\mathcal{A}_{\tau,t}} u_0(x - 4\pi t\xi, \xi), \tag{5.55}$$

where the representation $W_{\mathcal{A}_{\tau,t}}$ is of Cohen class:

$$W_{\mathcal{A}_{\tau,t}} f = Wf * \Sigma_{\tau,t}, \tag{5.56}$$

with kernel

$$\Sigma_{\tau,t}(x,\xi) = \Sigma_\tau(x + 4\pi t\xi, \xi),$$

where, for $\tau \neq 1/2$, the τ-kernel is given by

$$\Sigma_\tau(x,\xi) = \frac{2^d}{|2\tau - 1|^d} e^{2\pi i \rho(\tau)x\xi},$$

where $\rho(\tau) = \frac{2}{2\tau-1}$. The matrix $B_{\mathbf{A}_\tau}$ in (5.41) cab be computed as

$$B_{\mathbf{A}_\tau} = \begin{pmatrix} 0_{d\times d} & (\tau - \frac{1}{2})I_{d\times d} \\ (\tau - \frac{1}{2})I_{d\times d} & 0_{d\times d} \end{pmatrix}, \tag{5.57}$$

and by (5.53) (see also Proposition 4.4 in [31]),

$$B_{\mathcal{A}_{\tau,t}} = \chi_t^{-T} B_{\mathbf{A}_\tau} \chi_t^{-1} = \begin{pmatrix} 0_{d\times d} & (\tau - \frac{1}{2})I_{d\times d} \\ (\tau - \frac{1}{2})I_{d\times d} & (4\pi t)(1 - 2\tau)I_{d\times d} \end{pmatrix}.$$

The representation (5.56) can be equivalently written as (cf. (5.44))

$$W_{\mathcal{A}_{\tau,t}} f = Wf * \mathcal{F}^{-1}\Phi_{\mathcal{A}_{\tau,t}}.$$

Hence, the $\mathcal{A}_{\tau,t}$-Wigner representation computed in (5.48) with

$$A_{t,13} = 0_{d\times d}, \quad A_{t,11} = (1-\tau)I_{d\times d}, \quad A_{t,21} = -(4\pi t)(1-2\tau)I_{d\times d}$$

becomes

$$W_{\mathcal{A}_{\tau,t}}(f,g)(x,\xi) = \int_{\mathbb{R}^d} f(x+\tau\eta)\overline{g(x-(1-\tau)\eta)}e^{-2\pi i(\xi\cdot\eta+2\pi t(1-2\tau)\eta^2)}d\eta,$$

as desired.

5.4   Continuity on modulation spaces

For many quantizations, $Op_{\mathcal{A}}$ is an *integral superposition* of time-frequency shifts. Stated differently, these fundamental operators of time-frequency analysis represent the building blocks of pseudodifferential operators. Concretely, the Weyl quantization of a pseudodifferential operator with symbol $a \in \mathcal{S}'(\mathbb{R}^{2d})$ is given by

$$Op_w(a) = \int_{\mathbb{R}^{2d}} \hat{a}(\eta,-z)e^{-i\pi\eta\cdot z}\pi(z,\eta)dzd\eta.$$

On the other hand, if $f \in M_m^{p,q}$ for some $m \in \mathcal{M}_{v_s}$ and $0 < p,q \leq \infty$, then $\pi(z,\eta)f \in M_m^{p,q}$ for all $z,\eta \in \mathbb{R}^d$. This turns out to be one of the main reasons why modulation spaces appear in the theory of pseudodifferential operators.

In this section, we use the results in the first part of this paper to investigate the continuity properties of metaplectic pseudodifferential operators on modulation spaces. Since weighted modulation spaces measure the phase-space concentration of signals, as well as their decay properties, an investigation of their continuity on these spaces reveals how the time-frequency concentration of signals changes when a pseudodifferential operator is applied.

The first result we present involves the explicit expression of the symbol $b := (a \otimes 1) \circ \mathcal{A}^{-1}$, as in the equality (5.19) above, when $\mathcal{A}$ is totally Wigner-decomposable or covariant.

Proposition 5.32. Consider $\mathcal{A} \in \mathrm{Sp}(2d,\mathbb{R})$, $a \in \mathcal{S}'(\mathbb{R}^{2d})$ and $b = \sigma \circ \mathcal{A}^{-1}$, with $\sigma = a \otimes 1$ as defined in (5.16). For every $x,\xi,u,v \in \mathbb{R}^d$ we can state:
(i) if $\mathcal{A}$ is totally Wigner-decomposable with block decomposition as in Proposition 5.13, then

$$b(x,\xi,u,v) = a(A_{33}^T x - A_{23}^T v, -A_{41}^T \xi + A_{11}^T u); \qquad (5.58)$$

(ii) if $\mathcal{A}$ is covariant with block decomposition as in (5.40), then

$$b(x,\xi,u,v) = a(x - A_{13}u + (A_{11} - I)v, \xi + A_{11}^T u + A_{21}v). \qquad (5.59)$$

Proof. The proof follows by the straightforward calculation of

$$\mathcal{A}^{-1}(x, \xi, u, v)^T. \tag{5.60}$$

Namely, to get (5.58) one applies (5.60) with $\mathcal{A}^{-1}$ as in (5.29), whereas (5.59) is obtained applying (5.60) with

$$\mathcal{A}^{-1} = \begin{pmatrix} I_{d\times d} & 0_{d\times d} & -A_{13} & A_{11} - I_{d\times d} \\ I_{d\times d} & 0_{d\times d} & -A_{13} & A_{11} \\ 0_{d\times d} & I_{d\times d} & A_{11}^T & A_{21} \\ 0_{d\times d} & -I_{d\times d} & I_{d\times d} - A_{11}^T & -A_{21} \end{pmatrix}.$$

$\square$

For $a \in \mathcal{S}(\mathbb{R}^{2d})$, define $\sigma := a \otimes 1$ as in (5.16), and

$$\tilde{\sigma}(r, y, \rho, \eta) = 1_{(r,\rho)} \otimes \bar{a}(y, -\eta).$$

For $\mathcal{A} \in \mathrm{Sp}(2d, \mathbb{R})$ we set

$$b(x, \xi, u, v) = (\sigma \circ \mathcal{A}^{-1})(x, \xi, u, v), \tag{5.61}$$

$$\tilde{b}(x, \xi, u, v) = (\tilde{\sigma} \otimes \mathcal{A}^{-1})(x, \xi, u, v), \tag{5.62}$$

$$c(x, \xi, u, v) = b(x, \xi, u, v)\tilde{b}(x, \xi, u, v). \tag{5.63}$$

The following result extends Lemma 5.1 in [30] to general symplectic matrices.

Lemma 5.33. *Let $\mathcal{A} \in \mathrm{Sp}(2d, \mathbb{R})$, $a \in M^{\infty,q}_{1\otimes v_s}(\mathbb{R}^{2d})$, $0 < q \leq \infty$ and $s \geq 0$. Let $b, \tilde{b}$ and c be defined as in (5.61), (5.62) and (5.63), respectively. Then $b, \tilde{b}, c$ are in $M^{\infty,q}_{1\otimes v_s}(\mathbb{R}^{4d})$.*

Proof. The proof that b and $\tilde{b}$ are in $M^{\infty,q}_{1\otimes v_s}(\mathbb{R}^{2d})$ is analogous to that of [30, Lemma 5.1]. In fact, observe $1_{(y,\eta)}$ is in $M^{\infty,q}_{1\otimes v_s}(\mathbb{R}^{2d})$ for every $0 < q \leq \infty$ and $s \geq 0$. For $c = b\tilde{b}$, if $q \geq 1$ we use the product properties for modulation spaces in [29, Proposition 2.4.23], the quasi-Banach case $0 < q < 1$ is contained in [68]. $\square$

Recall the following boundedness result for Weyl quantization, see [65, Theorem 14.5.6], [116] and [117, Theorem 3.1].

Proposition 5.34. Assume that $0 < p, q, r \leq \infty$ with $r = \min\{1, p, q\}$, $s \in \mathbb{R}$, and $\sigma \in M^{\infty,r}_{1\otimes v_{|s|}}(\mathbb{R}^{2d})$. Then, $Op_w(\sigma) : \mathcal{S}(\mathbb{R}^d) \to \mathcal{S}'(\mathbb{R}^d)$ extends to a bounded operator on $\mathcal{M}^{p,q}_{v_s}(\mathbb{R}^d)$.

We generalize Proposition 5.34 to metaplectic pseudodifferential operators:

Theorem 5.35. *Let $\mathcal{A} \in \mathrm{Sp}(2d, \mathbb{R})$ be covariant and such that $B_{\mathcal{A}}$ in (5.41) is invertible. For $0 < p, q \leq \infty$, set $r = \min\{1, p, q\}$. If $a \in M^{\infty,r}_{1\otimes v_s}(\mathbb{R}^{2d})$, $s \geq 0$, then $Op_{\mathcal{A}}(a) : \mathcal{S}(\mathbb{R}^d) \to \mathcal{S}'(\mathbb{R}^d)$ extends to a bounded operator on $\mathcal{M}^{p,q}_{v_s}(\mathbb{R}^d)$.*

Proof. By [31, Proposition 3.3], $\mathcal{F}^{-1}\Phi_{B_\mathcal{A}} \in M_{v_s\otimes 1}^{r,\infty}$ for every $s \geq 0$, $0 < r \leq \infty$. Since $W_\mathcal{A}$ belongs to the Cohen class, for every $f, g \in \mathcal{S}(\mathbb{R}^d)$,

$$\begin{aligned}
\langle Op_\mathcal{A}(a)f, g\rangle &= \langle a, W_\mathcal{A}(g, f)\rangle = \langle a, W(g, f) * \mathcal{F}^{-1}\Phi_{-B_\mathcal{A}}\rangle \\
&= \langle \hat{a}, \mathcal{F}(W(g,f))e^{-i\pi\zeta\cdot B_\mathcal{A}\zeta}\rangle = \langle \hat{a}e^{i\pi\zeta\cdot B_\mathcal{A}\zeta}, \mathcal{F}(W(g,f))\rangle \\
&= \langle a * \mathcal{F}^{-1}\Phi_{B_\mathcal{A}}, W(g,f)\rangle = \langle Op_w(a * \mathcal{F}^{-1}\Phi_{B_\mathcal{A}})f, g\rangle.
\end{aligned}$$

By [4, Proposition 3.1]

$$\|a * \mathcal{F}^{-1}\Phi_{B_\mathcal{A}}\|_{M_{1\otimes v_s}^{\infty,r}} \lesssim \|a\|_{M_{1\otimes v_s}^{\infty,r}} \|\mathcal{F}^{-1}\Phi_{B_\mathcal{A}}\|_{M_{v_s\otimes 1}^{r,\infty}}.$$

The assertion follows from [117, Theorem 3.1]. □

We conclude this section by showing the validity of relations (5.18) on modulation spaces.

Theorem 5.36. *Consider* $\mathcal{A} \in \mathrm{Sp}(2d, \mathbb{R})$, $0 < p \leq \infty$, $a \in M_{1\otimes v_s}^{\infty,r}(\mathbb{R}^{2d})$, $s \geq 0$, $r = \min\{1, p\}$, *and* $b, \tilde{b}, c$ *defined as in (5.61), (5.62) and (5.63), respectively. For* $f, g \in \mathcal{M}_{v_s}^p(\mathbb{R}^d)$, *the following identities hold in* $\mathcal{M}_{v_s}^p(\mathbb{R}^{2d})$:

$$W_\mathcal{A}(Op_{w,2d}(a)f, g) = Op_{w,4d}(b)W_\mathcal{A}(f, g), \tag{5.64}$$

$$W_\mathcal{A}(f, Op_{w,2d}(a)g) = Op_{w,4d}(\tilde{b})W_\mathcal{A}(f, g), \tag{5.65}$$

$$W_\mathcal{A}(Op_{w,2d}(a)f) = Op_{w,4d}(c)W_\mathcal{A}(f). \tag{5.66}$$

Proof. If $f \in \mathcal{M}_{v_s}^p(\mathbb{R}^d)$, then $Op_w(a)f \in \mathcal{M}_{v_s}^p(\mathbb{R}^d)$ by [117, Theorem 3.1]. Hence, [31, Theorem 2.15] says that the distributions $W_\mathcal{A}(f)$, $W_\mathcal{A}(f, g)$, $W_\mathcal{A}(Op_w(a)f, g)$, $W_\mathcal{A}(f, Op_w(a)g)$, $W_\mathcal{A}(Op_w(a)f)$ belong to $\mathcal{M}_{v_s}^p(\mathbb{R}^{2d})$. Similarly, by Lemma 5.33, the symbols $b, \tilde{b}$ and c are in $M_{1\otimes v_s}^{\infty,q}(\mathbb{R}^{4d})$ and the right-hand sides of formulas (5.64), (5.65) and (5.66) are in $\mathcal{M}_{v_s}^p(\mathbb{R}^{2d})$. The equalities (5.64), (5.65) and (5.66) are obtained by using the same pattern as in the proof of [30, Theorem 5.1], namely replacing the symplectic matrix $\mathcal{A}_\tau$ with a general $\mathcal{A} \in \mathrm{Sp}(2d, \mathbb{R})$. □

Remark 5.37. Observe that the previous result extends [30, Theorem 5.1] to the quasi-Banach setting $0 < p < 1$.

5.5 Algebras of generalized metaplectic operators

In this section we introduce (quasi-)algebras of FIOs which extend the ones in [24, 25].

Given a Gabor frame $\mathcal{G}(g, \Lambda)$, the *Gabor matrix* of a linear continuous operator T from $\mathcal{S}(\mathbb{R}^d)$ to $\mathcal{S}'(\mathbb{R}^d)$ is

$$\langle T\pi(z)g, \pi(u)g\rangle, \quad z, u \in \mathbb{R}^{2d}. \tag{5.67}$$

Our goal: controlling the Gabor matrix of a metaplectic operator T (or more general one) related to the symplectic matrix $\chi \in \mathrm{Sp}(d, \mathbb{R})$ by

$$h(\mu - \chi\lambda), \quad \lambda, \mu \in \Lambda,$$

where h is a sequence leaving in a suitable (quasi-)algebra with respect to convolution.

The algebras already studied in [24, 25] where $\ell^1(\Lambda)$ and $\ell_{v_s}^\infty(\Lambda)$, $s > 2d$. Here we extend to the quasi-algebras $\ell_{v_s}^q(\Lambda)$, $0 < q < 1$, $s \geq 0$, enjoying the convolution property:

$$\ell_{v_s}^q(\Lambda) * \ell_{v_s}^q(\Lambda) \hookrightarrow \ell_{v_s}^q(\Lambda), \quad 0 < q < 1.$$

Recall that the Wiener amalgam spaces $W(C, L_{v_s}^p)(\mathbb{R}^{2d})$ is defined in (5.8) and the class $FIO(\chi, q, v_s)$ is defined in Definition 5.1.

The union

$$FIO(Sp(d, \mathbb{R}), q, v_s) = \bigcup_{\chi \in \mathrm{Sp}(d, \mathbb{R})} FIO(\chi, q, v_s)$$

is called the class of *generalized metaplectic operators*. Similarly to [25, Proposition 3.1] one can show:

Proposition 5.38. The definition of the class $FIO(\chi, q, v_s)$ is independent of the window function $g \in \mathcal{S}(\mathbb{R}^d)$.

Remark 5.39. (i) For $q = 1$ the original definition of $FIO(\chi, v_s)$ in [25] was formulated in terms of a function $H \in L_{v_s}^1(\mathbb{R}^{2d})$ instead of the more restrictive condition $H \in W(C, L_{v_s}^1)(\mathbb{R}^{2d})$. Though, it turns out that the two definitions are equivalent, see [25, Proposition 3.1].
(ii) Similarly to $q = 1$, one could consider the algebra of $FIO(\chi, \infty, v_s)$, $s > 2d$ such that

$$|\langle T\pi(z)g, \pi(w)g\rangle| \leq \langle w - \chi z\rangle^{-s}, \qquad \forall w, z \in \mathbb{R}^{2d}. \tag{5.68}$$

We shall not treat this case explicitly, but we remark that it enjoys similar properties to those we are going to establish for the cases above.

Theorem 5.40. *Consider T a continuous linear operator $\mathcal{S}(\mathbb{R}^d) \to \mathcal{S}'(\mathbb{R}^d)$, $\chi \in \mathrm{Sp}(d, \mathbb{R})$, $0 < q \leq 1$, $s \geq 0$. Let $\mathcal{G}(g, \Lambda)$ be a Gabor frame with $g \in \mathcal{S}(\mathbb{R}^d)$. Then the following properties are equivalent:*

(i) there exists a function $H \in W(C, L_{v_s}^q)(\mathbb{R}^{2d})$, such that the kernel of T with respect to time-frequency shifts satisfies the decay condition (5.9);

(ii) there exists a sequence $h \in \ell_{v_s}^q(\Lambda)$, such that

$$|\langle T\pi(\lambda)g, \pi(\mu)g\rangle| \leq h(\mu - \chi(\lambda)), \qquad \forall \lambda, \mu \in \Lambda. \tag{5.69}$$

Proof. It is a straightforward modification of the proof [24, Theorem 3.1]. □

We list a series of issues which follow by easy modifications of the earlier results contained in [24, 25], for a detailed proof we refer to [18].

Theorem 5.41. *(i) Boundedness. Fix $\chi \in \mathrm{Sp}(d,\mathbb{R})$, $0 < q \leq 1$, $s \geq 0$, $m \in \mathcal{M}_{v_s}$ and let T be generalized metaplectic operator in $FIO(\chi, q, v_s)$. Then T is bounded from $M_m^p(\mathbb{R}^d)$ to $M_{m\circ\chi^{-1}}^p(\mathbb{R}^d)$, $q \leq p \leq \infty$.*
(ii) Algebra property. Let $\chi_i \in \mathrm{Sp}(d,\mathbb{R})$, $s \geq 0$ and $T_i \in FIO(\chi_i, q, v_s)$, $i = 1, 2$. Then $T_1 T_2 \in FIO(\chi_1 \chi_2, q, v_s)$.

For the invertibility property, the algebra cases corresponding to the spaces of sequences $\ell_{v_s}^1$ where treated in [63] and [66] (see also earlier references therein). We extend those arguments to the quasi-Banach setting as follows.

Definition 5.42. Consider $\mathcal{B} = \ell_{v_s}^q(\Lambda)$, $0 < q \leq 1$, $s \geq 0$. Let A be a matrix on Λ with entries $a_{\lambda,\mu}$, for $\lambda, \mu \in \Lambda$, and let d_A be the sequence with entries $d_A(\mu)$ defined by

$$d_A(\mu) = \sup_{\lambda \in \Lambda} |a_{\lambda,\lambda-\mu}|. \qquad (5.70)$$

We say that the matrix A belongs to $\mathcal{C}_\mathcal{B}$ if d_A belongs to $\mathcal{B}$. The (quasi-)norm in $\mathcal{C}_\mathcal{B}$ is given by

$$\|A\|_{\mathcal{C}_\mathcal{B}} = \|d\|_\mathcal{B}.$$

The value $d_A(\mu)$ is the supremum of the entries in the $\mu - th$ diagonal of A, thus the $\mathcal{C}_\mathcal{B}$-norm describes a form of the off-diagonal decay of a matrix.

Theorem 5.43. *Consider the (quasi-)algebra $\mathcal{B}$ above. Then the following are equivalent:*
(i) $\mathcal{B}$ is inverse-closed in $B(\ell^2)$.
(ii) $\mathcal{C}_\mathcal{B}$ is inverse-closed in $B(\ell^2)$.
(iii) The spectrum $\widehat{\mathcal{B}} \simeq \mathbb{T}^d$.

Proof. The algebra case is already proved in [66]. The quasi-algebra case follows by a similar pattern, since, for $0 < q < 1$, it is easy to check that $\ell_{v_s}^q(\Lambda)$ is a solid convolution quasi-algebra of sequences. □

As a consequence, we can state:

Theorem 5.44. *The class of Weyl operators with symbols in $M_{1 \otimes v_s}^{\infty,q}(\mathbb{R}^{2d})$, $0 < q \leq 1$, is inverse-closed in $B(L^2(\mathbb{R}^d))$. In other words, if $\sigma \in M_{1 \otimes v_s}^{\infty,q}(\mathbb{R}^{2d})$ and $Op_w(\sigma)$ is invertible on $L^2(\mathbb{R}^d)$, then $(Op_w(\sigma))^{-1} = Op_w(b)$ for some $b \in M_{1 \otimes v_s}^{\infty,q}(\mathbb{R}^{2d})$.*

Proof. It follows the pattern of Theorem 5.5 in [66], using Theorem 5.43 in place of the corresponding Theorem 3.5 in the above-mentioned paper. □

Theorem 5.45 (Invertibility in the class $FIO(\chi, q, v_s)$)**.** *Let $T \in FIO(\chi, q, v_s)$ be invertible on $L^2(\mathbb{R}^d)$, then $T^{-1} \in FIO(\chi^{-1}, q, v_s)$.*

Proof. The pattern is similar to Theorem 3.7 in [24]. We detail the differences. We first show that the adjoint operator T^* belongs to the class $FIO(\chi^{-1}, q, v_s)$. By Definition 5.1:

$$|\langle T^*\pi(z)g, \pi(w)g\rangle| = |\langle \pi(z)g, T(\pi(w)g)\rangle| = |\langle T(\pi(w)g, \pi(z)g)\rangle|$$
$$\leq H(z - \chi(w)) = \mathcal{I}(H \circ \chi)(w - \chi^{-1}z).$$

It is easy to check that $\mathcal{I}(H \circ \chi) \in W(C, L_{v_s}^q)$ for $H \in W(C, L_{v_s}^q)$, since $v_s \circ \chi^{-1} \asymp v_s$, and the claim follows. Hence, by Theorem 5.41 (ii), the operator $P := T^*T$ is in $FIO(\mathrm{Id}, q, v_s)$ and satisfies the estimate (5.69), that is:

$$|\langle P\pi(\lambda)g, \pi(\mu)g\rangle| \leq h(\lambda - \mu), \quad \forall \lambda, \mu \in \Lambda,$$

and a suitable sequence $h \in \ell_{v_s}^q(\Lambda)$. The characterization for pseudodifferential operators in Theorem 3.2 [4] says that P is a Weyl operator $P = Op_w(\sigma)$ with a symbol σ in $M_{1 \otimes v_s}^{\infty, q}(\mathbb{R}^{2d})$. Since T and therefore T^* are invertible on $L^2(\mathbb{R}^d)$, P is also invertible on $L^2(\mathbb{R}^d)$. Now we apply Theorem 5.44 and conclude that the inverse $P^{-1} = Op_w(\tau)$ is a Weyl operator with symbol in $\tau \in M_{1 \otimes v_s}^{\infty, q}(\mathbb{R}^{2d})$. Hence P^{-1} is in $FIO(\mathrm{Id}, q, v_s)$. Eventually, using the algebra property of Theorem 5.41 (ii), we obtain that $T^{-1} = P^{-1}T^*$ is in $FIO(\chi^{-1}, q, v_s)$. $\square$

Theorem 5.46. *Fix $0 < q \leq 1$, $\chi \in \mathrm{Sp}(d, \mathbb{R})$. A linear continuous operator $T : \mathcal{S}(\mathbb{R}^d) \to \mathcal{S}'(\mathbb{R}^d)$ is in $FIO(\chi, q, v_s)$ if and only if there exist symbols $\sigma_1, \sigma_2 \in M_{1 \otimes v_s}^{\infty, q}(\mathbb{R}^{2d})$, such that*

$$T = Op_w(\sigma_1)\hat{\chi} \quad and \quad T = \hat{\chi}Op_w(\sigma_2). \tag{5.71}$$

The symbols σ_1 and σ_2 are related by

$$\sigma_2 = \sigma_1 \circ \chi. \tag{5.72}$$

Proof. It follows the same pattern of the proof of [25, Theorem 3.8]. The main tool is the characterization in Theorem 3.2 of [4] which extends Theorem 4.6 in [66] to the case $0 < q < 1$. We recall the main steps for the benefit of the reader.

Assume $T \in FIO(\chi, q, v_s)$ and fix $g \in \mathcal{S}(\mathbb{R}^d)$. We first prove the factorization $T = \sigma_1^w \hat{\chi}$. For every $\chi \in \mathrm{Sp}(d, \mathbb{R})$, the kernel of $\hat{\chi}$ with respect to time-frequency shifts can be written as

$$|\langle \hat{\chi}\pi(z)g, \pi(w)g\rangle| = |V_g(\hat{\chi}g)(w - \chi z)|.$$

Since both $g \in \mathcal{S}(\mathbb{R}^d)$ and $\hat{\chi}g \in \mathcal{S}(\mathbb{R}^d)$, we have $V_g(\hat{\chi}g) \in \mathcal{S}(\mathbb{R}^{2d})$ (see e.g., [29]). Consequently, we have found a function $H = |V_g(\hat{\chi}g)| \in \mathcal{S}(\mathbb{R}^{2d}) \subset W(C, L_{v_s}^q)$ such that

$$|\langle \hat{\chi}\pi(z)g, \pi(w)g\rangle| \leq H(w - \chi z) \quad w, z \in \mathbb{R}^{2d}. \tag{5.73}$$

Since $\hat{\chi}^{-1} = \widehat{\chi^{-1}}$ is in $FIO(\chi^{-1}, q, v_s)$ by Theorem 5.45, the algebra property of Theorem 5.41 (ii) implies that $T\widehat{\chi^{-1}} \in FIO(\mathrm{Id}, q, v_s)$. Now Theorem 3.2 in [4] implies the existence of a symbol $\sigma_1 \in M^{\infty,q}_{1\otimes v_s}(\mathbb{R}^{2d})$, such that $T\hat{\chi}^{-1} = Op_w(\sigma_1)$, as claimed. The rest goes exactly as in [25, Theorem 3.8]. $\qquad\square$

5.6   Applications to Schrödinger Equations

The theory developed in the previous sections finds a natural application in quantum mechanics. In particular, we focus on the Cauchy problems for Schrödinger equations announced in the introduction, cf. (5.3), with Hamiltonian of the form (5.4):

$$H = Op_w(a) + Op_w(\sigma),$$

where $Op_w(a)$ is the Weyl quantization of a real homogeneous quadratic polynomial on $\mathbb{R}^{2d}$ and $Op_w(\sigma)$ is a pseudodifferential operator with a symbol $\sigma \in M^{\infty,q}_{1\otimes v_s}(\mathbb{R}^{2d})$.

Proposition 5.34 (see also Theorem 5.41 (i) with $\chi = Id$ or [117, Theorem 3.1]) gives

Corollary 5.47. *If $\sigma \in M^{\infty,q}_{1\otimes v_s}(\mathbb{R}^{2d})$, $s \geq 0$, $0 < q \leq 1$, then the operator $Op_w(\sigma)$ is bounded on all modulation spaces $M^p_{v_s}(\mathbb{R}^d)$, for $q \leq p \leq \infty$. In particular, $Op_w(\sigma)$ is bounded on $L^2(\mathbb{R}^d)$.*

This implies that the operator H in (5.4) is a bounded perturbation of the generator $H_0 = Op_w(a)$ of a unitary group (cf. [108]), and H is the generator of a well-defined (semi-)group.

Theorem 5.48. *Let H be the Hamiltonian in (5.4) with homogeneous polynomial a and $\sigma \in M^{\infty,q}_{1\otimes v_s}(\mathbb{R}^{2d})$, $0 < q \leq 1$, $s \geq 0$. Let $U(t) = e^{itH}$ be the corresponding propagator. Then $U(t)$ is a generalized metaplectic operator for each $t \in \mathbb{R}$. Namely, the solution of the homogenous problem $iu_t + Op_w(a)u = 0$ is given by a metaplectic operator $\hat{\chi}_t$ in (5.6), and e^{itH} is of the from*

$$e^{itH} = \hat{\chi}_t Op_w(b_t)$$

for some symbol $b_t \in M^{\infty,q}_{1\otimes v_s}(\mathbb{R}^{2d})$.

Proof. The proof of the above result was shown for $q = 1$ in [25] and it easily extends to any $0 < q < 1$. In fact, the main ingredients to use are the invariance of $M^{\infty,q}_{1\otimes v_s}(\mathbb{R}^{2d})$ under metaplectic operators, plus the properties of that symbol class: the boundedness on modulation spaces and the algebra property of the corresponding Weyl operators. $\qquad\square$

Corollary 5.49. *Assume* $\sigma \in M^{\infty,q}_{1 \otimes v_s}(\mathbb{R}^{2d})$, $0 < q \le 1$, $s \ge 0$, $m \in \mathcal{M}_{v_s}$*. If the initial condition* u_0 *is in* $M^p_m(\mathbb{R}^d)$*, with* $q \le p \le \infty$*, then* $u(t, \cdot) \in M^p_{m \circ \chi^{-1}}(\mathbb{R}^d)$ *for every* $t \in \mathbb{R}$*. In particular, if* $m \circ \chi^{-1} \asymp m$ *for every* $\chi \in \mathrm{Sp}(d, \mathbb{R})$ *(as for* v_s*) the time evolution leaves* $M^p_m(\mathbb{R}^d)$ *invariant: the Schrödinger evolution preserves the phase space concentration of the initial condition.*

Proof of Corollary 5.49. It follows from Theorem 5.48 and the representation in Theorem 5.46 that $e^{itH} \in FIO(\chi, q, v_s)$, so that the claim is direct consequence of Theorem 5.41 (i). $\qquad\qquad\qquad\qquad\qquad\qquad\qquad\qquad\qquad\qquad\qquad\qquad\square$

We can now study the Wigner kernel of e^{itH}, namely $k(z, w)$, $w, z \in \mathbb{R}^{2d}$, such that
$$W(e^{itH} u_0)(z) = \int k(t, z, w) W u_0(w) \, dw,$$
and possible generalizations to $\mathcal{A}$-Wigner transforms.

For sake of clarity, we start with a symbol σ in the Hörmander class $S^0_{0,0}(\mathbb{R}^{2d})$, that is $\sigma \in \mathcal{C}^\infty(\mathbb{R}^{2d})$ such that for every $\alpha \in \mathbb{N}^d$ there exists a $C_\alpha > 0$ for which
$$|\partial^\alpha \sigma(z)| \le C_\alpha, \quad \forall z \in \mathbb{R}^{2d}.$$
We recall that $S^0_{0,0}(\mathbb{R}^{2d})$ can be viewed as the intersection of modulation spaces [4]
$$S^0_{0,0}(\mathbb{R}^{2d}) = \bigcap_{s \ge 0} M^{\infty,q}_{1 \otimes v_s}(\mathbb{R}^{2d}), \quad 0 < q \le \infty.$$
Let $\mathcal{A}$ be a covariant, shift-invertible matrix. Actually, when working in the L^2 setting, the assumption of shift-invertibility will be not essential in the sequel. We may argue in terms of the Cohen class Q_Σ in Theorem 5.24:
$$W_{\mathcal{A}}(f) = W(f) * \Sigma = Q_\Sigma(f)$$
where Σ is related to $\mathcal{A}$ by (5.43), (5.41).

Let us define $\Sigma_t(z) = \Sigma(\chi_t(z))$ and denote by $\mathcal{A}_t$ the corresponding covariant matrix, such that $W_{\mathcal{A}_t} = Q_{\Sigma_t}$, see Proposition 4.4 in [31] for details. Note that in the case of the standard Wigner transform we have $W = W_{\mathcal{A}} = W_{\mathcal{A}_t}$ for every t, since $\Sigma = \delta$.

The following proposition is the Wigner counterpart for e^{itH} of the almost-diagonalization in Definition 5.1.

Proposition 5.50. Under the assumptions above, for $z \in \mathbb{R}^{2d}$, $t \in \mathbb{R}$,
$$W_{\mathcal{A}}(e^{itH} u_0)(z) = \int_{\mathbb{R}^{2d}} k_{\mathcal{A}}(t, z, w)(W_{\mathcal{A}_t} u_0)(w) \, dw, \qquad (5.74)$$
where for every $N \ge 0$,
$$k_{\mathcal{A}}(t, z, w)\langle w - \chi_t^{-1}(z)\rangle^{2N}$$
is the kernel of an operator bounded on $L^2(\mathbb{R}^{2d})$.

We need the following preliminary result, cf. Proposition 4.1, formula (96) in [31]. To benefit the reader, we report here the proof.

Lemma 5.51. *Under the assumptions above,*

$$W_{\mathcal{A}}(\widehat{\chi_t} f)(z) = W_{\mathcal{A}_t} f(\chi_t^{-1} z).$$

Proof. From [29, Proposition 1.3.7] we have

$$W(\widehat{\chi_t} f)(z) = W f(\chi_t^{-1} z), \quad f \in \mathcal{S}(\mathbb{R}^d),$$

so that for any $\Sigma \in \mathcal{S}(\mathbb{R}^{2d})$, $f \in \mathcal{S}(\mathbb{R}^d)$,

$$
\begin{aligned}
Q_\Sigma(\widehat{\chi_t} f)(z) &= [\Sigma * W(\widehat{\chi_t} f)](z) \\
&= \int_{\mathbb{R}^{2d}} W(\widehat{\chi_t} f)(u) \Sigma(z - u) \, du \\
&= \int_{\mathbb{R}^{2d}} W f(\chi_t^{-1} u) \Sigma(\chi_t(\chi_t^{-1} z - \chi_t^{-1} u)) \, du \\
&= \int_{\mathbb{R}^{2d}} W f(\zeta) \Sigma(\chi_t(\chi_t^{-1} z - \zeta)) \, d\zeta \\
&= (W f * \Sigma_t)(\chi_t^{-1} z) = Q_{\Sigma_t} f(\chi_t^{-1} z).
\end{aligned}
$$

For $\Sigma \in \mathcal{S}'(\mathbb{R}^{2d})$ we may use standard approximation arguments. Since in our case $Q_\Sigma(\widehat{\chi_t} f) = W_{\mathcal{A}}(\widehat{\chi_t} f)$ and $Q_{\Sigma_t} f(\chi_t^{-1} z) = W_{\mathcal{A}_t} f(\chi_t^{-1} z)$, this concludes the proof. ☐

Proof of Proposition 5.50. From Theorem 5.48 we have

$$W_{\mathcal{A}}(e^{itH} u_0) = W_{\mathcal{A}}(\widehat{\chi_t} Op_w(b_t) u_0).$$

In view of Lemma 5.51

$$W_{\mathcal{A}}(e^{itH} u_0)(z) = W_{\mathcal{A}_t}(Op_w(b_t) u_0)(\chi_t^{-1} z).$$

We now apply formula (5.66) to obtain

$$W_{\mathcal{A}_t}(Op_w(b_t) u_0) = Op_w(c_t)(W_{\mathcal{A}_t} u_0)$$

where the symbol $c_t \in S_{0,0}^0(\mathbb{R}^{4d})$ is given by (5.63). Summing up

$$W_{\mathcal{A}}(e^{itH} u_0)(z) = Op_w(c_t)(W_{\mathcal{A}_t} u_0)(\chi_t^{-1} z). \tag{5.75}$$

Writing $h(t, z, w)$ for the kernel of $Op_w(c)$,

$$W_{\mathcal{A}}(e^{itH} u_0)(z) = \int h(t, \chi^{-1}(z), w)(W_{\mathcal{A}_t} u_0)(w) \, dw,$$

that is

$$k_{\mathcal{A}}(t, z, w) = h(t, \chi^{-1} z, w).$$

Now, observe that for every $N \geq 0$,

$$h_N(t, z, w) = \langle z - w \rangle^{2N} h(z, w)$$

is the kernel of bounded operator on $L^2(\mathbb{R}^d)$, see [30, Lemma 5.3]. Hence the operator with kernel

$$k_{\mathcal{A}}(t, z, w) \langle \chi^{-1}(z) - w \rangle^{2N} = h_N(t, \chi^{-1}(z), w)$$

is bounded as well. □

Definition 5.52. Fix $\mathcal{A} \in \mathrm{Sp}(2d, \mathbb{R})$ covariant and shift-invertible. For $f \in L^2(\mathbb{R}^d)$ we define $\mathcal{WF}_{\mathcal{A}}(f)$, the metaplectic Wigner wave front set of f, as follows. A point $z_0 = (x_0, \xi_0) \neq 0$ is not in $\mathcal{WF}_{\mathcal{A}}(f)$ if there exists a conic open neighbourhood $\Gamma_{z_0} \subset \mathbb{R}^{2d}$ of z_0 such that for every integer $N \geq 0$

$$\int_{\Gamma_{z_0}} \langle z \rangle^{2N} |W_{\mathcal{A}} f(z)|^2 dz < \infty.$$

In the case of the standard Wigner transform $W_{\mathcal{A}} = W$, we write for short $\mathcal{WF}_{\mathcal{A}}(f) = \mathcal{WF}(f)$. Note that $\mathcal{WF}_{\mathcal{A}}(f)$ is a closed cone in $\mathbb{R}^{2d} \setminus \{0\}$. We have $\mathcal{WF}_{\mathcal{A}}(f) = \emptyset$ if and only if $f \in \mathcal{S}(\mathbb{R}^d)$, cf. Proposition 4.7 in [31] and the arguments in the sequel.

First, we shall give the following extension of Theorem 1.6 in [30] concerning the τ-Wigner case.

Theorem 5.53. *Consider $a \in S^0_{0,0}(\mathbb{R}^{2d})$. Then, for every $f \in L^2(\mathbb{R}^d)$,*

$$\mathcal{WF}_{\mathcal{A}}(Op_w(a)f) \subset \mathcal{WF}_{\mathcal{A}}(f).$$

Proof. Arguing exactly as in the proof of Theorem 1.6 in [30] and replacing τ-Wigner with metaplectic Wigner distributions, we apply the identity

$$W_{\mathcal{A}}(Op_w(a)f) = Op_w(c)W_{\mathcal{A}}f$$

with the symbol c as in (5.63) and using (5.66) in Theorem 5.36 we obtain the inclusion. □

Theorem 5.54. *For $u_0 \in L^2(\mathbb{R}^d)$ we have*

$$\mathcal{WF}_{\mathcal{A}}(e^{itH}u_0) = \chi_t(\mathcal{WF}_{\mathcal{A}_t}(u_0)).$$

The proof follows the lines of the corresponding one in Theorem 1.6 [30], basing on the preceding Proposition 5.50, in particular on the identity in (5.75), see the sketch below. For the Wigner distribution the previous result reads as follows:

Corollary 5.55. *For $u_0 \in L^2(\mathbb{R}^d)$,*

$$\mathcal{WF}(e^{itH}u_0) = \chi_t(\mathcal{WF}(u_0)).$$

Proof of Theorem 5.54. Fix $t \in \mathbb{R}$, $z_0 \in \mathbb{R}^{2d} \setminus \{0\}$, Γ_{z_0} small conic neighbourhood of z_0, $\zeta_0 = \chi_t(z_0)$, $\Lambda_{\zeta_0} = \chi_t(\Gamma_{z_0})$ corresponding conic neighbourhood of ζ_0. Assume $\zeta_0 \notin \mathcal{WF}_{\mathcal{A}_t}(u_0)$, that is, for every $N \geq 0$,

$$\int_{\Lambda_{\zeta_0}} \langle \zeta \rangle^{2N} |W_{\mathcal{A}_t} u_0(\zeta)|^2 d\zeta < \infty.$$

We want to prove that $z_0 \notin \mathcal{WF}_{\mathcal{A}}(e^{itH}u_0)$, that is, for every $N \geq 0$,

$$I := \int_{\Gamma_{z_0}} \langle z \rangle^{2N} |W_{\mathcal{A}}(e^{itH}u_0)(z)|^2 dz < \infty.$$

By applying the basic identity (5.75) in the proof of Proposition 5.50 we obtain

$$I = \int_{\Gamma_{z_0}} \langle z \rangle^{2N} |[Op_w(c_t)W_{\mathcal{A}_t}u_0](\chi_t^{-1}z)|^2 dz$$

and after the change of variables $z = \chi_t \zeta$, observing that $\langle \chi_t \zeta \rangle \asymp \langle \zeta \rangle$:

$$I \asymp \int_{\Lambda_{\zeta_0}} \langle \zeta \rangle^{2N} |Op_w(c_t)W_{\mathcal{A}_t}u_0|^2 d\zeta.$$

We are therefore reduced to the pseudodifferential case, cf. the preceding Theorem 5.53. Arguing again as in the proof of Theorem 1.6 in [30] and using the assumption, we obtain $\mathcal{WF}_{\mathcal{A}}(e^{itH}u_0) \subset \chi_t(\mathcal{WF}_{\mathcal{A}_t}(u_0))$. Similarly, one can prove the opposite inclusion. $\square$

5.7   Comparison with the Hörmander wave front set

Corollary 5.55 is similar to other results in the literature, concerning propagation of micro-singularities for the Schrödinger equation, cf. [14, 24, 25, 27, 28, 29, 33, 69, 73, 74, 89, 93, 94, 109, 103, 102, 121, 124]. They mainly concern the global wave front set $\mathcal{WF}_G(f)$ of Hörmander [72]. It is interesting to compare the different microlocal contents of $\mathcal{WF}_{\mathcal{A}}(f)$ and $\mathcal{WF}_G(f)$. We recall the definition of $\mathcal{WF}_G(f)$, following the notation and the equivalent time-frequency setting in [29].

Definition 5.56. Consider $f \in L^2(\mathbb{R}^d)$ and $z_0 \in \mathbb{R}^{2d} \setminus \{0\}$. We say that $z_0 \notin \mathcal{WF}_G(f)$ if there exists a conic neighbourhood $\Gamma_{z_0} \subset \mathbb{R}^{2d}$ of z_0 such that for every integer $N \geq 0$

$$\int_{\Gamma_{z_0}} \langle z \rangle^{2N} |V_g f(z)|^2 dz < \infty, \tag{5.76}$$

where we fix $g \in \mathcal{S}(\mathbb{R}^d) \setminus \{0\}$ in the definition of the STFT $V_g f$.

As before, we assume $\mathcal{A} \in \mathrm{Sp}(2d, \mathbb{R})$ covariant and shift-invertible, then:

Theorem 5.57. *For all $f \in L^2(\mathbb{R}^d)$ we have*

$$\mathcal{W}\mathcal{F}_G(f) \subset \mathcal{W}\mathcal{F}_\mathcal{A}(f). \tag{5.77}$$

The proof requires the following preliminary issue.

Lemma 5.58. *Fix $g \in \mathcal{S}(\mathbb{R}^d) \setminus \{0\}$ and consider $\mathcal{A} \in \mathrm{Sp}(2d, \mathbb{R})$ covariant and shift-invertible. There exists $\Psi_\mathcal{A} \in \mathcal{S}(\mathbb{R}^{2d})$, depending on $\mathcal{A}$ and g such that for every $f \in L^2(\mathbb{R}^d)$*

$$|V_g f|^2 = \Psi_\mathcal{A} * W_\mathcal{A} f. \tag{5.78}$$

Proof. We start with the well-known identity

$$|V_g f|^2 = \mathcal{I}W g * W f, \tag{5.79}$$

where $\mathcal{I}W g(z) = W g(-z)$, see for example (156) in [30]. If $\mathcal{A}$ is covariant, we have from (5.42)

$$W_\mathcal{A} f = \sigma_\mathcal{A} * W f \tag{5.80}$$

with $\sigma_\mathcal{A}$ given by (5.43) $\sigma_\mathcal{A}(z) = \mathcal{F}^{-1}(e^{-\pi i \zeta \cdot B_\mathcal{A} \zeta})$. If we define

$$\tau_\mathcal{A}(z) = \mathcal{F}^{-1}(e^{\pi i \zeta \cdot B_\mathcal{A} \zeta})$$

we then have, for all $h \in L^2(\mathbb{R}^{2d})$,

$$\tau_\mathcal{A} * \sigma_\mathcal{A} * h = h,$$

hence from (5.79)

$$|V_g f|^2 = \mathcal{I}W g * \tau_\mathcal{A} * \sigma_\mathcal{A} * W f = \Psi_\mathcal{A} * W f,$$

with $\Psi_\mathcal{A} = \mathcal{I}W g * \tau_\mathcal{A}$.

To prove that $\Psi_\mathcal{A} \in \mathcal{S}(\mathbb{R}^{2d})$, we observe $\mathcal{I}W g \in \mathcal{S}(\mathbb{R}^{2d})$, in view of the regularity property of the Wigner distribution, and $\tau* : \mathcal{S}(\mathbb{R}^{2d}) \to \mathcal{S}(\mathbb{R}^{2d})$, since for every $h \in \mathcal{S}(\mathbb{R}^{2d})$ we have

$$e^{\pi i \zeta \cdot B_\mathcal{A} \zeta} h(\zeta) \in \mathcal{S}(\mathbb{R}^{2d}).$$

This concludes the proof.   □

Proof of Theorem 5.57. The pattern is similar to the the proof of Theorem 5.5 in [30], after replacing Lemma 5.4 in [30] with our present Lemma 5.58.   □

Corollary 5.59. *Let $\mathcal{A} \in \mathrm{Sp}(2d, \mathbb{R})$ as before and $f \in L^2(\mathbb{R}^d)$. We have $f \in \mathcal{S}(\mathbb{R}^d)$ if and only if $\mathcal{W}\mathcal{F}_\mathcal{A}(f) = \emptyset$.*

Proof. If $f \in \mathcal{S}(\mathbb{R}^d)$, then $W_\mathcal{A}(f) \in \mathcal{S}(\mathbb{R}^{2d})$ in view of Proposition 2.12 (*ii*). The estimates in Definition 5.52 are obviously satisfied for any $z_0 \in \mathbb{R}^{2d} \setminus \{0\}$, hence $\mathcal{WF}_\mathcal{A}(f) = \emptyset$. In the opposite direction, assume $\mathcal{WF}_\mathcal{A}(f) = \emptyset$. Theorem 5.57 yields $\mathcal{WF}_G(f) = \emptyset$ and this implies $f \in \mathcal{S}(\mathbb{R}^{2d})$, cf. [29]. Alternatively, one can follow the pattern of Theorem 5.4 in [30], using again Lemma 5.58. $\square$

Comparing now $\mathcal{WF}_G(f)$ and $\mathcal{WF}_\mathcal{A}(f)$, we first observe that the definition of $\mathcal{WF}_G(f)$ can be extended to $f \in \mathcal{S}'(\mathbb{R}^d)$, cf. [29], whereas Definition 5.52 refers to $f \in L^2(\mathbb{R}^d)$. With some more technicalities the definition of $\mathcal{WF}_\mathcal{A}(f)$ can be extended to $f \in \mathcal{S}'(\mathbb{R}^d)$ as well. The substantial difference between $\mathcal{WF}_G(f)$ and $\mathcal{WF}_\mathcal{A}(f)$ is that the inclusion in (5.77) is strict in general, since $\mathcal{WF}_\mathcal{A}(f)$ includes a ghost part depending on $\mathcal{A}$, as already observed in [30].

To better understand this issue, we will use the Shubin class of symbols H^m, $m \in \mathbb{R}$, defined by the estimates

$$|\partial^\alpha a(z)| \leq c_\alpha \langle z \rangle^{m-\alpha}, \quad z = (x, \xi) \in \mathbb{R}^{2d}. \tag{5.81}$$

Further, assume $a \in H^m_{cl}$, that is $a(z)$ has the homogeneous principal part $a_m(z)$:

$$a_m(\lambda z) = \lambda^m a_m(z), \quad \lambda > 0,$$

such that, cutting off $a_m(z)$ for small $|z|$, we have for some $\epsilon > 0$, $a - a_m \in H^{m-\epsilon}$.

Define the characteristic manifold

$$\Sigma = \{z \in \mathbb{R}^{2d}, a_m(z) = 0, z \neq 0\}.$$

Theorem 5.60. *Assume that $a \in H^m_{cl}$ is globally elliptic, i.e., $\Sigma = \emptyset$. Then for all $f \in L^2(\mathbb{R}^d)$,*
$$\mathcal{WF}_\mathcal{A}(Op_w(a)f) = \mathcal{WF}_\mathcal{A}(f).$$

Proof. The inclusion $\mathcal{WF}_\mathcal{A}(Op_w(a)f) \subset \mathcal{WF}_\mathcal{A}(f)$ follows from the easy variant of Theorem 5.53 for the class H^m. To obtain the opposite inclusion under the assumption of global ellipticity, we construct as in [114] a parametrix of $Op_w(a)$. Namely, there exists a $b \in H^{-m}_{cl}$ such that

$$Op_w(b)Op_w(a) = I + Op_w(r),$$

where I is the identity operator and the symbol r is in $\mathcal{S}(\mathbb{R}^{2d})$, hence $Op_w(r) : \mathcal{S}'(\mathbb{R}^d) \to \mathcal{S}(\mathbb{R}^d)$ is a regularizing operator. Therefore,

$$f = Op_w(b)Op_w(a)f - Op_w(r)f, \quad \forall f \in L^2(\mathbb{R}^d),$$

with $Op_w(r)f \in \mathcal{S}(\mathbb{R}^d)$. Invoking Theorem 5.53

$$\mathcal{WF}_\mathcal{A}(f) = \mathcal{WF}_\mathcal{A}(Op_w(b)Op_w(a)f) \subset \mathcal{WF}_\mathcal{A}(Op_w(a)f).$$

This completes the proof. $\square$

Theorem 5.60 shows a similarity of $\mathcal{WF}_{\mathcal{A}}(f)$ with $\mathcal{WF}_G(f)$. Though, in the non-elliptic case the classical microlocal inclusion

$$\mathcal{WF}_G(u) \subset \mathcal{WF}_G(Op_w(a)u) \cup \Sigma, \quad u \in \mathcal{S}'(\mathbb{R}^d),$$

fails for $\mathcal{WF}_{\mathcal{A}}(u)$. Consider for simplicity the case $v = Op_w(a)u \in \mathcal{S}(\mathbb{R}^d)$, so that for the solutions of $Op_w(a)u = v$ we have

$$\mathcal{WF}_G(u) \subset \Sigma \tag{5.82}$$

and test the same inclusion for $\mathcal{WF}_{\mathcal{A}}(u)$, $u \in L^2(\mathbb{R}^d)$, as follows. For simplicity, we will consider only the Wigner wave front $\mathcal{WF}(u)$ and consider in dimension $d = 1$ the operator

$$Pu = xD^2xu = Op_w(a)u$$

where the homogeneous principal part of $a \in H^4_{cl}$ is given by

$$a_4(x, \xi) = x^2\xi^2$$

so that Σ is the union of the x and ξ axes

$$\Sigma = \{(x, \xi) \in \mathbb{R}^2, x = 0 \,\text{or}\, \xi = 0, (x, \xi) \neq (0,0)\}. \tag{5.83}$$

We now address to the example at the end of [30], where $f, g \in L^2(\mathbb{R}^d)$ are defined such that

$$Df = i\delta - if' \tag{5.84}$$
$$xg = -i - ih, \tag{5.85}$$

with $f' \in \mathcal{S}(\mathbb{R})$, $h \in \mathcal{S}(\mathbb{R})$ and

$$\mathcal{WF}f = \mathcal{WF}_Gf = \{(x, \xi) \in \mathbb{R}^2, x = 0, \xi \neq 0\},$$

$$\mathcal{WF}g = \mathcal{WF}_Gg = \{(x, \xi) \in \mathbb{R}^2, \xi = 0, x \neq 0\}.$$

By using (5.84), (5.85), a simple calculation shows that $Pf \in \mathcal{S}(\mathbb{R}), Pg \in \mathcal{S}(\mathbb{R})$ and therefore for $u = f + g$ we have $Pu \in \mathcal{S}(\mathbb{R})$. Then for Σ as in (5.83) we obtain $\mathcal{WF}_Gu = \Sigma$ as expected from (5.82). Instead, the non-linearity of the Wigner transform (see [30]) gives

$$\mathcal{WF}u = \mathbb{R}^2 \setminus \{0\}.$$

To sum up, the appearance of ghost frequencies in the Wigner wave front is natural in Quantum Mechanics, but it contradicts Hörmander's result for micro-ellipticity.

Symplectic analysis of time-frequency spaces

The main results are exposed in Section 6.1 whereas Section 6.2 exhibits the most relevant examples. In the Appendix A we extend some of the results in [53] to general invertible matrices and to the quasi-Banach setting. In the Appendix B we compute the matrices associated to tensor products of metaplectic operators.

This chapter is part of an article published in *Journal de Mathématiques Pures et Appliquées* in 2023, cf. [19].

6.1 Shift-invertibility and modulation spaces

In this section we present the features of metaplectic operators that guarantee the representations of modulation and Wiener amalgam spaces by metaplectic operators.

Corollary 6.1. *Let $\hat{\mathcal{A}} \in \mathrm{Mp}(2d, \mathbb{R})$. Consider $g_1 \in \mathcal{S}'(\mathbb{R}^d)$, $g_2, g_3 \in \mathcal{S}(\mathbb{R}^d)$ with $\langle g_1, g_2 \rangle \neq 0$. For any $f \in \mathcal{S}'(\mathbb{R}^d)$,*

$$V_{g_3}f(w) = \frac{1}{\langle g_2, g_1 \rangle} \langle W_{\mathcal{A}}(f, g_1), W_{\mathcal{A}}(\pi(w)g_3, g_2) \rangle, \qquad w \in \mathbb{R}^{2d},$$

where $\langle \cdot, \cdot \rangle$ is the antilinear duality paring between $\mathcal{S}'(\mathbb{R}^{2d})$ and $\mathcal{S}(\mathbb{R}^{2d})$.

Proof. It is a straightforward consequence of the definition and main properties of metaplectic operators. Since $g_2, g_3 \in \mathcal{S}(\mathbb{R}^d)$, $W_{\mathcal{A}}(g_2, g_3) \in \mathcal{S}(\mathbb{R}^{2d})$, whereas $W_{\mathcal{A}}(f, g_1) \in \mathcal{S}'(\mathbb{R}^{2d})$ since $f, g_1 \in \mathcal{S}'(\mathbb{R}^d)$. Consequently,

$$\begin{aligned}
\langle W_{\mathcal{A}}(f, g_1), W_{\mathcal{A}}(\pi(w)g_3, g_2) \rangle &= \langle \hat{\mathcal{A}}(f \otimes \overline{g_1}), \hat{\mathcal{A}}(\pi(w)g_3 \otimes \overline{g_2})) \\
&= \langle f \otimes \overline{g_1}, \pi(w)g_3 \otimes \overline{g_2} \rangle \\
&= \langle f, \pi(w)g_3 \rangle \overline{\langle g_1, g_2 \rangle}.
\end{aligned}$$

This concludes the proof.

$\square$

If $\hat{\mathcal{A}} \in \mathrm{Mp}(2d, \mathbb{R})$, with $\mathcal{A} \in \mathrm{Sp}(2d, \mathbb{R})$ having block decomposition (2.20) then it was shown in [31] that

$$|W_{\mathcal{A}}(\pi(w)f, g)| = |\pi(E_{\mathcal{A}}w, F_{\mathcal{A}}w)W_{\mathcal{A}}(f, g)|, \quad w \in \mathbb{R}^{2d}, \quad \forall f, g \in L^2(\mathbb{R}^d),$$

where the matrices $E_{\mathcal{A}}$ and $F_{\mathcal{A}}$ are given as in (2.21).

We need the following representation formula.

Lemma 6.2. *Let $\hat{\mathcal{A}} \in Mp(2d, \mathbb{R})$, $\gamma, g \in \mathcal{S}(\mathbb{R}^d)$ be such that $\langle \gamma, g \rangle \neq 0$ and $f \in \mathcal{S}'(\mathbb{R}^d)$. Then,*

$$W_{\mathcal{A}}(f, g) = \frac{1}{\langle \gamma, g \rangle} \int_{\mathbb{R}^{2d}} V_g f(w) W_{\mathcal{A}}(\pi(w)\gamma, g) dw$$

with equality in $\mathcal{S}'(\mathbb{R}^{2d})$, the integral being intended in the weak sense.

Proof. Take any $\varphi \in \mathcal{S}(\mathbb{R}^{2d})$ and use the definition of vector-valued integral in a weak sense which entails

$$
\begin{aligned}
\langle W_{\mathcal{A}}(f, g)(z), \varphi \rangle &= \langle f \otimes \bar{g}, \hat{\mathcal{A}}^{-1}\varphi \rangle \\
&= \langle \frac{1}{\langle \gamma, g \rangle} \int_{\mathbb{R}^{2d}} V_g f(w)[(\pi(w)\gamma) \otimes \bar{g}]dw, \hat{\mathcal{A}}^{-1}\varphi \rangle \\
&= \frac{1}{\langle \gamma, g \rangle} \int_{\mathbb{R}^{2d}} V_g f(w)\langle [(\pi(w)\gamma) \otimes \bar{g}], \hat{\mathcal{A}}^{-1}\varphi \rangle dw \\
&= \frac{1}{\langle \gamma, g \rangle} \int_{\mathbb{R}^{2d}} V_g f(w)\langle \hat{\mathcal{A}}(\pi(w)\gamma \otimes \bar{g}), \varphi \rangle dw \\
&= \frac{1}{\langle \gamma, g \rangle} \int_{\mathbb{R}^{2d}} V_g f(w)\langle W_{\mathcal{A}}(\pi(w)\gamma, g)(z), \varphi \rangle dw.
\end{aligned}
$$

Therefore,

$$W_{\mathcal{A}}(f, g) = \frac{1}{\langle \gamma, g \rangle} \int_{\mathbb{R}^{2d}} V_g f(w) W_{\mathcal{A}}(\pi(w)\gamma, g) dw$$

with equality in $\mathcal{S}'(\mathbb{R}^{2d})$. $\square$

Theorem 6.3. *Let $W_{\mathcal{A}}$ be shift-invertible with $E_{\mathcal{A}}$ upper-triangular. Fix a non-zero window function $g \in \mathcal{S}(\mathbb{R}^d)$. For $m \in \mathcal{M}_v(\mathbb{R}^{2d})$ with $m \asymp m \circ E_{\mathcal{A}}^{-1}$, $1 \leq p, q \leq \infty$,*

$$f \in M_m^{p,q}(\mathbb{R}^d) \qquad \Leftrightarrow \qquad W_{\mathcal{A}}(f, g) \in L_m^{p,q}(\mathbb{R}^{2d}),$$

with equivalence of norms.

Proof. $\Rightarrow$. Assume $f \in M_m^{p,q}(\mathbb{R}^d)$. For any $\gamma \in \mathcal{S}(\mathbb{R}^d)$ such that $\langle \gamma, g \rangle \neq 0$, the inversion formula for the STFT (cf. Theorem 2.3.7 in [29]) reads

$$f = \frac{1}{\langle \gamma, g \rangle} \int_{\mathbb{R}^{2d}} V_g f(w) \pi(w) \gamma dw.$$

Multiplying both sides of the above equality by $\bar{g}(z_2)$, for any $z = (z_1, z_2) \in \mathbb{R}^{2d}$, we can write

$$f(z_1) \bar{g}(z_2) = (f \otimes \bar{g})(z) = \frac{1}{\langle \gamma, g \rangle} \int_{\mathbb{R}^{2d}} V_g f(w) [(\pi(w)\gamma) \otimes \bar{g}](z) dw.$$

Applying $\hat{\mathcal{A}}$ to $(f \otimes \bar{g})$ we obtain $\hat{\mathcal{A}}(f \otimes \bar{g}) = W_{\mathcal{A}}(f, g) \in \mathcal{S}'(\mathbb{R}^{2d})$. Using Lemma 6.2, we get:

$$W_{\mathcal{A}}(f, g) = \frac{1}{\langle \gamma, g \rangle} \int_{\mathbb{R}^{2d}} V_g f(w) W_{\mathcal{A}}(\pi(w)\gamma, g) dw,$$

with equality holding in $\mathcal{S}'(\mathbb{R}^{2d})$.

Now, if $f \in M_m^{p,q}(\mathbb{R}^d)$, the integral on the right-hand side is absolutely convergent as we shall see presently. For any $z \in \mathbb{R}^{2d}$,

$$
\begin{aligned}
|W_{\mathcal{A}}(f, g)(z)| &\leq \frac{1}{|\langle \gamma, g \rangle|} \int_{\mathbb{R}^{2d}} |V_g f(w)| |W_{\mathcal{A}}(\gamma, g)(z - E_{\mathcal{A}} w)| dw \\
&= \frac{|\det(E_{\mathcal{A}})|^{-1}}{|\langle \gamma, g \rangle|} \int_{\mathbb{R}^{2d}} |V_g f(E_{\mathcal{A}}^{-1} u)| |W_{\mathcal{A}}(\gamma, g)(z - u)| du \\
&= \frac{|\det(E_{\mathcal{A}})|^{-1}}{|\langle \gamma, g \rangle|} |V_g f \circ E_{\mathcal{A}}^{-1}| * |W_{\mathcal{A}}(\gamma, g)|(z).
\end{aligned}
\tag{6.1}
$$

Since $\gamma, g \in \mathcal{S}(\mathbb{R}^d)$, $W_{\mathcal{A}}(\gamma, g) \in \mathcal{S}(\mathbb{R}^{2d}) \subset L_v^1(\mathbb{R}^{2d})$. Moreover, by Theorem 6.14 and Theorem 6.15 both applied with $S = E_{\mathcal{A}}^{-1}$, we have that $V_g f \circ E_{\mathcal{A}}^{-1} \in L_m^{p,q}(\mathbb{R}^{2d})$. Young's convolution inequality applied to (6.1) entails

$$\|W_{\mathcal{A}}(f, g)\|_{L_m^{p,q}} \lesssim \|V_g f\|_{L_m^{p,q}} \|W_{\mathcal{A}}(\gamma, g)\|_{L_v^1} < \infty.$$

$\Leftarrow$. Assume that $W_{\mathcal{A}}(f, g) \in L_m^{p,q}(\mathbb{R}^{2d})$. Using Corollary 6.1 with $g_3 = g_1 = g$, $g_2 = \gamma$, for any $w \in \mathbb{R}^{2d}$,

$$
\begin{aligned}
|V_g f(w)| &\lesssim \frac{1}{|\langle \gamma, g \rangle|} |\langle W_{\mathcal{A}}(f, g), W_{\mathcal{A}}(\pi(w)g, \gamma) \rangle| \\
&\lesssim \int_{\mathbb{R}^{2d}} |W_{\mathcal{A}}(f, g)(u)| |W_{\mathcal{A}}(\pi(w)g, \gamma)(u)| du \\
&\lesssim \int_{\mathbb{R}^{2d}} |W_{\mathcal{A}}(f, g)(u)| |W_{\mathcal{A}}(g, \gamma)(u - E_{\mathcal{A}} w)| du \\
&\lesssim \int_{\mathbb{R}^{2d}} |W_{\mathcal{A}}(f, g)(u)| |[W_{\mathcal{A}}(g, \gamma)]^*(E_{\mathcal{A}} w - u)| du \\
&= |W_{\mathcal{A}}(f, g)| * |[W_{\mathcal{A}}(g, \gamma)]^*|(E_{\mathcal{A}} w).
\end{aligned}
\tag{6.2}
$$

Applying Theorem 6.14 and Theorem 6.15 with $S = E_\mathcal{A}$, we obtain

$$\|f\|_{M_m^{p,q}} \asymp \|V_g f\|_{L_m^{p,q}} \lesssim \||W_\mathcal{A}(f,g)| * |[W_\mathcal{A}(g,\gamma)]^*|\|_{L_m^{p,q}}$$
$$\lesssim \|W_\mathcal{A}(f,g)\|_{L_m^{p,q}} \|W_\mathcal{A}(g,\gamma)\|_{L_v^1} < \infty,$$

since we considered an even submultiplicative weight v. $\qquad\square$

Remark 6.4. Theorem 6.3 is sharp. Namely, if either $E_\mathcal{A}$ is not shift-invertible or $E_\mathcal{A}$ is not upper triangular, $W_\mathcal{A}$ may not characterize modulation spaces. We provide two counterexamples.

(*a*) If $E_\mathcal{A}$ is not shift-invertible, then $W_\mathcal{A}$ may not characterize modulation spaces. Let W_0 be the (cross-)Ryhaczek distribution defined in (2.6). Obviously, for every $f \in L^p(\mathbb{R}^d)$ and $g \in \mathcal{S}(\mathbb{R}^d)$, we obtain $\|W_0(f,g)\|_{L^{p,q}} = \|f\|_p \|\hat{g}\|_q$. This means that the $L^{p,q}$-norm of W_0 is not equivalent to the modulation norm in general. Observe that the corresponding matrix E_{A_0} is not shift-invertible. In fact,

$$E_{A_0} = \begin{pmatrix} I_{d\times d} & 0_{d\times d} \\ 0_{d\times d} & 0_{d\times d} \end{pmatrix}$$

is not invertible. Similarly, the (cross-)conjugate-Ryhaczek distribution W_1 in (2.7) is not shift-invertible and does not characterize modulation spaces [30, Remark 3.7].

(*b*) If $E_\mathcal{A}$ is not upper-triangular, then $W_\mathcal{A}$ may not characterize modulation spaces. Let $C \in \mathbb{R}^{2d\times 2d} \setminus \{0_{2d\times 2d}\}$ be any symmetric matrix. Then, up to a sign,

$$V_g(\widehat{V_C}f) = \widehat{A_{ST}}(\widehat{V_C}f \otimes \bar{g}) = \widehat{A_{ST}V_{\tilde{C}}}(f \otimes \bar{g}),$$

where

$$V_{\tilde{C}} = \begin{pmatrix} I_{d\times d} & 0_{d\times d} & 0_{d\times d} & 0_{d\times d} \\ 0_{d\times d} & I_{d\times d} & 0_{d\times d} & 0_{d\times d} \\ C & 0_{d\times d} & I_{d\times d} & 0_{d\times d} \\ 0_{d\times d} & 0_{d\times d} & 0_{d\times d} & I_{d\times d} \end{pmatrix},$$

see formula (6.8) in the Appendix B. Let $\mathcal{A} := A_{ST}V_{\tilde{C}}$ It is easy to verify that

$$E_\mathcal{A} = \begin{pmatrix} I_{d\times d} & 0_{d\times d} \\ C & I_{d\times d} \end{pmatrix},$$

which is always invertible and lower-triangular. The metaplectic operator $\widehat{V_C}$ is unbounded on $M^{p,q}(\mathbb{R}^d)$, $1 \le p,q \le \infty$, $p \ne q$, cf. [26, Proposition 7.1]. Namely, if $f \in M^{p,q}(\mathbb{R}^d)$, $\widehat{V_C}f \notin M^{p,q}(\mathbb{R}^d)$ for $p \ne q$ and, consequently, $\hat{\mathcal{A}}(f \otimes \bar{g}) \notin L^{p,q}(\mathbb{R}^{2d})$. Observe that a similar result with different methods is obtained in [53, Theorem 3.3].

As byproduct of the previous theorem we obtain new properties for shift-invertible representations $W_\mathcal{A}$, see ahead.

Corollary 6.5. *Let $\hat{\mathcal{A}} \in \mathrm{Mp}(2d, \mathbb{R})$ with $W_{\mathcal{A}}$ shift-invertible. Then, for all $f, g \in L^2(\mathbb{R}^d)$, we have $W_{\mathcal{A}}(f, g) \in L^{\infty}(\mathbb{R}^{2d})$ and it is everywhere defined.*

Proof. If $f \in L^2(\mathbb{R}^d)$ and $g, \gamma \in \mathcal{S}(\mathbb{R}^d)$, the inequality (6.1) holds pointwise (take $p = q = 2$, $m = 1$). Also, if $g \in L^2(\mathbb{R}^d)$ the right hand-side of (6.1) is also well defined for all $z \in \mathbb{R}^{2d}$, since $W_{\mathcal{A}}$ maps $L^2(\mathbb{R}^d) \times L^2(\mathbb{R}^d)$ to $L^2(\mathbb{R}^{2d})$. By Young's inequality,

$$\|W_{\mathcal{A}}(f, g)\|_{L^{\infty}(\mathbb{R}^{2d})} \lesssim \left\|V_g f \circ E_{\mathcal{A}}^{-1}\right\|_{L^2(\mathbb{R}^{2d})} \|W_{\mathcal{A}}(\gamma, g)\|_{L^2(\mathbb{R}^{2d})}$$
$$= \|f\|_2 \|g\|_2^2 \|\gamma\|_2 < \infty.$$

Hence, $W_{\mathcal{A}}(f, g) \in L^{\infty}(\mathbb{R}^{2d})$ and $W_{\mathcal{A}}(f, g)(z)$ is well defined for all $z \in \mathbb{R}^{2d}$. $\square$

If we limit to the case $p = q$, then $\mathfrak{T}_S : L^p(\mathbb{R}^{2d}) \to L^p(\mathbb{R}^{2d})$ is bounded for all $S \in \mathrm{GL}(2d, \mathbb{R})$, without any further assumption on its triangularity. In this case, arguing as above, but using Theorem 6.13, we obtain the following result.

Theorem 6.6. *Let $W_{\mathcal{A}}$ be shift-invertible and $m \in \mathcal{M}_v(\mathbb{R}^{2d})$ with $m \asymp m \circ E_{\mathcal{A}}^{-1}$. For $1 \le p \le \infty$ and $g \in \mathcal{S}(\mathbb{R}^d) \setminus \{0\}$, we have*

$$\|f\|_{M_m^p} \asymp \|W_{\mathcal{A}}(f, g)\|_{L_m^p}.$$

Corollary 6.7. *Under the assumptions of Theorem 6.3, assume that $(v \otimes v) \circ \mathcal{A}^{-1} \asymp v \otimes v$, then the window class can be enlarged to $M_v^1(\mathbb{R}^d)$.*

Proof. By Theorem 6.6, if $\gamma \in \mathcal{S}(\mathbb{R}^d)$ and $g \in M_v^1(\mathbb{R}^d)$, $W_{\mathcal{A}}(g, \gamma) \in L_v^1(\mathbb{R}^{2d})$, so that

$$|W_{\mathcal{A}}(f, g)(z)| \lesssim \frac{1}{|\langle \gamma, g \rangle|} |\det(E_{\mathcal{A}})|^{-1} |V_g f \circ E_{\mathcal{A}}^{-1}| * |W_{\mathcal{A}}(\gamma, g)|(z) \qquad (6.3)$$

is well defined by (6.1) provided that $W_{\mathcal{A}}(\gamma, g) \in L_v^1(\mathbb{R}^{2d})$.

By [31, Proposition 2.4],

$$W_{\mathcal{A}}(\gamma, g) = W_{\tilde{\mathcal{A}}}(\bar{g}, \bar{\gamma}) = \hat{\mathcal{A}} \widehat{\mathcal{D}_L}(\bar{g} \otimes \gamma),$$

with $\tilde{\mathcal{A}} = \mathcal{A}\mathcal{D}_L$. Now, $\bar{g} \otimes \gamma \in M_v^1(\mathbb{R}^d) \otimes \mathcal{S}(\mathbb{R}^d) \subset M_{v \otimes v}^1(\mathbb{R}^{2d})$ and $\widehat{\mathcal{D}_L}(\bar{g} \otimes \gamma) = \gamma \otimes \bar{g}$, so that $\widehat{\mathcal{D}_L} : M_{v \otimes v}^1(\mathbb{R}^{2d}) \to M_{v \otimes v}^1(\mathbb{R}^{2d})$. Indeed,

$$\left\|\widehat{\mathcal{D}_L}(\bar{g} \otimes \gamma)\right\|_{M_{v \otimes v}^1} \asymp \|\gamma\|_{M_v^1} \|g\|_{M_v^1}.$$

On the other hand, $\hat{\mathcal{A}} : M_{v \otimes v}^1(\mathbb{R}^{2d}) \to M_{v \otimes v}^1(\mathbb{R}^{2d})$ by [53, Theorem 3.2] and [53, Corollary 4.5]. Moreover, $M_{v \otimes v}^1(\mathbb{R}^{2d}) \hookrightarrow M_{v \otimes 1}^1(\mathbb{R}^{2d}) \hookrightarrow L_v^1(\mathbb{R}^{2d})$, since

$$v(z) \le v(z)v(w)$$

for all $z, w \in \mathbb{R}^{2d}$. Hence,

$$\|W_{\mathcal{A}}(\gamma, g)\|_{L_v^1} = \|W_{\tilde{\mathcal{A}}}(\bar{g}, \bar{\gamma})\|_{L_v^1} \leq \|W_{\tilde{\mathcal{A}}}(\bar{g}, \bar{\gamma})\|_{M_{v \otimes 1}^1} \leq \|W_{\tilde{\mathcal{A}}}(\bar{g}, \bar{\gamma})\|_{M_{v \otimes v}^1}$$
$$\lesssim_{\mathcal{A}} \left\|\widehat{\mathcal{D}_L \bar{g}} \otimes \gamma\right\|_{M_{v \otimes v}^1} \asymp \|\bar{g}\|_{M_v^1} \|\gamma\|_{M_v^1} \asymp_{\mathcal{A}, \gamma} \|g\|_{M_v^1} < \infty.$$

Going back to (6.3), we obtain

$$\|W_{\mathcal{A}}(f, g)\|_{L_m^{p,q}} \lesssim \|V_g f\|_{L_m^{p,q}} \|W_{\mathcal{A}}(\gamma, g)\|_{L_v^1} \asymp_{\mathcal{A}, \gamma, g} \|f\|_{M_m^{p,q}}.$$

Whence, if $g \in M_v^1(\mathbb{R}^d)$ and $f \in M_m^{p,q}(\mathbb{R}^d)$, the metaplectic Wigner $W_{\mathcal{A}}(f, g)$ is in $L_m^{p,q}(\mathbb{R}^{2d})$, with $\|W_{\mathcal{A}}(f, g)\|_{L_m^{p,q}} \lesssim \|f\|_{M_m^{p,q}}$.

Vice versa, we have shown that if $g \in M_v^1(\mathbb{R}^d)$ and $f \in M_m^{p,q}(\mathbb{R}^d)$, the metaplectic Wigner $W_{\mathcal{A}}(f, g)$ is in $L_m^{p,q}(\mathbb{R}^{2d})$. By (6.2), for all $w \in \mathbb{R}^{2d}$,

$$|V_g f(w)| \lesssim |W_{\mathcal{A}}(f, g)| * |[W_{\mathcal{A}}(g, \gamma)]^*|(E_{\mathcal{A}} w),$$

and Young's inequality gives

$$\|f\|_{M_m^{p,q}} \lesssim_{\mathcal{A}, g, \gamma} \|W_{\mathcal{A}}(f, g)\|_{L_m^{p,q}}.$$

In conclusion, $\|f\|_{M_m^{p,q}} \asymp \|W_{\mathcal{A}}(f, g)\|_{L_m^{p,q}}$, with $g \in M_v^1(\mathbb{R}^d)$. $\qquad \square$

Another consequence of Theorem 6.3 is the characterization of Wiener amalgam spaces $W(\mathcal{F}L_{m_1}^p, L_{m_2}^q)(\mathbb{R}^d)$.

Corollary 6.8. *Let $\hat{\mathcal{A}} \in \mathrm{Mp}(2d, \mathbb{R})$ be such that $W_{\mathcal{A}}$ is shift-invertible and $1 \leq p, q \leq \infty$. Let $m_1, m_2 \in \mathcal{M}_v(\mathbb{R}^d)$ be such that $m_2 \asymp \mathcal{I}m_2$, being $\mathcal{I}m_2(x) = m_2(-x)$, and $\mathcal{A} = \pi^{Mp}(\hat{\mathcal{A}})$ having block decomposition in (2.20). Fix $g \in \mathcal{S}(\mathbb{R}^d) \setminus \{0\}$ and define*

$$\tilde{E}_{\mathcal{A}} = J E_{\mathcal{A}} J. \tag{6.4}$$

If $m_1 \otimes m_2 \asymp (m_1 \otimes m_2) \circ \tilde{E}_{\mathcal{A}}^{-1}$ and $E_{\mathcal{A}}$ is lower triangular, then

$$\|f\|_{W(\mathcal{F}L_{m_1}^p, L_{m_2}^q)} \asymp \left(\int_{\mathbb{R}^d} \left(\int_{\mathbb{R}^d} |W_{\mathcal{A}}(f, g)(x, \xi)|^p m_1(\xi)^p d\xi \right)^{q/p} m_2(x)^q dx \right)^{1/q},$$

with the analogous for $\max\{p, q\} = \infty$.

Proof. Assume that $\max\{p, q\} < \infty$. We use (2.4). Let $f \in \mathcal{S}'(\mathbb{R}^d)$, $g \in \mathcal{S}(\mathbb{R}^d) \setminus \{0\}$. Then,

$$\left(\int_{\mathbb{R}^d} \left(\int_{\mathbb{R}^d} |W_{\mathcal{A}}(f, g)(x, \xi)|^p m_1(\xi)^p d\xi \right)^{q/p} m_2(x)^q dx \right)^{1/q}$$
$$= \left(\int_{\mathbb{R}^d} \left(\int_{\mathbb{R}^d} |W_{\mathcal{A}}(f, g)(J^{-1}(\xi, -x))|^p m_1(\xi)^p d\xi \right)^{q/p} m_2(x)^q dx \right)^{1/q}.$$

Now, $|W_{\mathcal{A}}(f,g) \circ J^{-1}| = |\widehat{\mathcal{D}_{J^{-1}}\hat{\mathcal{A}}}(f \otimes \bar{g})| = |\widehat{\mathcal{A}_0}(f \otimes \bar{g})| = |W_{\mathcal{A}_0}(f,g)|$, where

$$\pi^{Mp}(\widehat{\mathcal{A}_0}) = \mathcal{A}_0 := \mathcal{D}_{J^{-1}}\mathcal{A} = \begin{pmatrix} A_{21} & A_{22} & A_{23} & A_{24} \\ -A_{11} & -A_{12} & -A_{13} & -A_{14} \\ A_{41} & A_{42} & A_{43} & A_{44} \\ -A_{31} & -A_{32} & -A_{33} & -A_{34} \end{pmatrix}.$$

By [31, Proposition 2.7], $|W_{\mathcal{A}_0}(f,g)| = |W_{\tilde{\mathcal{A}}_0}(\hat{f},\hat{g})|$, where

$$\tilde{\mathcal{A}}_0 = \begin{pmatrix} -A_{23} & A_{24} & A_{21} & -A_{22} \\ A_{13} & -A_{14} & -A_{11} & A_{12} \\ -A_{43} & A_{44} & A_{41} & -A_{42} \\ A_{33} & -A_{34} & -A_{31} & A_{32} \end{pmatrix}.$$

Hence, using that $\mathcal{I}m_2 \asymp m_2$,

$$\left(\int_{\mathbb{R}^d} \left(\int_{\mathbb{R}^d} |W_{\mathcal{A}}(f,g)(x,\xi)|^p m_1(\xi)^p d\xi \right)^{q/p} m_2(x)^q dx \right)^{1/q}$$

$$\asymp \left(\int_{\mathbb{R}^d} \left(\int_{\mathbb{R}^d} |W_{\tilde{\mathcal{A}}_0}(\hat{f},\hat{g})(\xi,-x)|^p m_1(\xi)^p d\xi \right)^{q/p} m_2(x)^q dx \right)^{1/q}$$

$$= \left(\int_{\mathbb{R}^d} \left(\int_{\mathbb{R}^d} |W_{\tilde{\mathcal{A}}_0}(\hat{f},\hat{g})(\xi,x)|^p m_1(\xi)^p d\xi \right)^{q/p} \mathcal{I}m_2(x)^q dx \right)^{1/q}$$

$$\asymp \left\| W_{\tilde{\mathcal{A}}_0}(\hat{f},\hat{g}) \right\|_{L^{p,q}_{m_1 \otimes m_2}}.$$

Observe that $\tilde{E}_{\mathcal{A}} = E_{\tilde{\mathcal{A}}_0}$. Since $E_{\mathcal{A}}$ is invertible and lower triangular the matrix $\tilde{E}_{\mathcal{A}}$ in (6.4) is obviously invertible (and upper triangular). Hence, using the assumption $m_1 \otimes m_2 \asymp (m_1 \otimes m_2) \circ E_{\tilde{\mathcal{A}}_0}^{-1}$, we have

$$\left\| W_{\tilde{\mathcal{A}}_0}(\hat{f},\hat{g}) \right\|_{L^{p,q}_{m_1 \otimes m_2}} \asymp \left\| \hat{f} \right\|_{M^{p,q}_{m_1 \otimes m_2}} = \|f\|_{W(\mathcal{F}L^p_{m_1}, L^q_{m_2})}.$$

The same argument also proves the case $\max\{p,q\} = \infty$, simply replacing the corresponding integrals with the essential supremums. $\qquad\square$

Remark 6.9. Because of (2.8), Corollary 6.8 is significant only for $p \neq q$. For $p = q$ we refer to Theorem 6.6 with $m = m_1 \otimes m_2$.

6.2 Examples

We exhibit a manifold of new metaplectic Wigner distributions which may find application in time-frequency analysis, signal processing, quantum mechanics and pseudodifferential theory.

Example 6.10. This example generalizes the STFT by applying a metaplectic operator either on the window function g or on the function f as follows. First, consider the matrix

$$L = \begin{pmatrix} 0_{d\times d} & I_{d\times d} \\ -I_{d\times d} & I_{d\times d} \end{pmatrix}.$$

which allows to rewrite the STFT $V_g f$ as composition of the metaplectic operators $V_g f(x,\xi) = \mathcal{F}_2 \mathfrak{T}_L (f \otimes \bar{g})(x,\xi)$.

(i) We may act on the window g by replacing $\bar{g}$ with $\widehat{\mathcal{A}'}g$, $\widehat{\mathcal{A}'} \in \mathrm{Mp}(d,\mathbb{R})$. Namely, we consider the time-frequency representation

$$\mathcal{U}_g f(x,\xi) = \mathcal{F}_2 \mathfrak{T}_L (f \otimes \widehat{\mathcal{A}'}\bar{g})(x,\xi).$$

Denoting

$$\mathcal{A}' = \begin{pmatrix} A' & B' \\ C' & D' \end{pmatrix}, \tag{6.5}$$

by (6.8),

$$f \otimes \widehat{\mathcal{A}'}\bar{g} = \widehat{\mathcal{A}''}(f \otimes \bar{g}),$$

with

$$\mathcal{A}'' = \begin{pmatrix} I_{d\times d} & 0_{d\times d} & 0_{d\times d} & 0_{d\times d} \\ 0_{d\times d} & A' & 0_{d\times d} & B' \\ 0_{d\times d} & 0_{d\times d} & I_{d\times d} & 0_{d\times d} \\ 0_{d\times d} & C' & 0_{d\times d} & D' \end{pmatrix},$$

so that $\mathcal{U}_g f = W_{\mathcal{A}}(f,g)$ with

$$\mathcal{A} = \begin{pmatrix} I_{d\times d} & -A' & 0_{d\times d} & -B' \\ 0_{d\times d} & C' & I_{d\times d} & D' \\ 0_{d\times d} & -C' & 0_{d\times d} & -D' \\ -I_{d\times d} & 0_{d\times d} & 0_{d\times d} & 0_{d\times d} \end{pmatrix},$$

which is always shift-invertible with $E_{\mathcal{A}}$ diagonal. This is not surprising, since $\widehat{\mathcal{A}'}\bar{g} \in \mathcal{S}(\mathbb{R}^d)$ for $g \in \mathcal{S}(\mathbb{R}^d)$ and different windows in $\mathcal{S}(\mathbb{R}^d)$ yield equivalent norms.

(ii) A more interesting example comes out by applying $\widehat{\mathcal{A}'}$, with $\mathcal{A}' \in \mathrm{Sp}(d,\mathbb{R})$ having block decomposition in (6.5), to the function f. Namely, we consider

$$\widetilde{\mathcal{U}}_g f(x,\xi) = \mathcal{F}_2 \mathfrak{T}_L (\widehat{\mathcal{A}'}f \otimes \bar{g})(x,\xi).$$

Then $\widetilde{\mathcal{U}}_g f = W_{\mathcal{A}}(f,g)$ with

$$\mathcal{A} = \begin{pmatrix} A' & -I_{d\times d} & B' & 0_{d\times d} \\ C' & 0_{d\times d} & D' & I_{d\times d} \\ 0_{d\times d} & 0_{d\times d} & 0_{d\times d} & -I_{d\times d} \\ -A' & 0_{d\times d} & -B' & 0_{d\times d} \end{pmatrix},$$

and

$$E_{\mathcal{A}} = \mathcal{A}' = \begin{pmatrix} A' & B' \\ C' & D' \end{pmatrix},$$

in (6.5). This $W_{\mathcal{A}}$ characterizes modulation spaces if and only if the symplectic matrix $\mathcal{A}'$ is upper triangular, since $\widehat{\mathcal{A}'} : M^{p,q}(\mathbb{R}^d) \to M^{p,q}(\mathbb{R}^d)$, $p \neq q$, if and only if $\mathcal{A}'$ is an upper block triangular matrix [53].

Observe that these time-frequency representations find applications in signal processing, see Zhang et al. [127, 129].

Example 6.11. (i). For $z = (x, \xi) \in \mathbb{R}^{2d}$, the time-frequency shift $\pi(z)$ can be written as follows: $\pi(z)g(t) = \Phi_{\tilde{I}}(\xi, t) T_x g(t)$, where $\tilde{I} \in \mathbb{R}^{2d \times 2d}$ is the symmetric matrix

$$\tilde{I} = \begin{pmatrix} 0_{d \times d} & I_{d \times d} \\ I_{d \times d} & 0_{d \times d} \end{pmatrix}.$$

Thus, we can define a *generalized STFT* replacing the time-frequency atoms $\pi(z)g$ with the more general atoms $\varsigma(x, \xi) := \Phi_C(\xi, \cdot) T_x$, $x, \xi \in \mathbb{R}^d$, where Φ_C is the chirp function related to the symmetric matrix

$$C = \begin{pmatrix} C_{11} & C_{12} \\ C_{12}^T & C_{22} \end{pmatrix}$$

(hence $C_{11}^T = C_{11}$, $C_{22}^T = C_{22}$). Namely, we may define the *generalized STFT* $\mathcal{V}_{g,C} f$ as

$$\mathcal{V}_{g,C} f(x, \xi) = |\det(C_{12})|^{1/2} e^{-i\pi C_{11} \xi \cdot \xi} \int_{\mathbb{R}^d} f(t) \overline{g(t-x)} e^{-i\pi C_{22} t \cdot t} e^{-2\pi i C_{12}^T \xi \cdot t} dt$$

$$= \langle f, \varsigma(x, \xi) g \rangle,$$

$f, g \in L^2(\mathbb{R}^d)$. Observe that, if $C_{12} \in \mathrm{GL}(d, \mathbb{R})$, then $\mathcal{V}_{g,C} f = W_{\mathcal{A}}(f, g)$, with

$$\mathcal{A} = \begin{pmatrix} I_{d \times d} & -I_{d \times d} & 0_{d \times d} & 0_{d \times d} \\ -C_{12}^{-T} C_{22} & 0_{d \times d} & C_{12}^{-T} & C_{12}^{-T} \\ 0_{d \times d} & 0_{d \times d} & 0_{d \times d} & -I_{d \times d} \\ -C_{12} + C_{11} C_{12}^{-T} C_{22} & 0_{d \times d} & -C_{11} C_{12}^{-T} & -C_{11} C_{12}^{-T} \end{pmatrix},$$

which is always shift-invertible, but unless $C_{22} \neq 0_{d \times d}$, $E_{\mathcal{A}}$ is lower triangular. (ii) For $\tau \in \mathbb{R}$ consider the τ-Wigner distribution defined in (2.5) and replace the Gabor atoms $\pi(x, \xi)$ with the more general chirp functions Φ_C as before to obtain

$$\mathcal{W}_{\tau,C}(f, g)(x, \xi) = |\det(C_{12})|^{1/2} e^{-i\pi C_{11} \xi \cdot \xi}$$

$$\times \int_{\mathbb{R}^d} f(x + \tau t) \overline{g(x - (1-\tau)t)} e^{-i\pi C_{22} t \cdot t} e^{-2\pi i C_{12}^T \xi \cdot t} dt,$$

$f, g \in L^2(\mathbb{R}^d)$. Again, if $C_{12} \in \mathrm{GL}(d, \mathbb{R})$, then $\mathcal{W}_{\tau, C}(f, g) = W_{\mathcal{A}}(f, g)$ with

$$
\mathcal{A} = \begin{pmatrix}
(1 - \tau)I_{d \times d} & \tau I_{d \times d} & 0_{d \times d} & 0_{d \times d} \\
-C_{12}^{-T}C_{22} & -C_{12}^{-T}C_{22} & \tau C_{12}^{-T} & -(1 - \tau)C_{12}^{-T} \\
0_{d \times d} & 0_{d \times d} & I_{d \times d} & I_{d \times d} \\
C_{11}C_{12}^{-T}C_{22} - C_{12} & C_{11}C_{12}^{-T}C_{22} - C_{12} & -\tau C_{11}C_{12}^{-T} & (1 - \tau)C_{11}C_{12}^{-T}
\end{pmatrix}.
$$

This matrix is shift-invertible if and only if $\tau \neq 0, 1$, and in this case $E_{\mathcal{A}}$ is upper-triangular if and only if $C_{22} = 0_{d \times d}$.

Example 6.12. Every $\mathcal{A} \in \mathrm{Sp}(2d, \mathbb{R})$ can be written as $\Pi_{\mathcal{J}} V_Q \mathcal{D}_L V_{-P}^T$, where $L \in \mathrm{GL}(2d, \mathbb{R})$, the matrices $Q, P \in \mathbb{R}^{2d \times 2d}$ are symmetric and, if $1 \leq k \leq 2d$, $1 \leq j_1, \ldots, j_k \leq 2d$ and $\mathcal{J} = \{j_1, \ldots, j_k\}$, $\Pi_{\mathcal{J}} = \Pi_{j_1} \ldots \Pi_{j_k}$ is the matrix associated to the partial Fourier transform $\mathcal{F}_{\mathcal{J}} := \mathcal{F}_{j_1} \ldots \mathcal{F}_{j_k}$, cf. Example 2.7 (v). Set

$$
Q = \begin{pmatrix} Q_{11} & Q_{12} \\ Q_{12}^T & Q_{22} \end{pmatrix}, \quad P = \begin{pmatrix} P_{11} & P_{12} \\ P_{12}^T & P_{22} \end{pmatrix}, \quad L = \begin{pmatrix} L_{11} & L_{12} \\ L_{21} & L_{22} \end{pmatrix}
$$

and

$$
L^{-1} = \begin{pmatrix} L'_{11} & L'_{12} \\ L'_{21} & L'_{22} \end{pmatrix}.
$$

A direct computation shows

$$
V_Q \mathcal{D}_L V_{-P}^T = \begin{pmatrix}
L'_{11} & L'_{12} & -L'_{11}P_{11}^T - L'_{12}P_{12}^T & -L'_{11}P_{12} - L'_{12}P_{22}^T \\
L'_{21} & L'_{22} & -L'_{21}P_{11}^T - L'_{22}P_{12}^T & -L'_{21}P_{12} - L'_{22}P_{22}^T \\
M_{11} & M_{12} & N_{11} & N_{12} \\
M_{21} & M_{22} & N_{21} & N_{22}
\end{pmatrix}.
$$

In what follows the explicit expressions of $M_{11}, M_{12}, M_{21}, M_{22}, N_{11}, N_{12}, N_{21}, N_{22} \in \mathbb{R}^{d \times d}$ are irrelevant. We consider the case $\mathcal{J} = \{d + 1, \ldots, 2d\}$, i.e., $\mathcal{F}_{\mathcal{J}} = \mathcal{F}_2$. The effect of left-multiplying $V_Q \mathcal{D}_L V_{-P}^T$ by $\mathcal{A}_{FT2}$ is to swap the second column blocks of $V_Q \mathcal{D}_L V_{-P}^T$ with the fourth, up to change the sign of the latter. Hence, the matrix $E_{\mathcal{A}}$ associated to

$$
W_{\mathcal{A}}(f, g) = \mathcal{F}_2(\Phi_Q \cdot (\mathcal{F}^{-1}\Phi_P * (f \otimes \bar{g})))
$$

is

$$
E_{\mathcal{A}} = \begin{pmatrix} L'_{11} & -L'_{11}P_{11}^T - L'_{12}P_{12}^T \\ L'_{21} & -L'_{21}P_{11}^T - L'_{22}P_{12}^T \end{pmatrix}.
$$

This matrix is upper triangular if and only if $L'_{21} = 0_{d \times d}$ or, equivalently, if and only if L is upper triangular. In this case, we also can compute explicitly L^{-1} in terms of the blocks of L. Namely,

$$
L = \begin{pmatrix} L_{11} & L_{12} \\ 0_{d \times d} & L_{22} \end{pmatrix} \in \mathrm{GL}(2d, \mathbb{R}) \Rightarrow L^{-1} = \begin{pmatrix} L_{11}^{-1} & -L_{11}^{-1}L_{12}L_{22}^{-1} \\ 0_{d \times d} & L_{22}^{-1} \end{pmatrix}.
$$

So, the corresponding $E_{\mathcal{A}}$ is invertible if and only if $L_{22}^{-1}P_{12}^{T} \in \mathrm{GL}(d,\mathbb{R})$, i.e., if and only if $P_{12} \in \mathrm{GL}(d,\mathbb{R})$. In conclusion, any metaplectic Wigner distribution of the form

$$W_{\mathcal{A}}(f,g)(x,\xi) = \mathcal{F}_2(\Phi_Q \cdot (\mathcal{F}^{-1}\Phi_P * (f \otimes \bar{g})))(x,\xi)$$

with $P, Q \in \mathbb{R}^{2d \times 2d}$ symmetric, $P_{12} \in \mathrm{GL}(d,\mathbb{R})$, and $L \in \mathrm{GL}(2d,\mathbb{R})$ upper triangular, can be used to define modulation spaces.

6.3 Appendix A

In Appendix 6.3 we generalize the results in [53] to the quasi-Banach setting. Also, we observe that [53, Corollary 4.2] holds for general invertible matrices. For $S \in \mathrm{GL}(2d,\mathbb{R})$, recall the definition of the metaplectic operator

$$\mathfrak{T}_S f(z) = |\det(S)|^{\frac{1}{2}} f(Sz), \quad z \in \mathbb{R}^{2d},$$

defined in Example 2.7 (ii).

Theorem 6.13. *Let* $S \in \mathrm{GL}(2d,\mathbb{R})$ *and* $0 < p \leq \infty$. *The mapping* $\mathfrak{T}_S :$ $L^p(\mathbb{R}^{2d}) \to L^p(\mathbb{R}^{2d})$ *is everywhere defined and bounded with*

$$\|\mathfrak{T}_S\|_{L^p \to L^p} = |\det(S)|^{\frac{1}{2}-\frac{1}{p}}.$$

We use the convention $1/\infty = 0$.

Proof. Trivially, if $0 < p < \infty$ and $f \in L^p(\mathbb{R}^{2d})$,

$$\|\mathfrak{T}_S f\|_{L^p(\mathbb{R}^{2d})} = \|f \circ S\|_{L^p(\mathbb{R}^{2d})} = |\det(S)|^{\frac{1}{2}-\frac{1}{p}} \|f\|_{L^p(\mathbb{R}^{2d})}.$$

Also, $\|\mathfrak{T}_S f\|_{L^\infty(\mathbb{R}^{2d})} = |\det(S)|^{1/2} \|f\|_{L^\infty(\mathbb{R}^{2d})}$. $\qquad\square$

Theorem 6.14. *Consider* $A, D \in \mathrm{GL}(d,\mathbb{R})$, $B \in \mathbb{R}^{d \times d}$ *and* $0 < p, q \leq \infty$. *Define*

$$S = \begin{pmatrix} A & B \\ 0_{d \times d} & D \end{pmatrix}.$$

The mapping $\mathfrak{T}_S : L^{p,q}(\mathbb{R}^{2d}) \to L^{p,q}(\mathbb{R}^{2d})$ *is an isomorphism with bounded inverse* $\mathfrak{T}_{S^{-1}}$.

Proof. Let $f \in L^{p,q}(\mathbb{R}^{2d})$. Then,

$$\|\mathfrak{T}_S f\|_{L^{p,q}(\mathbb{R}^{2d})} = \left\| \xi \mapsto |\det(S)|^{1/2} \|f(A \cdot + B\xi, D\xi)\|_{L^p(\mathbb{R}^d)} \right\|_{L^q(\mathbb{R}^d)}$$

$$= \left\| \xi \mapsto |\det(S)|^{1/2} \|f(A\cdot, D\xi)\|_{L^p(\mathbb{R}^d)} \right\|_{L^q(\mathbb{R}^d)}$$

$$= \left\| \xi \mapsto |\det(S)|^{1/2} |\det(A)|^{-1/p} \|f(\cdot, D\xi)\|_{L^p(\mathbb{R}^d)} \right\|_{L^q(\mathbb{R}^d)}$$

$$= |\det(S)|^{1/2} |\det(A)|^{-1/p} |\det(D)|^{-1/q} \left\| \xi \mapsto \|f(\cdot, \xi)\|_{L^p(\mathbb{R}^d)} \right\|_{L^q(\mathbb{R}^d)}$$

$$= |\det(A)|^{\frac{1}{2} - \frac{1}{p}} |\det(D)|^{\frac{1}{2} - \frac{1}{q}} \|f\|_{L^{p,q}(\mathbb{R}^{2d})},$$

where $1/\infty = 0$. Observe that $\mathfrak{T}_S^{-1} = \mathfrak{T}_{S^{-1}}$. It remains to prove that $\mathfrak{T}_{S^{-1}}$ is also bounded. Since A (or, equivalently, D) is invertible, this follows by

$$S^{-1} = \begin{pmatrix} A^{-1} & -A^{-1}BD^{-1} \\ 0_{d \times d} & D^{-1} \end{pmatrix}$$

and by the first part of the statement. $\qquad\square$

Theorem 6.15. *Let* $m \in \mathcal{M}_v(\mathbb{R}^{2d})$, $S \in \mathrm{GL}(2d, \mathbb{R})$ *and* $0 < p, q \le \infty$. *Consider the operator*

$$(\mathfrak{T}_S)_m : f \in L^{p,q}_m(\mathbb{R}^{2d}) \mapsto |\det(S)|^{1/2} f \circ S.$$

If $m \circ S \asymp m$, *then* $\mathfrak{T}_S : L^{p,q}(\mathbb{R}^{2d}) \to L^{p,q}(\mathbb{R}^{2d})$ *is bounded if and only if* $(\mathfrak{T}_S)_m : L^{p,q}_m(\mathbb{R}^{2d}) \to L^{p,q}_m(\mathbb{R}^{2d})$ *is bounded.*

Proof. Observe that the condition $m \circ S \asymp m$ is equivalent to $m \circ S^{-1} \asymp m$. Assume that $\mathfrak{T}_S$ is bounded on $L^{p,q}(\mathbb{R}^{2d})$ and consider $f \in L^{p,q}_m(\mathbb{R}^{2d})$. Then, $fm \in L^{p,q}(\mathbb{R}^{2d})$ and

$$\|\mathfrak{T}_S f\|_{L^{p,q}_m(\mathbb{R}^{2d})} = \|\mathfrak{T}_S f \cdot m\|_{L^{p,q}(\mathbb{R}^{2d})} = \left\| \mathfrak{T}_S (f \cdot (m \circ S^{-1})) \right\|_{L^{p,q}(\mathbb{R}^{2d})}$$

$$\lesssim \|f \cdot (m \circ S^{-1})\|_{L^{p,q}(\mathbb{R}^{2d})} = \left\| \left(f \frac{m \circ S^{-1}}{m} \right) m \right\|_{L^{p,q}(\mathbb{R}^{2d})}$$

$$= \left\| f \frac{m \circ S^{-1}}{m} \right\|_{L^{p,q}_m(\mathbb{R}^{2d})} \lesssim \|f\|_{L^{p,q}_m(\mathbb{R}^{2d})}.$$

For the converse, assume that $(\mathfrak{T}_S)_m : L^{p,q}_m(\mathbb{R}^{2d}) \to L^{p,q}_m(\mathbb{R}^{2d})$ is bounded and take $f \in L^{p,q}(\mathbb{R}^{2d})$. Then, $f/m \in L^{p,q}_m(\mathbb{R}^{2d})$ and

$$\|\mathfrak{T}_S f\|_{L^{p,q}(\mathbb{R}^{2d})} \lesssim \left\| \mathfrak{T}_S f \left(\frac{m}{m \circ S} \right) \right\|_{L^{p,q}(\mathbb{R}^{2d})} \asymp \left\| \mathfrak{T}_S \left(\frac{f}{m} \right) \right\|_{L^{p,q}(\mathbb{R}^{2d})}$$

$$= \left\| \mathfrak{T}_S \left(\frac{f}{m} \right) \right\|_{L^{p,q}_m(\mathbb{R}^{2d})} \lesssim \|f/m\|_{L^{p,q}_m(\mathbb{R}^{2d})} = \|f\|_{L^{p,q}(\mathbb{R}^{2d})}.$$

$\qquad\square$

6.4   Appendix B

In this Appendix we study tensor products of metaplectic operators and refer to [76] for the theory of tensor products of HIlbert spaces. We are interested in proving the following result.

Theorem 6.16. *Let* $\hat{\mathcal{A}}, \widehat{\mathcal{B}} \in \mathrm{Mp}(d, \mathbb{R})$ *with* $\mathcal{A} = \pi^{Mp}(\hat{\mathcal{A}})$ *and* $\mathcal{B} = \pi^{Mp}(\widehat{\mathcal{B}})$ *having block decompositions*

$$\mathcal{A} = \begin{pmatrix} A & B \\ C & D \end{pmatrix}, \text{ and } \mathcal{B} = \begin{pmatrix} E & F \\ G & H \end{pmatrix}.$$

Then, the bilinear operator $S : L^2(\mathbb{R}^d) \times L^2(\mathbb{R}^d) \to L^2(\mathbb{R}^{2d})$ *defined for all* $f, g \in L^2(\mathbb{R}^d)$ *as*

$$S(f, g) = \hat{\mathcal{A}}f \otimes \widehat{\mathcal{B}}g$$

extends uniquely to a metaplectic operator $\widehat{\mathcal{C}} \in \mathrm{Mp}(2d, \mathbb{R})$ *with* $\mathcal{C} = \pi^{Mp}(\widehat{\mathcal{C}})$ *having block decomposition*

$$\mathcal{C} = \begin{pmatrix} A & 0_{d \times d} & B & 0_{d \times d} \\ 0_{d \times d} & E & 0_{d \times d} & F \\ C & 0_{d \times d} & D & 0_{d \times d} \\ 0_{d \times d} & G & 0_{d \times d} & H \end{pmatrix}.$$

Proof. By [76, Proposition 2.6.6], there exists a unique linear mapping $T : L^2(\mathbb{R}^d) \otimes L^2(\mathbb{R}^d) = L^2(\mathbb{R}^{2d}) \to L^2(\mathbb{R}^{2d})$ satisfying

$$T(f \otimes g) = \hat{\mathcal{A}}f \otimes \widehat{\mathcal{B}}g, \qquad f, g \in L^2(\mathbb{R}^d).$$

By [76, Proposition 2.6.12], this extension is also bounded. Moreover, T is invertible because $\hat{\mathcal{A}}$ and $\widehat{\mathcal{B}}$ are. In particular, T is surjective. To prove that T is a metaplectic operator, it remains to check that T preserves the L^2 inner product and that

$$T\rho(z, \tau) = \rho(\mathcal{C}z, \tau)T, \qquad z \in \mathbb{R}^{4d}, \ \tau \in \mathbb{R}. \tag{6.6}$$

For all $f, g, \varphi, \psi \in L^2(\mathbb{R}^d)$,

$$\langle T(f \otimes g), T(\varphi \otimes \psi) \rangle = \langle \hat{\mathcal{A}}f, \hat{\mathcal{A}}\varphi \rangle \langle \widehat{\mathcal{B}}g, \widehat{\mathcal{B}}\psi \rangle = \langle f, \varphi \rangle \langle g, \psi \rangle$$
$$= \langle f \otimes g, \varphi \otimes \psi \rangle.$$

If $\Phi \in L^2(\mathbb{R}^{2d})$, $\Phi = \sum_{j=1}^{\infty} c_j \varphi_j \otimes \psi_j$, with the sequence $(c_j)_j \subseteq \mathbb{C}$ vanishing definitely,

$$\langle T(f \otimes g), T\Phi \rangle = \sum_j \bar{c}_j \langle T(f \otimes g), T(\varphi_j \otimes \psi_j) \rangle = \sum_j \bar{c}_j \langle f \otimes g, \varphi_j \otimes \psi_j \rangle$$
$$= \langle f \otimes g, \Phi \rangle.$$

Now, consider $\Phi \in L^2(\mathbb{R}^{2d})$ and $(\Phi_j)_j \subseteq \mathrm{span}\{\varphi \otimes \psi : \varphi, \psi \in L^2(\mathbb{R}^d)\}$ satisfy $\lim_{j\to+\infty} \|\Phi - \Phi_j\|_{L^2(\mathbb{R}^{2d})} = 0$. Then, by the continuity of T and of the inner product,

$$\langle T(f \otimes g), T\Phi \rangle = \langle T(f \otimes g), T(\lim_{j\to+\infty} \Phi_j) \rangle = \lim_{j\to+\infty} \langle T(f \otimes g), T\Phi_j \rangle$$
$$= \lim_{j\to+\infty} \langle f \otimes g, \Phi_j \rangle = \langle f \otimes g, \Phi \rangle.$$

So, we proved that

$$\langle TF, T\Phi \rangle = \langle F, \Phi \rangle \tag{6.7}$$

holds for all $F = f \otimes g$, $f, g \in L^2(\mathbb{R}^d)$ and all $\Phi \in L^2(\mathbb{R}^{2d})$. The same argument applied to the first component of the inner product shows that (6.7) holds for all $F \in L^2(\mathbb{R}^{2d})$ as well. So, T is surjective and preserves the inner product, hence it is unitary. It remains to prove (6.6), which states that T is a metaplectic operator with $\pi^{Mp}(T) = \mathcal{C}$.

For, consider $f, g \in L^2(\mathbb{R}^d)$, $\tau \in \mathbb{R}$, $z = (x_1, x_2, \xi_1, \xi_2) \in \mathbb{R}^{4d}$ and $z_j = (x_j, \xi_j) \in \mathbb{R}^{2d}$ ($j = 1, 2$). First, observe that

$$\rho(z, \tau)(f \otimes g) = e^{-2\pi i \tau} \rho(z_1, \tau) f \otimes \rho(z_2, \tau) g$$

and

$$\pi(\mathcal{C}z)(f \otimes g) = \pi(\mathcal{A}z_1) f \otimes \pi(\mathcal{B}z_2) g,$$

so that

$$\rho(\mathcal{C}z, \tau) T(f \otimes g) = e^{2\pi i \tau} e^{-i\pi(Ax_1 + B\xi_1)(Cx_1 + D\xi_1)} e^{-i\pi(Ex_2 + F\xi_2)(Gx_2 + H\xi_2)}$$
$$\times \pi(\mathcal{C}z)(\hat{\mathcal{A}}f \otimes \widehat{\mathcal{B}}g)$$
$$= e^{2\pi i \tau} e^{-i\pi(Ax_1 + B\xi_1)(Cx_1 + D\xi_1)} e^{-i\pi(Ex_2 + F\xi_2)(Gx_2 + H\xi_2)}$$
$$\times \pi(\mathcal{A}z_1)\hat{\mathcal{A}}f \otimes \pi(\mathcal{B}z_2)\widehat{\mathcal{B}}g$$
$$= e^{-2\pi i \tau} \rho(\mathcal{A}z_1, \tau)\hat{\mathcal{A}}f \otimes \rho(\mathcal{B}z_2, \tau)\widehat{\mathcal{B}}g$$
$$= e^{-2\pi i \tau} \hat{\mathcal{A}}\rho(z_1, \tau)f \otimes \widehat{\mathcal{B}}\rho(z_2, \tau)g$$
$$= e^{-2\pi i \tau} T(\rho(z_1, \tau)f \otimes \rho(z_2, \tau)g)$$
$$= T\rho(z, \tau)(f \otimes g)$$

and (6.6) follows for tensor products. Next, if $F = \sum_{j=1}^{\infty} c_j f_j \otimes g_j$, $(c_j)_j \subseteq \mathbb{C}$ definitely zero, $f_j, g_j \in L^2(\mathbb{R}^d)$ ($j = 1, 2, \ldots$),

$$\rho(\mathcal{C}z, \tau)TF = \rho(\mathcal{C}z, \tau)T(\sum_j c_j f_j \otimes g_j) = \rho(\mathcal{C}z, \tau) \sum_j c_j T(f_j \otimes g_j)$$
$$= \sum_j c_j \rho(\mathcal{C}z, \tau)T(f_j \otimes g_j) = \sum_j c_j T\rho(z, \tau)(f_j \otimes g_j) = T\rho(z, \tau)F,$$

and the assertion follows by a standard density argument. $\qquad\square$

Remark 6.17. Under the same notation as in Theorem 6.16, if $\mathcal{A} = I_{d \times d}$, then

$$f \otimes \widehat{\mathcal{B}}g = \widehat{\mathcal{C}_1}(f \otimes g), \tag{6.8}$$

where

$$\mathcal{C}_1 = \begin{pmatrix} I_{d \times d} & 0_{d \times d} & 0_{d \times d} & 0_{d \times d} \\ 0_{d \times d} & E & 0_{d \times d} & F \\ 0_{d \times d} & 0_{d \times d} & I_{d \times d} & 0_{d \times d} \\ 0_{d \times d} & G & 0_{d \times d} & H \end{pmatrix}.$$

If $\mathcal{B} = I_{d \times d}$, we infer

$$\widehat{\mathcal{A}}f \otimes g = \widehat{\mathcal{C}_2}(f \otimes g),$$

where

$$\mathcal{C}_2 = \begin{pmatrix} A & 0_{d \times d} & B & 0_{d \times d} \\ 0_{d \times d} & I_{d \times d} & 0_{d \times d} & 0_{d \times d} \\ C & 0_{d \times d} & D & 0_{d \times d} \\ 0_{d \times d} & 0_{d \times d} & 0_{d \times d} & I_{d \times d} \end{pmatrix}.$$

Observe that $\mathcal{C} = \mathcal{C}_1 \mathcal{C}_2 = \mathcal{C}_2 \mathcal{C}_1$.

Metaplectic Gabor frames

Section 7.1 is devoted to metaplectic atoms, defined implicitly as

$$\langle f, \varphi \rangle = \frac{1}{\langle \gamma, g \rangle} \int_{\mathbb{R}^{2d}} W_{\mathcal{A}}(f, g)(z) \overline{W_{\mathcal{A}}(\varphi, \gamma)(z)} dz. \tag{7.1}$$

and to an equivalent of inversion formula of the STFT

$$f = \frac{1}{\langle \gamma, g \rangle} \int_{\mathbb{R}^{2d}} V_g f(x, \xi) \pi(x, \xi) \gamma \, dx d\xi, \qquad f \in L^2(\mathbb{R}^d), \tag{7.2}$$

for metaplectic Wigner distributions. In Section 7.2, we characterize shift-invertible Wigner distributions in terms of the STFT. We compute the metaplectic atoms of the distributions which belong to the Cohen's class in Section 7.3. In Section 7.4 we define metaplectic Gabor frames, characterizing those related to shift-invertible distributions. In Section 7.5 we complete the characterization of modulation spaces and Wiener amalgams in terms of shift-invertibility. We devote the Appendix to the proof of an intertwining formula between metaplectic operators and complex conjugation, which is used to obtain the expression of the adjoint of metaplectic atoms in Section 7.1.

This chapter is part of an article published in *Applied and Computational Harmonic Analysis* in 2024, cf. [20].

7.1 Metaplectic atoms

We start by generalizing the definition of time-frequency shifts. Differently from the classical theory, where time-frequency shifts are defined in terms of translations and modulations, and then used to define the STFT, we define them implicitly from metaplectic Wigner distributions.

Definition 7.1. Let $W_{\mathcal{A}}$ be a metaplectic Wigner distribution and $z \in \mathbb{R}^{2d}$. The **metaplectic atom** $\pi_{\mathcal{A}}(z)$ is the operator defined by its action on all $f \in \mathcal{S}(\mathbb{R}^d)$ as

$$\langle \varphi, \pi_{\mathcal{A}}(z) f \rangle := W_{\mathcal{A}}(\varphi, f)(z), \qquad \varphi \in \mathcal{S}(\mathbb{R}^d).$$

Observe that if $f, \varphi \in \mathcal{S}(\mathbb{R}^d)$, $W_{\mathcal{A}}(\varphi, f)(z)$ is well-defined for all $z \in \mathbb{R}^{2d}$, by Proposition 2.12.

Remark 7.2. Definition 7.1 says that metaplectic atoms play the game of time-frequency shifts for the STFT.

Metaplectic atoms map $\mathcal{S}(\mathbb{R}^d)$ to $\mathcal{S}'(\mathbb{R}^d)$, see Proposition 7.8 below. We put this detail aside and take it for granted in favour of some prior example.

Example 7.3. The metaplectic atoms associated to the STFT are the time-frequency shifts. In fact, for all $f, \varphi \in \mathcal{S}(\mathbb{R}^d)$ and all $z \in \mathbb{R}^{2d}$

$$\langle \varphi, \pi_{A_{ST}}(z)f \rangle = V_f \varphi(z) = \langle \varphi, \pi(z)f \rangle.$$

This implies that $\pi_{A_{ST}}(z)f$ and $\pi(z)f$ are tempered distributions with the same action on $\mathcal{S}(\mathbb{R}^d)$, i.e., $\pi_{A_{ST}}(z)f = \pi(z)f$.

Example 7.4. For $\hbar > 0$ and $f, g \in L^2(\mathbb{R}^d)$, we consider

$$V_g^\hbar f(x, \xi) = \langle f, (2\pi\hbar)^{-d/2} \pi^\hbar(x, \xi) g \rangle, \qquad (x, \xi) \in \mathbb{R}^{2d},$$

where $\pi^\hbar(x, \xi)g(t) := e^{i(\xi t - x \cdot \xi/2)/\hbar} g(t - x)$. These time-frequency representations were considered by M. de Gosson in [36]. For all $\hbar > 0$, up to a sign,

$$V_g^\hbar f(x, \xi) = (2\pi\hbar)^{-d/2} e^{2\pi i \frac{x \cdot \xi}{4\pi\hbar}} V_g f\left(x, \frac{\xi}{2\pi\hbar}\right), \qquad (x, \xi) \in \mathbb{R}^d, \quad f, g \in L^2(\mathbb{R}^d),$$

so that $V_g^\hbar f = W_{\mathcal{A}_\hbar}(f, g)$, where

$$\mathcal{A}_\hbar = \begin{pmatrix} I_{d \times d} & -I_{d \times d} & 0_{d \times d} & 0_{d \times d} \\ 0_{d \times d} & 0_{d \times d} & 2\pi\hbar I_{d \times d} & 2\pi\hbar I_{d \times d} \\ 0_{d \times d} & 0_{d \times d} & \frac{1}{2} I_{d \times d} & -\frac{1}{2} I_{d \times d} \\ -\frac{1}{4\pi\hbar} I_{d \times d} & -\frac{1}{4\pi\hbar} I_{d \times d} & 0_{d \times d} & 0_{d \times d} \end{pmatrix}.$$

In this case, we observe that

$$E_{\mathcal{A}_\hbar} = \begin{pmatrix} I_{d \times d} & 0_{d \times d} \\ 0_{d \times d} & 2\pi\hbar I_{d \times d} \end{pmatrix}.$$

The metaplectic atoms associated to $V^\hbar$ are

$$\pi_{\mathcal{A}_\hbar}(x, \xi)g = (2\pi\hbar)^{-d/2} e^{-i\frac{x \cdot \xi}{2\hbar}} \pi\left(x, \frac{\xi}{2\pi\hbar}\right) g$$

$$= |\det(E_{\mathcal{A}_\hbar})|^{-1/2} e^{-i\frac{x \cdot \xi}{\hbar}} \pi(E_{\mathcal{A}_\hbar}^{-1}(x, \xi))g,$$

$(x, \xi) \in \mathbb{R}^{2d}$, $g \in \mathcal{S}(\mathbb{R}^d)$.

Example 7.5. We compute the metaplectic atoms associated to the τ-Wigner distribution W_τ ($0 < \tau < 1$). For, let $z = (x, \xi) \in \mathbb{R}^{2d}$ and $f, \varphi \in \mathcal{S}(\mathbb{R}^d)$. Then,

$$W_\tau(\varphi, f)(x, \xi) = \int_{\mathbb{R}^d} \varphi(x + \tau t)\overline{f(x - (1 - \tau)t)}e^{-2\pi i \xi \cdot t}dt$$

$$= \frac{1}{\tau^d} \int_{\mathbb{R}^d} \varphi(s)\overline{f\left(x - (1 - \tau)\left(\frac{s - x}{\tau}\right)\right)}e^{-2\pi i \xi \cdot (\frac{s-x}{\tau})}ds$$

$$= \int_{\mathbb{R}^d} \varphi(s)\overline{f\left(\frac{1}{\tau}x - \frac{1 - \tau}{\tau}s\right)}e^{-2\pi i \xi \cdot \frac{s}{\tau}}e^{2\pi i \xi \cdot \frac{x}{\tau}}\frac{ds}{\tau^d}$$

$$= \langle \varphi, \pi_{A_\tau}(x, \xi)f \rangle,$$

where, if $\mathfrak{T}_\tau f(t) = \frac{(1-\tau)^{d/2}}{\tau^{d/2}}f\left(-\frac{1-\tau}{\tau}t\right)$,

$$\pi_{A_\tau}(x, \xi)f(t) = \frac{1}{\tau^d}e^{-2\pi i \frac{\xi \cdot x}{\tau}}e^{2\pi i t \cdot \frac{\xi}{\tau}}f\left(\left(-\frac{1 - \tau}{\tau}\right)\left(t - \frac{1}{1 - \tau}x\right)\right)$$

$$= \frac{1}{\tau^{d/2}(1 - \tau)^{d/2}}e^{-2\pi i \frac{x \cdot \xi}{\tau}}M_{\frac{\xi}{\tau}}T_{\frac{x}{1-\tau}}\mathfrak{T}_\tau f(t).$$

Observe that $\frac{1}{\tau^{d/2}|\tau - 1|^{d/2}} = |\det(E_{\mathcal{A}_\tau})|^{-1/2}$, so

$$\pi_{A_\tau}(x, \xi)f = |\det(E_{\mathcal{A}_\tau})|^{-1/2}e^{-2\pi i \frac{x \cdot \xi}{\tau}}\pi\left(\frac{1}{1 - \tau}x, \frac{1}{\tau}\xi\right)\mathfrak{T}_\tau f$$

$$= |\det(E_{\mathcal{A}_\tau})|^{-1/2}e^{-2\pi i \frac{x \cdot \xi}{\tau}}\pi(E_{A_\tau}^{-1}(x, \xi))\mathfrak{T}_\tau f.$$

Example 7.6. Consider the (cross)-Rihacek distribution W_0, defined for all $f, g \in L^2(\mathbb{R}^d)$ as

$$W_0(f, g)(x, \xi) = f(x)\overline{\hat{g}(\xi)}e^{-2\pi i \xi \cdot x}, \quad (x, \xi) \in \mathbb{R}^{2d}.$$

Then, if $z = (x, \xi) \in \mathbb{R}^{2d}$, $f, g \in \mathcal{S}(\mathbb{R}^d)$,

$$\langle \varphi, \pi_{A_0}(z)f \rangle = \varphi(x)\overline{\hat{f}(\xi)}e^{-2\pi i \xi \cdot x} = \langle \varphi, \hat{f}(\xi)e^{2\pi i \xi \cdot x}T_x\delta_0 \rangle.$$

Observe that $\pi_{A_0}(x, \xi)f = \hat{f}(\xi)e^{2\pi i \xi \cdot x}T_x\delta_0$ is a tempered distribution that does not define a function.

Example 7.7. Let $\hat{S} \in \mathrm{Sp}(d, \mathbb{R})$ with $S = \pi^{Mp}(\hat{S})$ having block decomposition

$$S = \begin{pmatrix} A & B \\ C & D \end{pmatrix} \tag{7.3}$$

and consider the metaplectic Wigner distribution defined in [19, Example 4.1 (ii)] as

$$\widetilde{\mathcal{U}}_g f(z) = V_g(\hat{S}f)(z) = W_{\mathcal{A}}(f, g)(z) = \langle f, \hat{S}^{-1}\pi(z)g \rangle = \langle f, \pi(S^{-1}z)\hat{S}^{-1}g \rangle,$$

$f, g \in L^2(\mathbb{R}^d)$, $x, \xi \in \mathbb{R}^d$, where

$$\mathcal{A} = \begin{pmatrix} A & -I_{d \times d} & B & 0_{d \times d} \\ C & 0_{d \times d} & D & I_{d \times d} \\ 0_{d \times d} & 0_{d \times d} & 0_{d \times d} & -I_{d \times d} \\ -A & 0_{d \times d} & -B & 0_{d \times d} \end{pmatrix}.$$

Clearly, $E_{\mathcal{A}} = S$ and $\pi_{\mathcal{A}}(z)g = \pi(S^{-1}z)\hat{S}^{-1}g$ for all $z \in \mathbb{R}^{2d}$.

As aforementioned, in the previous examples we took on trust that metaplectic atoms map $\mathcal{S}(\mathbb{R}^d)$ to $\mathcal{S}'(\mathbb{R}^d)$. This technicality, along with the linearity of metaplecitc atoms, is proved in the proposition that follows. Nevertheless, Example 7.6 shows that in general $\pi_{\mathcal{A}}(z)f$, $f \in \mathcal{S}(\mathbb{R}^d)$, is a tempered distribution that is not induced by any locally integrable function.

Proposition 7.8. Let $W_{\mathcal{A}}$ be a metaplectic Wigner distribution. For all $z \in \mathbb{R}^{2d}$, $\pi_{\mathcal{A}}(z)$ is a well-defined linear operator that maps $\mathcal{S}(\mathbb{R}^d)$ to $\mathcal{S}'(\mathbb{R}^d)$.

Proof. Let $f \in \mathcal{S}(\mathbb{R}^d)$. By definition, for any $\varphi, \psi \in \mathcal{S}(\mathbb{R}^d)$ and $\alpha \in \mathbb{C}$,

$$\begin{aligned} \langle \alpha\varphi + \psi, \pi_{\mathcal{A}}(z)f \rangle &= W_{\mathcal{A}}(\alpha\varphi + \psi, f)(z) = \hat{\mathcal{A}}((\alpha\varphi + \psi) \otimes \bar{f})(z) \\ &= \hat{\mathcal{A}}(\alpha\varphi \otimes \bar{f} + \psi \otimes \bar{f})(z) = \alpha\hat{\mathcal{A}}(\varphi \otimes \bar{f})(z) + \hat{\mathcal{A}}(\psi \otimes \bar{f})(z) \\ &= \alpha W_{\mathcal{A}}(\varphi, f)(z) + W_{\mathcal{A}}(\psi, f)(z) \\ &= \alpha\langle \varphi, \pi_{\mathcal{A}}(z)f \rangle + \langle \psi, \pi_{\mathcal{A}}(z)f \rangle. \end{aligned}$$

Then, we need to prove that $\pi_{\mathcal{A}}(z)f : \varphi \in \mathcal{S}(\mathbb{R}^d) \mapsto \langle \varphi, \pi_{\mathcal{A}}(z)f \rangle \in \mathbb{C}$ is continuous. Using the boundedness of $W_{\mathcal{A}} : \mathcal{S}(\mathbb{R}^d) \times \mathcal{S}(\mathbb{R}^d) \to \mathcal{S}(\mathbb{R}^{2d})$,

$$|\langle \varphi, \pi_{\mathcal{A}}(z)f \rangle| = |W_{\mathcal{A}}(\varphi, f)(z)| \leq \|W_{\mathcal{A}}(\varphi, f)\|_{L^\infty(\mathbb{R}^{2d})} = \rho_{0,0}(W_{\mathcal{A}}(\varphi, f))$$

$$\leq C \sum_{j=1}^{N} \rho_{\alpha_j, \beta_j}(\varphi) \sum_{j=1}^{M} \rho_{\gamma_j \delta_j}(f) = \tilde{C} \sum_{j=1}^{N} \rho_{\alpha_j, \beta_j}(\varphi).$$

Thus, it remains to check the linearity of $\pi_{\mathcal{A}}(z)$. For, let $\alpha \in \mathbb{C}$, $f, g \in \mathcal{S}(\mathbb{R}^d)$. For every $\varphi \in \mathcal{S}(\mathbb{R}^d)$,

$$\begin{aligned} \langle \varphi, \pi_{\mathcal{A}}(z)(\alpha f + g) \rangle &= W_{\mathcal{A}}(\varphi, \alpha f + g)(z) = \hat{\mathcal{A}}(\varphi \otimes \overline{(\alpha f + g)})(z) \\ &= \bar{\alpha}\hat{\mathcal{A}}(\varphi \otimes \bar{f})(z) + \hat{\mathcal{A}}(\varphi \otimes \bar{g})(z) \\ &= \bar{\alpha}W_{\mathcal{A}}(\varphi, f)(z) + W_{\mathcal{A}}(\varphi, g)(z) \\ &= \bar{\alpha}\langle \varphi, \pi_{\mathcal{A}}(z)f \rangle + \langle \varphi, \pi_{\mathcal{A}}(z)g \rangle \\ &= \langle \varphi, \alpha\pi_{\mathcal{A}}(z)f + \pi_{\mathcal{A}}(z)g \rangle. \end{aligned}$$

This concludes the proof. $\qquad\qquad\qquad\qquad\qquad\qquad\qquad\qquad\qquad\qquad\qquad\qquad$ □

The first question that we address is the validity of an equivalent of the inversion formula (7.2) for metaplectic Wigner distributions.

Theorem 7.9. *Let $W_{\mathcal{A}}$ be a metaplectic Wigner distribution and $f, g \in L^2(\mathbb{R}^d)$. If $\gamma \in \mathcal{S}(\mathbb{R}^d)$ satisfies $\langle \gamma, g \rangle \neq 0$, then*

$$f = \frac{1}{\langle \gamma, g \rangle} \int_{\mathbb{R}^{2d}} W_{\mathcal{A}}(f, g)(z) \pi_{\mathcal{A}}(z) \gamma dz \qquad (7.4)$$

where the integral must be interpreted in the weak sense of vector-valued integration.

Proof. We use the definition of vector-valued integral. For $\varphi \in L^2(\mathbb{R}^d)$, using (2.19),

$$\langle \frac{1}{\langle \gamma, g \rangle} \int_{\mathbb{R}^{2d}} W_{\mathcal{A}}(f, g)(z) \pi_{\mathcal{A}}(z) \gamma dz, \varphi \rangle = \frac{1}{\langle \gamma, g \rangle} \int_{\mathbb{R}^{2d}} W_{\mathcal{A}}(f, g)(z) \langle \pi_{\mathcal{A}}(z) \gamma, \varphi \rangle dz$$

$$= \frac{1}{\langle \gamma, g \rangle} \int_{\mathbb{R}^{2d}} W_{\mathcal{A}}(f, g)(z) \overline{W_{\mathcal{A}}(\varphi, \gamma)(z)} dz = \frac{1}{\langle \gamma, g \rangle} \langle W_{\mathcal{A}}(f, g), W_{\mathcal{A}}(\varphi, \gamma) \rangle$$

$$= \frac{1}{\langle \gamma, g \rangle} \langle f, \varphi \rangle \overline{\langle g, \gamma \rangle} = \langle f, \varphi \rangle.$$

This shows (7.4). $\qquad \square$

In what follows, we use the definitions of the submatrices $E_{\mathcal{A}}$, $F_{\mathcal{A}}$, $\mathcal{E}_{\mathcal{A}}$ and $\mathcal{F}_{\mathcal{A}}$ given in (2.21) and (2.22).

Lemma 7.10. *Let $W_{\mathcal{A}}$ be a metaplectic Wigner distribution. Then, for $z \in \mathbb{R}^{2d}$, $f, g \in L^2(\mathbb{R}^d)$, we have*

$$W_{\mathcal{A}}(\pi(z)f, g) = \Phi_{-M_{\mathcal{A}}}(z) \pi(E_{\mathcal{A}}z, F_{\mathcal{A}}z) W_{\mathcal{A}}(f, g),$$

where, if $\mathcal{A} = \pi^{Mp}(\hat{A})$ has block decomposition (2.20), $M_{\mathcal{A}}$ is the symmetric matrix

$$M_{\mathcal{A}} = \begin{pmatrix} A_{11}^T A_{31} + A_{21}^T A_{41} & A_{31}^T A_{13} + A_{41}^T A_{23} \\ A_{13}^T A_{31} + A_{23}^T A_{41} & A_{13}^T A_{33} + A_{23}^T A_{43} \end{pmatrix}. \qquad (7.5)$$

Proof. We use formula (41) in [19]. By definition of metaplectic operator, for all $\tau \in \mathbb{R}$, $z = (x, \xi) \in \mathbb{R}^{2d}$,

$$\hat{\mathcal{A}}(\rho(z; \tau)f \otimes \bar{g}) = \hat{\mathcal{A}}(\rho(x, 0, \xi, 0; \tau)f \otimes \bar{g})$$

$$= \rho(\mathcal{A}(x, 0, \xi, 0); \tau)\hat{\mathcal{A}}(f \otimes \bar{g})$$

$$= \rho(E_{\mathcal{A}}z, F_{\mathcal{A}}z; \tau) W_{\mathcal{A}}(f, g).$$

The assertion follows using that $\pi(x,\xi) = e^{i\pi x \cdot \xi}\rho(x,\xi;0)$:

$$
\begin{aligned}
W_{\mathcal{A}}(\pi(x,\xi)f,g) &= W_{\mathcal{A}}(e^{i\pi x \cdot \xi}\rho(x,\xi;0)f,g) \\
&= e^{i\pi x \cdot \xi}\rho(E_{\mathcal{A}}(x,\xi),F_{\mathcal{A}}(x,\xi);0)W_{\mathcal{A}}(f,g) \\
&= e^{i\pi x \cdot \xi}e^{-i\pi E_{\mathcal{A}}^T F_{\mathcal{A}}(x,\xi)\cdot(x,\xi)}\pi(E_{\mathcal{A}}(x,\xi),F_{\mathcal{A}}(x,\xi))W_{\mathcal{A}}(f,g).
\end{aligned}
$$

Using the definitions of $E_{\mathcal{A}}$ and $F_{\mathcal{A}}$, as well as the matrix L in (2.25), so that we rewrite the scalar product as

$$
x \cdot \xi = L(x,\xi)\cdot(x,\xi),
$$

we infer

$$
e^{i\pi x \cdot \xi}e^{-i\pi E_{\mathcal{A}}^T F_{\mathcal{A}}(x,\xi)\cdot(x,\xi)} = e^{-i\pi M_{\mathcal{A}}(x,\xi)\cdot(x,\xi)},
$$

where

$$
M_{\mathcal{A}} = \begin{pmatrix} A_{11}^T A_{31} + A_{21}^T A_{41} & A_{11}^T A_{33} + A_{21}^T A_{43} - I_{d\times d} \\ A_{13}^T A_{31} + A_{23}^T A_{41} & A_{13}^T A_{33} + A_{23}^T A_{43} \end{pmatrix}.
$$

The relations $(R1a)$, $(R2a)$ and $(R3a)$ imply that $M_{\mathcal{A}}$ is symmetric and it can be written as in (7.5).

$\square$

Remark 7.11. We stress that (7.5) introduces a new matrix associated to $W_{\mathcal{A}}$. Throughout this work, if $E_{\mathcal{A}}$ and $F_{\mathcal{A}}$ are defined as in (2.21), whereas P is the matrix given in (2.25), $M_{\mathcal{A}}$ denotes the symmetric $2d \times 2d$ matrix defined as $M_{\mathcal{A}} = E_{\mathcal{A}}^T F_{\mathcal{A}} - P$.

Theorem 7.12. *Let $\hat{\mathcal{A}} \in \mathrm{Mp}(2d,\mathbb{R})$, $\mathcal{A} = \pi^{Mp}(\hat{\mathcal{A}})$ and $W_{\mathcal{A}}$ be the associated metaplectic Wigner distribution. Consider the matrix $\mathcal{A}_* \in \mathrm{Sp}(2d,\mathbb{R})$ defined in (7.26) below. Then, for every $z \in \mathbb{R}^{2d}$,*

$$
\langle \pi_{\mathcal{A}}(z)f,g \rangle = \langle f,\pi_{\mathcal{A}_*}(z)g \rangle, \quad \forall\, f,g \in \mathcal{S}(\mathbb{R}^d).
$$

In particular, if $\pi_{\mathcal{A}}(z)$ extends to a bounded operator on $L^2(\mathbb{R}^d)$, then

$$
\pi_{\mathcal{A}}(z)^* = \pi_{\mathcal{A}_*}(z), \quad z \in \mathbb{R}^{2d}.
$$

Proof. It is an immediate consequence of Corollary 7.34 below. In fact, for all $f,g \in \mathcal{S}(\mathbb{R}^d)$,

$$
\langle \pi_{\mathcal{A}}(z)f,g \rangle = \overline{W_{\mathcal{A}}(g,f)(z)} = W_{\mathcal{A}_*}(f,g)(z) = \overline{\langle \pi_{\mathcal{A}_*}(z)g,f \rangle} = \langle f,\pi_{\mathcal{A}_*}(z)g \rangle.
$$

$\square$

7.2   Shift-invertibility unmasked

Among all metaplectic Wigner distributions, shift-invertible Wigner distributions are known to play a fundamental role in time-frequency analysis. It was proved in [31, 19] that they can be used to replace the STFT in the definition of modulation spaces $M_m^{p,q}(\mathbb{R}^d)$, for $1 \leq p, q \leq \infty$ and $m \in \mathcal{M}_v(\mathbb{R}^{2d})$ satisfying some inoffensive symmetry condition. In [19] it is observed that shift-invertibility is necessary for this characterization to hold, otherwise not even the $M^p(\mathbb{R}^d)$ spaces can be defined in terms of shift-invertible Wigner distributions. In this section, we investigate the properties of metaplectic atoms related to shift-invertible metaplectic Wigner distributions and characterize them in terms of the matrices $E_\mathcal{A}$, $F_\mathcal{A}$, $\mathcal{E}_\mathcal{A}$, $\mathcal{F}_\mathcal{A}$ and $M_\mathcal{A}$ defined in (2.21), (2.22) and (7.5), respectively.

Take any metaplectic Wigner distribution $W_\mathcal{A}$, and $z, w \in \mathbb{R}^{2d}$. Then Lemma 7.10 entails the equality

$$W_\mathcal{A}(\pi(w)f,g)(z) = \Phi_{-M_\mathcal{A}}(w)\pi(E_\mathcal{A}w, F_\mathcal{A}w)W_\mathcal{A}(f,g)(z), \qquad f, g \in L^2(\mathbb{R}^{2d}),$$

so that $|W_\mathcal{A}(\pi(w)f,g)(z)| = |W_\mathcal{A}(f,g)(z - E_\mathcal{A}w)|$.

Definition 7.13. A metaplectic Wigner distribution $W_\mathcal{A}$ is **shift-invertible** if $E_\mathcal{A} \in \mathrm{GL}(2d, \mathbb{R})$.

We shall need the following *lifting-type* result, proved in [19, Theorem B1]:

Lemma 7.14. *Let* $\hat{S}_1, \hat{S}_2 \in \mathrm{Mp}(d, \mathbb{R})$ *have block decompositions*

$$S_j = \begin{pmatrix} A_j & B_j \\ C_j & D_j \end{pmatrix}$$

($j = 1, 2$). Then, the bilinear operator

$$T(f,g) = \hat{S}_1 f \otimes \hat{S}_2 g$$

extends to a metaplectic operator $\hat{S} \in \mathrm{Mp}(2d, \mathbb{R})$, *where*

$$S = \begin{pmatrix} A_1 & 0_{d\times d} & B_1 & 0_{d\times d} \\ 0_{d\times d} & A_2 & 0_{d\times d} & B_2 \\ C_1 & 0_{d\times d} & D_1 & 0_{d\times d} \\ 0_{d\times d} & C_2 & 0_{d\times d} & D_2 \end{pmatrix}. \tag{7.6}$$

If $\hat{S} \in \mathrm{Mp}(d, \mathbb{R})$ and $\hat{T}(f \otimes g) = f \otimes \hat{S}g$, we set

$$\mathrm{Lift}(S) = \pi^{Mp}(\hat{T}) \in \mathrm{Sp}(2d, \mathbb{R}), \tag{7.7}$$

the corresponding matrix in (7.6).

Theorem 7.15. *Let $W_\mathcal{A}$ be a shift-invertible metaplectic Wigner distribution and $G_\mathcal{A} = L E_\mathcal{A}^{-1} \mathcal{E}_\mathcal{A}$ be the matrix of Lemma 2.14, with L as in (2.25). Then,*

$$\mathcal{A} = \mathcal{D}_{E_\mathcal{A}^{-1}} V_{M_\mathcal{A}} V_L^T \operatorname{Lift}(G_\mathcal{A}),$$

where $\operatorname{Lift}(G_\mathcal{A})$ *is defined in* (7.7).

Proof. We use the matrix

$$\mathcal{K} := \begin{pmatrix} I_{d\times d} & 0_{d\times d} & 0_{d\times d} & 0_{d\times d} \\ 0_{d\times d} & 0_{d\times d} & I_{d\times d} & 0_{d\times d} \\ 0_{d\times d} & I_{d\times d} & 0_{d\times d} & 0_{d\times d} \\ 0_{d\times d} & 0_{d\times d} & 0_{d\times d} & I_{d\times d} \end{pmatrix},$$

that permutes the central columns of $4d \times 4d$ matrices. This yields the following block decomposition of $\mathcal{A}$:

$$\mathcal{A} = \begin{pmatrix} E_\mathcal{A} & \mathcal{E}_\mathcal{A} \\ F_\mathcal{A} & \mathcal{F}_\mathcal{A} \end{pmatrix} \mathcal{K}.$$

Since $E_\mathcal{A} \in \operatorname{GL}(2d, \mathbb{R})$, we can write

$$\mathcal{A} = \begin{pmatrix} E_\mathcal{A} & 0_{2d\times 2d} \\ 0_{2d\times 2d} & E_\mathcal{A}^{-T} \end{pmatrix} \begin{pmatrix} I_{2d\times 2d} & E_\mathcal{A}^{-1}\mathcal{E}_\mathcal{A} \\ E_\mathcal{A}^T F_\mathcal{A} & E_\mathcal{A}^T \mathcal{F}_\mathcal{A} \end{pmatrix} \mathcal{K} = \mathcal{D}_{E_\mathcal{A}^{-1}} \begin{pmatrix} I_{2d\times 2d} & E_\mathcal{A}^{-1}\mathcal{E}_\mathcal{A} \\ E_\mathcal{A}^T F_\mathcal{A} & E_\mathcal{A}^T \mathcal{F}_\mathcal{A} \end{pmatrix} \mathcal{K}.$$

We proved in Lemma 7.10 that the matrix $M_\mathcal{A} = E_\mathcal{A}^T F_\mathcal{A} - P$ is symmetric, where P is defined as in (2.25). Therefore, $V_{M_\mathcal{A}}$ is a symplectic matrix and we have:

$$\mathcal{A} = \mathcal{D}_{E_\mathcal{A}^{-1}} \begin{pmatrix} I_{2d\times 2d} & 0_{2d\times 2d} \\ M_\mathcal{A} & I_{2d\times 2d} \end{pmatrix} \begin{pmatrix} I_{2d\times 2d} & E_\mathcal{A}^{-1}\mathcal{E}_\mathcal{A} \\ P & E_\mathcal{A}^T \mathcal{F}_\mathcal{A} - M_\mathcal{A} E_\mathcal{A}^{-1}\mathcal{E}_\mathcal{A} \end{pmatrix} \mathcal{K}$$

$$= \mathcal{D}_{E_\mathcal{A}^{-1}} V_{M_\mathcal{A}} \underbrace{\begin{pmatrix} I_{2d\times 2d} & E_\mathcal{A}^{-1}\mathcal{E}_\mathcal{A} \\ P & E_\mathcal{A}^T \mathcal{F}_\mathcal{A} - M_\mathcal{A} E_\mathcal{A}^{-1}\mathcal{E}_\mathcal{A} \end{pmatrix} \mathcal{K}}_{=:\, \mathcal{A}'}.$$

The matrix $\mathcal{A}'$ is symplectic, since $\mathcal{A}' = V_{-M_\mathcal{A}} \mathcal{D}_{E_\mathcal{A}} \mathcal{A}$ is the product of symplectic matrices. Getting rid of $\mathcal{K}$, we obtain

$$\mathcal{A}' = \begin{pmatrix} I_{d\times d} & A'_{12} & 0_{d\times d} & A'_{14} \\ 0_{d\times d} & A'_{22} & I_{d\times d} & A'_{24} \\ 0_{d\times d} & A'_{32} & I_{d\times d} & A'_{34} \\ 0_{d\times d} & A'_{42} & 0_{d\times d} & A'_{44} \end{pmatrix},$$

for suitable matrices A'_{ij}, $i = 1, 2, 3, 4$, $j = 2, 4$. Observe that

$$E_\mathcal{A}^{-1}\mathcal{E}_\mathcal{A} = \begin{pmatrix} A'_{12} & A'_{14} \\ A'_{22} & A'_{24} \end{pmatrix}.$$

The symplectic relations $(R1b)$, $(R1c)$, $(R2b)$, $(R2c)$, $(R3b)$, $(R3c)$ and $(R3d)$ for $\mathcal{A}' \in \mathrm{Sp}(2d, \mathbb{R})$ read respectively as

$(S1)$ $\quad A'_{32} = 0_{d \times d}$,

$(S2)$ $\quad {A'_{12}}^T A'_{32} + {A'_{22}}^T A'_{42} = {A'_{32}}^T A'_{12} + {A'_{42}}^T A'_{22}$,

$(S3)$ $\quad A'_{44}, = A'_{14}$,

$(S4)$ $\quad {A'_{14}}^T A'_{34} + {A'_{24}}^T A_{44} = {A'_{34}}^T A_{14} + {A'_{44}}^T A_{24}$

$(S5)$ $\quad A'_{34} = 0_{d \times d}$,

$(S6)$ $\quad A'_{12} = A'_{42}$

$(S7)$ $\quad {A'_{12}}^T A'_{34} + {A'_{22}}^T A'_{44} - ({A'_{32}}^T A'_{14} + {A'_{42}}^T A_{24}) = I_{d \times d}$.

The others being trivially satisfied. This yields:

$$\mathcal{A}' = \begin{pmatrix} I_{d \times d} & A'_{12} & 0_{d \times d} & A'_{14} \\ 0_{d \times d} & A'_{22} & I_{d \times d} & A'_{24} \\ 0_{d \times d} & 0_{d \times d} & I_{d \times d} & 0_{d \times d} \\ 0_{d \times d} & A'_{12} & 0_{d \times d} & A'_{14} \end{pmatrix}.$$

Observe that

$$\begin{pmatrix} A'_{22} & A'_{24} \\ A'_{12} & A'_{14} \end{pmatrix} = L E_{\mathcal{A}}^{-1} \mathcal{E}_{\mathcal{A}} = G_{\mathcal{A}},$$

which is symplectic by Lemma 2.14. A simple computation shows that $\mathcal{A}' = V_L^T \mathrm{Lift}(G_{\mathcal{A}})$, as desired. $\qquad \square$

The characterization of shift-invertible Wigner distributions is straightforward.

Corollary 7.16. *Let $W_{\mathcal{A}}$ be a metaplectic Wigner distribution. Then, $W_{\mathcal{A}}$ is shift-invertible if and only if, up to a sign,*

$$W_{\mathcal{A}}(f, g) = \mathfrak{T}_{E_{\mathcal{A}}^{-1}} \Phi_{M_{\mathcal{A}} + L} V_{\widehat{\delta_{\mathcal{A}} g}} f, \quad f, g \in L^2(\mathbb{R}^d), \tag{7.8}$$

where

$$\widehat{\delta_{\mathcal{A}} g} := \mathcal{F} \widehat{G_{\mathcal{A}}} g, \tag{7.9}$$

and $\widehat{G_{\mathcal{A}}}$ is the metaplectic operator defined in Proposition 7.33 below. In particular, if $W_{\mathcal{A}}$ is shift-invertible then, up to a sign,

$$\pi_{\mathcal{A}}(z) = |\det(E_{\mathcal{A}})|^{-1/2} \Phi_{-M_{\mathcal{A}} - L}(E_{\mathcal{A}}^{-1} z) \pi(E_{\mathcal{A}}^{-1} z) \widehat{\delta_{\mathcal{A}}}, \quad z \in \mathbb{R}^{2d}, \tag{7.10}$$

and

(i) $\pi_{\mathcal{A}}(z)$ is a surjective quasi-isometry of $L^2(\mathbb{R}^d)$ with

$$\|\pi_{\mathcal{A}}(z) f\|_2 = |\det(E_{\mathcal{A}})|^{-1/2} \|f\|_2, \quad f \in L^2(\mathbb{R}^d);$$

(ii) $\pi_{\mathcal{A}}(z)$ is a topological isomorphism on $\mathcal{S}(\mathbb{R}^d)$;
(iii) $\pi_{\mathcal{A}}(z)$ is a topological isomorphism on $\mathcal{S}'(\mathbb{R}^d)$.

Proof. By Theorem 7.15, $\mathcal{A}$ is shift-invertible if and only if

$$\mathcal{A} = \mathcal{D}_{E_{\mathcal{A}}^{-1}} V_{M_{\mathcal{A}}} V_L^T \operatorname{Lift}(G_{\mathcal{A}}).$$

Let A_{ST} be the symplectic matrix associated to the STFT, cf. (2.17). Observe that

$$A_{ST} = V_{-L} V_L^T \mathcal{A}_{FT2},$$

where $\mathcal{A}_{FT2}$ is the symplectic matrix associated to the partial Fourier transform with respect to the second variable defined in (2.12). Then,

$$\mathcal{A} = \mathcal{D}_{E_{\mathcal{A}}^{-1}} V_{M_{\mathcal{A}}} (V_L V_{-L}) V_L^T (\mathcal{A}_{FT2} \mathcal{A}_{FT2}^{-1}) \operatorname{Lift}(G_{\mathcal{A}})$$
$$= \mathcal{D}_{E_{\mathcal{A}}^{-1}} V_{M_{\mathcal{A}}+L} A_{ST} \mathcal{A}_{FT2}^{-1} \operatorname{Lift}(G_{\mathcal{A}}).$$

Therefore, up to a sign,

$$W_{\mathcal{A}}(f,g)(z) = \hat{\mathcal{A}}(f \otimes \bar{g})(z) = \widehat{\mathcal{D}_{E_{\mathcal{A}}^{-1}}} \widehat{V_{M_{\mathcal{A}}}} \widehat{V_L^T} \widehat{\operatorname{Lift}(G_{\mathcal{A}})}(f \otimes \bar{g})(z)$$
$$= \widehat{\mathcal{D}_{E_{\mathcal{A}}^{-1}}} \widehat{V_{M_{\mathcal{A}}+L}} \widehat{A_{ST}} \mathcal{F}_2^{-1} \widehat{\operatorname{Lift}(G_{\mathcal{A}})}(f \otimes \bar{g})(z)$$
$$= |\det(E_{\mathcal{A}})|^{-1/2} \Phi_{M_{\mathcal{A}}+L}(E_{\mathcal{A}}^{-1}z) \widehat{A_{ST}}(f \otimes (\mathcal{F}^{-1}\widehat{G_{\mathcal{A}}}\bar{g}))(E_{\mathcal{A}}^{-1}z).$$

Let $\widehat{\overline{G_{\mathcal{A}}}}$ be the symplectic operator such that $\widehat{G_{\mathcal{A}}}\bar{g} = \overline{\widehat{\overline{G_{\mathcal{A}}}}g}$, cf. Proposition 7.33. Then,

$$\mathcal{F}^{-1}\widehat{G_{\mathcal{A}}}\bar{g} = \mathcal{F}^{-1}\overline{\widehat{\overline{G_{\mathcal{A}}}}g} = \overline{\mathcal{F}\widehat{\overline{G_{\mathcal{A}}}}g} =: \overline{\widehat{\delta_{\mathcal{A}}}g}.$$

Therefore,

$$W_{\mathcal{A}}(f,g)(z) = |\det(E_{\mathcal{A}})|^{-1/2} \Phi_{M_{\mathcal{A}}+L}(E_{\mathcal{A}}^{-1}z) V_{\widehat{\delta_{\mathcal{A}}}g} f(E_{\mathcal{A}}^{-1}z),$$

which can also be restated as:

$$W_{\mathcal{A}}(f,g)(z) = \langle f, \pi_{\mathcal{A}}(z)g \rangle,$$

where $\pi_{\mathcal{A}}(z)$ is the operator in (7.10). Items (i) - (iii) are trivial consequences of (7.10). □

The metaplectic operator defined in (7.9) plays a crucial role in the characterization of metaplectic Gabor frames for shift-invertible metaplectic Wigner distributions. For this reason, it is worth giving it a name, in the spirit of the terminology used by M. de Gosson in [36]:

Definition 7.17. We call the metaplectic operator $\widehat{\delta_{\mathcal{A}}}$ in (7.9) the **deformation operator** associated to $W_{\mathcal{A}}$.

Example 7.18. τ-Wigner distributions can be rephrased as *rescaled STFT, up to chirps*, as in (7.8). Precisely, for $0 < \tau < 1$, set $\mathfrak{T}_\tau g(t) = \frac{(1-\tau)^{d/2}}{\tau^{d/2}} g(-\frac{1-\tau}{\tau} t)$ as in Example 7.5. We proved in the same Example that

$$W_\tau(f,g)(x,\xi) = \left\langle f, \frac{1}{\tau^{d/2}(1-\tau)^{d/2}} e^{-2\pi i \frac{x \cdot \xi}{\tau}} \pi\left(\frac{x}{1-\tau}, \frac{\xi}{\tau}\right) \mathfrak{T}_\tau g \right\rangle \qquad (7.11)$$

for all $f, g \in L^2(\mathbb{R}^d)$ and $x, \xi \in \mathbb{R}^d$. Consequently, we retrieve the expression of W_τ as a rescaled STFT:

$$W_\tau(f,g)(x,\xi) = \frac{1}{\tau^{d/2}(1-\tau)^{d/2}} e^{2\pi i \frac{x \cdot \xi}{\tau}} V_{\mathfrak{T}_\tau g} f\left(\frac{x}{1-\tau}, \frac{\xi}{\tau}\right).$$

We proved that metaplectic atoms of shift-invertible Wigner distributions are surjective isometries of $L^2(\mathbb{R}^d)$ and their adjoints are the atoms associated to $W_{\mathcal{A}_*}$, where $\mathcal{A}_*$ is the matrix defined in the statement of the Theorem 7.12.

We conclude this section with the explicit computation of $\pi_{\mathcal{A}}(z)^{-1}$ and $\pi_{\mathcal{A}}(z)^*$ for shift-invertible Wigner distributions.

Theorem 7.19. *Let $W_{\mathcal{A}}$ be a shift-invertible Wigner distribution and $\widehat{\delta_{\mathcal{A}}}$ the related deformation operator, cf. (7.9). Consider the matrices L and P defined as in (2.25) and the following matrices:*

$$Q = \begin{pmatrix} I_{d \times d} & 0_{d \times d} \\ 0_{d \times d} & -I_{d \times d} \end{pmatrix} = -LJ,$$

$$\delta_{\mathcal{A}} = -E_{\mathcal{A}}^{-1} \mathcal{E}_{\mathcal{A}} Q. \qquad (7.12)$$

Then, for every $z \in \mathbb{R}^{2d}$, up to a sign, the inverse $\pi_{\mathcal{A}}(z)^{-1}$ and the adjoint $\pi_{\mathcal{A}}(z)^*$ operators can be explicitly computed as

$$\pi_{\mathcal{A}}(z)^{-1} = |\det(E_{\mathcal{A}})|^{1/2} \Phi_{M_{\mathcal{A}}+L/2}(E_{\mathcal{A}}^{-1} z) \Phi_{L/2}(\mathcal{E}_{\mathcal{A}}^{-1} z) \pi(Q \mathcal{E}_{\mathcal{A}}^{-1} z) \widehat{\delta_{\mathcal{A}}}^{-1}, \qquad (7.13)$$

and

$$\pi_{\mathcal{A}}(z)^* = |\det(E_{\mathcal{A}})|^{-1} \pi_{\mathcal{A}}(z)^{-1}. \qquad (7.14)$$

Proof. We use the explicit expression of metaplectic Gabor atoms for shift-invertible $W_{\mathcal{A}}$ in (7.10), which yields

$$\pi_{\mathcal{A}}(z)^{-1} = |\det(E_{\mathcal{A}})|^{1/2} \Phi_{M_{\mathcal{A}}+L}(E_{\mathcal{A}}^{-1} z) \widehat{\delta_{\mathcal{A}}}^{-1} \pi(E_{\mathcal{A}}^{-1} z)^{-1}. \qquad (7.15)$$

By (2.3), if $E_{\mathcal{A}}^{-1} z = ((E_{\mathcal{A}}^{-1} z)_1, (E_{\mathcal{A}}^{-1} z)_2)$,

$$\pi(E_{\mathcal{A}}^{-1} z)^{-1} = e^{-2\pi i (E_{\mathcal{A}}^{-1} z)_1 \cdot (E_{\mathcal{A}}^{-1} z)_2} \pi(-E_{\mathcal{A}}^{-1} z) = \Phi_{-L}(E_{\mathcal{A}}^{-1} z) \pi(-E_{\mathcal{A}}^{-1} z).$$

Also, by (2.13), for all $z \in \mathbb{R}^{2d}$ and $\tau \in \mathbb{R}$,

$$\widehat{\delta_{\mathcal{A}}}^{-1} \rho(-E_{\mathcal{A}}^{-1}z; \tau)\widehat{\delta_{\mathcal{A}}} = \rho(-\delta_{\mathcal{A}}^{-1}E_{\mathcal{A}}^{-1}z; \tau).$$

Using the definition of ρ, for $\tau = 0$ this is equivalent to

$$\widehat{\delta_{\mathcal{A}}}^{-1} \pi(-E_{\mathcal{A}}^{-1}z) = e^{i\pi(E_{\mathcal{A}}^{-1}z)_1 \cdot (E_{\mathcal{A}}^{-1}z)_2} e^{-i\pi(\delta_{\mathcal{A}}^{-1}E_{\mathcal{A}}^{-1}z)_1 \cdot (\delta_{\mathcal{A}}^{-1}E_{\mathcal{A}}^{-1}z)_2} \pi(-\delta_{\mathcal{A}}^{-1}E_{\mathcal{A}}^{-1}z)\widehat{\delta_{\mathcal{A}}}^{-1},$$

where $\delta_{\mathcal{A}}^{-1}E_{\mathcal{A}}^{-1}z = ((\delta_{\mathcal{A}}^{-1}E_{\mathcal{A}}^{-1}z)_1, (\delta_{\mathcal{A}}^{-1}E_{\mathcal{A}}^{-1}z)_2)$. We compute explicitly the matrix $\delta_{\mathcal{A}}^{-1}E_{\mathcal{A}}^{-1}$. For, let us denote with

$$G_{\mathcal{A}} = \begin{pmatrix} A & B \\ C & D \end{pmatrix}$$

the block decomposition of the symplectic matrix $G_{\mathcal{A}}$, so that

$$G_{\mathcal{A}}^{-1} = \begin{pmatrix} D^T & -B^T \\ -C^T & A^T \end{pmatrix}, \quad \overline{G_{\mathcal{A}}} = \begin{pmatrix} A & -B \\ -C & D \end{pmatrix}$$

and

$$\overline{G_{\mathcal{A}}^T} = \overline{G_{\mathcal{A}}}^T = \begin{pmatrix} A^T & -C^T \\ -B^T & D^T \end{pmatrix}.$$

By definition, $\delta_{\mathcal{A}} = \pi^{Mp}(\widehat{\delta_{\mathcal{A}}}) = \pi^{Mp}(\widehat{\mathcal{F}G_{\mathcal{A}}})$, so that

$$\delta_{\mathcal{A}} = J\overline{G_{\mathcal{A}}}.$$

This, together with $\overline{G_{\mathcal{A}}}J\overline{G_{\mathcal{A}}}^T = J$ and $G_{\mathcal{A}} = LE_{\mathcal{A}}^{-1}\mathcal{E}_{\mathcal{A}}$, yields to:

$$\delta_{\mathcal{A}}^{-1}E_{\mathcal{A}}^{-1} = (-\overline{G_{\mathcal{A}}}^{-1}J)(LG_{\mathcal{A}}\mathcal{E}_{\mathcal{A}}^{-1}) = (-J\overline{G_{\mathcal{A}}}^T)(LG_{\mathcal{A}}\mathcal{E}_{\mathcal{A}}^{-1}),$$

where the invertibility of $\mathcal{E}_{\mathcal{A}}$ is guaranteed by Lemma 2.14. We use the block decompositions of the matrices at stake to get:

$$\begin{aligned}
\delta_{\mathcal{A}}^{-1}E_{\mathcal{A}}^{-1} &= \begin{pmatrix} 0_{d\times d} & -I_{d\times d} \\ I_{d\times d} & 0_{d\times d} \end{pmatrix} \begin{pmatrix} A^T & -C^T \\ -B^T & D^T \end{pmatrix} \begin{pmatrix} 0_{d\times d} & I_{d\times d} \\ I_{d\times d} & 0_{d\times d} \end{pmatrix} G_{\mathcal{A}}\mathcal{E}_{\mathcal{A}}^{-1} \\
&= \begin{pmatrix} B^T & -D^T \\ A^T & -C^T \end{pmatrix} \begin{pmatrix} 0_{d\times d} & I_{d\times d} \\ I_{d\times d} & 0_{d\times d} \end{pmatrix} G_{\mathcal{A}}\mathcal{E}_{\mathcal{A}}^{-1} \\
&= \begin{pmatrix} -D^T & B^T \\ -C^T & A^T \end{pmatrix} G_{\mathcal{A}}\mathcal{E}_{\mathcal{A}}^{-1} \\
&= \begin{pmatrix} -I_{d\times d} & 0_{d\times d} \\ 0_{d\times d} & I_{d\times d} \end{pmatrix} G_{\mathcal{A}}^{-1} G_{\mathcal{A}}\mathcal{E}_{\mathcal{A}}^{-1} = -Q\mathcal{E}_{\mathcal{A}}^{-1}.
\end{aligned}$$

This proves (7.12). A simple computation shows that

$$(\delta_{\mathcal{A}}^{-1}E_{\mathcal{A}}^{-1}z)_1 \cdot (\delta_{\mathcal{A}}^{-1}E_{\mathcal{A}}^{-1}z)_2 = (Q\mathcal{E}_{\mathcal{A}}^{-1}z)_1 \cdot (Q\mathcal{E}_{\mathcal{A}}^{-1}z)_2 = -(\mathcal{E}_{\mathcal{A}}^{-1}z)_1 \cdot (\mathcal{E}_{\mathcal{A}}^{-1}z)_2,$$

that entails

$$e^{-i\pi(\delta_{\mathcal{A}}^{-1}E_{\mathcal{A}}^{-1}z)_1 \cdot (\delta_{\mathcal{A}}^{-1}E_{\mathcal{A}}^{-1}z)_2} = e^{i\pi(\mathcal{E}_{\mathcal{A}}^{-1}z)_1 \cdot (\mathcal{E}_{\mathcal{A}}^{-1}z)_2} = \Phi_{L/2}(\mathcal{E}_{\mathcal{A}}^{-1}z).$$

Plugging all the information in (7.15), we find

$$\pi_{\mathcal{A}}(z)^{-1} = |\det(E_{\mathcal{A}})|^{1/2}\Phi_{M_{\mathcal{A}}+L}(E_{\mathcal{A}}^{-1}z)\Phi_{-L/2}(E_{\mathcal{A}}^{-1}z)\Phi_{L/2}(\mathcal{E}_{\mathcal{A}}^{-1}z)\pi(Q\mathcal{E}_{\mathcal{A}}^{-1}z)\widehat{\delta_{\mathcal{A}}}^{-1}.$$

This proves (i).

To prove (ii), we prove that $\pi_{\mathcal{A}}(z)^*$ is expressed by (7.15), up to the determinant factor. For, let $f, g \in L^2(\mathbb{R}^d)$ and $z \in \mathbb{R}^{2d}$. By (7.10),

$$\begin{aligned}
\langle \pi_{\mathcal{A}}(z)^* f, g \rangle &= \langle f, \pi_{\mathcal{A}}(z)g \rangle \\
&= \langle f, |\det(E_{\mathcal{A}})|^{-1/2}\Phi_{-M_{\mathcal{A}}-L}(E_{\mathcal{A}}^{-1}z)\pi(E_{\mathcal{A}}^{-1}z)\widehat{\delta_{\mathcal{A}}}g \rangle \\
&= \langle |\det(E_{\mathcal{A}})|^{-1/2}\Phi_{M_{\mathcal{A}}+L}(E_{\mathcal{A}}^{-1}z)\widehat{\delta_{\mathcal{A}}}^{-1}\pi(E_{\mathcal{A}}^{-1}z)^{-1}f, g \rangle \\
&= \langle |\det(E_{\mathcal{A}})|^{-1}\pi_{\mathcal{A}}(z)^{-1}f, g \rangle
\end{aligned}$$

and the assertion follows. $\qquad\square$

7.3 Atoms of Covariant Metaplectic Wigner distributions

In this section we derive the expression of metaplectic atoms of covariant metaplectic Wigner distributions. We recall their definition, cf. [31]

Definition 7.20. A metaplectic Wigner distribution $W_{\mathcal{A}}$ is **covariant** if

$$W_{\mathcal{A}}(\pi(z)f, \pi(z)g) = T_z W_{\mathcal{A}}(f, g)$$

holds for every $z \in \mathbb{R}^{2d}$ and all $f, g \in L^2(\mathbb{R}^d)$.

The following result summarizes [31, Proposition 2.10 and Theorem 2.11] and states that covariance characterises the Cohen's class of metaplectic Wigner distributions.

Proposition 7.21. Let $\hat{\mathcal{A}} \in \text{Mp}(2d, \mathbb{R})$ and $W_{\mathcal{A}}$ be the associated metaplectic Wigner distribution. The following statements are equivalent:
(i) $W_{\mathcal{A}}$ is covariant.
(ii) The matrix $\mathcal{A} = \pi^{Mp}(\hat{\mathcal{A}})$ has block decomposition

$$\mathcal{A} = \begin{pmatrix} A_{11} & I_{d\times d} - A_{11} & A_{13} & A_{13} \\ A_{21} & -A_{21} & I_{d\times d} - A_{11}^T & -A_{11}^T \\ 0_{d\times d} & 0_{d\times d} & I_{d\times d} & I_{d\times d} \\ -I_{d\times d} & I_{d\times d} & 0_{d\times d} & 0_{d\times d} \end{pmatrix}, \qquad (7.16)$$

with $A_{13} = A_{13}^T$ and $A_{21} = A_{21}^T$.

(iii) $W_{\mathcal{A}}$ belongs to the Cohen's class, namely

$$W_{\mathcal{A}}(f,g) = \Sigma_{\mathcal{A}} * W(f,g), \qquad f, g \in L^2(\mathbb{R}^d),$$

where $\Sigma_{\mathcal{A}} = \mathcal{F}^{-1}\Phi_{-B_{\mathcal{A}}}$, with $B_{\mathcal{A}}$ defined as in (2.24).

Theorem 7.22. *Let $W_{\mathcal{A}}$ be a covariant metaplectic Wigner distribution, $\mathcal{A}$ and $B_{\mathcal{A}}$ be as in (7.16) and (2.24), respectively. Then,*
(i) for every $z \in \mathbb{R}^{2d}$,

$$\pi_{\mathcal{A}}(z)g \overset{\mathcal{S}'}{=} 2^d \int_{\mathbb{R}^{2d}} \mathcal{F}\Phi_{B_{\mathcal{A}}}(z-w)\Phi_{-2L}(w)\pi(2w)\mathcal{I}gdw, \qquad (7.17)$$

where $\mathcal{I}g(t) = g(-t)$ and the integral must be interpreted in the weak sense of vector-valued integration.
(ii) If also $B_{\mathcal{A}} \in \mathrm{GL}(2d,\mathbb{R})$, then, for every $z \in \mathbb{R}^{2d}$,

$$\pi_{\mathcal{A}}(z)g \overset{\mathcal{S}'}{=} 2^d \int_{\mathbb{R}^{2d}} \Phi_{-B_{\mathcal{A}}^{-1}}(z-w)\Phi_{-2L}(w)\pi(2w)\mathcal{I}gdw, \qquad g \in \mathcal{S}(\mathbb{R}^d) \quad (7.18)$$

holds in the weak sense of vector-valued integration.
(iii) If $\mathcal{A}_*$ is the matrix defined in (7.26), then $W_{\mathcal{A}_*}$ is covariant with $B_{\mathcal{A}_*} = -B_{\mathcal{A}}$ and, consequently,

$$\pi_{\mathcal{A}}(z)^*g \overset{\mathcal{S}'}{=} 2^d \int_{\mathbb{R}^{2d}} \mathcal{F}\Phi_{-B_{\mathcal{A}}}(z-w)\Phi_{-2L}(w)\pi(2w)\mathcal{I}gdw,$$

for all $g \in \mathcal{S}(\mathbb{R}^d)$ and every $z \in \mathbb{R}^{2d}$. If $B_{\mathcal{A}}$ is invertible, then

$$\pi_{\mathcal{A}}(z)^*g \overset{\mathcal{S}'}{=} 2^d \int_{\mathbb{R}^{2d}} \Phi_{B_{\mathcal{A}}^{-1}}(z-w)\Phi_{-2L}(w)\pi(2w)\mathcal{I}gdw,$$

for every $g \in \mathcal{S}(\mathbb{R}^d)$ and $z \in \mathbb{R}^{2d}$.

Proof. (*i*) By Proposition 7.21, for all $\varphi, g \in \mathcal{S}(\mathbb{R}^d)$ and all $z \in \mathbb{R}^{2d}$,

$$\begin{aligned}
\langle \varphi, \pi_{\mathcal{A}}(z)g \rangle &= W_{\mathcal{A}}(\varphi, g)(z) \\
&= \Sigma_{\mathcal{A}} * W(\varphi, g)(z) \\
&= \int_{\mathbb{R}^{2d}} \Sigma_{\mathcal{A}}(z-w)W(\varphi,g)(w)dw \\
&= \int_{\mathbb{R}^{2d}} \overline{\mathcal{F}\Phi_{B_{\mathcal{A}}}(z-w)}\langle \varphi, \pi_{A_{1/2}}(w)g \rangle dw \\
&= \left\langle \varphi, \int_{\mathbb{R}^{2d}} \mathcal{F}\Phi_{B_{\mathcal{A}}}(z-w)\pi_{A_{1/2}}(w)gdw \right\rangle,
\end{aligned}$$

where we used that $\mathcal{F}^{-1}\Phi_{-B_\mathcal{A}} = \overline{\mathcal{F}\Phi_{B_\mathcal{A}}}$. Consequently,

$$\pi_\mathcal{A}(z)g = \int_{\mathbb{R}^{2d}} \mathcal{F}\Phi_{B_\mathcal{A}}(z-w)\pi_{A_{1/2}}(w)g\,dw.$$

Plugging $\tau = 1/2$ in (7.11), we infer the explicit metaplectic atom of the Wigner distribution: for $w = (x, \xi) \in \mathbb{R}^{2d}$,

$$\pi_{A_{1/2}}(x, \xi)g(t) = 2^d e^{-4\pi ix\cdot\xi}\pi(2x, 2\xi)\mathcal{I}g(t) = 2^d\Phi_{-2L}(w)\pi(2w)\mathcal{I}g(t).$$

Expression (7.17) follows consequently.

(ii) If $B_\mathcal{A}$ is invertible, then $\mathcal{F}\Phi_{B_\mathcal{A}} = \Phi_{-B_\mathcal{A}^{-1}}$, and (7.18) holds in the weak sense of vector-valued integration.

(iii) By (7.26) and (7.16), it follows that

$$\mathcal{A}_* = \begin{pmatrix} I_{d\times d} - A_{11} & A_{11} & -A_{13} & -A_{13} \\ -A_{21} & A_{21} & A_{11}^T & A_{11}^T - I_{d\times d} \\ 0_{d\times d} & 0_{d\times d} & I_{d\times d} & I_{d\times d} \\ -I_{d\times d} & I_{d\times d} & 0_{d\times d} & 0_{d\times d} \end{pmatrix}.$$

Therefore, $W_{\mathcal{A}_*}$ is covariant by Proposition 7.21 (ii), with

$$\begin{aligned} B_{\mathcal{A}_*} &= \begin{pmatrix} -A_{13} & \frac{1}{2}I_{d\times d} - (I_{d\times d} - A_{11}) \\ \frac{1}{2}I_{d\times d} - (I_{d\times d} - A_{11})^T & A_{21} \end{pmatrix} \\ &= \begin{pmatrix} -A_{13} & A_{11} - \frac{1}{2}I_{d\times d} \\ A_{11}^T - \frac{1}{2}I_{d\times d} & A_{21} \end{pmatrix} \\ &= -B_\mathcal{A}. \end{aligned}$$

So, (iii) follows by (i) and (ii). $\square$

7.4 Metaplectic Gabor frames

Definition 7.23. Let $W_\mathcal{A}$ be a metaplectic Wigner distribution such that every $\pi_\mathcal{A}(z)$ extends to a bounded operator on $L^2(\mathbb{R}^d)$ ($z \in \mathbb{R}^{2d}$). Let $g \in L^2(\mathbb{R}^d)$ and $\Lambda \subset \mathbb{R}^{2d}$ be a discrete subset. We call the set

$$\mathcal{G}_\mathcal{A}(g, \Lambda) = \{\pi_\mathcal{A}(\lambda)g\}_{\lambda\in\Lambda}$$

a **metaplectic Gabor system**. We call **metaplectic Gabor frame** of $L^2(\mathbb{R}^d)$ any metaplectic Gabor system $\mathcal{G}_\mathcal{A}(g, \Lambda)$ such that the following property holds: there exist $A, B > 0$ such that

$$A\|f\|_2^2 \le \sum_{\lambda\in\Lambda} |W_\mathcal{A}(f, g)(\lambda)|^2 \le B\|f\|_2^2, \tag{7.19}$$

for all $f \in L^2(\mathbb{R}^d)$.

Remark 7.24. By Definition 7.1, (7.19) is equivalent to

$$A \left\| f \right\|_2^2 \leq \sum_{\lambda \in \Lambda} |\langle f, \pi_{\mathcal{A}}(\lambda) g \rangle|^2 \leq B \left\| f \right\|_2^2, \quad \forall f \in L^2(\mathbb{R}^d).$$

Stated differently, a metaplectic Gabor frame is a frame for $L^2(\mathbb{R}^d)$.

Example 7.25. In [36], M. de Gosson introduced $\hbar$-Gabor frames as follows. Consider $g \in L^2(\mathbb{R}^d)$ and Λ a discrete subset of $\mathbb{R}^{2d}$. Under the same notation of Example 7.4, a family $\mathcal{G}_{\hbar}(g, \Lambda) = \{\pi^{\hbar}(\lambda) g\}_{\lambda \in \Lambda}$ is a $\hbar$-**Gabor frame** if

$$A \left\| f \right\|_2^2 \leq \sum_{\lambda \in \Lambda} |\langle f, \pi^{\hbar}(\lambda) g \rangle|^2 \leq B \left\| f \right\|_2^2, \qquad \forall f \in L^2(\mathbb{R}^d),$$

for $A, B > 0$. The time-frequency representation $z \mapsto \langle f, \pi^{\hbar}(z) g \rangle$ is, up to the constant $(2\pi\hbar)^{-d/2}$ (which is necessary to obtain a metaplectic operator in Example 7.4), the metaplectic Wigner distribution $V^{\hbar}$, as defined in Example 7.4. Hence, metaplectic Gabor frames $\mathcal{G}_{\mathcal{A}_{\hbar}}$ and $\hbar$-Gabor frames are basically the same objects. Namely, $\mathcal{G}_{\hbar}(g, \Lambda)$ is a $\hbar$-Gabor frame with frame bounds A, B if and only if $\mathcal{G}_{\mathcal{A}_{\hbar}}(g, \Lambda)$ is a metaplectic Gabor frame with frame bounds $(2\pi\hbar)^{-d} A$ and $(2\pi\hbar)^{-d} B$.

Metaplectic Gabor frames associated to shift-invertible Wigner distributions are completely characterized by the following consequence of Corollary 7.16.

Theorem 7.26. *Let $W_{\mathcal{A}}$ be shift-invertible and $\widehat{\delta_{\mathcal{A}}}$ be the corresponding deformation operator (see Definition 7.17). Let $g \in L^2(\mathbb{R}^d)$ and $\Lambda \subseteq \mathbb{R}^{2d}$ be a discrete subset. The following statements are equivalent:*
(i) $\mathcal{G}_{\mathcal{A}}(g, \Lambda)$ is a metaplectic Gabor frame with bounds A, B;
(ii) $\mathcal{G}(\widehat{\delta_{\mathcal{A}}} g, E_{\mathcal{A}}^{-1} \Lambda)$ is a Gabor frame with bounds $|\det(E_{\mathcal{A}})| A, |\det(E_{\mathcal{A}})| B$;
(iii) $\mathcal{G}(g, -Q \mathcal{E}_{\mathcal{A}}^{-1} \Lambda)$ is a Gabor frame with bounds $|\det(E_{\mathcal{A}})| A, |\det(E_{\mathcal{A}})| B$.

Proof. Consider $f \in L^2(\mathbb{R}^d)$. We use the representation of $\pi_{\mathcal{A}}$ in (7.10):

$$\sum_{\lambda \in \Lambda} |\langle f, \pi_{\mathcal{A}}(\lambda) g \rangle|^2 = \sum_{\lambda \in \Lambda} |\langle f, |\det(E_{\mathcal{A}})|^{-1/2} \pi(E_{\mathcal{A}}^{-1} \lambda) \widehat{\delta_{\mathcal{A}}} g \rangle|^2$$

$$= |\det(E_{\mathcal{A}})|^{-1} \sum_{\mu \in E_{\mathcal{A}}^{-1} \Lambda} |\langle f, \pi(\mu) \widehat{\delta_{\mathcal{A}}} g \rangle|^2.$$

This proves the equivalence $(i) \Leftrightarrow (ii)$. Now, using (2.13), we can write

$$|\det(E_{\mathcal{A}})|^{-1} \sum_{\mu \in E_{\mathcal{A}}^{-1} \Lambda} |\langle f, \pi(\mu) \widehat{\delta_{\mathcal{A}}} g \rangle|^2 = |\det(E_{\mathcal{A}})|^{-1} \sum_{\mu \in E_{\mathcal{A}}^{-1} \Lambda} |\langle f, \widehat{\delta_{\mathcal{A}}} \pi(\delta_{\mathcal{A}}^{-1} \mu) g \rangle|^2$$

$$= |\det(E_{\mathcal{A}})|^{-1} \sum_{\mu \in E_{\mathcal{A}}^{-1} \Lambda} |\langle \widehat{\delta_{\mathcal{A}}}^{-1} f, \pi(\delta_{\mathcal{A}}^{-1} \mu) g \rangle|^2$$

$$= |\det(E_{\mathcal{A}})|^{-1} \sum_{\nu \in \delta_{\mathcal{A}}^{-1} E_{\mathcal{A}}^{-1} \Lambda} |\langle \widehat{\delta_{\mathcal{A}}}^{-1} f, \pi(\nu) g \rangle|^2.$$

Observing that $\delta_{\mathcal{A}}^{-1} E_{\mathcal{A}}^{-1} = -Q \mathcal{E}_{\mathcal{A}}^{-1}$,

$$| \det(E_{\mathcal{A}})|^{-1} \sum_{\mu \in E_{\mathcal{A}}^{-1} \Lambda} |\langle f, \pi(\mu) \widehat{\delta_{\mathcal{A}}} g \rangle|^2 = | \det(E_{\mathcal{A}})|^{-1} \sum_{\nu \in -Q \mathcal{E}_{\mathcal{A}}^{-1} \Lambda} |\langle \delta_{\mathcal{A}}^{-1} f, \pi(\nu) g \rangle|^2.$$

Therefore, $\mathcal{G}_{\mathcal{A}}(g, \Lambda)$ is a metaplectic Gabor frame with frame bounds A and B if and only if

$$A \|f\|_2^2 \leq | \det(E_{\mathcal{A}})|^{-1} \sum_{\mu \in -Q \mathcal{E}_{\mathcal{A}}^{-1} \Lambda} |\langle \delta_{\mathcal{A}}^{-1} f, \pi(\mu) g \rangle|^2 \leq B \|f\|_2^2, \qquad f \in L^2(\mathbb{R}^d).$$

(7.20)

Since $\widehat{\delta_{\mathcal{A}}}^{-1}$ is a unitary operator on $L^2(\mathbb{R}^d)$, it follows that (7.20) holds for all $f \in L^2(\mathbb{R}^d)$ if and only if

$$| \det(E_{\mathcal{A}})| A \|f\|_2^2 \leq \sum_{\mu \in -Q \mathcal{E}_{\mathcal{A}}^{-1} \Lambda} |\langle f, \pi(\mu) g \rangle|^2 \leq | \det(E_{\mathcal{A}})| B \|f\|_2^2$$

holds for every $f \in L^2(\mathbb{R}^d)$. This proves the equivalence $(i) \Leftrightarrow (iii)$. $\qquad \square$

Remark 7.27. For $\hbar$-Gabor frames, Example 7.25 shows that Theorem 7.26 applied to the metaplectic Wigner distributions of Example 7.4 recovers [36, Proposition 7].

We now introduce the metaplectic Gabor frame operator and related properties.

First, consider a lattice $\Lambda \subset \mathbb{R}^{2d}$ and a metaplectic Gabor frame $\mathcal{G}_{\mathcal{A}}(g, \Lambda) = \{\pi_{\mathcal{A}}(\lambda) g\}_{\lambda \in \Lambda}$ for $L^2(\mathbb{R}^d)$. We compute the expressions of coefficient, reconstruction and frame operators, see, e.g., [29, Definitions 3.1.8 and 3.1.13]. The coefficient (or analysis) operator $C_{\mathcal{A}} : L^2(\mathbb{R}^d) \to \ell^2(\Lambda)$ is given by

$$C_{\mathcal{A}} f = (\langle f, \pi_{\mathcal{A}}(\lambda) g \rangle)_{\lambda \in \Lambda} = (W_{\mathcal{A}}(f, g)(\lambda))_{\lambda \in \Lambda}, \quad f \in L^2(\mathbb{R}^d).$$

Its adjoint $D_{\mathcal{A}} = C_{\mathcal{A}}^* : \ell^2(\Lambda) \to L^2(\mathbb{R}^d)$ is called the reconstruction (or synthesis) operator: for any sequence $c = (c_\lambda)_{\lambda \in \Lambda} \in \ell^2(\Lambda)$,

$$D_{\mathcal{A}} c = \sum_{\lambda \in \Lambda} c_\lambda \pi_{\mathcal{A}}(\lambda) g.$$

The frame operator is defined as $S_{\mathcal{A}} = D_{\mathcal{A}} C_{\mathcal{A}} : L^2(\mathbb{R}^d) \to L^2(\mathbb{R}^d)$:

$$S_{\mathcal{A}} f = \sum_{\lambda \in \Lambda} \langle f, \pi_{\mathcal{A}}(\lambda) g \rangle \pi_{\mathcal{A}}(\lambda) g = \sum_{\lambda \in \Lambda} W_{\mathcal{A}}(f, g)(\lambda) \pi_{\mathcal{A}}(\lambda) g.$$

Let us compute $\pi_\mathcal{A}(\mu)^{-1}S_\mathcal{A}\pi_\mathcal{A}(\mu)$, for $\mu \in \Lambda$. We make use of the explicit expression of the inverse and the adjoint of the metaplectic atom (7.10) in (7.13), and (7.14), respectively. Observing that the phase factors cancel, we obtain

$$\pi_\mathcal{A}(\mu)^{-1}S_\mathcal{A}\pi_\mathcal{A}(\mu)f = \sum_{\lambda \in \Lambda}\langle\pi_\mathcal{A}(\mu)f, \pi_\mathcal{A}(\lambda)g\rangle\pi_\mathcal{A}(\mu)^{-1}\pi_\mathcal{A}(\lambda)g$$

$$= \sum_{\lambda \in \Lambda}\langle f, \pi_\mathcal{A}(\mu)^*\pi_\mathcal{A}(\lambda)g\rangle\pi_\mathcal{A}(\mu)^{-1}\pi_\mathcal{A}(\lambda)g$$

$$= |\det(E_\mathcal{A})|^{-1}\sum_{\lambda \in \Lambda}\langle f, \pi_\mathcal{A}(\mu)^{-1}\pi_\mathcal{A}(\lambda)g\rangle\pi_\mathcal{A}(\mu)^{-1}\pi_\mathcal{A}(\lambda)g$$

$$= |\det(E_\mathcal{A})|^{-1}\sum_{\lambda \in \Lambda}\langle f, \widehat{\delta_\mathcal{A}}^{-1}\pi(E_\mathcal{A}^{-1}\mu)^{-1}\pi(E_\mathcal{A}^{-1}\lambda)\widehat{\delta_\mathcal{A}}g\rangle$$

$$\times \widehat{\delta_\mathcal{A}}^{-1}\pi(E_\mathcal{A}^{-1}\mu)^{-1}\pi(E_\mathcal{A}^{-1}\lambda)\widehat{\delta_\mathcal{A}}g$$

$$= |\det(E_\mathcal{A})|^{-1}\sum_{\lambda \in \Lambda}\langle f, \widehat{\delta_\mathcal{A}}^{-1}\pi(E_\mathcal{A}^{-1}(\lambda-\mu))\widehat{\delta_\mathcal{A}}g\rangle\widehat{\delta_\mathcal{A}}^{-1}\pi(E_\mathcal{A}^{-1}(\lambda-\mu))\widehat{\delta_\mathcal{A}}g$$

$$= |\det(E_\mathcal{A})|^{-1}\sum_{\lambda \in \Lambda}\langle f, \widehat{\delta_\mathcal{A}}^{-1}\pi(E_\mathcal{A}^{-1}\lambda)\widehat{\delta_\mathcal{A}}g\rangle\widehat{\delta_\mathcal{A}}^{-1}\pi(E_\mathcal{A}^{-1}\lambda)\widehat{\delta_\mathcal{A}}g$$

$$= \sum_{\lambda \in \Lambda}\langle f, \widehat{\delta_\mathcal{A}}^{-1}\pi_\mathcal{A}(\lambda)g\rangle\widehat{\delta_\mathcal{A}}^{-1}\pi_\mathcal{A}(\lambda)g$$

$$= \sum_{\lambda \in \Lambda}\langle\widehat{\delta_\mathcal{A}}f, \pi_\mathcal{A}(\lambda)g\rangle\widehat{\delta_\mathcal{A}}^{-1}\pi_\mathcal{A}(\lambda)g$$

$$= \widehat{\delta_\mathcal{A}}^{-1}S_\mathcal{A}\widehat{\delta_\mathcal{A}}f,$$

since $\widehat{\delta_\mathcal{A}}^{-*} = \widehat{\delta_\mathcal{A}}$.

The equality

$$\pi_\mathcal{A}(\mu)^{-1}S_\mathcal{A} = \widehat{\delta_\mathcal{A}}^{-1}S_\mathcal{A}\widehat{\delta_\mathcal{A}}\pi_\mathcal{A}(\mu)^{-1}$$

yields

$$S_\mathcal{A}^{-1}\pi_\mathcal{A}(\mu) = \pi_\mathcal{A}(\mu)\widehat{\delta_\mathcal{A}}^{-1}S_\mathcal{A}^{-1}\widehat{\delta_\mathcal{A}}.$$

Hence the canonical dual frame of $\mathcal{G}_\mathcal{A}(g, \Lambda)$ is still a metaplectic Gabor frame

$$\mathcal{G}_\mathcal{A}(\gamma_\mathcal{A}, \Lambda) = \{\pi_\mathcal{A}(\lambda)\gamma_\mathcal{A}\}_{\lambda \in \Lambda}$$

with canonical dual window

$$\gamma_\mathcal{A} = \widehat{\delta_\mathcal{A}}^{-1}S_\mathcal{A}^{-1}\widehat{\delta_\mathcal{A}}g. \tag{7.21}$$

Consequently, if $\mathcal{G}_\mathcal{A}(g, \Lambda)$ is a frame with bounds $0 < A \le B$, then every

$f \in L^2(\mathbb{R}^d)$ possesses the expansions

$$f = \sum_{\lambda \in \Lambda} \langle f, \pi_{\mathcal{A}}(\lambda)g \rangle \pi_{\mathcal{A}}(\lambda)\gamma_{\mathcal{A}} \tag{7.22}$$

$$= \sum_{\lambda \in \Lambda} \langle f, \pi_{\mathcal{A}}(\lambda)\gamma_{\mathcal{A}} \rangle \pi_{\mathcal{A}}(\lambda)g \tag{7.23}$$

with unconditional convergence in $L^2(\mathbb{R}^d)$. Besides, we have the norm equivalences

$$A\|f\|_2^2 \leq \sum_{\lambda \in \Lambda} |\langle f, \pi_{\mathcal{A}}(\lambda)g \rangle|^2 \leq B\|f\|^2$$

$$B^{-1}\|f\|^2 \leq \sum_{\lambda \in \Lambda} |\langle f, \pi_{\mathcal{A}}(\lambda)\gamma_{\mathcal{A}} \rangle|^2 \leq A^{-1}\|f\|_2^2.$$

7.5 Characterization of Time-frequency spaces

A direct application of the theory developed so far is the whole characterization of modulation spaces. Namely, the issue below generalizes Theorem 1.1 in [19] to the quasi-Banach space setting, extending the indices $p, q \in [1, \infty]$ to $0 < p, q \leq \infty$. Whenever $p \neq q$ we need the assumption $E_{\mathcal{A}}$ upper-triangular, that is, the 2×1 block of $E_{\mathcal{A}}$ in (2.21) satisfies $A_{21} = 0_{d \times d}$. This requirement is needed for the use of Theorem 6.15.

Theorem 7.28. *Fix a non-zero window function $g \in \mathcal{S}(\mathbb{R}^d)$. Consider $0 < p, q \leq \infty$, $W_{\mathcal{A}}$ shift-invertible and a weight $m \in \mathcal{M}_v(\mathbb{R}^{2d})$ with $m \asymp m \circ E_{\mathcal{A}}^{-1}$. Then*
(i) For $0 < p \leq \infty$ and we have

$$f \in M_m^p(\mathbb{R}^d) \qquad \Leftrightarrow \qquad W_{\mathcal{A}}(f, g) \in L_m^p(\mathbb{R}^{2d}),$$

with equivalence of norms.
(ii) If we add the assumption that $E_{\mathcal{A}}$ is upper-triangular, then

$$f \in M_m^{p,q}(\mathbb{R}^d) \qquad \Leftrightarrow \qquad W_{\mathcal{A}}(f, g) \in L_m^{p,q}(\mathbb{R}^{2d}),$$

with equivalence of norms.

Proof. Take $f \in M_m^{p,q}(\mathbb{R}^d)$. From the equality (7.8) we infer

$$|W_{\mathcal{A}}(f, g)|(z) = |\mathfrak{T}_{E_{\mathcal{A}}^{-1}} \Phi_{M_{\mathcal{A}}+L} V_{\widehat{\delta_{\mathcal{A}}g}} f|(z) = |\mathfrak{T}_{E_{\mathcal{A}}^{-1}} V_{\widehat{\delta_{\mathcal{A}}g}} f|(z)$$

$$= |\det(E_{\mathcal{A}})|^{-1/2} |V_{\widehat{\delta_{\mathcal{A}}g}} f|(E_{\mathcal{A}}^{-1}z).$$

Since $\widehat{\delta_{\mathcal{A}}} : \mathcal{S}(\mathbb{R}^d) \to \mathcal{S}(\mathbb{R}^d)$, we can choose the window $\widehat{\delta_{\mathcal{A}}g} \in \mathcal{S}(\mathbb{R}^d)$ to compute the modulation space norm so that

$$\|W_{\mathcal{A}}(f, g)\|_{L_m^{p,q}} \asymp \|V_{\widehat{\delta_{\mathcal{A}}g}} f(E_{\mathcal{A}}^{-1}\cdot)\|_{L_m^{p,q}}.$$

The conclusion follows from Theorem 6.15. □

In what follows we generalize [19, Corollary 3.12] to the quasi-Banach space setting $0 < p, q \leq \infty$.

Theorem 7.29. *Fix a non-zero window function* $g \in \mathcal{S}(\mathbb{R}^d)$. *Consider* $0 < p, q \leq \infty$, $W_{\mathcal{A}}$ *shift-invertible and* $m_1, m_2 \in \mathcal{M}_v(\mathbb{R}^d)$ *such that* $m_2 \asymp \mathcal{I}m_2$, *with* $\mathcal{I}m_2(x) = m_2(-x)$. *Fix* $g \in \mathcal{S}(\mathbb{R}^d) \setminus \{0\}$ *and define*

$$\tilde{E}_{\mathcal{A}} = JE_{\mathcal{A}}J,$$

with the symplectic matrix J *defined in (2.9). (Observe that* $E_{\mathcal{A}}^{-1}$ *is lower triangular if and only if* $\tilde{E}_{\mathcal{A}}$ *is upper triangular). If* $m_1 \otimes m_2 \asymp (m_1 \otimes m_2) \circ \tilde{E}_{\mathcal{A}}^{-1}$ *and* $E_{\mathcal{A}}$ *is lower triangular, then*

$$\|f\|_{W(\mathcal{F}L^p_{m_1}, L^q_{m_2})} \asymp \left(\int_{\mathbb{R}^d} \left(\int_{\mathbb{R}^d} |W_{\mathcal{A}}(f,g)(x,\xi)|^p m_1(\xi)^p d\xi \right)^{q/p} m_2(x)^q dx \right)^{1/q},$$

with the analogous for $\max\{p, q\} = \infty$.

Proof. As in the proof of Corollary 3.12 in [19], assuming $m_2(-x) = m_2(x)$, we can write

$$\left(\int_{\mathbb{R}^d} \left(\int_{\mathbb{R}^d} |W_{\mathcal{A}}(f,g)(x,\xi)|^p m_1(\xi)^p d\xi \right)^{q/p} m_2(x)^q dx \right)^{1/q} \asymp \left\| W_{\tilde{\mathcal{A}}_0}(\hat{f}, \hat{g}) \right\|_{L^{p,q}_{m_1 \otimes m_2}},$$

$$\tilde{\mathcal{A}}_0 = \begin{pmatrix} -A_{23} & A_{24} & A_{21} & -A_{22} \\ A_{13} & -A_{14} & -A_{11} & A_{12} \\ -A_{43} & A_{44} & A_{41} & -A_{42} \\ A_{33} & -A_{34} & -A_{31} & A_{32} \end{pmatrix},$$

so that $\tilde{E}_{\mathcal{A}} = E_{\tilde{\mathcal{A}}_0}$. The conclusion is due to Theorem 7.28 $\qquad \square$

If $p = q$ the additional assumption $E_{\mathcal{A}}^{-1}$ lower triangular is not needed. Observe that in this case $\|f\|_{W(\mathcal{F}L^p_{m_1}, L^p_{m_2})} \asymp \|f\|_{M^p_{m_2 \otimes m_1}}$, and the norm equivalence follows from Theorem 7.28 above. In fact, notice that

$$(m_1 \otimes m_2) \circ E_{\mathcal{A}}^{-1} \asymp (\mathcal{I}m_2 \otimes m_1) \otimes \tilde{E}_{\mathcal{A}}^{-1}.$$

Consider a metaplectic Gabor frame $\mathcal{G}_{\mathcal{A}}(g, \Lambda)$ and assume

$$m \asymp m \circ E_{\mathcal{A}}^{-1}, \tag{7.24}$$

then, for any $f \in M^{p;q}_m(\mathbb{R}^d)$ we can use (7.10) to express the coefficient operator's entries

$$|C_{\mathcal{A}}f(\lambda)| = |\langle f, \pi_{\mathcal{A}}(\lambda)g \rangle| = |\det(E_{\mathcal{A}})|^{-1/2}|\langle f, \pi(E_{\mathcal{A}}^{-1}\lambda)\widehat{\delta_{\mathcal{A}}g} \rangle|.$$

Observe that $\widehat{\delta_{\mathcal{A}}}g \in \mathcal{S}(\mathbb{R}^d)$ for $g \in \mathcal{S}(\mathbb{R}^d)$, by Theorem 7.26 (ii); further-more, $\mathcal{G}(\widehat{\delta_{\mathcal{A}}}g, E_{\mathcal{A}}^{-1}\Lambda)$ is a Gabor frame with coefficient operator C satisfying $\|Cf\|_{\ell_m^{p,q}(E_{\mathcal{A}}^{-1}\Lambda)} \lesssim \|f\|_{M_m^{p,q}}$, so that the equivalence of weights in (7.24) gives

$$\|C_{\mathcal{A}}f\|_{\ell_m^{p,q}(\Lambda)} = |\det(E_{\mathcal{A}})|^{-1/2}\|Cf\|_{\ell_m^{p,q}(E_{\mathcal{A}}^{-1}\Lambda)} \lesssim \|f\|_{M_m^{p,q}},$$

that is the boundedness of $C_{\mathcal{A}} : M_m^{p,q}(\mathbb{R}^d) \to \ell_m^{p,q}(\Lambda)$.

Using the relation between $\pi_{\mathcal{A}}(\lambda)$ and the time-frequency shift $\pi(E_{\mathcal{A}}^{-1}\lambda)$ displayed in (7.10), and the equivalence of weights in (7.24), for any sequence $c_\lambda \in \ell_m^{p,q}(\Lambda)$, the sequence $\widetilde{c}_\mu := c_{E_{\mathcal{A}}\mu}\Phi_{M_{\mathcal{A}}+L}(\mu) \in \ell_m^{p,q}(E_{\mathcal{A}}^{-1}\Lambda)$ so that

$$\|D_{\mathcal{A}}c_\lambda\|_{M_m^{p,q}(\mathbb{R}^d)} = \left\|\sum_{\lambda\in\Lambda} c_\lambda \pi_{\mathcal{A}}(\lambda)g\right\|_{M_m^{p,q}(\mathbb{R}^d)} \asymp \left\|\sum_{\mu\in E_{\mathcal{A}}^{-1}\Lambda} \widetilde{c}_\mu \pi(E_{\mathcal{A}}^{-1}\lambda)\widehat{\delta_{\mathcal{A}}}g\right\|_{M_m^{p,q}(\mathbb{R}^d)}$$

$$\lesssim \|(\widetilde{c}_\mu)\|_{\ell_m^{p,q}(E_{\mathcal{A}}^{-1}\Lambda)} \asymp \|(c_\lambda)\|_{\ell_m^{p,q}(\Lambda)}.$$

For the Banach space case $p,q \in [1,+\infty]$, the window class can be extended from $\mathcal{S}(\mathbb{R}^d)$ to $M_v^1(\mathbb{R}^d)$. In fact, under the assumption (7.24), the metaplectic operator $\widehat{\delta_{\mathcal{A}}}$ and its inverse are bounded on $M_v^1(\mathbb{R}^d)$, cf. [53, Theorem 4.6]. Hence, $g \in M_v^1(\mathbb{R}^d) \iff \widehat{\delta_{\mathcal{A}}}g \in M_v^1(\mathbb{R}^d)$. Arguing as for the Schwartz class and using the results for Gabor frames [65, Chapter 12] we infer that the coefficient operator $C_{\mathcal{A}}$ is bounded from $M_m^{p,q}(\mathbb{R}^d)$ to $\ell_m^{p,q}(\Lambda)$ and the other way round for the reconstruction operator $D_{\mathcal{A}}$.

The observations above, together with the characterization of modulation spaces via Gabor frames (see, e.g., [29, Theorem 3.2.37] and [54]) yield an equivalent discrete norm for modulation spaces in terms of metaplectic Gabor frames. Namely,

Theorem 7.30. *Consider $\mathcal{G}_{\mathcal{A}}(g, \Lambda)$ a metaplectic Gabor frame for $L^2(\mathbb{R}^d)$ with bounds $0 < A \leq B$, with $g \in \mathcal{S}(\mathbb{R}^d)$ and canonical dual window $\gamma_{\mathcal{A}}$ in (7.21). Assume $W_{\mathcal{A}}$ shift-invertible and $m \in \mathcal{M}_v(\mathbb{R}^{2d})$, with $m \asymp m \circ E_{\mathcal{A}}^{-1}$. Then,*
(i) For every $0 < p,q \leq \infty$, $C_{\mathcal{A}} : M_m^{p,q}(\mathbb{R}^d) \to \ell_m^{p,q}(\Lambda)$ and $D_{\mathcal{A}} : \ell_m^{p,q}(\Lambda) \to M_m^{p,q}(\mathbb{R}^d)$ continuously. If $f \in M_m^{p,q}(\mathbb{R}^d)$, then the expansions in (7.22) converge unconditionally in $M_m^{p,q}$ for $0 < p,q < \infty$, and weak*-$M_{1/v}^\infty$ unconditionally if $p = \infty$ or $q = \infty$.
(ii) The following (quasi-)norms are equivalent on $M_m^{p,q}(\mathbb{R}^d)$

$$A\|f\|_{M_m^{p,q}(\mathbb{R}^d)} \leq \|(\langle f, \pi_{\mathcal{A}}(\lambda)g\rangle)_{\lambda\in\Lambda}\|_{\ell_m^{p,q}(\Lambda)} \leq B\|f\|_{M_m^{p,q}(\mathbb{R}^d)},$$

$$B^{-1}\|f\|_{M_m^{p,q}(\mathbb{R}^d)} \leq \|(\langle f, \pi_{\mathcal{A}}(\lambda)\gamma_{\mathcal{A}}\rangle)_{\lambda\in\Lambda}\|_{\ell_m^{p,q}(\Lambda)} \leq A^{-1}\|f\|_{M_m^{p,q}(\mathbb{R}^d)}.$$

Remark 7.31. Assume $g, \gamma \in M_v^1(\mathbb{R}^d)$ with v satisfying (7.24) and such that

$$S_{\mathcal{A},g,\gamma} = D_{\mathcal{A},\gamma}C_{\mathcal{A},g} = I, \quad \text{on} \quad L^2(\mathbb{R}^d).$$

For $p,q \in [1,\infty]$, the statements of the previous theorem hold in the larger window class $M_v^1(\mathbb{R}^d)$, with the canonical dual window $\gamma_{\mathcal{A}}$ replaced by γ.

7.6   Appendix C

In [31], the authors proved the following result, cf. [31, Proposition 2.6]:

Proposition 7.32. Let $\hat{\mathcal{A}} \in \mathrm{Mp}(2d, \mathbb{R})$ and $W_{\mathcal{A}}$ be the corresponding metaplectic Wigner distribution. Then, there exists $\widehat{\mathcal{A}_*} \in \mathrm{Mp}(2d, \mathbb{R})$ such that for all $f, g \in L^2(\mathbb{R}^d)$,

$$W_{\mathcal{A}}(g, f) = \overline{W_{\mathcal{A}_*}(f, g)} \tag{7.25}$$

up to a sign.

In what follows we shall improve Proposition 7.32, carrying over the explicit expression of the projection $\mathcal{A}_*$ in (7.25). First, we need to compute the intertwining relation between complex conjugation and metaplectic operators.

Proposition 7.33. Let $\hat{S} \in \mathrm{Mp}(d, \mathbb{R})$ be a metaplectic operator and $S = \pi^{Mp}(\hat{S})$ have block decomposition (7.3). Define

$$\bar{S} := \begin{pmatrix} A & -B \\ -C & D \end{pmatrix}.$$

Then, for all $f \in L^2(\mathbb{R}^d)$,

$$\hat{S}\bar{f} = \overline{\hat{\bar{S}}f}.$$

Proof. Let T the operator defined by

$$Tf = \overline{\hat{S}\bar{f}}, \quad f \in L^2(\mathbb{R}^d).$$

Since $\hat{S}$ is a unitary operator on $L^2(\mathbb{R}^d)$, T is a unitary operator on $L^2(\mathbb{R}^d)$. We have to prove that T satisfies the intertwining relation in (2.13) for $\mathcal{A} = \bar{S}$. For, let $z = (x, \xi) \in \mathbb{R}^{2d}$ and take $\tau \in \mathbb{R}$. Then,

$$
\begin{aligned}
T\rho(z; \tau)f &= \overline{\hat{S}\overline{\rho(z; \tau)f}} \\
&= \overline{\hat{S}\rho(x, -\xi; -\tau)\bar{f}} \\
&= \overline{\rho(S(x, -\xi); -\tau)\hat{S}\bar{f}} \\
&= \overline{e^{-2\pi i \tau} e^{-i\pi(Ax - B\xi)\cdot(Cx - D\xi)}\pi(Ax - B\xi, Cx - D\xi)\hat{S}\bar{f}} \\
&= e^{2\pi i \tau} e^{-i\pi(Ax - B\xi)\cdot(-Cx + D\xi)}\pi(Ax - B\xi, -Cx + D\xi)\overline{\hat{S}\bar{f}} \\
&= \rho(\bar{S}(x, \xi); \tau)Tf,
\end{aligned}
$$

as desired.   □

Corollary 7.34. *Under the assumptions of Proposition 7.32, we have*

$$\mathcal{A}_* = \overline{\mathcal{A}}\mathcal{D}_L$$

with the matrix L defined in (2.25). Namely, if $\mathcal{A}$ has block decomposition (2.20),
$\mathcal{A}_*$ *is given by*

$$\mathcal{A}_* = \begin{pmatrix} A_{12} & A_{11} & -A_{14} & -A_{13} \\ A_{22} & A_{21} & -A_{24} & -A_{23} \\ -A_{32} & -A_{31} & A_{34} & A_{33} \\ -A_{42} & -A_{41} & A_{44} & A_{43} \end{pmatrix}. \tag{7.26}$$

Proof. Observe that $\widehat{\mathcal{D}_L}F(x,y) = F(y,x)$, so that, for every $f, g \in L^2(\mathbb{R}^d)$,

$$g \otimes f(x,y) = f(y)g(x) = f \otimes g(y,x) = f \otimes g(\mathcal{D}_L(x,y)) = \widehat{\mathcal{D}_L}(f \otimes g)(x,y).$$

By Proposition 7.33, it follows that, up to a sign,

$$W_{\mathcal{A}}(f,g) = \hat{\mathcal{A}}(f \otimes \bar{g}) = \hat{\mathcal{A}}(\overline{\bar{f} \otimes g}) = \overline{\hat{\bar{\mathcal{A}}}(\bar{f} \otimes g)} = \overline{\widehat{\bar{\mathcal{A}}\mathcal{D}_L}(g \otimes \bar{f})} = \overline{W_{\mathcal{A}_*}(g,f)}.$$

Assuming that $\mathcal{A}$ exhibits the block decomposition (2.20), a straightforward computation yields (7.26). This concludes the proof. ☐

Remark 7.35. A straightforward computation shows that $\overline{S}^T = \overline{S^T}$. In fact, if S has block decomposition (7.3),

$$\overline{S}^T = \begin{pmatrix} A^T & -C^T \\ -B^T & D^T \end{pmatrix},$$

whereas

$$S^T = \begin{pmatrix} A^T & C^T \\ B^T & D^T \end{pmatrix}, \quad \text{so that} \quad \overline{S^T} = \begin{pmatrix} A^T & -C^T \\ -B^T & D^T \end{pmatrix} = \overline{S}^T.$$

Conclusions and future directions

8.1 Tuning parameters selection

We discussed the selection of tuning parameters for weighted and generalized LASSO problems in Chapters 3 and 4.

8.1.1 The weighted LASSO

In Chapter 3 we studied the equivalent of Lagrange multipliers for minimization problems with inequality constrains in the framework of weighted LASSO:

$$\text{minimize } \|Ax - b\|_2^2 + \sum_{j=1}^{n} \lambda_j |x_j|, \text{ for } x \in \mathbb{R}^n.$$

The relation between $\lambda_1, \ldots, \lambda_n$ and the constraints of the corresponding constrained problem

$$\text{minimize } \|Ax - b\|_2^2 \text{ subject to } |x_j| \le \tau_j, \, j = 1, \ldots, n$$

is computed in the following settings:

- $A^T A$ diagonal,

- the derivatives of $\|Ax - b\|_2^2$ have constant sign in $\prod_{j=1}^{n} [-\tau_j, \tau_j]$,

with the purpose of getting insights about the relation $\lambda = \lambda(\tau)$ in this particular scenario, where $\lambda = (\lambda_1, \ldots, \lambda_n)$ and $\tau = (\tau_1, \ldots, \tau_n)$.

As long as $A^T A$ is not a diagonal matrix, the geometries of the sets $\mathcal{G}$ and $\mathcal{A}$ of the points satisfying (3.22) and (3.23) respectively, become more involved, along with the possible casuistry. However, the general case in which $A^T A$ is not diagonal would be of great importance in applications. Indeed, as long as the approximate Lagrange multipliers are proved to act as effective tuning parameters, the behavior of approximate Lagrange multipliers for the weighted LASSO

problem (3.4) in terms of voxel-wise estimates would provide a way to control the tuning parameters via estimates of the τ_j.

Another open problem is whether it is possible to apply the same procedure to compute the Lagrange multipliers for (1.13). Clearly, the corresponding sets $\mathcal{G}$ and $\mathcal{A}$ lie in $\mathbb{R}^2$ so that the function describing the boundary of $\mathcal{A}$, that we called g, maps $\mathbb{R}$ to itself. Despite this simplifying fact, the set $\mathcal{G}$ is characterized by:

$$\begin{cases} u = s(x)^T x - \tau, \\ t = \|Ax - b\|_2^2 \end{cases} \qquad \text{for some } x \in \mathbb{R}^n,$$

where $s(x) \in \mathbb{R}^n$ is a vector such that $\operatorname{diag}(s(x)_j) \in \operatorname{sgn}(x)$ and, in this case, u and x belong to different spaces and a closed form for $t = t(u)$ is even more difficult to provide.

Finally, we stress that it would be important to generalize (3.17) up to consider different inner products on $\mathbb{R}^n$. Namely, this is the situation that occurs in MRI when the undersampling pattern is non-Cartesian. Problem (3.4) in this case becomes:

$$\min_x \|Ax - b\|_W^2 + \sum_j \lambda_j |x_j|,$$

where

$$\|x\|_W = x^T W^T W x \qquad (x \in \mathbb{R}^n),$$

for a definite positive diagonal matrix W. Since this topic falls beyond the purpose of this work, we limit ourselves to mention the very mathematical reason why the weighted norm shall definitely replace the Euclidean norm over $\mathbb{R}^n$ when sampling is not performed on a cartesian grid. Indeed, non-Cartesian sampling patterns require appropriate discretizations of the Fourier transform integral. Roughly speaking,

$$\hat{f}(\xi) \approx \sum_j f(x_j) e^{-2\pi i \xi \cdot x_j} \Delta x_j = \langle f, e^{2\pi i \xi \cdot} \rangle_W,$$

where Δx_j is the Lebesgue measure of an adequate neighborhood of x_j, weighting the contribution of the sample x_j, and W is the diagonal matrix whose entries are $\sqrt{\Delta x_j}$. The inversion formula of the Fourier transform shall be modified accordingly. For instance, if the sampling follows a radial/spiral trajectory, Δx_j shall be bigger the further x_j is from the origin, since this value serves as an avarage of f on a portion of sphere that is larger as x_j is far from the origin.

8.1.2 ALMA for tuning and reconstruction

In Chapter 4, we achieved our three main objectives:

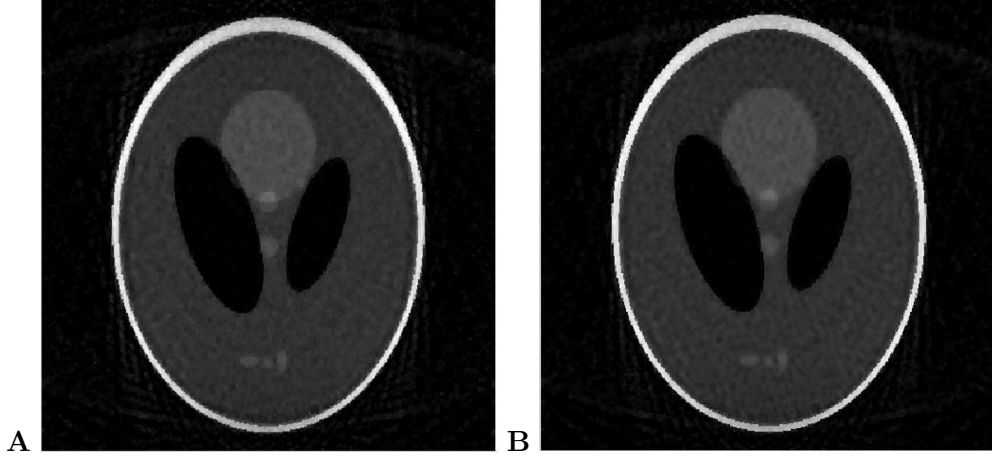- We defined an iterative procedure to approximate Lagrange multipliers.

Figure 8.1: Reconstructions of the Shepp-Logan brain phantom under radial sampling, with $NL_\% = 15/100$ and $UR_\% = 15\%$. The reconstruction obtained with the ALM is displayed on the left. The reconstruction obtained with the parameter that maximizes the mSSIM is displayed on the right. Observe that the two images are almost indistinguishable.

- We demonstrated the efficiency of ALM as tuning parameters for TV-weighted g-LASSO in the context of MRI.

- We assessed the quality of the reconstructions using image quality metrics, including mSSIM, pSNR, and CJV.

Our results show that ALMA performs almost optimally across varying levels of noise and undersampling, consistently yielding high-quality reconstructions in terms of image quality metrics. This iterative algorithm offers significant advantages by actively computing the tuning parameter during reconstruction, which enhances computational efficiency and ease of implementation.

The strength of ALMA, however, does not limit to TV based LASSO denoising, or to Cartesian undersampling. For example, we repeated our experimental framework in extreme conditions ($NL_\% = 15/100$ and $UR_\% = 15\%$), but with radial sampling. The quality of the reconstruction is undoubtedly comparable to the best reconstruction in terms of mSSIM, as displayed in fig. 8.1.

Therefore, while our focus was on TV-LASSO, the principles underlying ALMA can be adapted to other models, paving the way for broader applications. For practical MRI applications, however, accurate estimates of the norm of the noise remain a fundamental challenge for the implementation of ALMA. Indeed, to apply ALMA concretely to MRI, an efficient way to estimate the parameter η, estimating $\left\| Ax^{\#} - b \right\|_2$ from above, where $x^{\#}$ is the reconstruction and b is the sampled data, has to be found. Moreover, it is still unclear whether a small perturbations of η correspond to small variations of the estimated ALM.

8.2 Metaplectic Wigner distributions

We proved that shift-invertibility is really the key property that metaplectic Wigner distributions must satisfy to characterize modulation spaces quasi-norms. Nevertheless, the research on metaplectic Wigner distributions does not limit to the results detailed in the previous chapters. The question of whether

$$M_m^{p,q}(\mathbb{R}^d) = \{f \in \mathcal{S}'(\mathbb{R}^d) : \|W_{\mathcal{A}}(f,g)\|_{L_m^{p,q}} < \infty\}$$

for some $W_{\mathcal{A}}$ not shift-invertible, was not approached in this thesis. Nevertheless, this was proved in [58]. To be precise, we proved that for every $0 < p \leq \infty$ and for every $W_{\mathcal{A}}$ not shift-invertible,

$$M^p(\mathbb{R}^d) \neq \{f \in \mathcal{S}'(\mathbb{R}^d) : \|W_{\mathcal{A}}(f,g)\|_{L^p} < \infty\}.$$

Consequently, a metaplectic Wigner distribution $W_{\mathcal{A}}$ defines the quasi-norms of (all) modulation spaces if and only if $W_{\mathcal{A}}$ is shift-invertible, in addition to further compatibility conditions on the submatrix $E_{\mathcal{A}}$ of the projection $\mathcal{A}$ with respect to the weight m. As far as other properties of metaplectic Wigner distributions are concerned, it is easy to verify (sneak peek) that $W_{\mathcal{A}}f$ is a real-valued function if and only if $W_{\mathcal{A}}$ is a rescaled (classical) Wigner distribution. In [22], the metaplectic Wigner distributions $W_{\mathcal{A}}$ having the property that

$$W_{\mathcal{A}}(f,g) = V_{\varphi}f\overline{V_{\psi}g}, \qquad f,g \in \mathcal{S}(\mathbb{R}^d),$$

for some $\varphi, \psi \in \mathcal{S}'(\mathbb{R}^d)$, are characterized. Time-frequency representations of this form are called *generalized spectrograms*. Let us mention that to expand the class of metaplectic generalized spectrograms, so that it encompasses Gaussians, metaplectic Wigner distributions with complex symplectic projection are needed. Indeed, the chirp $e^{i\pi Ct \cdot t}$, C symmetric and $t \in \mathbb{R}^d$, becomes a Gaussian when $C = iI_{d \times d}$.

After studying metaplectic Wigner distributions, along with Cordero, Rodino, Pucci and Valenzano, we introduced Wigner analysis of operators. This analysis was briefly introduced at the end of Chapter 5 and roughly speaking, it is about providing an implicit way of representing globally Fourier integral operators (FIO), with suitable phases, avoiding the so-called caustics. Wigner analysis and metaplectic Wigner distributions are not separate: let us mention that the approach of metaplectic Wigner distributions allowed to prove the following result in [21]:

$$k_T \in M_m^p(\mathbb{R}^{2d}) \qquad \Longleftrightarrow \qquad k_W \in M_m^p(\mathbb{R}^{4d}),$$

when either $m = 1 \otimes v_s$ or $m = v_s$ ($s \geq 0$, $v_s = (1 + |\cdot|^2)^{s/2}$), for every $0 < p \leq \infty$, where K_T is the Schwartz kernel of a linear operator T, and k_W is its Wigner kernel. To conclude, an open project with prof. Cordero and Rodino consists of studying wavefront sets and Wigner kernels corresponding to metaplectic Wigner distributions, other than the classical τ-Wigner distributions and the STFT. In short, Wigner analysis of operators by means of metaplectic Wigner distributions.

8.3 Conclusions

Despite being widely studied and seemingly well understood, tuning parameters remain a challenging issue in practical applications. Numerous studies address their approximation, yet their use in MRI frameworks remains limited. More recently, machine learning approaches have been adopted to bypass traditional parameter estimation methods. However, in medical imaging, the lack of available data often limits the use of such learning algorithms. Compressed sensing, which does not rely on extensive datasets, and LASSO problems are still widely used for MRI reconstructions. Our work provides a solid foundation for further research aimed at improving parameter estimation and advancing MRI reconstruction techniques.

On the other hand, time-frequency analysis offers valuable tools to examine local frequencies in signals that evolve over time, though its potential is still poorly explored in the context of medical imaging. MRI of moving organs, such as the heart and eyes, requires techniques to segment data in the k-space according to motion phases, enabling the capture of clear images or footage. Current methods rely heavily on specialized hardware during scans to track motion. In principle, time-frequency analysis could automate the identification of motion phases by selecting appropriate time-frequency representations. Representations such as fractional Fourier transforms, Wigner distributions, and the ambiguity function, as well as metaplectic generalized spectrograms, hold significant potential for application in MRI of moving organs.

Looking forward, time-frequency analysis on graphs, which is currently being developed in collaboration with Professors Bulai, Cordero, and Saliani, may further advance this field. While there is still much work to be done, this approach could play a key role in realizing the full potential of MRI, setting us on a promising path in the search for its *Holy Grail*.

Acknowledgements

Bibliography

[1] B. Adcock and A. C. Hansen. *Compressive imaging: structure, sampling, learning.* Cambridge University Press, 2021.

[2] K. Asada and D. Fujiwara. On some oscillatory integral transformations in $L^2(\mathbb{R}^n)$. *Japanese Journal of Mathematics. New series*, 4(2):299–361, 1978.

[3] R.-F. Bai, B.-Z. Li, and Q.-Y. Cheng. Wigner-Ville distribution associated with the linear canonical transform. *Journal of Applied Mathematics*, 2012(1):740161, 2012.

[4] F. Bastianoni and E. Cordero. Characterization of smooth symbol classes by Gabor matrix decay. *Journal of Fourier Analysis and Applications*, 28:1–20, 2021.

[5] A. Bényi and K. A. Okoudjou. *Modulation Spaces: With Applications to Pseudodifferential Operators and Nonlinear Schrödinger Equations.* Springer-Verlag New York, 2021.

[6] A. M. Bianchi, L. T. Mainardi, and S. Cerutti. Time-frequency analysis of biomedical signals. *Transactions of the Institute of Measurement and Control*, 22(3):215–230, 2000.

[7] F. Bloch, W. W. Hansen, and M. E. Packard. Nuclear induction. *Phys Rev*, 70:127, 1946.

[8] B. Boashash. *Time-frequency signal analysis and processing: a comprehensive reference.* Academic press, 2015.

[9] J. Bobin, J.-L. Starck, and R. Ottensamer. Compressed sensing in astronomy. *IEEE Journal of Selected Topics in Signal Processing*, 2(5):718–726, 2008.

[10] A. Bora, A. Jalal, E. Price, and A. G. Dimakis. Compressed sensing using generative models. In *International conference on machine learning*, pages 537–546. PMLR, 2017.

[11] S. P. Boyd and L. Vandenberghe. *Convex optimization.* Cambridge university press, 2004.

[12] L. Braunstorfer, J. Romanowicz, A. J. Powell, J. Pattee, L. P. Browne, R. J. van der Geest, and M. H. Moghari. Non-contrast free-breathing whole-heart 3d cine cardiovascular magnetic resonance with a novel 3d radial leaf trajectory. *Magnetic resonance imaging*, 94:64–72, 2022.

[13] I. M. Bulai and S. Saliani. Spectral graph wavelet packets frames. *Applied and Computational Harmonic Analysis*, 66:18–45, 2023.

[14] E. Carypis and P. Wahlberg. Propagation of exponential phase space singularities for Schrödinger equations with quadratic Hamiltonians. *Journal of Fourier Analysis and Applications*, 23:530–571, 2017.

[15] J. W. Choi, B. Shim, Y. Ding, B. Rao, and D. I. Kim. Compressed sensing for wireless communications: Useful tips and tricks. *IEEE Communications Surveys & Tutorials*, 19(3):1527–1550, 2017.

[16] L. Cohen. Generalized phase-space distribution functions. *Journal of Mathematical Physics*, 7(5):781–786, 1966.

[17] L. Cohen. *Time-frequency analysis*, volume 778. Prentice Hall PTR New Jersey, 1995.

[18] E. Cordero and G. Giacchi. Quasi-Banach algebras and Wiener properties for pseudodifferential and generalized metaplectic operators. *Journal of Pseudo-Differential Operators and Applications*, 14(1):9, 2023.

[19] E. Cordero and G. Giacchi. Symplectic analysis of time-frequency spaces. *Journal de Mathématiques Pures et Appliquées*, 177:154–177, 2023.

[20] E. Cordero and G. Giacchi. Metaplectic Gabor frames and symplectic analysis of time-frequency spaces. *Applied and Computational Harmonic Analysis*, 68:101594, 2024.

[21] E. Cordero, G. Giacchi, and E. Pucci. Understanding of linear operators through Wigner analysis. *Journal of Mathematical Analysis and Applications*, 543(1):128955, 2025.

[22] E. Cordero, G. Giacchi, and L. Rodino. A unified approach to time-frequency representations and generalized spectrogram. *arXiv preprint arXiv:2401.03882*, 2024.

[23] E. Cordero, G. Giacchi, and L. Rodino. Wigner analysis of operators. part ii: Schrödinger equations. *Communications in Mathematical Physics*, 405(7):156, 2024.

[24] E. Cordero, K. Gröchenig, F. Nicola, and L. Rodino. Wiener algebras of fourier integral operators. *Journal de mathématiques pures et appliquées*, 99(2):219–233, 2013.

[25] E. Cordero, K. Gröchenig, F. Nicola, and L. Rodino. Generalized metaplectic operators and the Schrödinger equation with a potential in the Sjöstrand class. *Journal of Mathematical Physics*, 55(8), 2014.

[26] E. Cordero, F. Nicola, and L. Rodino. Time-frequency analysis of fourier integral operators. *Communications on Pure and Applied Mathematics*, 9(1):1–21, 2010.

[27] E. Cordero, F. Nicola, and L. Rodino. Propagation of the Gabor wave front set for Schrödinger equations with non-smooth potentials. *Reviews in Mathematical Physics*, 27(01):1550001, 2015.

[28] E. Cordero, F. Nicola, and L. Rodino. Wave packet analysis of Schrödinger equations in analytic function spaces. *Advances in Mathematics*, 278:182–209, 2015.

[29] E. Cordero and L. Rodino. *Time-frequency analysis of operators*, volume 75. Walter de Gruyter GmbH & Co KG, 2020.

[30] E. Cordero and L. Rodino. Wigner analysis of operators. part I: Pseudodifferential operators and wave fronts. *Applied and Computational Harmonic Analysis*, 58:85–123, 2022.

[31] E. Cordero and L. Rodino. Characterization of modulation spaces by symplectic representations and applications to Schrödinger equations. *Journal of Functional Analysis*, 284(9):109892, 2023.

[32] E. Cordero and S. I. Trapasso. Linear perturbations of the Wigner distribution and the Cohen class. *Analysis and Applications*, 18(03):385–422, 2020.

[33] W. Craig, T. Kappeler, and W. Strauss. Microlocal dispersive smoothing for the schrödinger equation. *Communications on Pure and Applied Mathematics*, 48(8):769–860, 1995.

[34] T. Çukur, M. Lustig, E. U. Saritas, and D. G. Nishimura. Signal compensation and compressed sensing for magnetization-prepared MR angiography. *IEEE transactions on medical imaging*, 30(5):1017–1027, 2011.

[35] M. A. De Gosson. *Symplectic methods in harmonic analysis and in mathematical physics*, volume 7. Springer Science & Business Media, 2011.

[36] M. A. de Gosson. Hamiltonian deformations of Gabor frames: first steps. *Applied and computational harmonic analysis*, 38(2):196–221, 2015.

[37] M. A. de Gosson. *Quantum Harmonic Analysis: An Introduction*, volume 4. Walter de Gruyter GmbH & Co KG, 2021.

[38] L. Deligiannidis and H. R. Arabnia. *Emerging trends in image processing, computer vision and pattern recognition.* Morgan Kaufmann, 2014.

[39] L. Di Sopra, D. Piccini, S. Coppo, M. Stuber, and J. Yerly. An automated approach to fully self-gated free-running cardiac and respiratory motion-resolved 5D whole-heart MRI. *Magnetic resonance in medicine*, 82(6):2118–2132, 2019.

[40] N. C. Dias, M. A. De Gosson, and J. N. Prata. Metaplectic formulation of the Wigner transform and applications. *Reviews in Mathematical Physics*, 25(10):1343010, 2013.

[41] T. T. Do, Y. Chen, D. T. Nguyen, N. Nguyen, L. Gan, and T. D. Tran. Distributed compressed video sensing. In *2009 16th IEEE International Conference on Image Processing (ICIP)*, pages 1393–1396. IEEE, 2009.

[42] J. H. Ender. On compressive sensing applied to radar. *Signal Processing*, 90(5):1402–1414, 2010.

[43] H. G. Feichtinger. Banach spaces of distributions of Wiener's type and interpolation. In *Functional Analysis and Approximation: Proceedings of the Conference held at the Mathematical Research Institute at Oberwolfach, Black Forest, August 9–16, 1980*, pages 153–165. Springer, 1981.

[44] H. G. Feichtinger. *Modulation spaces on locally compact abelian groups.* Citeseer, 1983.

[45] H. G. Feichtinger. Generalized amalgams, with applications to Fourier transform. *Canadian Journal of Mathematics*, 42(3):395–409, 1990.

[46] H. G. Feichtinger and W. Kozek. *Quantization of TF lattice-invariant operators on elementary LCA groups*, pages 233–266. Birkhäuser Boston, Boston, MA, 1998.

[47] W. Y. R. Fok, Y. C. I. Chan, J. Romanowicz, J. Jang, A. J. Powell, and M. H. Moghari. Accelerated free-breathing 3d whole-heart magnetic resonance angiography with a radial phyllotaxis trajectory, compressed sensing, and curvelet transform. *Magnetic resonance imaging*, 83:57–67, 2021.

[48] G. B. Folland. *Harmonic analysis in phase space.* Number 122 in Annals of Mathematics Studies. Princeton university press, 1989.

[49] S. Foucart and H. Rauhut. *A Mathematical Introduction to Compressive Sensing.* Applied and Numerical Harmonic Analysis. Birkhäuser New York, NY, 1 edition, 2013.

[50] J. E. Fowler, S. Mun, E. W. Tramel, et al. Block-based compressed sensing of images and video. *Foundations and Trends® in Signal Processing*, 4(4):297–416, 2012.

[51] B. Franceschiello, L. Di Sopra, S. Ionta, D. Zeugin, M. Notter, J. A. Basti-aansen, J. Jorge, J. Yerly, M. Stuber, and M. Murray. Motion-resolved 3d magnetic resonance imaging of the human eye. *Investigative Ophthalmology & Visual Science*, 60(9):6112–6112, 2019.

[52] B. Franceschiello, S. Rumac, T. Hilbert, M. Nau, M. Dziadosz, G. Degano, C. W. Roy, A. Gaglianese, G. Petri, J. Yerly, et al. Hi-Fi fMRI: High-resolution, fast-sampled and sub-second whole-brain functional MRI at 3T in humans. *bioRxiv*, pages 2023–05, 2023.

[53] H. Führ and I. Shafkulovska. The metaplectic action on modulation spaces. *Applied and Computational Harmonic Analysis*, 68:101604, 2024.

[54] Y. V. Galperin and S. Samarah. Time-frequency analysis on modulation spaces $M_m^{p,q}$ $0 \leq p, q \leq \infty$. *Applied and Computational Harmonic Analysis*, 16(1):1–18, 2004.

[55] M. Ganzetti, N. Wenderoth, and D. Mantini. Intensity inhomogeneity correction of structural mr images: a data-driven approach to define input algorithm parameters. *Frontiers in neuroinformatics*, 10:10, 2016.

[56] Z. Gao, L. Dai, S. Han, I. Chih-Lin, Z. Wang, and L. Hanzo. Compressive sensing techniques for next-generation wireless communications. *IEEE Wireless Communications*, 25(3):144–153, 2018.

[57] M. Ghahremani, Y. Liu, P. Yuen, and A. Behera. Remote sensing image fusion via compressive sensing. *ISPRS journal of photogrammetry and remote sensing*, 152:34–48, 2019.

[58] G. Giacchi. Boundedness of metaplectic operators within L^p spaces, applications to pseudodifferential calculus, and time-frequency representations. *Journal of Fourier Analysis and Applications*, Accepted.

[59] G. Giacchi, I. Iakovidis, B. Milani, M. Stuber, M. Murray, and B. Franceschiello. ALMA: a mathematics-driven approach for determining tuning parameters in generalized LASSO problems, with applications to MRI. *arXiv preprint arXiv:2406.19239*, 2024.

[60] G. Giacchi, B. Milani, and B. Franceschiello. On the determination of Lagrange multipliers for a weighted LASSO problem using geometric and convex analysis techniques. *Applied Mathematics & Optimization*, 89(2):31, 2024.

[61] G. H. Glover. Spiral imaging in fMRI. *Neuroimage*, 62(2):706–712, 2012.

[62] G. Goelman, R. Dan, F. Růžička, O. Bezdicek, E. Růžička, J. Roth, J. Vymazal, and R. Jech. Frequency-phase analysis of resting-state functional MRI. *Scientific reports*, 7(1):43743, 2017.

[63] K. Gröchenig. Time-frequency analysis of Sjöstrand's class. *Revista matemática iberoamericana*, 22(2):703–724, 2006.

[64] K. Gröchenig. Weight functions in time-frequency analysis. In *Pseudodifferential Operators: Partial Differential Equations and Time-Frequency Analysis*, volume 52, pages 343–366. AMS and Fields Institute Comm., 2007.

[65] K. Gröchenig. *Foundations of time-frequency analysis*. Springer Science & Business Media, 2013.

[66] K. Gröchenig and Z. Rzeszotnik. Banach algebras of pseudodifferential operators and their almost diagonalization. In *Annales de l'institut Fourier*, volume 58, pages 2279–2314, 2008.

[67] D. Gross, Y.-K. Liu, S. T. Flammia, S. Becker, and J. Eisert. Quantum state tomography via compressed sensing. *Physical review letters*, 105(15):150401, 2010.

[68] W. Guo, J. Chen, D. Fan, and G. Zhao. Characterizations of some properties on weighted modulation and Wiener amalgam spaces. *Michigan Mathematical Journal*, 68(3):451–482, 2019.

[69] A. Hassell and J. Wunsch. The Schrödinger propagator for scattering metrics. *Annals of Mathematics*, pages 487–523, 2005.

[70] K. Hayashi, M. Nagahara, and T. Tanaka. A user's guide to compressed sensing for communications systems. *IEICE transactions on communications*, 96(3):685–712, 2013.

[71] M. Herman and T. Strohmer. Compressed sensing radar. In *2008 IEEE Radar Conference*, pages 1–6. IEEE, 2008.

[72] L. Hörmander. Quadratic hyperbolic operators. *Microlocal analysis and applications (Montecatini Terme, 1989), Lecture Notes in Math*, 1495:118–160, 1989.

[73] K. Ito. Propagation of singularities for Schrödinger equations on the Euclidean space with a scattering metric. *Communications in Partial Differential Equations*, 31(12):1735–1777, 2006.

[74] K. Ito and S. Nakamura. Singularities of solutions to the Schrödinger equation on scattering manifold. *American journal of mathematics*, 131(6):1835–1865, 2009.

[75] R. Jaroudi, G. Baravdish, B. T. Johansson, and F. Åström. Numerical reconstruction of brain tumours. *Inverse Problems in Science and Engineering*, 27(3):278–298, 2019.

[76] R. V. Kadison and J. R. Ringrose. *Fundamentals of the theory of operator algebras. Volume I: Elementary theory.* Now York: Academic press, 1997.

[77] A. Kapoor, R. Viswanathan, and P. Jain. Multilabel classification using bayesian compressed sensing. *Advances in neural information processing systems*, 25, 2012.

[78] K. Kato, M. Kobayashi, and S. Ito. Representation of Schrödinger operator of a free particle via short-time Fourier transform and its applications. *Tohoku Mathematical Journal, Second Series*, 64(2):223–231, 2012.

[79] M. Kobayashi. Modulation spaces $M^{p,q}$ for $0 < p, q \leq \infty$. *Journal of Function Spaces*, 4(3):329–341, 2006.

[80] R. Kumar, H. Wason, and F. J. Herrmann. Source separation for simultaneous towed-streamer marine acquisition—a compressed sensing approach. *Geophysics*, 80(6):WD73–WD88, 2015.

[81] P. C. Lauterbur. Image formation by induced local interactions: examples employing nuclear magnetic resonance. *nature*, 242(5394):190–191, 1973.

[82] J.-R. Liao, J. M. Pauly, T. J. Brosnan, and N. J. Pelc. Reduction of motion artifacts in cine MRI using variable-density spiral trajectories. *Magnetic resonance in medicine*, 37(4):569–575, 1997.

[83] B. Likar, M. A. Viergever, and F. Pernus. Retrospective correction of MR intensity inhomogeneity by information minimization. *IEEE transactions on medical imaging*, 20(12):1398–1410, 2001.

[84] M. Lopes. Estimating unknown sparsity in compressed sensing. In *International Conference on Machine Learning*, pages 217–225. PMLR, 2013.

[85] T.-T. Lu and S.-H. Shiou. Inverses of 2×2 block matrices. *Computers & Mathematics with Applications*, 43(1-2):119–129, 2002.

[86] M. Lustig, D. Donoho, and J. M. Pauly. Sparse MRI: The application of compressed sensing for rapid MR imaging. *Magnetic Resonance in Medicine: An Official Journal of the International Society for Magnetic Resonance in Medicine*, 58(6):1182–1195, 2007.

[87] M. Lustig, D. L. Donoho, J. M. Santos, and J. M. Pauly. Compressed sensing MRI. *IEEE signal processing magazine*, 25(2):72–82, 2008.

[88] L. E. Ma, J. Yerly, D. Piccini, L. Di Sopra, C. W. Roy, J. C. Carr, C. K. Rigsby, D. Kim, M. Stuber, and M. Markl. 5D flow MRI: a fully self-gated, free-running framework for cardiac and respiratory motion–resolved 3D hemodynamics. *Radiology: Cardiothoracic Imaging*, 2(6):e200219, 2020.

[89] A. Martinez, S. Nakamura, and V. Sordoni. Analytic wave front set for solutions to Schrödinger equations. *Advances in Mathematics*, 222(4):1277–1307, 2009.

[90] D. W. McRobbie, E. A. Moore, M. J. Graves, and M. R. Prince. *MRI from Picture to Proton*. Cambridge university press, 2017.

[91] C. Mosher, C. Li, L. Morley, Y. Ji, F. Janiszewski, R. Olson, and J. Brewer. Increasing the efficiency of seismic data acquisition via compressive sensing. *The Leading Edge*, 33(4):386–391, 2014.

[92] J. E. Moyal. Quantum mechanics as a statistical theory. In *Mathematical Proceedings of the Cambridge Philosophical Society*, volume 45, pages 99–124. Cambridge University Press, 1949.

[93] S. Nakamura. Propagation of the homogeneous wave front set for Schrödinger equations. *Duke Mathematical Journal*, 126(2):349–367, January 2005.

[94] F. Nicola and L. Rodino. Propagation of Gabor singularities for semilinear Schrödinger equations. *Nonlinear Differential Equations and Applications NoDEA*, 22:1715–1732, 2015.

[95] C. O'Neill. Compressed sensing reconstruction of sparse geophysical data: an example from regional magnetics. *Exploration Geophysics*, 55(2):139–152, 2024.

[96] R. B. Pachori. *Time-frequency analysis techniques and their applications*. CRC Press, 2023.

[97] M. Packard, F. Bloch, and W. Hansen. The nuclear induction experiment. *Physical Review*, 70(7-8):474–485, 1946.

[98] H. Palangi, R. Ward, and L. Deng. Distributed compressive sensing: A deep learning approach. *IEEE Transactions on Signal Processing*, 64(17):4504–4518, 2016.

[99] Z. Pan, J. Yu, H. Huang, S. Hu, A. Zhang, H. Ma, and W. Sun. Super-resolution based on compressive sensing and structural self-similarity for remote sensing images. *IEEE Transactions on Geoscience and Remote Sensing*, 51(9):4864–4876, 2013.

[100] J. Y. Park and M. B. Wakin. A multiscale framework for compressive sensing of video. In *2009 Picture Coding Symposium*, pages 1–4. IEEE, 2009.

[101] D. Piccini, A. Littmann, S. Nielles-Vallespin, and M. O. Zenge. Spiral phyllotaxis: the natural way to construct a 3D radial trajectory in MRI. *Magnetic resonance in medicine*, 66(4):1049–1056, 2011.

[102] K. Pravda-Starov. Generalized Mehler formula for time-dependent non-selfadjoint quadratic operators and propagation of singularities. *Mathematische Annalen*, 372(3):1335–1382, 2018.

[103] K. Pravda-Starov, L. Rodino, and P. Wahlberg. Propagation of Gabor singularities for Schrödinger equations with quadratic Hamiltonians. *Mathematische Nachrichten*, 291(1):128–159, 2018.

[104] S. Pudlewski, A. Prasanna, and T. Melodia. Compressed-sensing-enabled video streaming for wireless multimedia sensor networks. *IEEE Transactions on Mobile Computing*, 11(6):1060–1072, 2012.

[105] E. M. Purcell, H. C. Torrey, and R. V. Pound. Resonance absorption by nuclear magnetic moments in a solid. *Physical review*, 69(1-2):37, 1946.

[106] I. I. Rabi, S. Millman, P. Kusch, and J. R. Zacharias. The molecular beam resonance method for measuring nuclear magnetic moments. the magnetic moments of $_3\mathrm{Li}^6$, $_3\mathrm{Li}^7$ and $_9\mathrm{F}^{19}$. *Physical review*, 55(6):526, 1939.

[107] H. Rauhut. Wiener amalgam spaces with respect to quasi-Banach spaces. *Colloquium Mathematicum*, 109(2):345–362, 2007.

[108] M. Reed, B. Simon, and S. Reed. *Methods of Modern Mathematical Physics. II. Fourier Analysis, self-adjointness*. Academic Press [Harcourt Brace Jovanovich Publishers], New York, 1975.

[109] L. Robbiano and C. Zuily. Microlocal analytic smoothing effect for the Schrödinger equation. *Duke Mathematical Journal*, pages 93–129, 1999.

[110] R. T. Rockafellar. *Convex Analysis*, volume 13. Princeton University Press, December 1970.

[111] R. T. Rockafellar and R. J.-B. Wets. *Variational analysis*, volume 317. Springer Science & Business Media, 3rd edition edition, 2009.

[112] W. Rudin. *Functional Analysis*. McGraw-Hill, 1991.

[113] M. W. Seeger and H. Nickisch. Compressed sensing and Bayesian experimental design. In *Proceedings of the 25th international conference on Machine learning*, pages 912–919, 2008.

[114] M. A. Shubin. *Pseudodifferential operators and spectral theory*. Springer, 2 edition, 2001.

[115] M. Sushma, A. Gupta, and J. Sivaswamy. Time-frequency analysis based motion detection in perfusion weighted MRI. In *2013 Fourth National Conference on Computer Vision, Pattern Recognition, Image Processing and Graphics (NCVPRIPG)*, pages 1–4. IEEE, 2013.

[116] J. Toft. Continuity properties for modulation spaces, with applications to pseudo-differential calculus, II. *Annals of Global Analysis and Geometry*, 26:73–106, 2004.

[117] J. Toft. Continuity and compactness for pseudo-differential operators with symbols in quasi-banach spaces or Hörmander classes. *Analysis and Applications*, 15(03):353–389, 2017.

[118] R. B. Van Heeswijk, G. Bonanno, S. Coppo, A. Coristine, T. Kober, and M. Stuber. Motion compensation strategies in magnetic resonance imaging. *Critical Reviews™ in Biomedical Engineering*, 40(2), 2012.

[119] S. S. Vasanawala, M. T. Alley, B. A. Hargreaves, R. A. Barth, J. M. Pauly, and M. Lustig. Improved pediatric MR imaging with compressed sensing. *Radiology*, 256(2):607–616, 2010.

[120] S. S. Vasanawala, M. Murphy, M. T. Alley, P. Lai, K. Keutzer, J. M. Pauly, and M. Lustig. Practical parallel imaging compressed sensing MRI: Summary of two years of experience in accelerating body MRI of pediatric patients. In *2011 IEEE international symposium on biomedical imaging: From nano to macro*, pages 1039–1043. IEEE, 2011.

[121] P. Wahlberg. Propagation of polynomial phase space singularities for Schrödinger equations with quadratic hamiltonians. *Mathematica scandinavica*, pages 107–140, 2018.

[122] Z. Wang, E. P. Simoncelli, and A. C. Bovik. Multiscale structural similarity for image quality assessment. In *The Thrity-Seventh Asilomar Conference on Signals, Systems & Computers, 2003*, volume 2, pages 1398–1402. Ieee, 2003.

[123] E. Wigner. On the quantum correction for thermodynamic equilibrium. *Physical review*, 40(5):749, 1932.

[124] J. Wunsch. Propagation of singularities and growth for Schrödinger operators. *Duke Mathematical Journal*, pages 137–186, 1999.

[125] H. Yu and G. Wang. Compressed sensing based interior tomography. *Physics in medicine & biology*, 54(9):2791, 2009.

[126] X. Yuan, P. Llull, X. Liao, J. Yang, D. J. Brady, G. Sapiro, and L. Carin. Low-cost compressive sensing for color video and depth. In *Proceedings of the IEEE Conference on Computer Vision and Pattern Recognition*, pages 3318–3325, 2014.

[127] Z. Zhang. Uncertainty principle of complex-valued functions in specific free metaplectic transformation domains. *Journal of Fourier Analysis and Applications*, 27(4):68, 2021.

[128] Z. Zhang and M. Luo. New integral transforms for generalizing the Wigner distribution and ambiguity function. *IEEE Signal Processing Letters*, 22(4):460–464, 2015.

[129] Z. Zhang, X. Shi, A. Wu, and D. Li. Sharper N-D Heisenberg's uncertainty principle. *IEEE Signal Processing Letters*, 28:1665–1669, 2021.